AN INVESTIGATION OF THE FUNCTIONAL SIGNIFICANCE OF 5'-FLANKING REGION POLYMORPHISMS OF INTERLEUKIN-6 IN SYSTEMIC ARTHRITIS

RACHEL CAROLINE SUSAN JEFFERY

A thesis submitted for the degree of Doctor of Philosophy to University College London at the University of London

July 2003

Centre for Paediatric and Adolescent Rheumatology
Department of Immunology and Molecular Pathology
Windeyer Institute of Medical Sciences
University College London
46 Cleveland Street
London
W1T 4FJ

ProQuest LLC
789 East Eisenhower Parkway
P.O. Box 1346
Ann Arbor, MI 48106-1346

Preface

Interleukin-6 (IL-6) is a pleotropic cytokine produced by a wide range of mammalian cell types, with actions on a variety of cellular mechanisms. It is predominantly involved in mediating adaptive immune responses to inflammation, both in the acute and chronic setting, regulating B-cell and T-cell function, stimulating the acute phase reaction, influencing haemopoiesis and cellular bone formation.

The systemic arthritis (SA) form of juvenile idiopathic arthritis (JIA) is characterised by an inflammatory arthritis, a daily spiking fever and an evanescent rash, with serositis, lymphadenopathy, hepatosplenomegaly, thrombocytosis, anaemia, hypergammaglobulinaemia, osteoporosis and growth retardation also occurring. This is the most severe form of JIA, associated with the highest morbidity and mortality.

Several observations implicate IL-6 as having a pivotal role in the pathogenesis of SA. IL-6 levels together with the soluble IL-6 agonist receptor sIL-6R are significantly elevated in the serum and synovial fluid of children with SA, more so than in other forms of JIA or in inflammatory arthritides occurring in the adult population. Serum peaks of IL-6 precede the daily fever spike and are associated with the appearance of rash, and unlike other inflammatory conditions such as infection or rheumatoid arthritis, the peak in IL-6 is not preceded by a rise in levels of other inflammatory cytokines such as IL-1 and TNFα. In addition, many of the manifestations of SA involve mechanisms in which IL-6 is involved in the pathogenesis. IL-6 was therefore considered a candidate gene for susceptibility and severity of SA.

Several polymorphisms have been identified in the 5'-flanking region of the IL-6 gene, a G to C at position –174, a G to C at –572, a G to A at –597 and a variable length AT-tract from –373 to –392. As IL-6 is predominantly regulated by transcription, these polymorphisms were considered to potentially influence the production of IL-6. This thesis set out to investigate the association of these IL-6 polymorphisms with SA using case-control genotype studies. This led to an investigation of the functional significance and possible mechanisms of the polymorphisms found to be associated with SA using transfection studies and electrophoretic mobility shift assays.

Abstract

This thesis investigates the hypothesis that the high levels of IL-6 in SA is pathogenic and is influenced by polymorphisms in the 5'-flanking region of IL-6, resulting in altered IL-6 transcriptional regulation, susceptibility to and severity of SA.

Genotype studies of SA cases and controls found the –174G/C polymorphism to be associated with SA. The –174CC genotype was under-represented in SA and this was due to under-representation of this genotype in the early disease onset group (≤5 years of age), indicating association with susceptibility and severity of SA. The –572G/C and –597G/A polymorphisms were not associated with disease despite strong allelic association between –174C & –597A and weak allelic association between –174G & –572C. The most common naturally occurring haplotypes were –597G–572G–174G and –597A–572G–174C.

In HeLa cell transfections with luciferase reporter constructs stimulated with IL-1β or TNFα, the –174G allele was associated with higher levels of expression than the –174C allele. The –597 polymorphism lacked independent function, whereas the –572G allele was associated with higher levels of expression than –572C. The AT-tract polymorphism showed functional influence, with A_8T_{12} associated with higher levels of expression than A_9T_{11}. These effects were cell-specific, with no difference in levels of transcription between haplotypes in Huh7 cells. Deletion mutant constructs indicated that the –174G/C allelic effect was modulated by a region between –310 and –550, which includes the AT-tract. Dexamethasone inhibition of IL-1-induced IL-6 transcription was associated with significantly more inhibition of expression for the –174G allele than –174C.

Electrophoretic mobility shift assays with HeLa cell nuclear extracts found a transcription factor(s) bound to the IL-6 gene between –134 and –184 more strongly with the –174C allele than –174G. This appeared to involve C/EBPβ, and NF1 may have been involved. An additional novel finding was the binding of an IL-1β inducible factor between –161 and –235.

Contents

List of figures

Chapter 1

Chapter 2

Chapter 5

List of tables

Abbreviations

ACR	American College of Rheumatology
AEBSF	(4-[2-aminoethyl]benzenesulfonylfluoride
AIA	Antigen induced arthritis
AMPS	Ammonium persulphate
AP1	Activating protein 1
APC	Antigen presenting cell
APP	Acute phase protein
APR	Acute phase response
ARC	Arthritis research campaign
ATF	Activating transcription factor
ATP	Adenosine triphosphate
AT-tract	Adenosine-thymidine tract
AUBP	AU-rich region RNA binding protein
AU-rich	Adenosine-uracil rich
BCA	Bicinchoninic acid
BiP	Immunoglobulin binding protein
BMD	Bone mineral density
bp	Base pairs
BPRG	British Paediatric Rheumatology Group
BSA	Bovine serum albumin
mBSA	Methylated bovine serum albumin
bZIP	Basic zipper region
C/EBP	CCAAT/enhancer binding protein
cAMP	Cyclic-adenosine monophosphate
CAT	Chloramphenicol acetyltransferase
CBF1	C-promoter binding factor 1
CBM	Cytokine binding module
CBP	CREB binding protein
cDNA	Copy deoxyribonucleic acid
cf	Compared with
CFDA SE	5-(and-6)-carboxyfluorescein diacetate, succinimidyl ester
CFSE	Carboxyfluorescein succinimidyl ester
cfu	Colony forming units
CIS	Cytokine inducible SH2 protein
CLC	Cardiotrophin-like cytokine
CNTF	Ciliary neurotrophic factor
cps	Counts per second
CRE	cAMP response element
CREB	cAMP response element binding protein
CREM	cAMP response element modulator
CsCl	Caesium chloride
CstF-64	Cleavage stimulation factor
CT-1	Cardiotrophin 1
DAT1	Dopamine transporter gene
DEPC	Diethyl pyrocarbonate
dex	dexamethasone
df	Degrees of freedom
DMEM	Dulbecco's modified Eagles medium
DMSO	Dimethyl sulphoxide
DNA	Deoxyribonucleic acid
dsDNA	Double-stranded DNA
ssDNA	Single-stranded DNA
dNTP	Deoxynucleotide triphosphate

dATP	Deoxyadenosine triphosphate
dCTP	Deoxycytosine triphosphate
ddNTP	Dideoxynucleotide triphosphate
DTT	Dithiothreitol
E. coli	*Escherichia coli*
ECL	Enhanced chemiluminescence
ECV304	Human cell line, possibly endothelial cell
EDTA	Ethylene glycol-bis (b-aminoethylether) N, N, N', N'-tetraacetic acid
EH	Estimation of haplotype
ELISA	Enzyme-linked immunosorbent assay
EMSA	Electrophoretic mobility shift assay
ER	Oestrogen receptor
ERK	Extracellular regulated kinase
EULAR	European League Against Rheumatism
FACS	Fluorescence-activated cell sorter
FCS	Foetal calf serum
FITC	Fluorescein isothiocynate
FLSs	Fibroblast-like synoviocytes
Fras	Fos-related antigens
G418	Neomycin analogue
β-gal	β-galactosidase
X-gal	5-bromo-4-chloro-3-indolyl-β-D-galactopyranoside
Gab	Grb2-associated binder protein
GC	Glucocorticosteroid
G-CSF	Granulocyte colony stimulating factor
GM-CSF	Granulocyte macrophage colony stimulating factor
GOOD	Goodinge controls
gp130	Glycoprotein 130
sgp130	Soluble glycoprotein 130
Grb2	Growth factor receptor bound protein
GR	Glucocorticoid receptor
GRE	Glucocorticoid response element
dH_2O	Distilled water
HBS	Hanks buffered saline
HCl	Hydrochloric acid
HeLa	Human epithelial cell line
HEPES	N-2-hydroxyethylpiperazine-N'-2-ethanesulphonic acid
HepG2	Human hepatoma cell line
HGMP	Human genome mapping project
HLA	Human leukocyte antigen
HPV18	Human papilloma virus type 18
HRP	Horseradish peroxidase
Hsp	Heat shock protein
HSV-TK	Herpes simplex virus-thymidine kinase
HTLV1	Human T-cell leukaemia virus 1
Huh7	Human hepatoma cell line
HUVEC	Human umbilical vein endothelial cell
H-W	Hardy-Weinberg
ICAM	Intercellular adhesion molecule
ICER	Inducible cAMP early repressor
IFNγ	Interferon gamma
Ig	Immunoglobulin
IGF1	Insulin-like growth factor 1
IKK	Inhibitor of kappa B kinase
IL-1	Interleukin-1

IL-1 stim	IL-1β stimulated
IL-1R	Interleukin-1 receptor
IL-1RI	Type I interleukin-1 receptor
IL-4	Interleukin-4
IL-6	Interleukin-6
IL-6R	Ineterleukin-6 receptor
hIL-6	Human interleukin-6
rIL-6	Recombinant human IL-6
sIL-6R	Soluble Interleukin-6 receptor
vIL-6	Viral interleukin-6
IL-8	Interleukin-8
IL-10	Interleukin-10
IL-11	Interleukin-11
ILAR	International League Against Rheumatism
Inr	Transcription initiation region
IPTG	Isopropyl β-D thiogalactopyranoside
IRAK1	Interleukin-1 receptor associated kinase 1
IRF	Interferon regulatory factor
IκB	Inhibitor of kappa B
JAK	Janus kinase
JCA	Juvenile chronic arthritis
JIA	Juvenile idiopathic arthritis
JRA	Juvenile rheumatoid arthritis
$K_4Fe(CN)_6$	Potassium ferrous cyanate
KAc	Potassium acetate
KCl	Potassium chloride
kDa	kiloDaltons
KH_2PO_4	Potassium hydrogen phosphate
LAP	Liver-enriched transcription activating protein (C/EBPβ)
LB	Luria-Bertani medium
LIF	Leukaemia inhibitory factor
LIFR	Leukaemia inhibitory factor receptor
LIP	Liver transcription inhibitory protein (truncated form of C/EBPβ)
Ln(L)	Log likelihood of allelic association
LPS	Lipopolysaccharide
mAb	Monoclonal antibody
MADGE	Micro-titre array diagonal gel electrophoresis
MAPK	Mitogen activated protein kinase
MAPKAP kinase2	MAPK-activated protein kinase 2
MCP1	Macrophage chemotactic protein 1
M-CSF	Macrophage colony stimulating factor
M-CSFR	Macrophage colony stimulating factor receptor
$MgCl_2$	Magnesium chloride
mgp130	Membrane bound gp130
$MgSO_4$	Magnesium sulphate
MHC	Human major histocompatibility complex
MIF	Migratory inhibitory factor
MIP	Macrophage inflammatory protein
$MnCl_2$	Manganese chloride
MRA	Myeloma regression antibody, mAb to IL-6R
MRC	Medical research council
NaAc	Sodium acetate
Na_2HPO_4	Sodium hydrogen phosphate
NaCl	Sodium chloride
NaOH	Sodium hydroxide

N-CoR	Nuclear receptor co-receptor
NF1	Nuclear factor 1
NF-IL6	Nuclear factor of IL-6 (also known as C/EBPβ)
NF-κB	Nuclear factor for kappa B
NH_4Ac	Ammonium acetate
NIH3T2	Mouse adipocyte cell line
NIK	NF-κB inducing kinase
NLS	Nuclear localisation sequence
NP-40	Nonidet P-40
NPH	Northwick Park Hospital controls
NRD	Negative regulatory domain
Nun	Nuneaton controls
OCT1&2	Octamer binding transcription factors
OD	Optical density
OR	Odds ratio
OSM	Oncostatin M
OSMR	Oncostatin M receptor
PAGE	Polyacrylamide gel electrophoresis
PBMC	Peripheral blood mononuclear cell
PBS	Phosphate buffered saline
PC	Personal computer
PCR	Polymerase chain reaction
PE	Phycoerythrin
Pfu	*Pyrococcus furiosus*
PHA	Phytohaemagglutinin
PIAS	Protein inhibitors of activated STATs
PI3K	Phosphatidylinositol 3-kinase
PMA	Phorbo-13-myristate-12-acetate
PMSF	Phenylmethylsulfonyl fluoride
PolydI.dC	Poly(dI-dC).poly(dI-dC), synthetic double stranded polymer of inosine and cytosine
Pr	Probe
PTH	Parathyroid hormone
PVDF	Polyvinylidene difluoride
QR	Quantum red
RA	Rheumatoid arthritis
RANK	Receptor activator of nuclear factor
RANKL	RANK ligand
RBP	Recombination binding protein
RBP-Jκ	Recombination signal sequence binding protein-Jκ
RCE	Retinoblastoma control element
RD	Regulatory domain
RFLP	Restriction fragment length polymorphism
RHD	Rel homology domain
RIP	Receptor interacting protein
RNA	Ribonucleic acid
mRNA	Messenger RNA
rpm	Revolutions per minute
RSV	Respiratory syncitial virus
RT-PCR	Reverse transcription polymerase chain reaction
SA	Systemic arthritis
SAA	Serum amyloid A
SDS	Sodium dodecyl sulphate
SDW	Sterile distilled water
SH2	Src homology domain

SHP2	Two-SH2 domain-containing tyrosine-phosphatase
SLE	Systemic lupus erythematosus
SNP	Single nucleotide polymorphism
SOCS	Suppressor of cytokine signalling
Sp1	Specificity protein 1
SRC-1	Steroid receptor coactivator-1
SRE	Serum response element
SSC	Salt sodium citrate
SSc	Systemic sclerosis
SSCP	Single-strand conformational polymorphism
SSOP	Sequence specific oligonucleotide probing
STAT	Signal transducers and activators of transcription
str-FCS	Stripped foetal calf serum
SV40	Simian virus type 40
TAE	Tris acetic acid EDTA
Taq	*Thermus aquaticus*
TBE	Tris boric acid EDTA
TBP	TATA binding protein, also known at TFIID
TDT	Transmission disequilibrium test
TE	Tris EDTA buffer
TEMED	Tetraethylmethylene diamine
TFIIB	Transcription factor IIB
TH	T-helper cell
THP1	Human monocyte cell line
TIMP	Tissue inhibitor of metalloproteinases
Tm	Melting temperature
TNF	Tumour necrosis factor
TNFR	Tumour necrosis factor receptor
TPA	Tetradecanoyl phorbo-13-acetate
TPO	Thrombopoietin
TRADD	TNF-receptor associated death domain protein
TRAF	TNF-receptor associated factor
Tween	Polyoxyethelenesorbitan monolaurate
Tyk	Tyrosine kinase
Tyr	Tyrosine
Ub	Ubiquitination
UHG	Universal heteroduplex generator
UK	United Kingdom
Unstim	Unstimulated
US	United States
UTR	Untranslated region
UV	Ultraviolet
VCAM	Vascular cell adhesion molecule
VNTR	Variable number of tandem repeats
WEDC	West-end donor controls
YY1	Ying yang 1
ZIA	Zymosan induced arthritis
p	probability-value (statistical measure)
Δ	Delta co-efficient (linkage disequilibrium)
χ^2	Chi-square
λs	Sibling relative risk of disease

Publication list

Papers

Fishman D, Faulds G, **Jeffery R**, Mohamed-Ali V, Yudkin JS, Humphries S and Woo P (1998). The effect of novel polymorphisms in the interleukin-6 (IL-6) gene on IL-6 transcription and plasma IL-6 levels, and an association with systemic-onset juvenile chronic arthritis. *J Clin Invest*, **102**, 1369-76.

Jeffery R and Mitchison NA (2001). IL-6 polymorphism, anti-IL-6 therapy and animal models of multiple myeloma. *Cytokine*, **16**, 87.

Garnero P, Borel O, Sornay-Rendu E, Duboeuf F, **Jeffery R**, Woo P and Delmas PD (2002). Association between a functional interleukin-6 gene polymorphism and peak bone mineral density and postmenopausal bone loss in women: the ofely study. *Bone*, **31**, 43-50.

Jeffery R, Fife M, Luong AL, Ogilvie E, Humphries S and Woo P (submitted). Differential binding of a transcription factor complex to the –174 G>C variant of the interleukin-6 gene: rationale for disease susceptibility.

Abstracts

Jeffery R, Luong L, Fishman D, Xia C, Humphries S and Woo P (2001). Functional interleukin-6 (IL-6) polymorphisms in systemic juvenile idiopathic arthritis (sJIA): the G/C polymorphism at –174 has a dominant influence on transcription. *Rheumatol*, **40** Suppl, 138.

Jeffery R, Luong L, Xia C, Ogilvie E, Humphries S & Woo P (2001). The –174 polymorphism of IL-6 alters binding of a HeLa transcription factor and forms functionally significant allelic associations with other 5'-flanking region polymorphisms. *J Leuk Biol*, **Suppl**, 132.

Jeffery R, Luong L, Ogilvie E, Xia C, Humphries S and Woo P, 2002. The –174 polymorphism of IL-6 alters transcription factor binding and forms functionally significant allelic associations in systemic arthritis. *Rheumatol*, **41** Suppl, OP28.

Jeffery R, Luong AL, Ogilvie E, Xia C, Humphries S and Woo P (2002). The –174 single nucleotide polymorphism (SNP) of the Interleukin-6 gene associated with systemic arthritis is functionally significant in the context of common haplotypes, alters transcription factor binding and repression by glucocorticoids. *Arthritis Rheum*, **46** Suppl, 1555.

Twine N, Fife M, Ogilvie E, Lewis C, **Jeffery R** and Woo P (2003). Does the IL6 AnTn tract modify the effect of the –174 polymorphism in systemic arthritis? *Rheumatol*, **42** Suppl, 89.

Awards

American College of Rheumatology Paediatric Rheumatology Research Award 2000

Royal Society of Medicine President's Prize in Clinical Immunology and Allergy 2001

British Society of Rheumatology Young Investigator Award 2002

Acknowledgements

I would like to thank Prof Patricia Woo for giving me the opportunity to develop my scientific training and for supervising me through the ups-and-downs of the time that I was doing my PhD. I am grateful to her for her faith in me, for her support and advice. I am grateful to Prof David Latchman for his advice as my second supervisor and to Dr Mark Fife who kindly took on the unofficial role of a second supervisor after Prof Latchman left. I am grateful to the Arthritis Research Campaign (UK) for enabling me to undertake my PhD by supporting me with a Research Fellowship (grant JO522).

I acknowledge the help of our collaborators Prof Steve Humphries and Dr Le-Ann Luong, in the department of Cardiovascular Genetics at UCL. For the many meetings we spent together critically analysing results and for the equipment and techniques we shared between laboratories. The collection of patient samples for this study would not have been possible without the help of the British Paediatric Rheumatology Group and Dr Wendy Thompson and Dr Rachelle Donn from the ARC DNA repository at Manchester University. I thank the patients, their families and control individuals for their willingness to donate blood samples.

I also thank all the members of the Paediatric and Adolescent Rheumatology Research Group at UCL, many of whom continued to advise on technical matters and provide helpful discussion even after they had left the department. In particular, I acknowledge the help and encouragement of David Faulkes, Ray Fellowes, Sharon Cole, John Cheshire, Daniel Fishman, Chulin Xia and Lucy Wedderburn. Hemlata, Alka, Himarkshi, Emma and Nicole have been invaluable friends. I am grateful to Dr Catherine Lewis for help and tutoring regarding statistical methods used in this research. Not least, I thank my husband Fraser for his constant love, support and encouragement.

Dedication

To my father, who always taught me to have an enquiring mind

CHAPTER 1

INTRODUCTION

1.1. Interleukin 6

1.1.1. The history of interleukin 6

The cytokine interleukin 6 (IL-6) is a mammalian glycoprotein involved in adaptive immune responses to inflammatory stimuli, with regulatory roles on B-cell and T-cell function, haematopoiesis and acute phase reactions. In humans, IL-6 is a single polypeptide chain 184 amino acids in length (212 amino-acid precursor), with a molecular weight of between 21 and 28 kDaltons depending on the glycosylation state. It was initially identified as a protein produced by fibroblasts stimulated with poly(I)poly(C) in the presence of cyclohexamide and named interferon-β_2 (Weissenbach et al., 1980). Independently, it was identified and described by another group as a mitogen-inducible lymphokine acting on B-cells to promote their terminal maturation into immunoglobulin-producing cells, and was named B-cell differentiation factor (Yoshizaki et al., 1984). Subsequently it was changed to B-cell stimulatory factor-2 after purification and characterization (Hirano et al., 1985). The name interleukin 6 (first proposed by Poupart et al., 1987) was universally adopted, as molecular cloning and nucleotide sequencing revealed that these previously described and differently named molecules were identical (Sehgal et al., 1989). Additional previous names for IL-6 reflect the pleiotropic actions of this cytokine; hepatocyte stimulatory factor, hybridoma/plasmacytoma growth factor, monocyte granulocyte inducer type 2 and cytotoxic T-cell differentiation factor (Gauldie et al., 1987, Van Damme et al., 1987, Takai et al., 1988). IL-6 additionally has roles in induction of T-cell growth, thrombopoiesis, bone metabolism and neuronal differentiation. The diversity of cell types that can produce IL-6 also reflects its pleiotropic biological activity. This includes lymphoid cells (B-cells and T-cells), macrophages, bone marrow stromal cells, fibroblasts, chondrocytes, adipocytes, keratinocytes, mesangial cells, astrocytes, endothelial cells, epithelial cells, hepatocytes and osteoblasts.

1.1.2. The IL-6 family of cytokines and their receptors

Cytokines can be classified according to the structure of their receptors. IL-6 is the prototype for the IL-6 family of cytokines that in combination with their specific receptors, signal through a common signal transducer gp130. Other members of this family are interleukin 11 (IL-11), leukaemia inhibitory factor (LIF), oncostatin M (OSM), ciliary neurotrophic factor (CNTF), cardiotrophin 1 (CT-1) and cardiotrophin-like cytokine (CLC). These other members have many similarities in biological

activities to IL-6 including enhancement of immunoglobulin secretion, stimulation of erythropoiesis and thrombopoiesis, involvement in maturation and activation of macrophages, activation of osteoclasts, stimulation of acute phase protein synthesis and regulation of neuronal differentiation. There is homology between amino acids 153-165 of IL-6 and equivalent regions in OSM, CNF, LIF and IL-11, indicating a common region involved in signalling via gp130 (de Hon et al., 1995, Heinrich et al., 2003).

The receptors for the IL-6 family of cytokines form a sub-type of class I cytokine receptors characterised by an extracellular cytokine binding module (CBM), a haematopoietin-binding homologous domain with 4 positionally conserved cysteine residues and a conserved 5 amino-acid C-terminal domain motif (WSXWS) (Bazan, 1990). The receptors also contain a common immunoglobulin homologous domain, a transmembrane domain and a short, non-signalling intra-cellular domain. Despite these structural similarities, each of the α-chain receptors is cytokine specific and occurs in cell membrane anchored and soluble extra-cellular form. Cellular response to cytokine is regulated by the distribution (spacial and temporal) of α-chain receptors (Taga and Kishimoto, 1997). The α-chain receptor is a low affinity receptor. For IL-6, IL-11 and CNTF, cytokine binding to the α-chain receptor initiates ordered assembly of cytokine/α-chain receptor with membrane bound gp130, which increase the receptor affinity. This forms the receptor-signalling complex. IL-6 and IL-11 signal via a gp130 homodimer, whereas the other IL-6 family cytokines signal via a heterodimer of gp130 and LIF receptor (LIFR) for LIF, CNTF, CT-1 and CLC, or gp130 and OSM receptor (OSMR) for OSM (Heinrich et al., 2003).

1.1.3. The IL-6 protein structure and its binding to receptor

The crystal structure of human recombinant IL-6 has confirmed predictions that it is a long-chain helical cytokine. It consists of four helices, two running in one direction (designated A and B) and two running anti-parallel (C and D), with two long linking loops (between A-B, and C-D) and one short loop (between B-C), (figure 1.1, Somers et al., 1997). A network of hydrophobic interactions at the core of the molecule stabilises the helical structure and a series of hydrogen bonds formed by water molecules in surface clefts link the helices and loops of the crystallised structure. This

tertiary structure is common to the other IL-6-type cytokines, such as LIF and CNTF (Robinson et al., 1994, McDonald et al., 1995a). Comparison of known and predicted structures for other related long-chain α-helix-bundle cytokine/haemopoietic factors, such as granulocyte colony-stimulating factor (G-CSF), also show close structural similarity despite low amino acid homology (Somers et al., 1997).

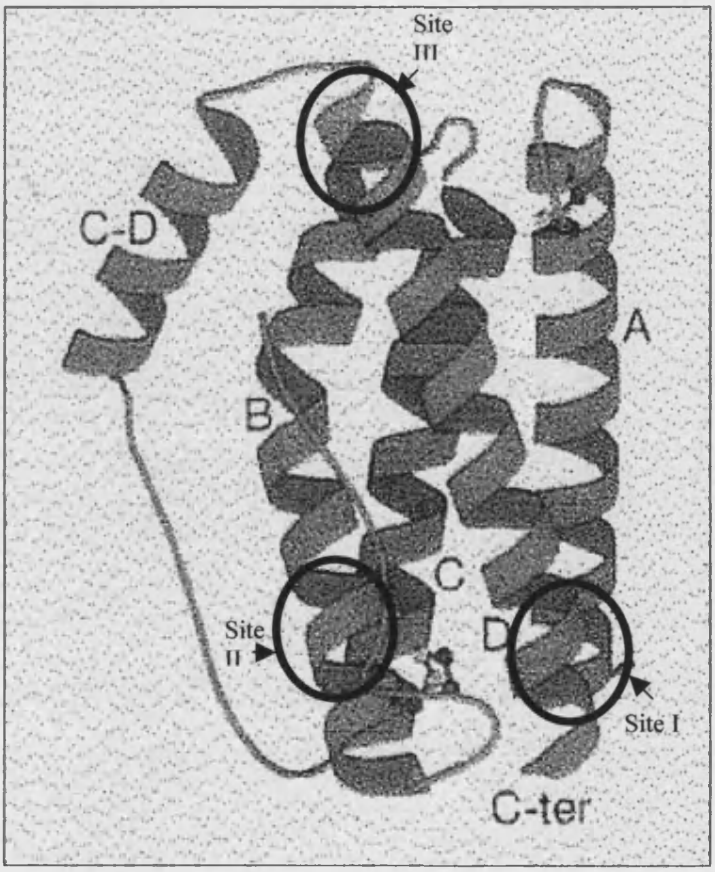

Figure 1.1. Ribbon diagram of the structure of the human IL-6 protein.
As determined by 1.9Å x-ray crystallography (Brookhaven databank accession number IL6). A & B = parallel helices, C & D =anti-parallel helices, C-D =long linking loop between C & D domain, C-ter = C-terminal end of protein. Site I interacts with IL-6R, sites II and III with gp130 (Somers et al., 1997).

Distinct sites on the IL-6 protein are important for binding the α-chain specific receptor for IL-6 (IL-6R) and for signal transduction via gp130. Brakenhoff and co-workers (1994) found that neutralising monoclonal antibodies (mAbs) to a region of the A-B loop of human IL-6 inhibited IL-6R-binding, while neutralising mAbs to a distinct second region permitted IL-6R binding but interfered with signal transduction in bioassays. Further analysis of the A-B loop region (amino acids 41-95) using

chimeric human/murine IL-6 proteins, where murine IL-6 does not permit binding to the human IL-6R, identified a region of 7-10 amino acids in the C-terminal portion of the loop that was necessary to confer human IL-6R binding capacity to IL-6 (Ehlers et al., 1994). In addition, the region of amino acids 175-181 appears to be important in binding to soluble IL-6R as single base mutations within this region resulted in reduced IL-6 biological activity, correlating with reduced affinity for soluble IL-6R (Savino et al, 1993). The region corresponds to a cleft in the 3D structure of the C-terminal region of helix D that may accept amino acid bases from the IL-6R as is seen with the similarly structured molecule human growth hormone when it engages with its specific receptor (Somers et al., 1997). The crystal structure of IL-6 shows the C-terminal A-B loop and the C-terminal portion of helix D to lie in close proximity, to form one binding interface for IL-6R. Mutational studies of two regions of the A & C helices, and a region of the terminal part of the C-D loop, resulted in reduced or abolished signal transduction without altering the binding affinity for IL-6R (Paonessa et al., 1995). This was due to prevention of gp130 binding and dimerization. IL-6 has an essential role in the formation of the IL-6 signalling complex binding directly to IL-6R and gp130 via specific domains and facilitating activation of gp130 (see 1.1.4&5).

Immunoprecipitation, size-exclusion chromatography and analytical centrifugation analysis of the assembled soluble receptor-signalling complex have shown it to consist of two IL-6, two IL-6R and two gp130 molecules (Ward et al., 1994, Paonessa at al., 1995). Therefore, a hexameric model for complex assembly has been proposed. Although study has shown that dimeric-IL-6 bound with higher affinity to sIL-6R by cross-linking two sIL-6R molecules (Ward et al., 1996), this 4-unit complex resulted in reduced biological potency due to decreased ability to couple with gp130. The hexameric complex was therefore proposed to arise from the formation of two trimeric complexes of IL-6/IL-6R/gp130 (in a 1:1:1 ratio) coupling via dimerization of the complexed gp130 molecules (see figure 1.2).

1.1.4. The IL-6 receptor

IL-6R is expressed on a range of cell types facilitating pleiotropic actions of IL-6. This includes activated but not resting B-lymphocytes, plasma cells, T-lymphocytes, monocytes, macrophages, epithelial cells, fibroblasts, hepatocytes, neural cells and osteoclasts. The crystal structure of IL-6-type receptors has yet to be resolved, but

predictions have been made from the amino-acid sequence and the structure of IL-6 and gp130. Residues in the cytokine-binding motif (CBM) of IL-6R, near the hinge region between the upper and lower domains, are involved in IL-6 binding (figure 1.2), (Kalai et al., 1997, Grötzinger et al., 1997). Large aromatic and hydrophobic residues, surrounded by hydrophilic amino acids, are necessary for the IL-6/IL-6R interaction. The immunoglobulin (Ig)-like domain is not required for signal transduction by IL-6 through gp130 and therefore not necessary for IL-6 binding (Yawata et al., 1993). The cytoplasmic domain of IL-6R though not required for receptor complex formation or signal transduction, has a role in targeting the receptor complex to the basolateral membrane of polarised cells (Martens et al., 2000). This targeting of the receptor may influence specific signalling functions of the receptor complex.

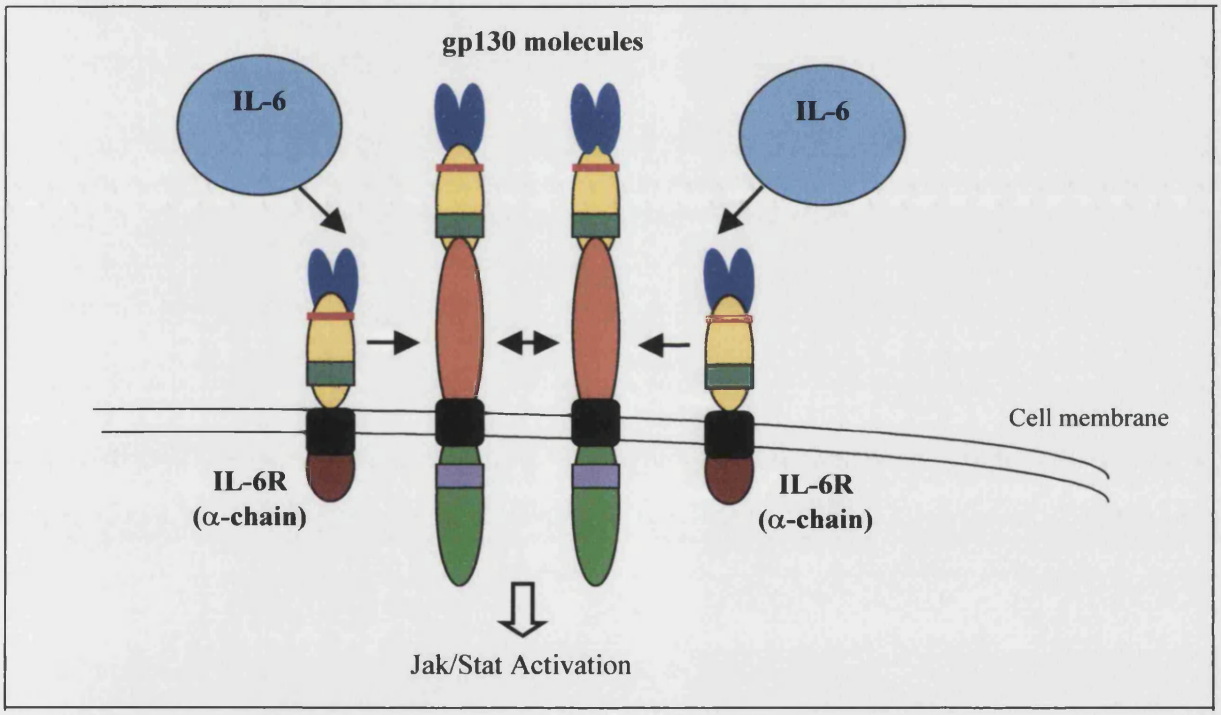

Figure 1.2. The IL-6 receptor-signalling complex - a hexameric model for IL-6/IL-6R/gp130 signal-transduction complex assembly (adapted from Heinrich et al., 1998).
The IL-6/IL-6R complex binds membrane bound gp130 and induces gp130 homodimerization. This results in specific tyrosine phosphorylation in the intracellular cytoplasmic tail of gp130 and Jak/Stat pathway activation (see section 1.1.6).

=Immunoglobulin homologous domain

=Cytokine binding module (CBM)
(red band = 4 conserved cysteine residues, green band = conserved WSXWS motif)

= Transmembrane domain

=60 amino acid intracellular domain essential for signal transduction
(Murakami et al., 1991)

1.1.5. The gp130 molecule

The gp130 molecule is ubiquitously expressed, with cellular response limited by the expression and binding of specific α-receptors such as IL-6R. The Ig-like domain as well as the CBM domain of gp-130 (figure 1.2) and particularly a valine residue at position 252, are necessary for gp130 interaction with IL-6/IL-6R complex (Horsten et al., 1997, Moritz et al., 1999). The crystal structure has been determined for the uncomplexed CBM domain of gp130 and recently for ligand-bound extracellular part of gp130 (with viral IL-6 (vIL-6) capable of signalling through gp130 without the requirement of α-chain receptor), (Bravo et al., 1998, Chow et al., 2001). As predicted from the amino acid sequence, the extracellular fragment of gp130 comprises three domains; a seven-stranded β-sandwich module with an Ig fold (Ig-like domain), a proline-rich linker, and two β-sandwich fibronectin type III domains (CBM). The gp130 molecule appears to be a rigid structure with little or no structural adaptation to cytokine/ligand binding. The exposed hydrophobic residues on the surface of the CBM in combination with an amphipathic-binding surface (capable of polar and non-polar interactions) possibly explain the diversity of cytokine/receptor ligands that can bind and activate gp130. Anti-gp130 mAbs have been created that specifically block signalling by a single member of the IL-6 family, but not by other members (Wijdenes et al., 1995, Chevalier et al., 1996). This indicates that distinct regions of the gp130 molecule facilitate signalling by different IL-6-family cytokines and goes some way to explaining how a common signal transducer may elicit different cellular responses with different cytokine ligands. This is supported by more recent work where gp130 mutants, lacking the Ig-like domain, were unresponsive to IL-6 and IL-11 but still capable of signal transduction in response to LIF or OSM that dimerize gp130 to LIFR or OSMR (Timmermann et al., 2000). Point mutations in the CBM of gp130 also severely impaired signal transduction by IL-6 and IL-11, but differentially affected LIF and OSM responses. Similar to the IL-6R, the cytoplasmic domain of gp130 contains a motif that targets gp130 to the basolateral membrane of polarised cells (Heinrich et al., 2003). In certain cell types localisation of gp130 to specific sites such as lipid rafts and caveolae may facilitate special signalling functions.

1.1.6. IL-6 signal transduction through gp130

IL-6 bound IL-6R induces disulphide-linked homodimerization of gp130 and only once dimerized is gp130 associated with tyrosine kinase activity (Murakami et al., 1993). Two serine residues (amino acids 656 and 658) in the cytoplasmic tail of gp130 were found to be essential for this tyrosine kinase activity. Dimerization of gp130 alone however, may not be sufficient for receptor activation as a single mAb, though inducing dimerization, did not result in efficient activation (Müller-Newen et al., 2000).

Dimerization of gp130 by IL-6 bound IL-6R leads to activation of three of the four known mammalian Janus kinases (Jak1, Jak2 and Tyk2), with different cell types having different patterns of Jak-Tyk phosphorylation (Narazaki et al., 1994, Stahl et al., 1994). The gp130-mediated activation of other tyrosine kinases, Hck, Fes, Btk and Tec, has also been reported in certain cell types (Heinrich et al., 1998). The N-terminal region of Jaks is involved in their association with the cytoplasmic part of receptors (Yan et al., 1998). Heinrich et al. (1998) observed that close contact between Jaks, appears to be sufficient to trigger cross-activation, as over-expression of Jaks without stimulation is associated with tyrosine phosphorylation. Jak1 deficient cells could not respond to IL-6-family cytokines, but Jak-2 deficient cells could, suggesting that in at least some cell types Jak-1 plays an essential role in IL-6 signalling (Rodig et al., 1998, Parganas et al., 1998). Jaks associate with gp130 via two sequences in the membrane-proximal cytoplasmic tail (conserved between Jak-activating cytokine receptors). Mutations in box 1 of gp130 (an 8 amino acid proline-rich motif, figure 1.3) reduced gp130 association with Jaks and abolished both Jak1 and Jak2 activation, while deletion of box 2 (a cluster of hydrophobic residues, figure 1.3) reduced only Jak2 binding and activation (Tanner et al., 1995, Narazaki et al., 1994, Murakami et al., 1993). The inter-box region of gp130 is also important in Jak association. Distinct amino acids appear to regulate Jak binding and Jak activation in association with gp130. Mutation of the tryptophan residue at position 666 of gp130 (in the inter-box region) reduced Jak binding (Haan et al., 2000), where as mutation of the tryptophan residue at position 652 (within the box 1 region) reduced Jak1 activation, though binding was not altered (Haan et al., 2002).

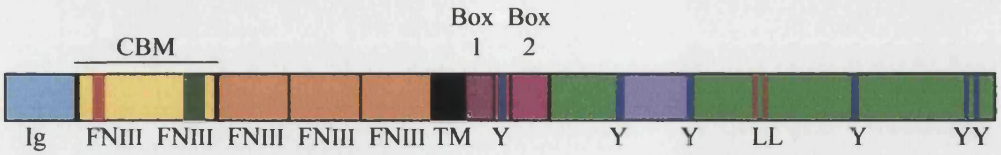

Figure 1.3. The structural organisation of the gp130 molecule
(adapted from Heinrich et al., 2003).
Ig=Immunoglobulin-like domain, FNIII=fibronectin type III domain, CBM=cytokine binding module (consisting of 2 FNIII domains with 4 conserved cysteine residues [shown in red] & a conserved WSXWS motif [shown in green]), TM=transmembrane region, Y=specific tyrosine residues that undergo phosphorylation, LL=di-leucine motif, Box 1&2 are important for Jak interaction.

The context of the Jak binding site is clearly important. Transfer of the box1/2 region to the C-terminal region instead of the proximal part of the intra-cellular gp130 sequence did not permit Jak binding (Greiser et al., 2002). The N-terminal domain of Jaks, the FERM domain (so called as it is also contained in four-point-one, ezrin, radixin and moesin) is crucial for Jak association with gp130 (Heinrich et al., 2003, figure 1.4).

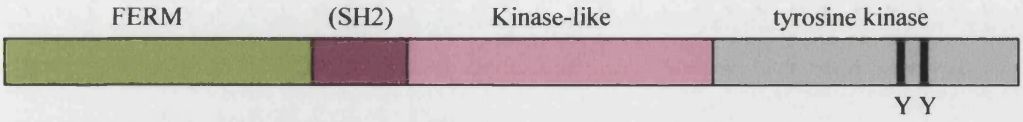

Figure 1.4. The structural organisation of Jak molecules.
FERM=4.1/ezrin/radixin/moesin domain, (SH2)=potential Src homology 2 domain, Y=tyrosine residue.

Multiple Jaks become activated by gp130 dimerization, resulting in the induction of distinct intracellular signalling pathways. The pathways are dependent not on the Jak that is activated, but on phospho-tyrosines in the cytoplasmic tail of gp130 (figure 1.3). These specific tyrosine motifs, once phosphorylated by tyrosine kinase activity, act as docking sites for specific signal transducers and activators of transcription (STATs), (Stahl et al., 1995, Hemman et al., 1996). IL-6 activated gp130 has two tyrosine motifs within the cytoplasmic tail that specifically mediate STAT3 activation and two other motifs that specifically recruit STAT1 and STAT3 (Gerhartz et al., 1996). The highly conserved STAT src homology domain (SH2, figure 1.5) determines the binding specificity to tyrosine motifs (Hemman et al., 1996). STAT3 seems to be preferentially activated compared to STAT1 by cytokine-induced gp130 activation regardless of which Jak/Tyk kinases are activated (Boulton et al., 1995). Once recruited to the gp130 molecule STATs become tyrosine phosphorylated on a specific tyrosine residue

(Kaptein et al., 1996). This phosphorylation was found to be essential for STAT dimerization via the SH2 domain and the dimerization is essential for STAT dissociation from the receptor and for its nuclear translocation, DNA binding and gene activation (Shuai et al., 1993, Shuai et al., 1994).

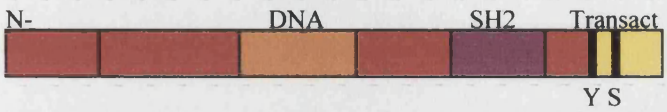

Figure 1.5. The structural organisation of STAT molecules.
N=N-terminal, DNA=DNA binding domain, SH2=Src homology 2 domain, Transact=transactivation domain, Y=tyrosine residue & S=serine residue that undergo phosphorylation.

STAT1 and STAT3 can form homo- or hetero-dimers that are probably translocated to the nucleus via associated shuttle proteins with nuclear localisation sequences (NLSs). STATs themselves do not seem to contain any conventional NLSs (Heinrich et al., 1998). More recently in transfection studies, Zhang and Darnell (2001) have demonstrated that tetrameric complexes of STAT3, forming via N-terminal domain interactions, were required for maximal IL-6 induction of the acute phase protein promoter α2-macroglobulin. Serine/threonine protein kinases in the cytoplasm result in phosphorylation of STAT1 and STAT3 and this augments their transactivating potential (Wegenka et al., 1993, Boulton et al., 1995, Wen and Darnell, 1997). Serine phosphorylation of STAT may regulate the DNA binding of some STAT dimer combinations (STAT3 homo-dimers), but not of others (STAT1 homo-dimers or STAT1/STAT3 hetero-dimers), (Zhang et al., 1995). The DNA-binding domain is located centrally in the STAT dimer (figure 1.5) and may be stabilised by the SH2 phosphotyrosine domains (Chen et al., 1998a). The DNA element recognised is principally determined by the STATs involved (Seidel et al., 1995, Lamb et al., 1995). STAT1 and STAT3 preferentially bind a six base sequence ($TTCN_3GAA$) with the central spacing of the two halves of the recognition site being critical. STAT1 and STAT3 induce a range of target genes including acute phase protein genes, transcription factors, apoptosis regulators and gp130.

The signal transduction of IL-6 via gp130 and the negative regulatory mechanisms involved are summarised in figure 1.6.

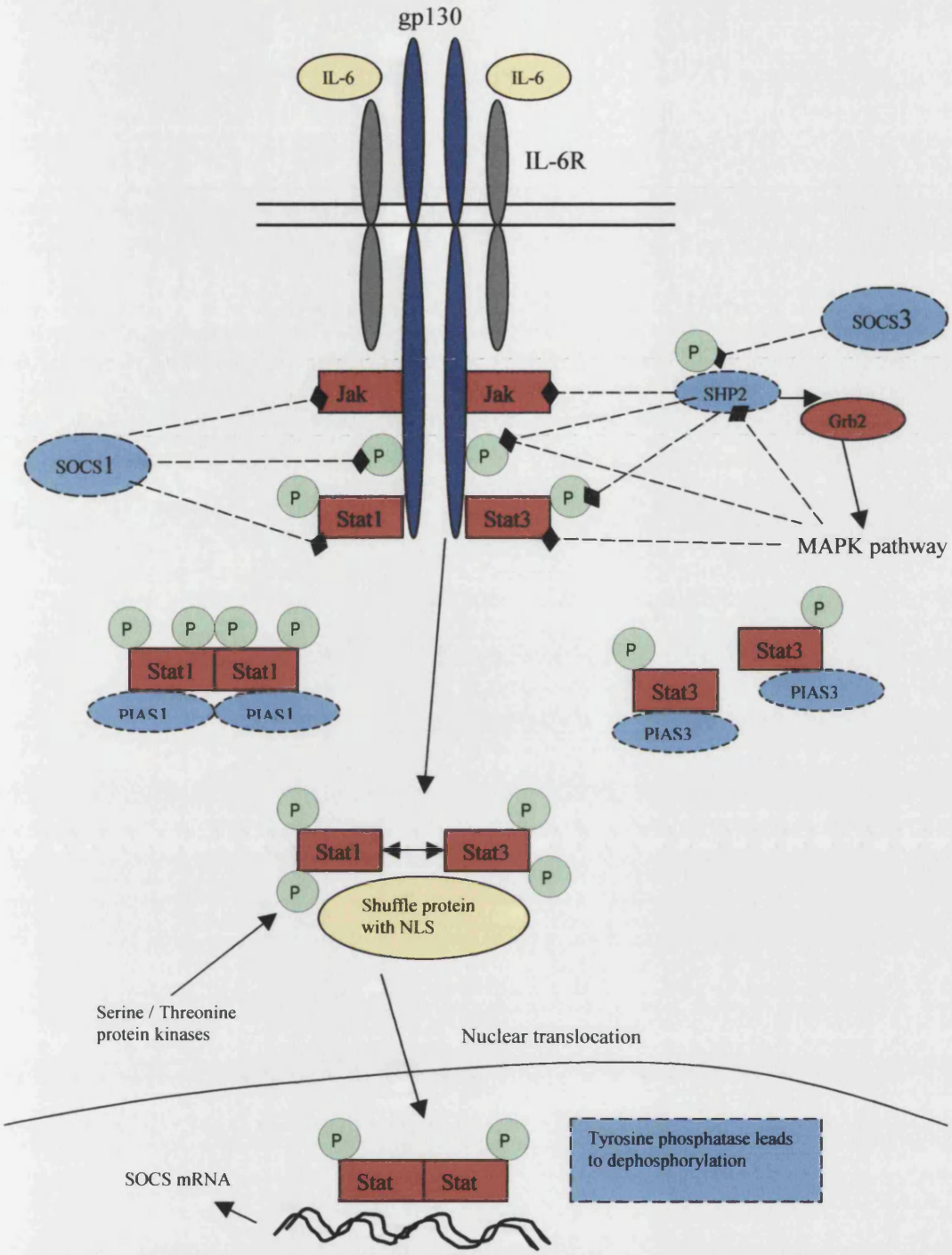

Figure 1.6. The signal transduction pathway of IL-6 via gp130 and negative regulatory mechanisms (adapted from Heinrich et al., 1998).
Dimerisation of gp130 by binding of IL-6/IL-6R results in recruitment & activation of cytoplasmic Janus kinases (Jaks). Phosphorylation of specific tyrosines in the cytoplasmic tail of gp130 allows signal transducers and activators of transcriptions (STAT1 & STAT3) to dock and become tyrosine phosphorylated. STAT phosphorylation is essential for dimerisation of STAT molecules and for nuclear translocation via a shuttle protein containing a nuclear localisation signal (NLS). Further phosphorylation via serine/threonine protein kinases may influence STAT DNA binding. Dephosphorylation of STAT occurs in the nucleus via tyrosine phosphatases. The two SH2 domain-containing tyrosine-phosphatase (SHP2) is also recruited, phosphorylated and activated by gp130 signal transduction, dependent on phosphoryplation of gp130 tyrosine-759 and the presence of Jak1. Activated SHP2 can bind growth factor receptor bound protein (grb2) and activate the mitogen-activated protein kinase (MAPK) pathway in some cells. The MAPK pathway can inhibit tyrosine phosphorylation of STAT1, gp130 and SHP2. SHP2 has inhibitory effects on the Jaks, STATs & gp130. STAT specific protein inhibitors of activated STATs (PIAS) bind & inhibit activated STATs. Suppressors of cytokine signalling (SOCS), induced by the Jak/STAT pathway inhibit tyrosine phosphorylation of STATs & gp130.

1.1.7. Negative regulation of IL-6 signal transduction

STAT activation is transient. Phosphorylated STATs enter the nucleus and then return to the cytoplasm in a dephosphorylated (de-activated) state (Haspel et al., 1996). Tyrosine phosphatases in the nucleus are required for dephosphorylation of STAT1 (Haspel and Darnell, 1999). Dephosphorylation by these phosphatases requires the N-terminal region of STAT1, as N-terminal mutants of STAT1 did not undergo nuclear dephosphorylation, resulting in prolonged phosphorylation. Three families of proteins are involved in the down-regulation of IL-6 signalling; SH2 domain-containing protein-tyrosine phosphatases, protein inhibitors of activated STATs (PIAS) and suppressors of cytokine signalling (SOCS).

Signal transduction through gp130, in addition to activation of Jaks and STATs, results in recruitment and activation of the two-SH2 domain-containing tyrosine-phosphatase SHP2 (Schaper et al., 1998). This SHP2 activation is dependent on the presence of phosphotyrosine-759 (Tyr 759) in the cytoplasmic domain of gp130 and requires Jak1. The main effect of SHP2 seems to be as an inhibitor of IL-6 induced Jak/STAT activation. Mutation of the gp130 recruitment site for SHP2, preventing its recruitment and activation, resulted in elevated and prolonged activation of STAT1 and STAT3, Jaks and gp130 (Kim et al., 1998, Schaper et al., 1998). Only one SHP2-recruiting Tyr-759 was required on the cytoplasmic tail of dimerized gp130 to allow SHP2 association with gp130 and attenuate IL-6 signal transduction (Anhuf et al., 2000). The Tyr-759 did not have to be on the same gp130 molecule in the dimer as the STAT recruitment sites. There is evidence that modulation of Jaks and STATs occurs via direct interaction with SHP2, as in vitro at least, binding to SHP2 has been demonstrated (Yin et al., 1997). In addition, phosphorylated SHP2 can bind the growth factor receptor bound protein (grb2), and links to activation of the mitogen-activated protein kinase (MAPK) pathway, which is activated in some IL-6-stimulated cells. MAPK stimulated by phorbo-13-myristate-12-acetate (PMA) inhibited IL-6 induced STAT3 activation and inhibited tyrosine phosphorylation of STAT1, gp130 and SHP2 (Terstegen et al., 2000). The inhibitory effect of MAPK was dependent on the Tyr-759 residue of gp130 indicating a requirement for SHP2 recruitment. The grb2-associated binder 1 (gab1) protein, involved in activation of the MAPK cascade, becomes tyrosine phosphorylated by IL-6 activation of gp130 and can then bind to SHP2 and phosphatidylinositol 3-kinase (Takahashi-Tezuka et al., 1998). Although no direct

interaction is required between gp130 and gab1, the Tyr-759 residue of gp130 is required, indicating that activated SHP2 is required for the interaction. Gab1 binding to SHP2 leads to activation of ERK2 MAPK. The functional significance of Tyr-759 has been demonstrated in a mouse strain generated to contain a gp130 knock-in point mutation of Tyr-759. These mice died sooner and at a higher rate than controls when exposed to Listeria infection (Kamimura et al., 2002).

Protein inhibitors of activated STATs (PIAS) are important regulators of the Jak/STAT pathway. PIAS bind to a specific STAT molecules only after ligand stimulation and once bound are able to block STAT-DNA binding and gene activation (Chung et al., 1997, Liu et al., 1998). PIAS1 is specific for STAT1, requiring the STAT1 phosphotyrosine-701 (figure 1.5) for interaction, the same phosphotyrosine that is critical for STAT dissociation from gp130 and formation of STAT dimers. PIAS3 is specific for STAT3. Another member of the PIAS family, PIASy, inhibits STAT1 gene activation though not DNA-binding (Liu et al., 2001). Methylation of STAT1 by methyltransferases reduces STAT1 interaction with PIAS, permitting increased DNA binding (Mowen et al., 2001). The methylation is independent of tyrosine or serine phosphorylation. Though complex interactions are clearly involved in STAT inhibition by PIAS, little is known at present about the mechanism of the inhibitory actions.

A further negative regulatory mechanism for IL-6 signalling is induced by Jak/STAT pathway activation. This induces suppressors of cytokine signalling (SOCS), leading to feedback inhibition of STATs, Jaks and gp130 by inhibition of their tyrosine phosphorylation by Jaks (Naka et al., 1997). SOCS family members share a common C-terminal domain (the SOCS box) but have different lengths of N-terminal domain (figure 1.7). The N-terminal domain is required for activity, though for SOCS1 and SOCS3 this region is functionally interchangeable (Nicholson et al., 1999). The conserved SOCS box can mediate SOCS binding to elongins B & C, and may target SOCS with coupled proteins such as Jak2 to proteasomal degradation (Zhang et al., 1999, Ungureanu et al., 2002). SOCS family members also contain an SH2 domain preceding the SOCS box that is involved in their inhibitory function via interaction with respective targets. In the case of SOCS1, an inhibitor of STAT1 and STAT3, the SH2 domain interacts directly with the kinase domain of Jak2 (Endo et al., 1997). In the case of SOCS3, the SH2 domain recognises the phosphotyrosine-759 of gp130, the

binding site for SHP2 and can reduce SHP2 phosphorylation (Schmitz et al., 2000). Expression of SOCS family members SOCS1, 2, 3 and cytokine inducible SH2 protein (CIS) can be induced by IL-6. However, SOCS1, 2, 3 & 5 inhibit IL-6 signalling (Starr et al., 1997, Nicholson et al., 1999). SOCS proteins may have an additional role in mediating cross-communication between cytokine signalling pathways. They inhibit the signalling of other cytokines that influence expression levels of IL-6 and IL-6 signal transduction mediators, for example, TNFα can inhibit IL-6-induced STAT3 activation via up-regulation of SOCS3 in macrophages (Bode et al., 1999).

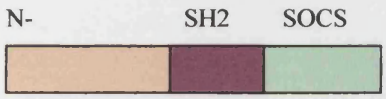

Figure 1.7. The structural organisation of SOCS molecules.
N=N-terminal domain, SH2=Src homology 2 domain, SOCS=conserved SOCS box.

Mechanisms of inhibition of IL-6 signalling that are independent of Jak/STAT pathways have also been demonstrated (Thiel et al., 1998). Rapid removal of radiolabelled IL-6 from the circulation was observed in rat hepatocytes, T-cells and macrophages, with internalisation and degradation of cell surface bound IL-6 (Sonne et al., 1990, Munck et al., 1990). This effect is IL-6R dependent and results from endocytosis of the IL-6/IL-6R/gp130 complex (Zohlnhofer et al., 1992). Replenishment of IL-6 binding sites on the cell surface required *de novo* protein synthesis. Truncated forms of the cytoplasmic domain of gp130, but not IL-6R, prevented IL6-receptor complex endocytosis, with the di-leucine internalisation motif of gp130 sufficient to mediate and target endocytosis to lysosomes (Dittrich et al., 1996). Though internalisation of gp130 can occur independent of ligand binding, it is modulated by phosphorylation of the serine residue at position 782, adjacent to the di-leucine motif (figure 1.3, Gibson et al., 2000). Mechanisms of inhibition of IL-6 signalling are still not fully understood, however they are clearly of major importance in regulating the effects of IL-6.

1.1.8. Soluble IL-6R and soluble gp130

Soluble forms of IL-6R (sIL-6R) and gp130 (sgp130) are found in human plasma. Although the soluble form of IL-6R can be generated by proteolytic cleavage of the membrane bound receptor, *in vivo,* both sIL-6R and sgp130 are also generated by translation of alternatively spliced mRNA transcripts (Müller-Newen et al., 1996, Diamant et al., 1997). In the presence of IL-6, sIL-6R can combine with membrane-bound gp130 (mgp130) to initiate signal transduction and in this way function as an agonist. This contrasts to many other cytokine soluble-receptors which act as antagonists of cytokine activity by blocking cytokine binding to cell-surface receptors. sIL-6R can therefore widen the effects of IL-6 in some cells that only have mgp130 but not membrane bound IL-6R. However, sgp130 antagonises IL-6/sIL-6R signal transduction by competing for binding to mgp130 and sIL-6R enhances the neutralising effect of sgp130 (Müller-Newen et al., 1998). It is therefore not clear whether sIL-6R plays a predominantly agonist or antagonist role *in vivo*. The relative concentrations of sIL-6R, sgp130 and mgp130 may be a deciding factor. In conditions where high plasma levels of sIL-6R occur, it is more likely to act as an agonist, enhancing IL-6 signalling via mgp130. Hence, sIL-6R has the potential to regulate both local and systemic IL-6 effects.

1.2. Biological and pathological effects of IL-6

In common with other cytokines, IL-6 acts as an intercellular communicator in multi-cellular organisms, regulating target cell functions, at nanomolar to picomolar concentrations. In response to a myriad of immunological stimuli, it is rapidly synthesised by cells in secretory form and released without storage. In keeping with the diversity of cells expressing IL-6 and IL-6R, the actions of IL-6 are diverse.

1.2.1. IL-6 as a B-cell differentiation and growth factor

IL-6 plays a crucial role in the maturation of B-cells to immunoglobulin-secreting plasma cells (Takatsu, 1997). The principal factor from rheumatoid synovium found to induce B-cells to secrete immunoglobulins, was IL-6 produced by synovial monocytes (Nawata et al., 1989). C57BL/6 mice transgenic for the human IL-6 gene had massive polyclonal plasmacytosis with associated hypergammaglobulinaemia (Hirano et al., 1992). Although IL-6 deficient mice had normal levels of anitgen-specific immunoglobulin (IgM), levels of IgG isotypes were reduced (Kopf et al., 1998). Re-

exposure of cultured cells from the germinal centres of these IL-6 deficient mice to IL-6 resulted in increased levels of antibody production. In humans, IL-6 is implicated in the hypergammaglobulinaemia associated with atrial myxoma (a benign intra-arterial neoplasm) and multicentric Castleman's disease (a lymphoproliferative disorder of mononuclear cells) with both conditions producing high levels of IL-6 (Parissis et al., 1996, Nishimoto et al., 2000). Surgical removal of the tumour in the case of atrial myxoma, or treatment with anti-IL-6R blocking antibodies in the case of Castleman's disease resulted in remission of clinical disease and normalisation of gammaglobulin levels. In peripheral blood mononuclear cells (PBMCs) from patients with systemic lupus erythematosus (SLE), IL-6 neutralising antibody produced a 30% reduction in spontaneous polyclonal IgG production and a 44% reduction of IgG mAb production (Linker-Israeli et al., 1991).

IL-6 has been shown to induce IgM, IgG and IgA synthesis without affecting B-cell proliferation and it can enhance IL-4-dependent T-cell driven IgE production by immature B-cells *in vitro* (Muraguchi et al., 1988, van Kooten et al., 1990 and Bjorck et al., 1998). Two mechanisms seem to be involved, transcriptional up-regulation of the immunoglobulin gene (Tanner and Tosato, 1992) and altered transcriptional termination to select secretory rather than membrane-specific polyadenylation sites (Raynal et al., 1989). The transcription factors Oct-2 and C/EBPβ can be induced by IL-6 in B-cells, both having specific binding sites in the 5'-flanking region of the immunoglobulin gene with enhancer actions (Natkunam et al., 1994, Cooper et al., 1992). In a chicken B-cell line, over-expression of the polyadenylation/cleavage stimulation factor CstF-64 was sufficient to switch IgM heavy chain expression from membrane-bound to the secreted form (Takagaki et al., 1996). In a human B-cell line however, IL-6 induced switching to secretory Ig mRNA by shifts in poly(A) site preference and occurred without an increase in CstF-64 (Martincic et al., 1998).

In addition to induction of immunoglobulin secretion, IL-6 can act as a B-cell growth factor, stimulating the growth of B-cell and plasma cell tumour lines from multiple myelomas, non-malignant plasmablasts, B-cell lymphomas, and chronic lymphocytic leukaemias (Wang et al., 2001, Jego et al., 2001, Eray et al., 2003).

Furthermore, IL-6 is implicated in autoantibody production in SLE and systemic sclerosis (SSc). In a mouse model of SLE induced by pristane, high levels of IgG autoantibodies were produced to ssDNA, dsDNA and chromatin in IL-6 competent mice, but not IL-6 knockout mice (Richards et al., 1998). The generation of other autoantibodies (anti-nRNP/Sm and anti-Su) were not affected by the absence of IL-6, suggesting that there may be IL-6-dependent and IL-6-independent mechanisms of autoantibody generation. *In vitro* studies of the ability of Topoisomerase I specific T-cell clones from patients with SSc to induce HLA-DR matched SSc B-cells to produce anti-topoisomerase I antibodies showed close correlation to the IL-2 and IL-6 producing ability of the T-cells (Kuwana et al., 2000). In kinetic studies, IL-6 was found to be important in the late phase of the T-cell dependent B-cell activation. In summary, IL-6 has important roles in B-cell differentiation, proliferation and antibody production.

1.2.2. IL-6 as a macrophage differentiation factor

Monocytes from the circulation, attracted to an area of inflammation or injury that facilitates crossing of the endothelium, will differentiate under local tissue influences into either dendritic cells or macrophages. It has been reported that IL-6 released by fibroblasts during monocyte-fibroblast contact resulted in preferential differentiation of monocytes into CD14+CD1a- macrophage phenotype cells displaying characteristic macrophage morphology with numerous vacuoles (Chomarat et al., 2000). This was despite culture in the presence of granulocyte macrophage-colony stimulating factor (GM-CSF) and IL-4 that favours dendritic cell formation (CD14-CD1a+, high HLA-DR expressing cells). Anti-IL-6 and anti-IL-6R blocking monoclonal antibodies (mAbs) prevented fibroblast induced macrophage differentiation, favouring dendritic cell differentiation. The mechanism of IL-6 induced macrophage differentiation was via up-regulation of functional macrophage-colony stimulating factor (M-CSF) receptors on monocytes. Neutralisation of M-CSF activity with anti-M-CSF or anti-M-CSFR blocking antibodies prevented IL-6-mediated macrophage differentiation.

Although IL-6 does not induce maturation of dendritic cells, it may have a role in the generation of auto-immunity by allowing dendritic cells to present previously cryptic and weakly presented epitopes to T-cells, resulting in an antigenic response (Drakesmith et al., 1998). Dendritic cells treated *ex-vivo* with IL-6 and exposed to the

antigen hen-egg lysozyme (HEL), once injected into mice were able to prime T-cells *in vivo* against cryptic epitopes. Mice immunised with HEL and incomplete Freund's adjuvant together with IL-6 exposure, also produced T-cell responses to cryptic determinants. The IL-6 treated dendritic cells contained endosomes that were more acidic than control dendritic cells and this may have resulted in altered processing and presentation of antigen.

1.2.3. IL-6 as a T-helper cell proliferation and differentiation factor

As well as potential influences on antigen presentation to T-cells, IL-6 acts as a potent enhancer of the proliferation of naïve CD4+ T-helper (TH) cells (Joseph et al., 1998). TH cells are classified into TH1 and TH2 subsets based on the cytokines they produce. TH1 cells produce IL-2, interferon-γ (IFNγ) and tumour necrosis factor-β (TNFβ), cytokines involved in regulation of cell-mediated immune responses. TH2 cells produce IL-4, IL-5, IL-6, IL-10 and IL-13, cytokines that mediate T-cell dependent B-cell activation and antibody production. The local cytokine environment plays a critical role in determining TH1 and TH2 differentiation. IL-12, IL-18 and IFN-γ direct differentiation to the TH1 phenotype and IL-4 produces TH2 phenotypic differentiation (Murphy, 1998). IL-6-deficient mice fail to efficiently control infections with facultative intracellular pathogens due to impaired T-cell dependent antibody mediated responses (Kopf et al., 1994, Anguita et al., 1997). Studies of TH2 specific response to injected *Schistosoma* eggs in IL-6 deficient mice, have shown that though IL-6 is not essential for TH2 cell differentiation it is important for TH-proliferation, possibly through induction of the IL-2 receptor (La Flamme et al., 1999). Rincón et al. (1997) showed that IL-6 could modulate the TH phenotype. IL-4 production was significantly less in naïve TH cells differentiated in the presence of antigen presenting cells (APCs) from IL-6 deficient mice compared to in the presence of wild-type (IL-6 producing) APCs. Anti-IL-4 mAbs blocked IL-6 induced TH2 differentiation in the presence of IL-6 or IL-4, and mRNA transcripts of IL-4 were 100-fold higher in TH cells differentiated with IL-6 or IL-4. There was no evidence of differential distribution of IL-6R between TH sub-types to account for differential response to IL-6. These results support a role for IL-6 as a TH2 differentiation factor, mediated via up regulation of IL-4 expression.

In addition to stimulation of TH2 differentiation, IL-6 has been reported to inhibit TH1 differentiation. IL-6 inhibited IFNγ production and stimulated IL-4 synthesis by TH1 cells differentiated with IL-12 (Rincón et al., 1997). The inhibition of IFNγ production by IL-6 was independent of IL-4. It was not blocked by anti-IL-4 mAbs, though IL-4 synthesis was blocked (Diehl et al., 2000). IFNγR-/- CD4+ T-cells, from IFNγR deficient mice, prevented IL-6 from inhibiting TH1 differentiation, although IL-6 treatment itself did not affect levels of IFNγR expression on wild-type CD4+ T-cells during activation (Diehl et al., 2000). STAT1, the main signal transducer for IFNγR, showed decreased levels of tyrosine phosphorylation (indicative of reduced activation), in the presence of IL-6 when wild-type CD4+ T-cells were stimulated with IFNγ. This IL-6 inhibition of IFNγ-induced STAT1 phosphorylation was prevented by SOCS1 deficient CD4+ T-cells. STAT3, a known mediator of IL-6-induced SOCS1 expression was unregulated in activated CD4+ T-cells in the presence of IL-6. IL-6 inhibition of TH1 differentiation therefore seems to be mediated by increased expression of SOCS1 because of IL-6-induced STAT3 expression. SOCS1 expression then reduces signalling via IFNγR and results in reduced autocrine production of IFNγ.

A different group, found that IL-6 only augmented IL-4 synthesis and inhibited IFNγ production in *primed* CD4+ T-cells from wild-type and IL-6 deficient mice, but inhibited IL-4-induced TH2 differentiation in *naïve* T-cells (Tanaka et al., 2001). The nature of the antigenic stimulus may be important in determining TH cell response to IL-6. IL-6 deficient mice infected with *Candida albicans* showed preferential augmentation of the TH2 response (Romani et al., 1996), whereas IL-6 deficient mice infected with *Streptococcus pneumoniae* or injected with lipopolysaccharide (LPS) showed augmented IFNγ synthesis, associated with a TH1 response (Poll et al., 1997, Xing et al., 1998). IL-6 appears to have a complex role in T-cell differentiation and proliferation.

1.2.4. IL-6 and bone metabolism

Bone metabolism is regulated by a balance between osteoclast-induced bone resorption and osteoblast derived bone formation. Ishimi et al. (1990) showed that IL-6 was produced by a murine osteoblast cell line, inducible by agents such as IL-1, TNF, LPS and parathyroid hormone (PTH), (Greenfield et al., 1993). PTH is a key regulator of

bone metabolism in response to serum calcium levels. IL-6 appears to act as a downstream effector of PTH as neutralising IL-6 antibodies block PTH-induced bone resorption (Greenfield et al., 1995). IL-6 stimulates osteoclast formation and activation. Murine bone cultures with IL-6 exposure had three-times more osteoclasts than control cultures grown without the addition of IL-6, and osteoclast calcium efflux was stimulated in a dose dependent manner by IL-6 (Ishimi et al., 1990). The IL-6R is necessary for IL-6 induced osteoclast formation from bone marrow (Tamura et al., 1993). Interestingly, IL-6R expression was required on osteoblasts rather than osteoclasts, indicating that the IL-6 effect on osteoclastogenesis is mediated via osteoblasts, at least *ex vivo* (Udagawa et al., 1995). The mechanisms by which IL-6 may mediate bone cell effects is unknown. However, an inter-play between cytokines and their signalling systems is likely to be involved. Neutralising antibodies to IL-1 inhibited recombinant IL-6-induced osteoclast differentiation from normal human bone marrow cultures (Kurihara et al., 1990). In turn, it has also been shown that antagonism of IL-6R signalling can inhibit the effects of IL-1 and TNF-induced osteoclastogenesis (Devlin et al., 1998).

Serum from patients with Paget's or Gorham-Stout disease, conditions characterised by increased bone remodelling and osteolysis, were found to stimulate osteoclast-like multinucleated cell formation from normal bone marrow cultures (Roodman et al., 1992, Devlin et al., 1996). The sera from these patients contained high levels of IL-6 when compared to normal controls, and neutralising antibody to IL-6 was able to block induced osteoclast formation by disease serum. Osteoblast levels of mRNA for IL-6, IL-6R and C/EBPβ (an IL-6 transcription factor, see section 1.3.2.2) were significantly higher from Pagetic bone than from non-Pagetic bone (Hoyland et al., 1994). In addition, osteoclasts from Pagetic bone expressed IL-6 mRNA where as osteoclasts from control bone did not. *Ex vivo* studies on mouse parietal bone confirmed osteoblasts and stromal cells, rather than osteoclasts, as the main source of IL-6 in normal bone (Holt et al., 1996). There is indirect evidence that IL-6 plays a role in pathological bone resorption in rheumatoid arthritis (RA). This inflammatory arthropathy is associated with periarticular osteopenia and bony erosions of affected joints. IL-6 mRNA expression was found to be significantly elevated in the absence of elevation of other pro-inflammatory cytokines, IL-1β and TNFα, in periarticular cancellous bone from RA patients with radiological bone loss (Sugiyama, 2001).

Osteoblast-lineage cells derived from RA affected bone produced higher IL-6 expression than osteoblast-lineage cells derived from non-RA bone.

In a murine model of post-menopausal osteoporosis, oestrogen loss as a result of oophorectomy resulted in increased osteoclast development, increased bone turnover and a significant loss in bone mass (Poli et al., 1994). IL-6 was essential for this process as IL-6 deficiency in IL-6 knockout mice undergoing the same procedure, completely prevented the bone changes. Interestingly, the IL-6 knockout mice had normal amounts of trabecular bone, but had higher rates of bone turnover (formation and resorption) when compared to control mice. This may be due to increased numbers of osteoblasts and osteoclasts. Mice transgenic for human IL-6 had reduced numbers of osteoblasts, osteoblast precursors and osteoclasts, with suppressed bone turnover (formation and resorption), (Kitamura et al., 1995). This indicates a complex role for IL-6 in the metabolism of bone *in vivo*. Although the predominant effects of IL-6 appear to be on osteoclasts, this may require osteoblasts to mediate the IL-6 effects, as was seen *in vitro*. Oestrogen has an inhibitory effect on IL-6 expression (see section 1.3.2.6), so its removal by oophorectomy in the murine model of postmenopausal osteoporosis (Poli et al., 1994) would permit IL-6 levels to rise and increase bone resorption. In support of this in humans, oestrogen-deficient women when compared to oestrogen competent women, were found to have significantly higher levels of IL-6 expression from bone marrow aspirates (as well as other bone-resorbing cytokines), (Bismar et al., 1995). In a longitudinal study of 137 post-menopausal women, serum levels of IL-6 were highly predictive of femoral bone loss during the first decade past menopause in nonusers of hormone replacement therapy, and was independent of potential confounders or plasma sex hormone levels (Scheidt-Nave et al., 2001). Bone explants from patients with osteoporotic vertebral fractures show enhanced IL-6 mRNA expression (Ralston, 1994). Recently, IL-6 genotypes associated with lower IL-6 expression have been associated in postmenopausal women with lower bone resorption and reduced loss of bone mass, and in healthy pubertal men with higher peak bone mass (Ferrari et al., 2001, Lorentzon et al., 2000, discussed in section 6.9).

The effects of IL-6 on physiological and pathological bone resorption can at least in part be explained by the induction of receptor activator for nuclear factor (RANK) ligand on the cell surface of osteoblasts and stromal cells (Horowitz et al., 2001).

RANK ligand (RANKL) interacts with RANK expressed on osteoclast-precursors and induces terminal differentiation into mature osteoclasts with bone-resorbing function.

1.2.5. IL-6 and growth retardation

IL-6 transgenic mice (of the rat neurospecific enolase promoter-hIL-6 construct), expressing high levels of circulating human IL-6 from shortly after birth, were found to be 50-70% smaller than non-transgenic littermates (De Benedetti et al., 1997a). This growth retardation could be partially prevented by blocking the actions of IL-6 with administration of anti-murine IL-6 receptor antibodies. The mechanism is probably via the inhibition of insulin-like growth factor-1 (IGF-1) before completion of skeletal growth. Serum levels of IGF-1 were significantly reduced in the IL-6 transgenic mice, while circulating and pituitary cell growth hormone levels were normal. IL-6 administered to non-transgenic mice produced a reduction in IGF-1 levels. In children with systemic arthritis-associated growth retardation, reduced circulating IGF-1 levels have been reported and found to negatively correlate with the degree of active inflammation, which in turn correlates with the levels of IL-6 (Davies et al., 1997).

1.2.6. IL-6 and the acute phase response

Both acute and chronic inflammation trigger a series of systemic reactions characterised by altered hepatic production of a family of proteins called the acute phase proteins (APPs), the process known as the acute phase response (APR). APPs mediate various inflammatory functions: inhibition of phagocyte-derived proteases and cathepsins (α_1-antitrypsin, α_1-antichymotrypsin, haptoglobulin), control of inflammatory mediator pathways (antithrombin III, complement C1, factor I and factor H), activation of clotting (factor VIII, prothrombin and fibrinogen), activation and opsonisation of complement (plasminogen and C-reactive protein), chemotaxis and mast cell degranulation (complement components), free-radical scavenging (caeruloplasmin), removal of cellular debris (haptoglobulin, C-reactive protein) and promotion of fibroblast growth (α_1-acid glycoprotein), (Banks et al., 1998). These APPs can be classified into two types depending on the main inducing cytokine stimulus (Baumann and Gauldie, 1994). Type-1 APPs, including C-reactive protein, complement component C3, serum amyloid A protein and α_1-acid glycoprotein, are mainly induced by IL-1 and TNF, but can also be induced by IL-6. IL-6 synergistically

enhances IL-1- and TNF-mediated production of type-1 APPs. In contrast, type-2 APPs, including fibrinogen, α_1-antitrypsin, α_1-antichymotrypsin, haptoglobulin and caeruloplasmin, are specifically induced by IL-6, with IL-1 or TNF having little effect. IL-6 therefore plays a key role in mediating activation of the acute phase response and the resultant effects.

1.2.7. IL-6 as a thrombopoietic factor

In mice, monkeys and humans IL-6 is a potent thrombopoietic factor stimulating megakaryocytopoiesis and thrombocytosis. Recombinant human IL-6 (rIL-6) increased the size and proportion of megakaryocytes (platelet producing stem cells) in the bone marrow of mice after 48-72 hours of treatment (Hill et al., 1991). Mice implanted with an IL-6 secreting murine fibroblast, developed elevated peripheral blood platelet counts and increased numbers of megakaryocyte-colony forming units in the bone marrow and spleen (Cao et al., 1998). In primates, rIL-6 alone produced a 2 to 3 fold increase in platelet count, with no additional synergy from concomitant administration of IL-3, GM-CSF or LIF (Zeidler et al., 1993). Monkeys that had undergone bone marrow irradiation and received rIL-6 therapy underwent a shortened time of thrombocytopenia (3 days instead of 5) compared to irradiated animals with the same degree of thrombocytopenia that did not receive rIL-6. Megakaryocyte numbers were not altered by IL-6 treatment in healthy or irradiated animals but the ploidy of the megakaryocytes was increased, indicating a stimulation of megakaryocytes to rapidly produce platelets. Though IL-6 is not the main inducer of megakaryocytopoiesis and thrombocyte production, these roles are fulfilled by megakaryocyte-colony stimulating factor and thrombopoietin (TPO). IL-6 clearly has modulatory effects on platelet production and may account for the secondary thrombocytosis seen in association with many inflammatory conditions. Levels of IL-6 and associated biological activity closely correlate with circulating platelet counts in inflammatory conditions in humans (Gastl et al., 1993, Heits et al., 1999). Subcutaneous rIL-6 in a phase 1 trial for the treatment of refractory cancer produced a dose-related induced thrombocytosis (Olencki et al., 2000). A polymorphism in the 5'-flanking region of IL-6, associated with lower levels of IL-6 transcription, correlated with lower circulating platelet counts in healthy subjects (Fernandez-Real et al., 2001). The effects of IL-6 on thrombopoiesis appear to be mediated by TPO. IL-6-induced thrombopoiesis could be abrogated in mice by neutralising antibodies to TPO (Kaser et al., 2001), and plasma

TPO levels were elevated in cancer patients who had received rIL-6. Hepatic TPO mRNA was induced by IL-6 in human hepatoma cell lines (Wolber and Jelkmann, 2000). It remains unclear however whether IL-6 has a role in the normal thrombopoiesis in man.

1.2.8. Anti-inflammatory effects of IL-6

IL-6 is critically involved in the generation of the immune response via effects on T-cells, B-cells, macrophages, induction of the acute phase response, fever and corticosteroid release. Use of neutralising antibodies to IL-6 in chronic inflammatory conditions such as rheumatoid arthritis has shown reduction in joint damage and clinical indices of inflammation (discussed in section 1.2.9). IL-6 may in addition have anti-inflammatory or inflammation modulatory functions, particularly in acute inflammation. IL-6 knockout mice (-/-) with local endotoxin-induced acute lung inflammation or systemically induced endotoxaemia had significantly worse markers of acute inflammation and lower survival rates than IL-6 competent mice (Xing et al., 1998). Levels of pro-inflammatory cytokines were significantly higher in IL-6 -/- mice after induced inflammation (TNFα and macrophage inflammatory protein (MIP)-2 in lung injury, TNFα, MIP-2, GM-CSF and IFNγ in endotoxaemia) with an associated higher neutrophilic response. Similar results were reported for mice induced to develop pneumococcal meningitis. Increased levels of TNFα, IL-1β and MIP-2 mRNA and increased cerebrospinal fluid leukocytosis was detected in the brain of IL-6 -/- mice compared with IL-6 competent wild-type animals (Paul et al., 2003). Administration of rIL-6 to IL-6 -/- mice abolished these differences. In hyperoxic acute lung injury, transgenic IL-6 mice over-expressing IL-6 in the lung, showed enhanced survival compared to wild-type mice (Ward et al., 2000). Improved survival correlated with significant reduction in endothelial and epithelial damage, reduced cell-death and diminished DNA fragmentation. Levels of the cell-death inhibitor Bcl-2 and regulator tissue inhibitor of metalloproteinase-1 (TIMP-1) were enhanced in the IL-6 transgenic mice. *In vitro,* IL-6 can prevent apoptosis in lymphoid cell-lines via activation of Bcl-2 (Rollwagen et al., 1998). *In vivo,* in mice with haemorrhagic shock induced intestinal apoptosis, mice fed oral IL-6 showed reduced apoptosis and increased Bcl-2 gene expression relative to non-IL-6 treated animals. In wild-type mice given intra-tracheal injections of endotoxin to induce local inflammation, co-injection with IL-6 was found

to inhibit the acute neutrophilic infiltrate and resulted in reduced levels of TNFα in bronchoalveolar lavage (Ulich et al., 1994). Interestingly, endogenous IL-6 was up regulated by IL-6 co-injection suggesting a possible auto-regulatory mechanism. Cancer patients who had received rIL-6 in phase 1 and phase 2 trials were found after IL-6 infusion to have elevated levels of IL-1 receptor antagonist (IL-1Ra) and soluble TNF receptor p55 (sTNFRp55), antagonists to the pro-inflammatory cytokines IL-1 and TNF respectively (Tilg et al., 1994). A neutralising antibody to IL-6 used in mice with orally induced Yersinia enterocolitis, showed inhibition of IL-1Ra expression locally and systemically (Jordan et al., 1995). This anti-IL-6 antibody directly inhibited the expression of IL-1Ra from macrophages and polymorphonuclear leukocytes in culture. Increased bone resorption was seen in dental-pulp induced infection in IL-6 -/- mice compared to wild type mice and was associated with an increase in the bone-resorptive cytokines, IL-1-α and -β and reduced expression of the anti-inflammatory cytokine IL-10 (Balto et al., 2001).

These experiments indicate two main mechanisms by which IL-6 may exert anti-inflammatory effects in acute inflammation: via induction of apoptosis regulatory genes Bcl-2 and TIMP-1 and via induction of pro-inflammatory cytokine antagonists IL-1Ra and sTNFRp55 with down-regulation of TNF. In chronic inflammation, the balance of cytokines may differ and the effect of IL-6 may favour inflammation. Different inflammatory stimuli may induce a differing profile of cytokine induction with influences on IL-6 effects. IL-6 knockout mice have shown impaired inflammatory responses to turpentine and *Candida albicans*, but preserved or exaggerated responses to endotoxin (Fattori et al., 1994, Romani et al., 1996, Xing et al., 1998). A paper by Marin and co-workers (2001) suggests that IL-6-sIL-6R may act as an intermediate between acute and chronic inflammation in activated endothelium, though the context of activation may be relevant. Human umbilical vein endothelial cells (HUVECs) activated *in vitro* with thrombin, induced IL-8 secretion, neutrophil infiltration, IL-6 and macrophage chemotactic protein (MCP)-1 production. IL-8 induced IL-6R shedding from neutrophil membranes to produce a rise in sIL-6R levels. sIL-6R increased the amounts of MCP-1 produced by activated HUVECs, which could be blocked by anti-IL-6 or anti-IL-6R antibody indicating that IL-6 is required as a complex with sIL-6R. Increased levels of MCP-1 lead to infiltration by monocytes and the establishment of a chronic inflammatory picture. An *in vivo* model of

inflammation, antigen-induced arthritis in mice, also supports a role for IL-6 in the progression of initial joint inflammation into chronic inflammation (de Hooge et al., 2000 and discussed below).

1.2.9. IL-6 and arthritis

Mouse models of inflammatory arthritis demonstrate an important role for IL-6 in the generation and propagation of inflammatory joint disease. When mice from the DBA/1J strain, susceptible to arthritis induced by immunisation with collagen II antigens, were crossed with IL-6 knockout mice to prevent IL-6 production, collagen induced arthritis was completely abolished (Alonzi et al., 1998). This could not simply be explained by a reduction in antibody production involved in the pathogenesis in this model. Anti-collagen IgG levels were reduced in IL-6 -/- mice, however IgG1, IgG2a and IgG2b isotypes were equally present in IL-6 -/- and IL-6 competent mice compatible with disease inducibility. Histological joint examination revealed an absence of inflammatory cells and tissue damage in IL-6 -/- mice after collagen induction. In another mouse model with a C57BL/6 genetic background, also susceptible to antigen-induced arthritis (AIA) with methylated bovine serum albumin (mBSA), cross-breeding with IL-6 -/- mice resulted in only mild arthritis and preserved articular cartilage, compared to severe arthritis and cartilage destruction in IL-6 producing littermates (Ohshima et al., 1998). Levels of the pro-inflammatory cytokines IL-1β and TNFα were not different between IL-6 -/- and IL-6 competent mice suggesting that IL-6 plays a crucial role in induction of arthritis as well as in cartilage destruction. Antigen-specific lymph node cell proliferative-responses *in vitro* and antibody production *in vivo* were present though reduced in IL-6 -/- mice. Interestingly, IL-6 -/- lymph node cells produced more TH2 cytokines (IL-4 and IL-10) than IL-6 competent lymph node cells, in response to antigen-specific and non-specific stimuli *in vitro*. IL-4 and IL-10 are thought to play a preventative role in arthritis generation (Jorgensen et al., 1998). de Hooge and co-workers (2000), found onset of inflammation in mBSA injected joints of IL-6 -/- C57BL/6-AIA mice at day 1, which then disappeared within 1-week, but which developed into a chronic, severe destructive arthritis in IL-6 competent C57BL/6-AIA animals. Even low levels of antigen-induction in IL-6 competent mice produced chronic arthritis though only low levels of antibody were produced, indicating that lower antibody levels in IL-6 -/- mice were not primarily responsible for a milder inflammatory reaction. In IL-6 -/- animals,

a similar non-sustained inflammatory response was seen in zymosan-induced arthritis (ZIA), a non-immunological, irritant-induced arthritis. Inflammation was equal in the joints of IL-6 -/- and IL-6 competent ZIA mice at day-7, but cleared from IL-6 -/- joints by day-21 while chronic inflammation became established in IL-6 competent joints. TNFα, IL-1β, MCP-1, MIP-2, intercellular adhesion molecule (ICAM)-1, vascular cell adhesion molecule (VCAM)-1, e- and p-selectin expression were not reduced in IL-6 -/- synovium. The type of inflammatory stimulus may be important in determining the cytokine profile induced, as with bronchial or intravenous endotoxin and cerebral pneumococcus TNF and IL-1 were reduced in IL-6 -/- mice (see section 1.2.8). Polymorphonuclear cells and macrophages from the IL-6 -/- ZIA mice did not display any differences in chemotaxis *in vitro* compared to IL-6 competent cells. Even after transfer of antigen-specific lymph node cells from IL-6 competent AIA mice to IL-6 -/- mice, though producing increased acute joint inflammation and cartilage damage at day-2, it did not lead to sustained chronic inflammation at day-7 or -14. Transfer of antigen-specific lymph node cells from IL-6 -/- AIA mice to other IL-6 -/- mice or to IL-6 competent mice, had no influence on joint inflammation. Transfer of bone marrow cells from antigen immunised AIA mice was able to establish an arthritis in recipient irradiated non-immunised wild type mice, when the donor bone marrow cells were from IL-6 competent mice but not from IL-6 -/- mice (Kobayashi et al., 2002). IL-6 appears to have an important role in maintaining inflammatory infiltrate and propagating chronic arthritis. The effects of IL-6 in the acute inflammatory setting may be different to the chronic inflammatory environment. Research from de Hooge and co-workers (2002) implicates a balance between activation levels of STAT1 and STAT3 in influencing the chronicity of arthritis. In the ZIA mouse model, activated STAT3 was found in the synovium during the acute and chronic phase of arthritis in IL-6 competent mice. Activated STAT1 was only detected in the synovium during the chronic inflammatory phase. In IL-6 -/- mice where no chronic arthritis is established, no STAT1 activation was detected and only transient STAT3 activation. STAT1 -/- ZIA mice developed an increased granulomatous joint inflammation, suggesting that STAT1 may have a regulatory role on the inflammatory response in the chronic phase. This model suggests that the balance between STAT3 activation, up regulating inflammation, and STAT1 activation, down regulating inflammation, both STATs induced by IL-6 in the synovium, could influence the switch between acute and chronic inflammation. Interestingly, another inflammatory arthritis mouse model, a

DBA/1 mouse strain expressing the human TNF-α transgene and spontaneously developing arthritis, still developed arthritis when crossed with the IL-6 -/- mouse (Alonzi et. al, 1998). This suggests that the TNF-α over-expression model may represent a different disease process, involving a pathogenic mechanism independent of IL-6.

Transgenic mice with a C-terminal gp130 mutation such that STAT binding and signalling were prevented on activation of the gp-130 receptor, developed severe destructive joint disease (Ernst et al., 2001). Although at first this may seem contradictory to expectation, the mutation resulted in impaired SOCS protein inhibition of gp-130 signalling via the SHP-2/ras/Erk MAPK pathway. This indicates the dual role for SHP2 in inhibition of the STAT pathway but activation of the MAPK pathway. SHP-2 and STAT seem to have mutually inhibitory mechanisms. If both SHP2 and STAT binding to gp130 are inhibited then the net result is reduced signal transduction. However, if only one pathway is blocked as in this model, then the net result is loss of inhibition of the other pathway and hence increased signal transduction. Increased gp130 signal transduction resulted in reduced circulating IgA and IgG levels, synovial hyperplasia, establishment of chronic joint inflammation and cartilage destruction, gastrointestinal ulceration and failure of uterine implantation. An enhanced mitotic response was seen in synovial fibroblasts when IL-6 was applied.

Anti-IL-6R antibodies that block IL-6-gp130 signal transduction have been used in animal trials and early clinical trials in humans as potential treatment for arthritis. In Cynomolgus monkeys with collagen-induced arthritis, such an antibody infused from the day of collagen immunisation resulted in inhibition of the acute phase response and suppression of joint inflammation and destruction (Mihara et al., 2001). In two randomised controlled trials, adults with active rheumatoid arthritis showed significant reduction in joint inflammation and improvement in inflammatory markers after treatment with IL-6 neutralising monoclonal antibody therapy (Choy et al., 2002, Nishimoto et al., 2002, and discussed in section 6.32). Initial studies of this monoclonal antibody therapy in children with systemic arthritis have also shown significant reduction in systemic and joint inflammatory symptoms and normalisation of inflammatory markers (Yokota et al., 2002, discussed in section 6.32).

1.2.10. IL-6 and the systemic arthritis form of juvenile idiopathic arthritis

Systemic arthritis (SA) is the most severe and disabling form of a group of arthritides that affect children, called juvenile idiopathic arthritis (Laxer and Schneider, 1998). The annual incidence of juvenile idiopathic arthritis (JIA) in the UK is approximately 1 in 10,000 with 11% suffering from SA (Symmons et al., 1996), making it one of the most common causes of chronic childhood disability. These diseases are characterised primarily by arthritis of unknown aetiology persisting for a minimum of 6-weeks, once other causes have been excluded. This encompasses a heterogeneous group of arthritides that are sub-classified according to the number of joints involved, the pattern of extra-articular involvement and the associated features (Petty et al., 1998, table 1.1). Many different terms have been used over the years for this group of diseases, however international collaboration has now resulted in a unified classification as JIA (Petty et al., 1998, Hofer et al., 2001), enabling standardisation and comparison of genetic, immunological, epidemiological and therapeutic trial data from around the World. Previous terminology included juvenile rheumatoid arthritis (American College of Rheumatology, ACR, Cassidy et al., 1986, used in Europe only to refer to a specific sub-group of children with rheumatoid factor positive disease), juvenile chronic arthritis (European League Against Rheumatism, Wood, 1978) and Still's disease for what is now called SA. The terminology is not interchangeable however, underlying the need for a unifying classification such as JIA, as the ACR classification juvenile rheumatoid arthritis excludes the sub-type juvenile ankylosing spondylitis (JAS), where as, juvenile chronic arthritis includes JAS, but required 3-months of arthritis before establishing a diagnosis.

Despite immunosuppressive treatments, many children with JIA (particularly the polyarticular and SA forms that tend to be more aggressive) have prolonged active disease throughout childhood and into adulthood. This is associated with joint destruction, poor function, need for surgical joint replacement and fatality secondary to disease and treatment (Wallace and Levinson, 1991, Zak and Pedersen, 2000). Current treatment strategies with corticosteroids and immunosuppressive drugs (such as methotrexate, sulphasalazine, cyclosporin, cyclophosphamide, azathioprine and more recently anti-TNF therapy) are toxic and may be ineffective, particularly in SA. However, a more detailed knowledge of factors affecting disease phenotype and responsiveness may allow more specific and targeted treatments.

Systemic Arthritis	Arthritis – any pattern Daily fever for at least 2 weeks (documented to be quotidian for at least 3 days) PLUS one or more of: • evanescent erythematous rash • generalised lymph node enlargement • hepatomegaly and/or splenomegaly • serositis Exclusion by investigation of infectious or malignant disorders
Oligoarthritis	Arthritis affecting 1 – 4 joints during the first 6 months of disease Can be: Persistent: never more than 4 joints involved throughout disease Extended: cumulative involvement of 5 or more joints after first 6 months HLA-B27 negative if male and ≥ 8 years of age No family history of psoriasis or HLA-B27 associated disease No systemic features
Polyarthritis	Arthritis affecting 5 or more joints during first 6 months Rheumatoid factor negative Tests negative for rheumatoid factor, no systemic features Rheumatoid factor positive Positive rheumatoid factor test on 2 occasions at least 3 months apart
Psoriatic Arthritis	Arthritis and psoriasis OR Arthritis and 2 or more of: • dactylitis • nail pitting/onycholysis • family history of psoriasis Rheumatoid factor negative, no systemic features
Enthesitis Related Arthritis	Arthritis and enthesitis OR Arthritis or enthesitis PLUS 2 or more of: • sacroiliac joint tenderness/inflammatory spine pain • HLA-B27 positive • family history of HLA-B27 assoc. disease • anterior uveitis • male ≥ 8 years No psoriasis, no systemic features
Other Arthritis	Arthritis of unknown cause for 6 weeks or more • not fulfilling criteria for other categories • fulfilling criteria for more than one other category

Table 1.1. Classification of Juvenile Idiopathic Arthritis.

International League of Associations for Rheumatology, Durban 1997 (adapted from Petty et al, 1998).

SA has an equal prevalence between the sexes, with the youngest median age of onset of any form of JIA at 4-years of age (Symmons et al., 1996). It is associated with extra-articular features and characterised by a cyclical spiking fever, a salmon pink rash, lymphadenopathy, hepatosplenomegaly, serositis, myalgia and arthritis, together with an acute phase response, anaemia, hypergammaglobulinaemia, thrombocytosis, linear growth retardation and osteoporosis (Laxer and Schneider, 1998). IL-6 is implicated in the pathogenesis of this disease.

Serum and synovial fluid levels of IL-6 are elevated in patients with SA and are higher than levels in other forms of JIA (oligoarticular or polyarticular) or than in adult arthritides such as rheumatoid arthritis (De Benedetti et al., 1991, 1992, 1997b, Rooney et al., 1995). IL-6 levels correlate with disease activity as determined by the number of joints involved and the acute phase response. The levels of other inflammatory cytokines such as IL-1β, IL-1ra, TNFα, IL-2, IFN-γ and –β did not correlate with disease activity in SA (Lepore et al., 1994, De Benedetti et al., 1995). In SA, the already elevated serum levels of IL-6 have been shown to rise just preceding, and to fall in parallel with, the cyclical fever (Rooney et al., 1995, Prieur et al., 1996). IL-1ra was found to rise after the fever spike, probably driven by IL-6. The rise in IL-6 levels in SA were not preceded by a rise in other pro-inflammatory cytokines, IL-1 and TNF, known to induce IL-6 production and thought to be the mechanism of elevated IL-6 in rheumatoid arthritis (Feldmann et al., 1998). In addition to elevation of IL-6 in SA, levels of sIL-6R and IL-6/sIL-6R complex are elevated in SA and correlate with disease activity (De Benedetti et al., 1994). In two patients with SA in whom IL-6 levels were shown to correspond to the fever curve, sIL-6R levels also tended to follow the fever (Keul et al., 1998). Levels of sgp130 were no different in SA patients than matched controls. The unique IL-6-fever association of SA and the multiple features of SA that can be induced by IL-6, implicates IL-6 in the pathogenesis of SA and hence the IL-6 gene as a candidate for susceptibility and/or severity of disease.

An estimation of the genetic component of susceptibility to a disease can be derived from the ratio of disease prevalence in affected siblings to disease prevalence in the general population, λs. If there were no genetic component, λs would be expected to be 1.0. The higher the value of λs the stronger the genetic component is likely to be.

From the JIA affected sib-pairs registry in the US, compared to the prevalence of JIA in the general US population, the λs for JIA as a whole has been calculated as 15, suggesting a significant genetic component in these diseases (Glass and Giannini, 1999).

1.3. The human IL-6 gene

The human IL-6 gene is approximately 5 kb in length, consisting of 5 exons and 4 introns (Yasukawa et al., 1987, figure 1.8). The gene is located on the short arm of chromosome 7 at 7p21 (Bowcock et al., 1988). Sequence homology in the coding region of the gene is moderately conserved between species (human versus mouse 65%, human versus rat 68%). However, it is highly conserved in the 5' flanking region, particularly within the first 300bp with greater than 80% homology between human and mouse (Tanabe et al., 1988) and highly conserved across other species such as rat and bovine (figure 1.9). Humans and mice are thought to have diverged from a common mammalian ancestor tens of millions of years ago (Gojobori et al., 1984). It has been estimated that random mutational events during this time would have resulted in approximately two out of every three nucleotides having been changed. The fact that the first 300bp of the 5'-flanking region of IL-6 have been so highly conserved over evolution indicates that this region is likely to be important in regulation of the gene.

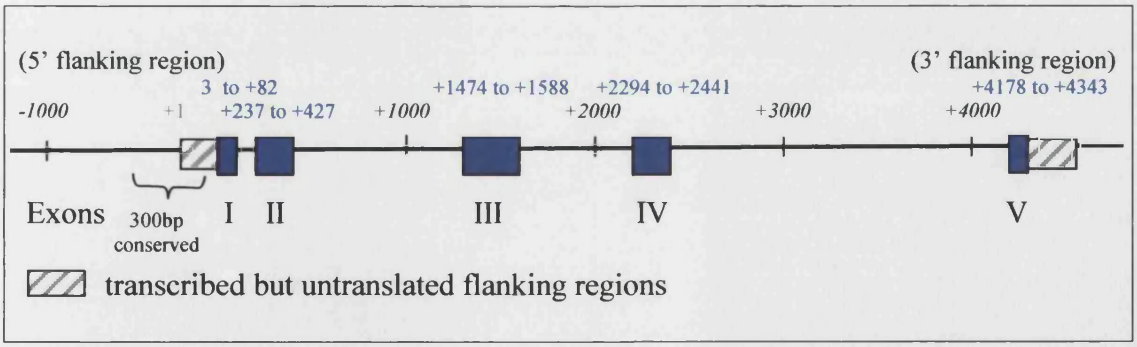

Figure 1.8. The human IL-6 gene.
Schematic representation based on sequencing information from Yasukawa et al., 1987. The positions of exons are marked in relation to the primary start site of transcription.

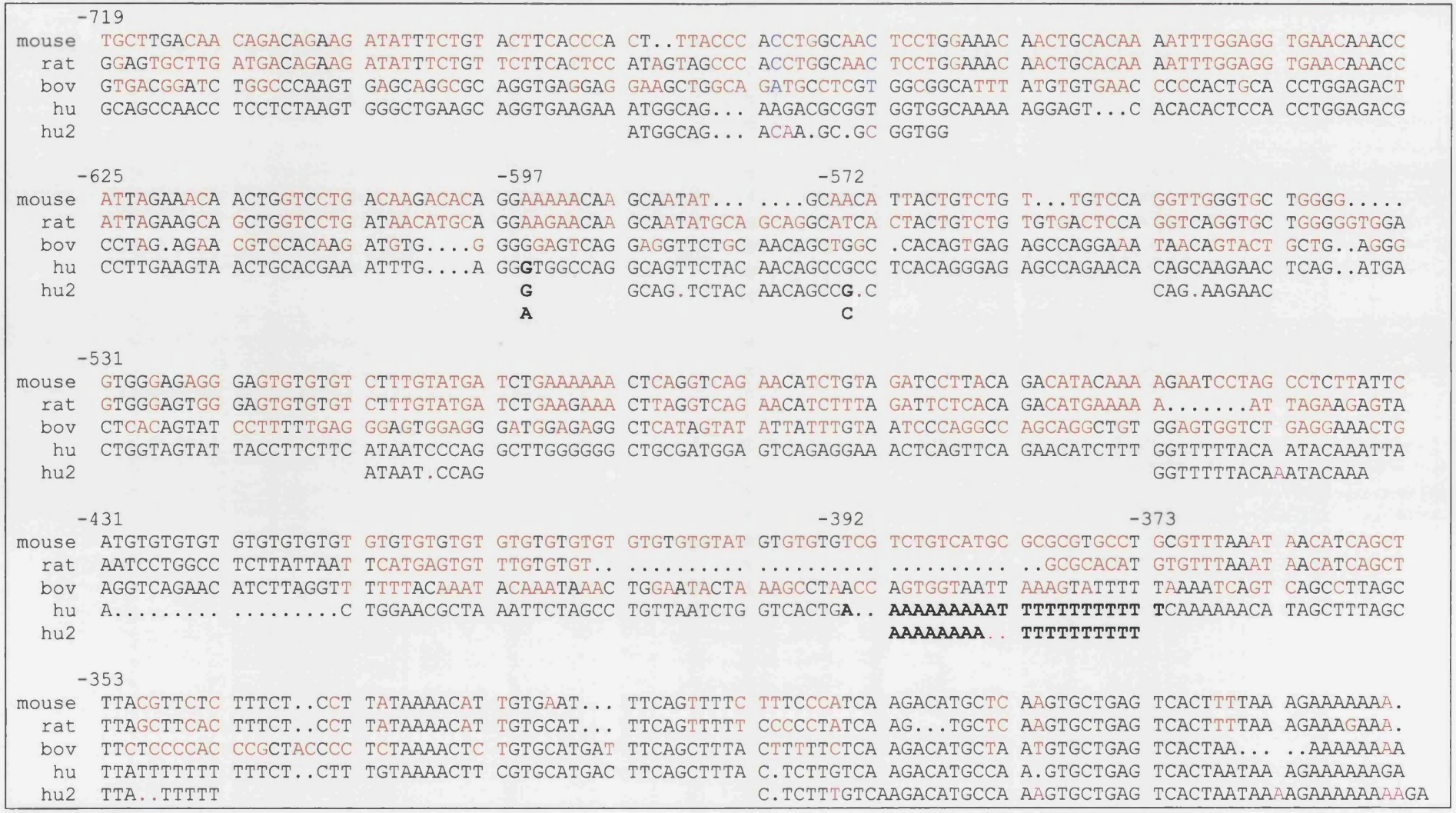
-719
mouse TGCTTGACAA CAGACAGAAG ATATTTCTGT ACTTCACCCA CT..TTACCC ACCTGGCAAC TCCTGGAAAC AACTGCACAA AATTTGGAGG TGAACAAACC
rat GGAGTGCTTG ATGACAGAAG ATATTTCTGT TCTTCACTCC ATAGTAGCCC ACCTGGCAAC TCCTGGAAAC AACTGCACAA AATTTGGAGG TGAACAAACC
bov GTGACGGATC TGGCCCAAGT GAGCAGGCGC AGGTGAGGAG GAAGCTGGCA GATGCCTCGT GGCGGCATTT ATGTGTGAAC CCCCACTGCA CCTGGAGACT
hu GCAGCCAACC TCCTCTAAGT GGGCTGAAGC AGGTGAAGAA ATGGCAG... AAGACGCGGT GGTGGCAAAA AGGAGT...C ACACACTCCA CCTGGAGACG
hu2 ATGGCAG... ACAA.GC.GC GGTGG
-625 -597 -572
mouse ATTAGAAACA ACTGGTCCTG ACAAGACACA GGAAAAACAA GCAATAT... ....GCAACA TTACTGTCTG T...TGTCCA GGTTGGGTGC TGGGG.....
rat ATTAGAAGCA GCTGGTCCTG ATAACATGCA GGAAGAACAA GCAATATGCA GCAGGCATCA CTACTGTCTG TGTGACTCCA GGTCAGGTGC TGGGGGTGGA
bov CCTAG.AGAA CGTCCACAAG ATGTG....G GGGGAGTCAG GAGGTTCTGC AACAGCTGGC .CACAGTGAG AGCCAGGAAA TAACAGTACT GCTG..AGGG
hu CCTTGAAGTA ACTGCACGAA ATTTG....A GGGTGGCCAG GCAGTTCTAC AACAGCCGCC TCACAGGGAG AGCCAGAACA CAGCAAGAAC TCAG..ATGA
hu2 G GCAG.TCTAC AACAGCCG.C CAG.AAGAAC
A C
-531
mouse GTGGGAGAGG GAGTGTGTGT CTTTGTATGA TCTGAAAAAA CTCAGGTCAG AACATCTGTA GATCCTTACA GACATACAAA AGAATCCTAG CCTCTTATTC
rat GTGGGAGTGG GAGTGTGTGT CTTTGTATGA TCTGAAGAAA CTTAGGTCAG AACATCTTTA GATTCTCACA GACATGAAAA A.......AT TAGAAGAGTA
bov CTCACAGTAT CCTTTTTGAG GGAGTGGAGG GATGGAGAGG CTCATAGTAT ATTATTTGTA ATCCCAGGCC AGCAGGCTGT GGAGTGGTCT GAGGAAACTG
hu CTGGTAGTAT TACCTTCTTC ATAATCCCAG GCTTGGGGGG CTGCGATGGA GTCAGAGGAA ACTCAGTTCA GAACATCTTT GGTTTTTACA ATACAAATTA
hu2 ATAAT.CCAG GGTTTTTACAAATACAAA
-431 -392 -373
mouse ATGTGTGTGT GTGTGTGTGT GTGTGTGTGT GTGTGTGTGT GTGTGTGTAT GTGTGTGTCG TCTGTCATGC GCGCGTGCCT GCGTTTAAAT AACATCAGCT
rat AATCCTGGCC TCTTATTAAT TCATGAGTGT TTGTGTGT.. ....GCGCACAT GTGTTTAAAT AACATCAGCT
bov AGGTCAGAAC ATCTTAGGTT TTTTACAAAT ACAAATAAAC TGGAATACTA AAGCCTAACC AGTGGTAATT AAAGTATTTT TAAAATCAGT CAGCCTTAGC
hu A..... .....C TGGAACGCTA AATTCTAGCC TGTTAATCTG GTCACTGA.. AAAAAAAAAT TTTTTTTTTT TCAAAAAACA TAGCTTTAGC
hu2 AAAAAAAA.. TTTTTTTTTT
-353
mouse TTACGTTCTC TTTCT..CCT TATAAAACAT TGTGAAT... TTCAGTTTTC TTTCCCATCA AGACATGCTC AAGTGCTGAG TCACTTTTAA AGAAAAAAA.
rat TTAGCTTCAC TTTCT..CCT TATAAAACAT TGTGCAT... TTCAGTTTTT CCCCCTATCA AG...TGCTC AAGTGCTGAG TCACTTTTAA AGAAAGAAA.
bov TTCTCCCCAC CCGCTACCCC TCTAAAACTC TGTGCATGAT TTCAGCTTTA CTTTTTCTCA AGACATGCTA ATGTGCTGAG TCACTAA... ..AAAAAAAA
hu TTATTTTTTT TTTCT..CTT TGTAAAACTT CGTGCATGAC TTCAGCTTTA C.TCTTGTCA AGACATGCCA A.GTGCTGAG TCACTAATAA AGAAAAAAGA
hu2 TTA..TTTTT C.TCTTTGTCAAGACATGCCA AAGTGCTGAG TCACTAATAAAGAAAAAAAAGA

Figure 1.9.....

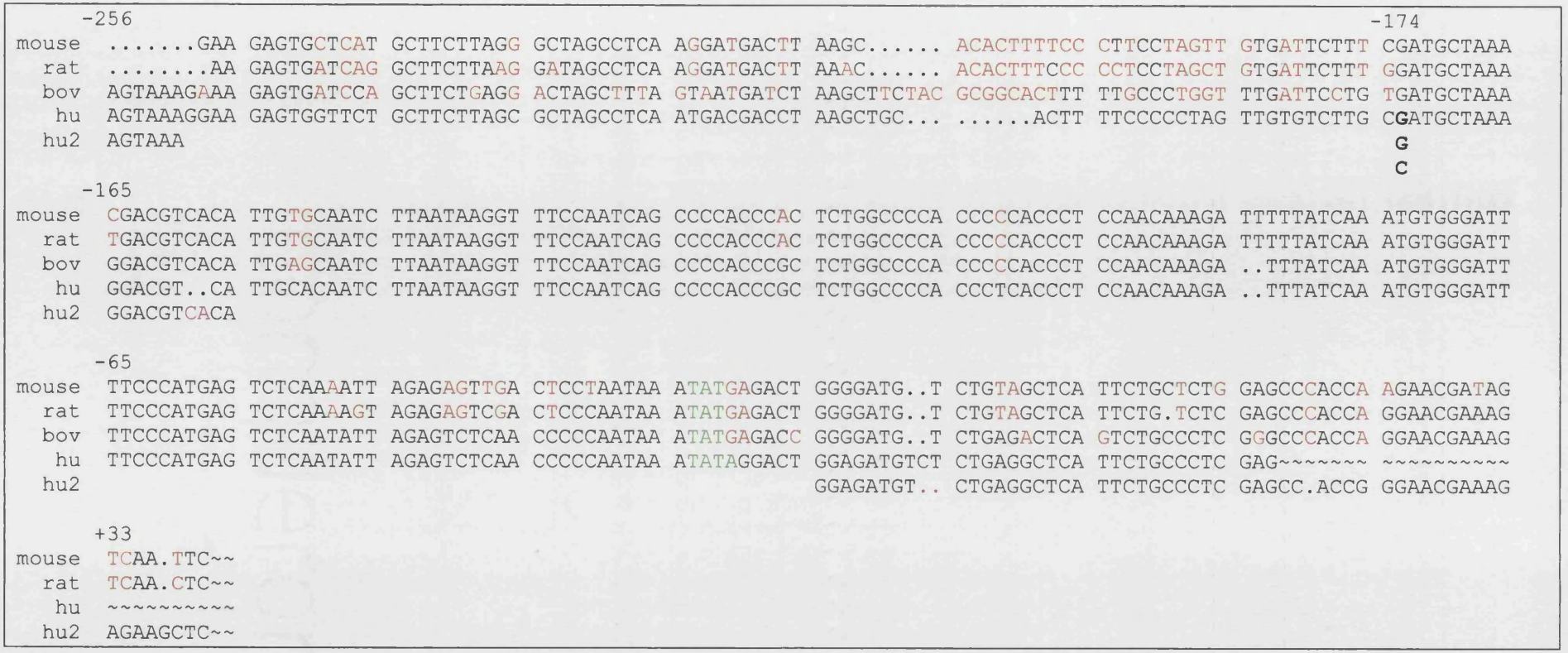

Figure 1.9. DNA sequence of the 5' flanking region of the human IL-6 gene (+40 to –719) **compared to rat, mouse and bovine sequences.**
The sequences show many conserved regions between species, particularly from the transcriptional start site to –344. Only the human sequence has a TATA-site and an AT-tract.
hu =human (Ray et. al, 1988), hu2 =human (Yasukawa et al., 1987), rat (Northemann et al., 1989), mouse (Tanabe et al., 1988), bov =bovine (Droogmans et al., 1992).
Red lettering = differences compared to human sequence; pink lettering = differences between Yasukawa et al. and Ray et al. human sequence; green lettering =TATA site; **bold** lettering = polymorphisms in human sequence.
Numbering is from the transcriptional start site based on the human sequence (Yasukawa et al., 1987 GenBank Accession number Y00081; Ray et al. GenBank Accession number M22111).

1.3.1. Transcriptional control of IL-6

As with other eukaryotic genes, IL-6 expression is mainly controlled at the level of transcription (Latchman, 1998), though post-transcriptional mechanisms play a modifying role. Three potential sites of transcriptional initiation in the human IL-6 gene have been identified by S1 nuclease mapping and primer extension analysis. Each site is associated with TATA-like sequences (Yasukawa et al., 1987, figure 1.10). Different cell types may preferentially use different initiation sites to produce IL-6 mRNA transcripts. Yasukawa et al. (1987) detected three lengths of transcript in a glioblastoma cell line SK-MG-4 stimulated with IL-1β, compatible with transcriptional initiation from each of the three potential sites, C1, C2 and C3. Phytohaemagglutinin (PHA) stimulation produced two transcript lengths in an epithelial cell line (bladder carcinoma T24), in a tonsillar lymphocyte-derived line and in a human T-cell leukaemia virus (HTLV)-1 transformed T-lymphocyte line. These were compatible with transcription initiation at sites C1 and C3. In a fibroblast cell line stimulated with poly(I).poly(C), the main transcript product arose from initiation of transcription at site C1, with a second weaker initiation site compatible with C2 (Zilberstein et al., 1986, Haegeman et al., 1986). The C1 site seems to be the main transcription initiation site in most cell lines expressing IL-6 and producing the 212 amino acid protein product. It has been proposed that the upstream initiation sites C2 and C3 would code for a protein with a hydrophobic N-terminus tail, which could act as a membrane bound form of IL-6 (Hirano et al., 1986), though the existence of such a variant has not been established.

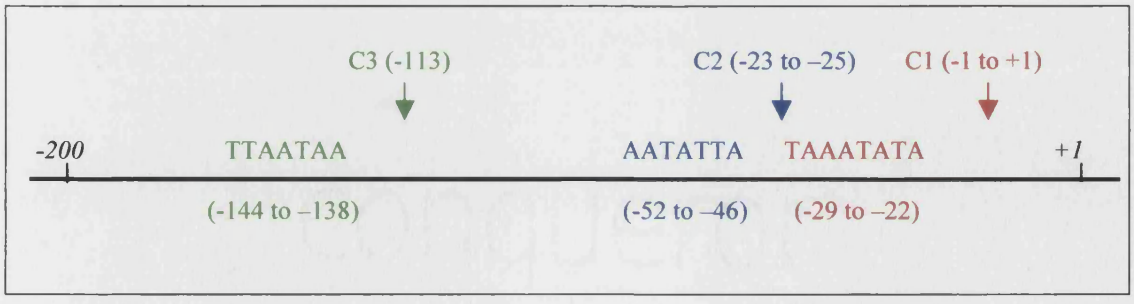

Figure 1.10. The human IL-6 gene promoter, potential transcription initiation sites and TATA boxes.
Based on S1 nuclease mapping with primer extension analysis and sequence information from Yasukawa et al., 1987. Three potential transcription initiation sites were identified C1, C2 and C3. C1 is the main initiation site in most cell lines and base numbering for the gene is determined with respect to C1 initiation site.

1.3.2. Regulation of IL-6 transcription

Specific transcription factors can act as enhancers or repressors of transcription (Ptashne, 1986, 1988). Each transcription factor binds to a sequence specific element, which in eukaryotes can be position-, orientation- or strand-independent to the transcriptional initiation site, and may be located within introns, 3'- or more commonly 5'-flanking regions of the gene, with some acting over several kilobases. More than one member of a transcription factor family may bind to a specific regulatory element, multiple regulatory elements may be present within one gene and each transcription factor may bind more than one regulatory sequence. This allows a large diversity of transcriptional control for eukaryotic genes and enables cell-specific diversity depending on which transcription factors are expressed in a cell-type.

Hybrid-protein genetic engineering techniques allowing expression of individual transcription factors, deletion mutations and domain interchanges, have enabled detailed analysis of the structure, binding and function of transcription factors. In common, they tend to have bi-modular domains, one making specific DNA contact and the other interacting with transcription initiation factors, either directly or indirectly (Pabo and Sauer, 1992). The DNA between regulatory elements and the promoter can loop out (Schleif, 1992) facilitating transcription regulatory and initiation factors to interact. Transcription factors can act as enhancers by increasing the binding affinity or speed of assembly of the transcription initiation complex, facilitating opening of double helical DNA, recruiting other transcription factors that increase the rate of transcription, or preventing repressor factors from acting, either by blocking their binding to DNA or by blocking their protein action domain (Mitchell and Tjian, 1989). Transcription factors can act as repressors by competing with transcription initiation or enhancer factors for DNA binding sites, masking protein activation domains on other transcription factors, binding and mopping up transcription factor availability, or blocking protein-protein interactions required for transcription complex assembly (Jackson, 1991). As complexes, transcription factors can act synergistically to increase binding affinity, where one factor alone may have too weak an affinity to bind. Factors binding the DNA may not contain the effector site themselves, but may enable other co-factors with effector-domains to bind via protein-protein interactions (Lemon and Tjian, 2000). The same transcription factor or co-factor may have different effects in different complexes, depending on which portions are bound and

exposed. It is clear that these multiple steps in gene regulation facilitate an enormous diversity of transcriptional control.

Transcription regulatory sites in the IL-6 gene have been demonstrated in the 5'-flanking region. There is no evidence that sites elsewhere in the IL-6 gene play an active role in controlling the rate of gene expression. Figure 1.11 shows schematically the location of many of these transcription regulatory sites, discussed below.

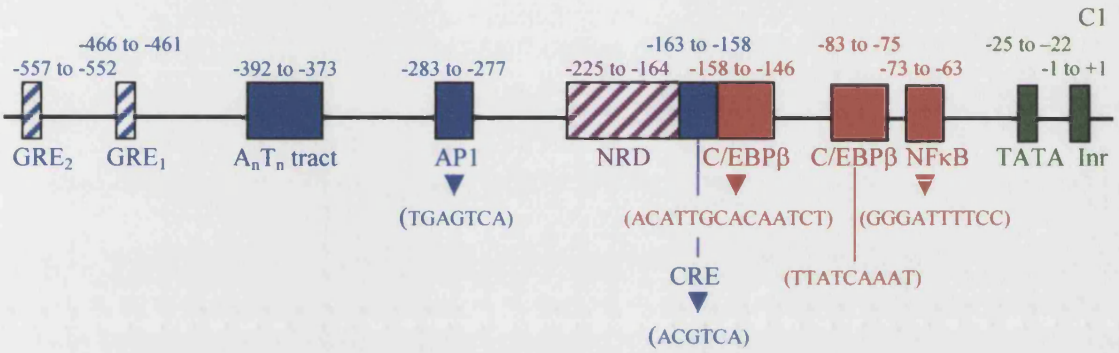

Figure 1.11. Transcriptional regulatory sites in the human IL-6 gene.
Schematic representation of transcription factor sites in the 5'-flanking region of IL-6 (see discussion below for references to each site). Base numbering is in relation to the transcription initiation site C1. Confirmed transcription factor sites are shown as solid boxes with the DNA sequence indicated below, putative transcription regulatory sites are shown as hatched boxes.

1.3.2.1. NF-κB

Deletion mutants of the 5'-flanking region of hIL-6 revealed an essential IL-1 response element, and strong TNFα and LPS response element, in the region –63 to –73 that bound the nuclear factor binding protein NF-κB, (Libermann and Baltimore, 1990, Shimizu et al., 1990, Zhang et al., 1990). Site-directed mutagenesis of this NF-κB site confirmed the importance of NF-κB in activation of IL-6 transcription by LPS (Matsusaka et al., 1993, Dendorfer et al., 1994). Electrophoretic mobility shift assay (EMSA) showed that NF-κB p50 and p65 homodimers (see below), and p50/p65 heterodimers, bind avidly to this site (Matsusaka et al., 1993).

NF-κB is a eukaryotic transcription factor, first discovered in B-cells as a nuclear factor that bound as an enhancer of the immunoglobulin κ light-chain gene (Sen and

Baltimore, 1986). It is strongly evolutionarily conserved in terms of sequence homology and signal transduction pathways from *Drosophila* to human (Gonzalez-Crespo and Levine, 1994, Medzhitov et al., 1997). Numerous mammalian genes are regulated by NF-κB including many cytokines, acute phase response proteins and cell adhesion molecules, and hence it plays a key role in co-ordinating and enhancing the adaptive immune response to situations of infection, stress or injury. NF-κB exists as a dimer of specific proteins, members of the Rel homology domain (RHD) family, containing a 300 amino acid N-terminal conserved domain (figure 1.12). The RHD determines the DNA-binding, dimerization and protein interaction characteristics of the molecule. In humans, NF-κB forms as homodimers or heterodimers of p50, p52, p65 or c-rel, each with unique DNA binding capacity and transactivation potential (Kunsch et al., 1992). The majority of dimeric combinations, such as p50/p65, p50/c-rel, p65/p65 or p65/c-rel, activate gene transcription. However, the homodimers p50 and p52 appear to repress transcription, probably due to their lack of a variable C-terminal activation domain and by competing with transactivation complexes for binding sites (Plaskin et al., 1993, Brown et al., 1994). X-ray crystallography of p50 homodimers and p50/p65 heterodimers bound to a κB site, showed each molecule to comprise two domains linked by a flexible region (Ghosh et al., 1995, Chen et al., 1998b). Dimerization occurred exclusively via the interaction of hydrophobic amino-acid side chains in the C-terminal domain of RHD. Differential contributions of key residues may dictate selectivity of dimer formation between NF-κB members (Sengchanthalangsy et al., 1999). Both N- and C-terminal regions of RHD are involved in binding to DNA, with multiple contacts between loop regions (joining β-sheet domains of the protein) and the nucleotide bases and sugar phosphate backbone of specific DNA sequences. Mutational analyses have revealed the importance of DNA sequence specificity at the binding site and the bases involved in the interactions (Toledano et al., 1993, Liu et al., 1994). For example, the p65 homodimer, though sharing the same basic structure as p50, binds asymmetrically to DNA target sites with one subunit binding to a specific four-base half-site, but the second sub-unit requiring only partial specificity in the other half-site (Chen et al., 1998c). This contributes to the diversity of DNA sequences recognised by NF-κB. In addition, NF-κB-induced transcription may be influenced by the context of the binding site(s) within a promoter, producing different degrees of DNA bend within different promoter sequences

(Berkowitz et al., 2002). This may influence the transactivation function of NF-κB or other promoter bound factors.

Messenger RNA for p50 & p52 encodes for larger precursor proteins, p105 & p100 that are then cleaved post translation, to produce the p50 & p52 molecules, respectively (figure 1.12), (Ghosh et al., 1990, Schmid et al., 1991). Within the C-terminal region of the larger proteins, an ankyrin-repeat motif masks the nuclear localisation signals of p50 & p52, and enables the unprocessed proteins to function as IκB-like (see below) domains (Henkel et al., 1992, Blank et al., 1991, Rice et al., 1992). Degradation of this C-terminal region to release p50 or p52 appears to be regulated by a signal-dependent mechanism in cells stimulated with NF-κB activating agents, and by a signal-independent mechanism in unstimulated cells. Cellular stimulation results in an increased rate of degradation of the C-terminus (Mellits et al., 1993). A glycine-rich region in the N-terminus portion of p105 & p100 is necessary and sufficient for cleavage of the C-terminal region (Lin and Ghosh, 1996, Betts and Nabel, 1996). In the signal-dependent mechanism, this requires phosphorylation of the C-terminus resulting from cell stimulation.

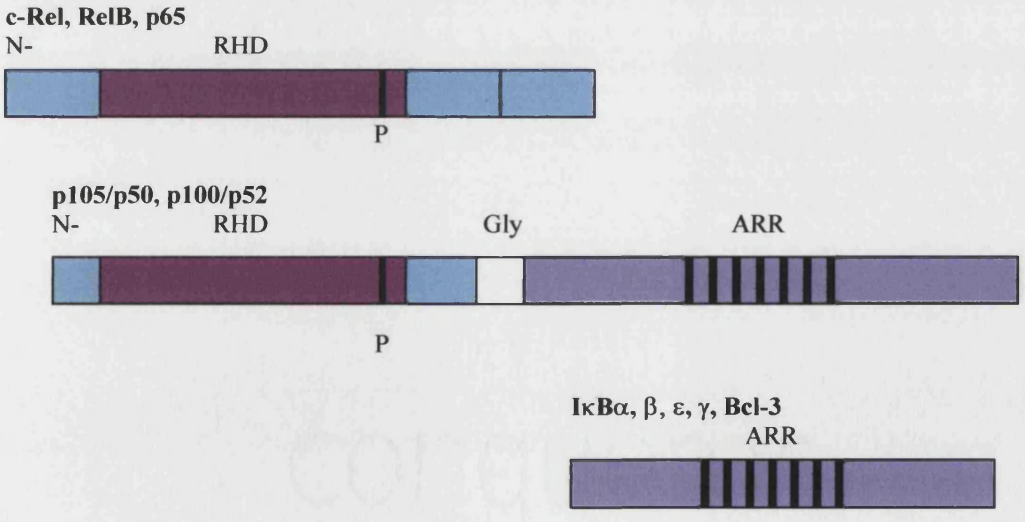

Figure 1.12. The structural organisation of NF-κB and IκB molecules.
N=N-terminus, RHD=Rel homology domain, P=phosphorylation site, Gly=glycine-rich motif, ARR=ankyrin repeat regions.

NF-κB is pre-formed in the cytoplasm of most cells and maintained in an inactive form bound to its cytoplasmic inhibitor, IκB. IκB acts as the main regulator of NF-κB activation by masking the NF-κB nuclear localisation signals and retaining it in the cytoplasm (Verma et al., 1995). At least five IκB family members have been identified to date (IκBα, IκBβ, IκBε, IκBγ, Bcl-3), each containing multiple ankyrin-repeat regions that specifically interact with the RHD of NF-κB (figure 1.12). The number of ankyrin-repeats influences the specificity for RHD. This inhibitory mechanism is further tuned by members of the IκB family having different kinetics of degradation and re-synthesis in response to simulators of NF-κB. Both IκBα and IκBβ regulate p50/p65 and p50/c-rel heterodimers (Thompson et al., 1995). IκBα and IκBβ both rapidly degrade after stimulation of NF-κB inducing pathways, however only IκBα is rapidly re-transcribed, maintaining only a transient effect of inducing agents. Levels of IκBβ remain low until the NF-κB activating signal is attenuated. This is explained by the fact that the IκBα gene, but not the IκBβ gene, contain an NF-κB enhancer site (Brown et al., 1993, Chiao et al., 1994). IκBε exclusively binds p65/p65 and p65/c-rel (Whiteside et al., 1997). It is slowly degraded on activation of the NF-κB pathway. IκBγ (only detected in lymphoid cells) is generated from the same gene as p105 (Heron et al., 1995). It seems only to bind and inhibit p50 and p52 homodimers (Bell et al., 1996). Bcl-3 is unique in that it localises to the nucleus rather than the cytoplasm and can act as a transactivator by specifically binding and removing the inhibitory p50 & p52 homodimers (Nolan et al., 1993).

Multiple activators of NF-κB stimulate cells to signal tissue injury, inflammation and infection. These activators include cytokines IL-1 & TNFα, products from infection such as lipopolysaccharide (bacterial), double-stranded RNA & tax nuclear proteins (viral), CD30 & CD40 ligands, lymphotoxin-α & β, and stress mediators such as reactive oxygen intermediates & UV light (May and Ghosh, 1998, McDonald et al., 1995b, Nakano et al., 1996). In the context of IL-6 gene induction, the IL-1β and TNFα mediated signalling pathways resulting in activation of NF-κB, and hence induction of IL-6 transcription, are shown in figure 1.13.

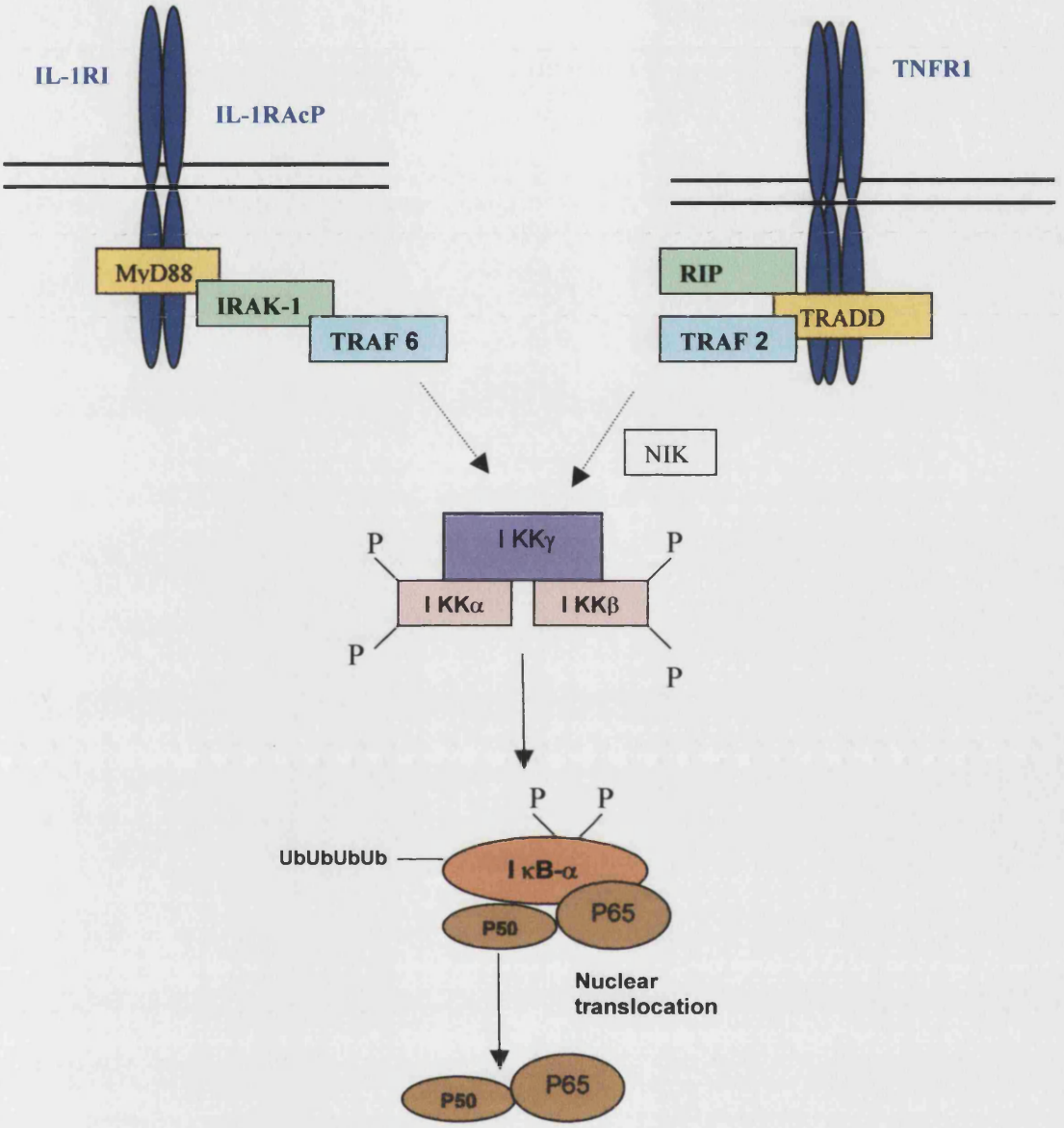

Figure 1.13. Signal transduction pathways for IL-1β and TNFα mediated activation of NF-κB via their specific receptors.

IL-1β binding to the IL-1R1 and IL-1R accessory protein receptor complex induces association of MyD88 (a cytosolic adapter molecule) with the intracellular domain of IL1R complex (Wesche et al., 1997). This triggers the recruitment and phosphorylation of Interleukin-1 Receptor Associated Kinase-1 (IRAK-1). Activated IRAK-1 can then associate with TNF-receptor associated factor 6 (TRAF6). TNFα binding to the TNFR1 (p55) receptor complex allows TNF-receptor-associated death domain protein (TRADD) to bind and recruit receptor interacting protein (RIP) and TRAF2 (Hsu et al., 1996). RIP and TRAF2 activate NF-κB inducing kinase (NIK), (Malinin et al., 1997). Both activated NIK and TRAF6 activate the IKK complex (the common component of both pathways), though mechanisms are not fully understood, and result in phosphorylation of IKKα and IKKβ. This in turn leads to phosphorylation of IκBα, leading to ubiquitination and degradation of the protein to release the dimeric NF-κB molecule that can then translocate to the nucleus and activate target genes.

Via their own specific cell surface receptor, IL-1β and TNFα activate members of the TRAF family of proteins that in turn activate an IκB kinase (IKK) complex of at least three proteins (IKKα, IKKβ, IKKγ). The activated IKK's specifically phosphorylate two critical serine residues on IκBα (Ser-32 and Ser-36) and IκBβ (Ser-19 and Ser-23), (DiDonato et al., 1996). This specific phosphorylation leads to ubiquitin-proteasome degradation of IκB, with release and nuclear translocation of NF-κB (Brown et al., 1995).

1.3.2.2 C/EBP

In addition to the NF-κB activation site in the hIL-6 gene, another IL-1 response element was identified as a 14bp site around position –150 that bound a nuclear factor designated nuclear factor IL-6, NF-IL6 (Isshiki et al., 1990). This NF-IL6 site was also shown by site-directed mutagenesis to be necessary for LPS-induced IL-6 expression (Zhang et al., 1994). Zhang and co-workers (1994) identified a second NF-IL6 site from position –75 to –83 that conferred LPS and lipoarabinomannan (a constituent of *Mycobacterium* cell walls) inducibility to IL-6 in a human monocyte cell line. It was subsequently shown by site-directed mutagenesis that this downstream NF-IL6 site was essential in combination with the NF-κB site for IL-6 induction by IL-1β in an osteoblast cell line (Stein and Yang, 1995). The up-stream NF-IL6 site (-146 to –158) however, did not seem important for IL-1β-induced expression of IL-6 in these osteoblasts, as deletion of this region in transfected constructs did not significantly affect levels of induction. NF-IL6 is a member of the CCAAT/enhancer binding protein (C/EBP) family and has been re-designated C/EBPβ (Akira et al., 1990, Poli et al., 1990). Matsusaka and co-workers (1993) showed that C/EBPβ and NF-κB act synergistically in the activation of IL-6 gene transcription. More recently, a third C/EBP site has been identified within the region –45 to –74 of the IL-6 gene (Vales and Friedl, 2002, and see section 1.3.2.9). This site was shown to be functionally significant in co-activation of IL-6 expression in HepG2 and COS cells.

C/EBP is a family of eukaryotic transcription factors comprising six known members, C/EBPα, β, δ, ε, γ and ζ, encoded by different genes with a tissue-specific pattern of expression (Lekstrom-Himes and Xanthopoulos, 1998). They are highly conserved in evolution and are important in normal tissue development, cellular function, cellular

proliferation and differentiation, as determined from studies with C/EBP knockout mice. Each member has a different pattern of cell-specific expression. They contain three functional domains, an activation, a dimerization and a DNA-binding domain. The C-terminal dimerization domain is highly conserved between members and has a basic-leucine zipper (bZIP) structure (figure 1.14), allowing homo- and hetero-dimers to form. Electrostatic interactions between amino-acids along the dimerization interface determine the specificity of dimer formation with other C/EBP family members and with other transcription factors such as NF-κB and Fos/Jun family members (Vinson et al., 1993). Dimerization is necessary for DNA binding (Landschultz et al., 1989). The DNA binding specificity of C/EBP is determined by a 20 amino-acid region in the C-terminal domain of the molecule that contains three key residues for protein-DNA interaction (Johnson, 1993). The bZIP domain assumes an α-helical configuration and from DNA modelling based on x-ray crystallographic studies, is thought to form an inverted Y-shaped structure with the bZIP region of the other dimerized C/EBP molecule to enable binding to a palindromic DNA recognition site (Ramji and Foka, 2002). The optimal C/EBP binding site has a symmetrical repeat sequence, however, most sites contain a conserved half-site paired with a more divergent sequence, indicating that considerable variation in binding sequence is tolerated (Osada et al., 1997a).

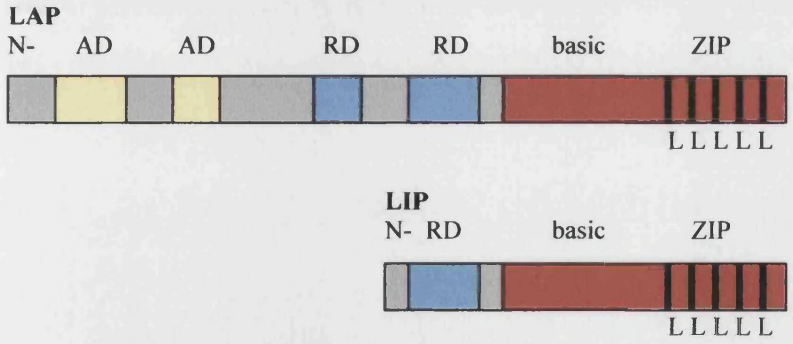

Figure 1.14. The structural organisation of C/EBPβ (LAP & LIF isoforms), adapted from Ramji and Foka, 2002.
LAP=liver-enriched transcriptional activating protein (full-length C/EBPβ), a 35kDa polypeptide, LIP=liver transcription inhibitory protein (truncated isoform of C/EBPβ), a 20kDa polypeptide (see text below).
N=N-terminus, AD=activation domain, RD=negative regulatory domain (influencing DNA binding), basic=region containing basic amino acid residues, ZIP=leucine zipper region (together with the basic region this forms the bZIP region that facilitates dimerization and DNA-binding), L=leucine residue.

The activation domains at the N-terminal end of the protein are least conserved between family members, most interact with the basal transcription machinery to enhance transcription, however, in several C/EBP molecules the N-terminal region also contains negative regulatory regions that can act as dominant-negative repressors (Williams et al., 1995). C/EBPγ lacks an activation domain and acts only as a repressor of gene transcription (Cooper et al., 1995).

C/EBPβ, though initially identified and cloned as a transcriptional activator of IL-6, also binds many other genes involved in inflammation, haemopoiesis and acute phase response such as TNFα, IL-8, G-CSF and class I APR genes (Akira et al., 1990, Poli et al., 1990, Betts et al., 1993). It is constitutively expressed in liver, intestine, lung, adipose cells and myeloid cells, though it can also be strongly induced by cell stimulation with LPS, IL-6, IL-1, dexamethasone and glucagon. Cytokine stimulation promotes nuclear localisation of C/EBPβ and enhances its binding to DNA (Yin et al., 1996). This may involve post-translational modification of C/EBPβ, via protein kinase specific phosphorylation, which has been shown to increase the transcriptional enhancing activity of C/EBPβ (Nakajima et al., 1993). In the serum amyloid A gene, increased transactivation by C/EBPβ or δ was seen in the presence of inhibition of cellular phosphatases and associated with increased DNA binding activity (Ray and Ray, 1994). Auto-regulation of the C/EBPβ gene also occurs in response to inflammatory stimuli (cytokines, turpentine oil, LPS) via C/EBPβ binding sites contained within the C/EBPβ promoter (Akira and Kishimoto, 1997, Niehof et al., 2001a). The C/EBPβ promoter contains two cAMP-response element (CRE)-like sites (see section 1.3.2.3) that can bind the transcription factor CRE-binding protein (CREB) to up-regulate C/EBPβ transcription (Niehof et al., 1997). The CRE-like sites are required for IL-6-mediated induction of C/EBPβ (Niehof et al., 2001b), producing an auto-regulatory feed-back-loop as C/EBPβ induces IL-6, which in turn can induce C/EBPβ. In addition, inflammatory stimuli in hepatocytes and macrophages, have been shown to alter the balance of C/EBP members by reducing the levels of C/EBPα transcription while inducing C/EBPβ and δ transcription to varying degrees (Alam et al., 1992, Tengku-Muhammad et al., 2000). In this way, the kinetics and magnitude of response for different C/EBP members can be influenced to favour enhanced

transcription of genes containing binding sites for the up-regulated factors (such as IL-6 in the case of C/EBPβ).

A further complexity in the tissue-specific regulation of C/EBPβ is added by translational control of the formation of isoforms. Two isoforms of the protein can occur, generated through initiation of translation from two separate AUG sequences within the same reading frame of a single mRNA transcript (Descombes and Schibler, 1991). The larger generated polypeptide is 35kDa (liver-enriched transcriptional activating protein LAP, figure 1.14) and contains the conserved C/EBP activation domain, two negative regulatory domains (RD) that influence DNA binding (Williams et al., 1995) and the bZIP domain. The truncated form is 20kDa (liver transcription inhibitory protein LIP, figure 1.14) and contains only one RD and the bZIP dimerization domain, but no activation domain. Heterodimers of LAP and LIP can form, with LIP acting as a dominant negative repressor, inhibiting the transactivational function of C/EBPβ (Descombes and Schibler, 1991).

The C/EBP family members can form dimers via protein-protein interactions with other bZIP and non-bZIP containing transcription factors. C/EBPβ has been shown to interact with the p50 & p65 subunits of NF-κB, CREB/activating transcription factor (ATF), Fos & Jun, glucocorticoid receptor and retinoblastoma protein (Hsu et al., 1994, Xia et al., 1997, Ramji and Foka, 2002). These heterodimers may have different transactivation potential and binding specificity compared to homodimers for each factor. For example, Fos and Jun hetero-dimerization to C/EBPβ, reduced the C/EBPβ binding affinity for the C/EBPβ consensus sequence, and repressed transcription of a reporter gene containing C/EBPβ sites in the promoter (Hsu et al., 1994). In contrast, NF-κB interaction with C/EBPβ is co-operative and results in enhancement of transcriptional activation (Matsusaka et al., 1993, Xia et al., 1997). This interaction and co-operation requires both the Rel homology domain (RHD) of NF-κB (figure 1.12) and the leucine-zipper domain of C/EBPβ (figure 1.14). Each factor binding to DNA can increase the DNA binding affinity of the other (Ruocco et al., 1996). Up-regulation of C/EBPβ after an inflammatory stimulus is slow compared to the early availability of pre-transcribed NF-κB (Poli, 1998). In genes such as IL-6 that have dual responsiveness to NF-κB and C/EBPβ, C/EBPβ may provide a slower, more sustained

induction of transcription, while NF-κB provides a faster, more immediate response, enhanced by the availability of small amounts of constitutive C/EBPβ, probably activated by phosphorylation as discussed above. The influence of synergy between C/EBPβ and NF-κB in possible prolongation of transcriptional transactivation is not known.

Though C/EBPβ can clearly up-regulate IL-6 transcription, it may not be essential for IL-6 induction in some cell types. Peritoneal macrophages from C/EBPβ deficient mice still resulted in induction of IL-6 following bacterial infection and in fact, basal levels of IL-6 mRNA were elevated (Tanaka et al., 1995). Screpanti and co-workers (1996) found elevated serum IL-6 levels with associated pathological features similar to Castleman's disease (see section 1.2.1) in C/EBPβ -/- mice. Targeted elimination of C/EBPβ mRNA to prevent C/EBPβ expression in human fibroblasts did not inhibit IL-6 expression though the expression of other pro-inflammatory cytokines with C/EBPβ sensitive promoters (TNFα, G-CSF) was inhibited (Tanaka et al., 1995). This suggests that redundancy may occur between transcription factors and transduction pathways in the transcription of IL-6. Indeed, LPS-induced IL-6 expression was restored in a murine lymphocytic cell line deficient for C/EBPα, β and δ (shown to poorly express IL-6 in response to LPS), by transfection with any one of the three C/EBP members (Hu et al., 1998). This contrasts however, with the findings of Gorgoni and co-workers (2002) who found LPS- and IFNγ/LPS-induced IL-6 levels to be impaired in splenic macrophages from C/EBPβ deficient mice compared to wild-type mice. In some cell types, C/EBPα or δ may be able to substitute for C/EBPβ in transactivation of IL-6 transcription induced by certain stimuli. C/EBPδ may be a more likely candidate as it is up regulated by LPS and other inflammatory stimuli, where C/EBPα is down regulated. C/EBPδ and α have been shown *in vitro* to induce reporter gene expression through a region of the human IL-6 promoter and bind to the same DNA-sequences as C/EBPβ (Kinoshita et al., 1992, Vales and Friedl, 2002). In fact, C/EBPδ and α were associated with stronger induction than C/EBPβ, displaying synergy with NF-κB p65, and C/EBPδ forming heterodimers with C/EBPβ. The significance of these regulatory mechanisms *in vivo* remains to be established.

1.3.2.3 cAMP response element and negative regulatory domain

Ray et al. (1989) reported 70% sequence homology between the IL-6 5'-flanking region –124 to –170 and the serum response element (SRE) of the c-Fos gene promoter. On electrophoretic mobility shift assay, HeLa nuclear factors bound to the –151 to –173 region of IL-6 could be competed out by the SRE sequence of c-Fos, suggesting that similar factors could bind each regulatory region. The –151 to –173 sequence of IL-6 was found to confer responsiveness to serum, tetradecanoyl phorbo-13-acetate (TPA), IL-1 and TNFα when inserted up stream of a herpes simplex virus-thymidine kinase (HSV-TK) promoter driving CAT reporter gene expression. Within this sequence, the motif CGTCA at –158 to –163 (a cAMP response element, CRE, consensus sequence) was found to be essential for TPA inducible transcription, but not for serum, IL-1 or TNFα induction. Site-directed mutagenesis confirmed that the CGTCA motif was functional in conferring cAMP responsiveness (Ray et al., 1989), although IL-6 inducibility by cAMP and prostaglandin E1 was not completely abolished by mutation of this site (Dendorfer et al., 1994). Mutation of three additional sites of the IL-6 5'-flanking region, the AP1, C/EBPβ and NF-κB sites, also contributed to reduction of IL-6 responsiveness to cAMP. This suggests that cAMP can act through multiple, partially redundant regulatory elements, including the CRE.

Intracellular levels of cyclic 3',5'-monophosphate (cAMP) rise in response to activation of the membrane-associated enzyme adenylyl cyclase by engagement of cell specific receptors by stimulating factors such as adrenaline, glucagons, vasopressin or thyroid stimulating hormone (Montminy, 1997). A family of CRE binding factors has been identified, known as the CRE binding protein/activating transcription factor (CREB/ATF) family, and share a common basic DNA-binding domain and leucine zipper structure (figure 1.15). CREB, a 43kDa protein, binds to the CRE as a dimer. In unstimulated cells, this is in an inactive form producing no activation of transcription. As cellular levels of cAMP are stimulated to rise, this results in activation of the enzyme protein kinase A, which produces phosphorylation of the serine residue at position 133 (ser-133) of CREB (McKnight et al., 1988). Phosphorylation of ser-133 produces a conformational change in CREB that permits activation of transcription.

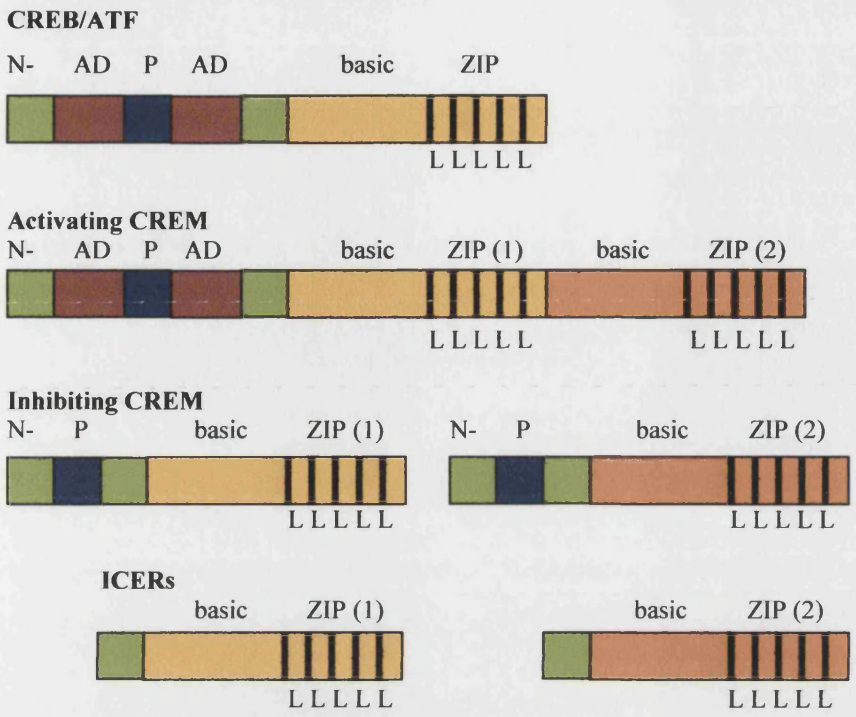

Figure 1.15. The structural organisation of CREB, CREM and ICERs.
The inhibiting forms of CREM are alternative splice products of a single RNA transcript of CREM. They compete with CREB and activating CREM for CRE binding, but lack the activation domain. ICERs are formed from a distinct promoter within the CREM gene that is activated in response to cAMP to produce transcripts encoding these short proteins. They also exert an inhibitory effect by competing with CREB and activating CREM (Sassone-Corsi, 1998).
CREB=CRE-binding protein, ATF=activating transcription factor, CREM=CRE modulator, ICERs=inducible cAMP early repressors. N=N-terminus, AD=activation domain, P=phosphorylated region, in response to cAMP, basic=basic domain, ZIP=leucine-zipper domain.

Screening of cDNA expression libraries, revealed a 265kDa protein CREB-binding protein (CBP) that binds to phosphorylated CREB, but not to unphosphorylated CREB (Chrivia et al., 1993). Screening of cDNA expression libraries, revealed a 265kDa protein CREB-binding protein (CBP) that binds to phosphorylated CREB, but not to unphosphorylated CREB (Chrivia et al., 1993). The activation domain of CREB undergoes a structural change from a coiled to a two α-helices structure when it interacts with CBP (Radhakrishnan et al., 1997). CBP acts as a co-activator and appears to be essential for gene activation by cAMP as antibodies to CBP injected into cells before stimulation prevented activation of transcription by cAMP. CBP may mediate activation of transcription by bridging between CREB and the basal transcriptional complex. It has been identified as part of the RNA polymerase II/ basal transcription factor holoenzyme complex and has been shown to produce protein-to-protein interactions with components such as transcription factor IIB, TFIIB (Nakajima

et al., 1997). Another possible mechanism is via alteration of the DNA chromatin structure. CBP has been shown to have histone-acetyltransferase activity (Ogryzko et al., 1996), and this may produce a more open chromatin structure facilitating transcription (Wade et al., 1997). CBP is not exclusive to CREB but can also act as a co-activator to other transcription factors such as AP1, nuclear receptors and NF-κB (Shikama et al., 1997). A limited amount of CBP within a cell will result in competition and mutual antagonism between transcription factors for this co-activator.

The CRE modulator (CREM) is another member of the CREB/ATF family that can bind to the CRE and activate transcription in response to cAMP via a similar mechanism to CREB requiring the co-activator CBP (Sassone-Corsi, 1998). Alternative splicing products of CREM, that lack the activation domain (figure 1.15) but can still form dimers and bind to DNA, inhibit transcriptional activation by competing with CREB or CREM for the CRE site. This is a cell specific regulatory mechanism with different proportions of activating and inhibitory CREM influencing the level of transcriptional activation following cAMP stimulation. In addition, there are two distinct exons in the CREM gene coding for distinct DNA-binding domains (bZIP (1) & (2), figure 1.15) and hence alternative splicing can result in a molecule with a different DNA-binding specificity in different cells. The rate of production of these CREM splice-variants is not affected by levels of cAMP. However, the CREM gene promoter contains a CRE that induces the production of short protein transcripts. These short proteins (inducible cAMP early repressors, ICERs), like the splice-variants of CREM, lack the activation domain (figure 1.15). ICERs act as repressors of cAMP activation by inhibiting CREB and the activating form of CREM from binding to the CRE. This limits the cAMP response via CRE to a transient effect on gene expression. This contrasts with the constitutive expression of CREB and the activating form of CREM, expression of which is not induced by cAMP, but which are activated by cAMP solely at the post-translational level by phosphorylation through protein kinase A followed by recruitment of CBP.

During investigation of the cAMP response element of IL-6, Ray and co-workers (1989) found that the region –111 to –164 of IL-6, inserted up stream of the HSV-TK-CAT reporter construct, was associated with higher levels of expression than similar constructs with the region –111 to –225. This suggested that the region –165 to –225

contained a negative regulatory domain (NRD). The only known transcription factor site with inhibitory action localised within the NRD is a glucocorticoid receptor site at –201 to –210 (see section 1.3.2.5).

1.3.2.4 AP1

An AP1 consensus sequence between –277 and –283 of the IL-6 gene was initially thought unimportant in the regulation of gene expression. Deletion constructs of this region had not altered levels of IL-6 transcription when induced by IL-1, TNFα, virus components or LPS (Ray et al., 1988, Shimizu et al., 1990). However, site-directed mutagenesis of the AP1 site by Dendorfer and co-workers (1994) showed that this site was important in mediating cAMP responsiveness.

Several cellular proteins have been identified as capable of binding AP1 sites including Jun, Jun B, Fos and Fos-related antigens (Fras), (Karin et al., 1997). Jun homodimers can bind an AP1 site, though Fos-Jun heterodimers have an approximately 30-fold higher binding affinity for the site. Fos cannot bind AP1 without the presence of Jun (Rauscher et al., 1988). Fos and Jun were originally identified as oncogenes from retroviruses, however, cellular counterparts have since been identified and function as transcription factors that can be induced by serum, phorbol esters such as TPA, or by treatment with growth factors (Lamph et al., 1988). Fos and Jun induction is usually only transient, and plays a critical role in genes involved in cell growth. Uncontrolled growth with persistently elevated levels of Fos and Jun is seen as part of malignant transformation (Land et al., 1983). The Fos/Jun complex requires the co-activator CBP to activate transcription. This can result in competition for limited quantities of CBP between the Fos-Jun-AP1 system and other CBP dependent systems such as the nuclear receptors (Kamei et al., 1996) or CREB (see 1.3.2.3), with mutual repression of the systems dependent on the relative concentration of factors. This illustrates cross talk between different induced pathways, via shared co-activators (Janknecht and Hunter, 1996).

1.3.2.5 Glucocorticoid response element

Glucocorticosteroids (GCs) are strong repressors of the transcription of IL-6 (Ray et al., 1990). They complex in the cytoplasm with the specific glucocorticoid receptor (GR), this activates the receptor and leads to translocation of the complex to the

nucleus, where the GR can bind DNA as a homodimer, or heterodimer with other members of the nuclear receptor family such as mineralocorticoid, progesterone or androgen receptors (Wang et al., 1995). *In vitro* foot-printing studies of short constructs of the 5'-flanking region of IL-6 revealed that GR could bind at several sites on the IL-6 gene, at the TATA box and transcription initiation site (Inr), at the region between –145 and –173 (overlapping the CRE) and at the region between –201 and –210. The consensus sequence for GR binding (the glucocorticoid response element, GRE) is a palindrome AGAACAnnnTGTTCT, but can vary significantly between genes. Two GRE consensus sequences occur in the IL-6 gene between positions –461 to –466 and –552 to –557, though GR binding has not been confirmed.

The glucocorticoid receptor is a member of an evolutionarily related gene family known as the nuclear receptor family that code for steroid hormone, thyroid hormone and retinoic acid receptors that share a common structure with distinct DNA-binding, hormone-binding and transcriptional effector domains (figure 1.16), (Mangelsdorf et al., 1995). The most conserved region between nuclear receptors is the multi-cysteine, zinc-finger motif that forms the DNA-binding domain, resulting in the similarity of binding-sites between receptors. This DNA-binding is dependent on the presence of zinc. Nuclear receptors in the intact cell are only found bound to DNA in the presence of the hormone, though nuclear receptors uncoupled to hormone have been shown to bind to DNA *in vitro* in electrophoretic mobility shift assays and footprint studies. In the absence of hormone, the GR is found in the cytoplasm bound to a 90kDa heat-inducible chaperone protein, hsp90 (Pratt, 1997). Exposure to steroid results in dissociation of this complex and release of the GR that is then able to dimerize and move to the nucleus. In addition to inducing dissociation of hsp90 from the nuclear receptor, hormone binding induces a conformational change in the C-terminal effector domain that unmasks transcriptional activity. Other steroid hormone receptors are similarly bound to hsp90 in the cytoplasm and released by specific hormone binding, however the related nuclear receptors for thyroid hormone and retinoic acid are not associated with hsp90 and are already bound to DNA prior to exposure to ligand (Mangelsdorf and Evans, 1995). With all nuclear receptors, ligand binding brings the effector domain into close association with the hormone-binding domain and allows co-activator proteins to bind the receptor, including CBP (Glass et al., 1997, Torchia et al., 1998).

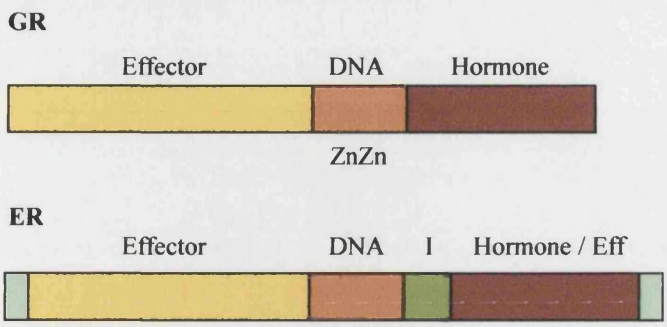

Figure 1.16. The structural organisation of nuclear receptors.
GR=glucocorticoid receptor, ER=oestrogen receptor. Effector=transcriptional effector domain, DNA=DNA-binding domain containing conserved multi-cysteine zinc-finger motif (ZnZn), Hormone=hormone/ligand-binding domain, I=interaction domain of ER, necessary for binding to NF-κB & C/EBPβ, Eff=C-terminus transcriptional effector region of ER.

Three mechanisms have been shown by which GR can produce repression of gene expression once DNA bound; direct inhibition of transcription via the effector domain, neutralisation of an enhancing factor, or competition with a co-activator. These mechanisms all require activation of the receptor by ligand binding as described above. Negative effects of GR on transcription seem to be mediated by binding to distinct GRE sites. Although related in sequence to the GRE associated with positive effects on transcription, the receptor may bind these negative-GREs in a different configuration to the positive-GREs. For example, in the pro-opiomelanocortin gene, GR has been shown to bind as a trimer to the negative–GRE rather than as a dimer (Drouin et al., 1993). The bound GR can then act by exerting a direct inhibitory influence on transcription, or by preventing binding of a positive acting factor. GR binding in the human glycoprotein hormone α-subunit gene only results in repression of gene expression when the CRE is intact (Akerblom et al., 1988). The GRE overlaps the CRE in this gene. Interestingly, mutation of the GRE or GR DNA-binding domain did not abolish repression (Stauber et al., 1992). It was also found that inhibition by GR was only effective when transcription was activated by CREB. *In vitro*, no high affinity protein-to-protein interactions were identified between GR and CREB implicating a third protein in the interaction. The nuclear factors, like CREB (see 1.3.2.3), can bind CBP resulting in mutual repression (Kamei et al., 1996) and this may be the mechanism involved for this gene. A similar mechanism could be postulated for the IL-6 gene where the –145 to –173 GRE site overlaps the CRE. Co-repressor molecules play a role in gene inhibition by nuclear receptors as identified for the

thyroid hormone and retinoic acid receptors. Nuclear receptor co-receptor (N-CoR), together with two other proteins mSIN3 and mRPD3, bind to the nuclear receptors as a co-repressor complex (Heinzel et al., 1997, Horlein et al., 1995). In addition to transcriptional inhibition by binding to GRE, the GR can inhibit transcription in genes that do not contain a GRE, such as the collagenase promoter (Yang-Yen et al., 1990). This is via direct protein–to–protein interactions with the transcriptional activators Fos and Jun resulting in repression of AP-1 activity. NF-κB induced expression of IL-6 can be inhibited by GR association with the p65 subunit of NF-κB (Ray and Prefontaine, 1994). Mutual repression has been shown between NF-κB p65 and GR, and was dependent upon the co-activators CBP and steroid receptor coactivator-1 (SRC-1), (Sheppard et al., 1998). Increased levels of CBP were able to relieve glucocorticoid repression of NF-κB, while CBP and SRC-1 were able to relieve NF-κB repression of GR activity. This is another example of cross-talk between transcriptional pathways. GR inhibition of NF-κB activity can also occur via an indirect inhibitory mechanism. In some genes, GR can have enhancing roles on transcription. This is seen with the IκBα gene where glucocorticoid exposure induces expression, resulting in increased levels of IκBα protein and increased inhibition of NF-κB activity (Scheinman et al., 1995, also see section 1.3.2.1).

The predominant influence of glucocorticoids on the transcription of IL-6 is inhibitory. This is via direct effects of activated GR binding to GREs, with potential inhibition of CREB binding, competition of co-activators such as CBP, inhibition of Fos and Jun activation through the AP1 site, and possibly also by direct inhibitory mechanisms on the basal transcription machinery. Other mechanisms include non-DNA-bound GR-protein interactions such as described with NF-κB.

1.3.2.6. Oestrogens and androgens

Oestrogen has been shown to down-regulate IL-6 expression in osteoblasts and bone marrow stromal cells (Girasole et al., 1992). This inhibition occurs at the level of transcription and is oestrogen receptor (ER) dependent. However, it does not involve ER binding to the IL-6 5'-flanking region where there are no known binding sites for oestrogen or androgen receptors (Pottratz et al., 1994, Ray et al., 1994). ER repression is via direct protein-protein interaction with the transcriptional activators NF-κB (p65

and p50 subunits) and C/EBPβ, inhibiting their ability to bind DNA (Stein and Yang, 1995, Ray et al., 1997). Mutation studies revealed that a region adjacent to the DNA-binding domain of the ER was necessary for these protein interactions (see figure 1.16). ER interaction was via the Rel homology domain of NF-κB and the leucine-zipper domain of C/EBP. Although the DNA-binding domain was not necessary for ER interaction with NF-κB or C/EBPβ, it was necessary, together with the hormone-binding domain and C-terminus effector region (figure 1.16), for repression of the IL-6 promoter (Stein and Yang, 1995). In Cos-7 monkey cells, oestrogen was found to inhibit NF-κB but not C/EBPβ induced IL-6 transcription, a process that may involve oestrogen induced conformational changes of the ER hormone-binding domain (Kurebayashi et al., 1997). Like GR, ER has been shown to bind AP1 Jun, but not Fos, transcription factors, via direct protein-protein interaction requiring a similar interaction domain as for NF-κB and C/EBPβ (Doucas et al., 1991, Teyssier et al., 2001). It is not known however whether such interactions have a modulatory effect on IL-6 transcription. Androgens, in contrast to oestrogens, have been shown to inhibit the expression of IL-6 through maintenance of IκBα levels and hence inhibition of NF-κB activation, and not via direct interaction with NF-κB (Keller et al., 1996). Oestrogens were shown not to significantly modulate IκBα levels (Stein and Yang, 1995).

1.3.2.7. Interferon regulatory factor

Interferon regulatory factor-1 (IRF-1) is an interferon-γ inducible transcription factor that in HeLa cells was shown to bind the 5'-flanking region of the IL-6 gene from –254 and –267, and in the co-presence of NF-κB (p65) to up-regulate IL-6 expression (Faggioli et al., 1997). This co-operative induction required the concomitant removal of the negative effect of a retinoblastoma control element (RCE) and involved the presence of the transcription factor Sp1 (Sanceau et al., 1995).

1.3.2.8. Sp1

Deletion mutation studies of the human IL-6 gene indicated a negative regulatory region between –73 and –181 (Shimizu et al., 1990, Sanceau et al., 1995). This region contains a consensus sequence for retinoblastoma control element (RCE) and Sp1. EMSA studies using interferon-γ and TNFα induced nuclear extracts from THP1 cells (a human monocyte cell line), showed the presence of Sp1 in the protein-complex

binding to this negative regulatory region (Sanceau et al., 1995). It is not known whether this is a cell specific phenomenon, as studies in other cell-types have not been reported. However, in murine IL-6 studies, Sp1 binding to three CCACC motifs between the NF-κB and C/EBPβ binding sites was important in both basal and inducible expression (Kang et al., 1996). Deletion mutant constructs revealed that these Sp1 sites were necessary for murine IL-6 transcription via NF-κB and C/EBPβ. It remains to be established whether this is an important mechanism in human IL-6 transcription.

1.3.2.9. Recombination binding protein

The transcriptional repressor recombination binding protein (RBP, also known as CBF1 or RBP-Jκ) has been shown in transient-expression assays to repress IL-6 transcription (Kannabiran et al., 1997). EMSA studies with nuclear extracts from an embryonal carcinoma cell line F9, showed binding from –62 to –69 (AAAGGGT) of the IL-6 gene, a site overlapping the NF-κB site. Studies with nuclear extracts from a mouse fibrosarcoma cell line L929, reported RBP to be constitutively bound to this site at a 10-fold lower affinity than NF-κB and suggested that RBP may have a role in the constitutive repression of the IL-6 gene under normal physiological conditions (Plaisance et al., 1997). Kannabiran and co-workers (1997) showed that RBP repressed co-operative activation of IL-6 expression by NF-κB and C/EBPβ. This required all three sites, the RBP, NF-κB and C/EBPβ to be bound by their transcription factors for repression to occur. The mechanism is therefore not simply due to prevention of NF-κB or C/EBPβ binding, but involves inhibition of interaction between NF-κB and C/EBPβ. In HeLa cells, RBP has also been shown to bind at this site on the hIL-6 gene and inhibits transcription (Palmieri et al., 1999). This inhibition may be effected through conformational change in the IL-6 promoter region as the topology of the RBP-DNA bound complex was influenced by surrounding sequences, and in IL-6 induced a bend in the DNA. In the course of investigating the mechanism of RBP inhibition of NF-κB and C/EBPβ transactivation of IL-6, a third C/EBP site was identified that overlaps the RBP site in hIL-6 (Vales and Friedl, 2002). Deletion mutant constructs of IL-6 lacking the two up-stream C/EBP sites (–146 to –154 & -75 to –83) were found to still bind C/EBPβ, δ and α via direct DNA-binding. Interestingly, these constructs could bind NF-κB p65 or C/EBP family members alone,

but combined C/EBP & p65 binding was not seen in the absence of the up-stream C/EBP site. This suggests that co-operative binding between NF-κB and C/EBP at this down-stream site requires co-operation from the up-stream C/EBP site. Site-directed mutagenesis of the RBP site produced a mutant construct with reduced RBP binding that could still bind NF-κB p65, but had reduced binding of C/EBP family members. This construct produced significantly lower levels (similar to those of wild-type construct inhibited with RBP) of IL-6 transcription in response to NF-κB and C/EBPβ exposure in HepG2 and COS cell transient transfections and could not be repressed by exposure to RBP (Vales and Friedl, 2002). A second mutant prevented RBP binding but still facilitated similar levels of NF-κB and C/EBP binding as the wild-type sequence. This construct displayed levels of IL-6 expression similar to the wild-type construct, but was not repressed by RBP. This confirms that RBP repression requires DNA-binding of RBP and that the third, down-stream C/EBP site, over-lapping the RBP site, is functionally significant for optimal induction of IL-6 expression. In addition, it suggests that RBP binding may produce its repressor effect by disruption of C/EBP binding to the third C/EBP site. RBP has also been shown to have two other mechanisms of transcriptional repression. It can interact with co-repressors such as N-CoR (see 1.3.2.5) and histone deacetylase (see 1.3.2.3), and can interact with the basic transcriptional machinery to reduce transcriptional activation (Kao et al., 1998, Olave et al., 1998). These mechanisms may also be relevant to inhibition of IL-6 transcription.

1.3.2.10. Regulation of IL-6 expression in rheumatoid fibroblast-like synoviocytes

Cell-type specific differences in the regulation of the human IL-6 gene are evident. In a murine monocyte/macrophage cell line, PU5-1.8, the AP1 site, CRE and adjacent C/EBPβ and NF-κB sites were all important for IL-6 expression (Dendorfer et al., 1994). In a human monocytic cell line, THP1, two C/EBPβ binding sites (-75 to –83 & –148 to –155) were important together with NF-κB (Zhang et al., 1994). In contrast, cells infected with the human T-cell leukaemia virus type-I required only NF-κB for full expression of IL-6 (Mori et al., 1994).

In the inflammatory arthritis, rheumatoid arthritis, the main producer of IL-6 with in an inflamed joint is believed to be fibroblast-like synoviocytes (Firestein et al., 1990,

Guerne et al., 1989). Site-specific mutagenesis studies of IL-6 promoter constructs in rheumatoid fibroblast-like synoviocytes (FLSs) identified regulation by C/EBPβ, NF-κB and RBP as important for IL-6 expression (Miyazawa et al., 1998a). NF-κB (p65/p65 and p50/p65 dimers) were the main enhancers of IL-1 induced expression of IL-6 in these cells, but were not significantly involved in basal IL-6 regulation. C/EBPβ in contrast was a significant enhancer of both basal and IL-1 induced expression of IL-6. RBP binding was thought by this group to be a positive regulator of IL-1-induced expression of IL-6. However, in light of the findings by Vales and Friedl (2002, discussed in section 1.3.2.9), who identified a third C/EBP site overlapping the RBP site, it is likely that the mutation preventing RBP binding was also preventing C/EBP binding to this down-stream site. The reduced expression seen with this construct was probably due to loss of C/EBP activity rather than RBP.

In addition, the p38 mitogen activated protein kinase (MAPK) pathway was activated in response to IL-1β stimulation of human FLSs (Miyazawa et al., 1998b). Using a pyridinylimidazole inhibitor specific for p38 MAPK, SB203580, Miyazawa and co-workers (1998b) showed that levels of IL-6 protein and mRNA were inhibited in a dose and time dependent manner. This appeared to be a mechanism independent of transcription, as the inhibition was not prevented by the blocking of transcription with actinomycin D, nor did SB203580 alter the levels of transcription of transfected IL-6 reporter constructs. Activation of the p38 MAPK pathway appeared to stabilise IL-6 mRNA, with SB203580 significantly reducing the half-life in FLSs. This may be a cell specific, species specific and/or inducer specific effect, as in the mouse fibrosarcoma cell line L929, SB203580 repressed TNFα-induced expression of human IL-6 reporter constructs indicating an action at the level of transcription (Berghe et al., 1998). Although NF-κB plays an important role in the induction of IL-6 expression by TNFα, blocking the p38 MAPK pathway did not affect levels of NF-κB binding to DNA. Glucocorticoid inhibition of IL-6 expression was mediated at the level of transcription in FLSs, with no effect on the stability of IL-6 mRNA (Miyazawa et al., 1998c). This was dependent on *de novo* protein synthesis as exposure to cyclohexamide to block protein synthesis prevented dexamethasone inhibition of IL-6 expression. Levels of IκBα (a cytoplasmic inactivator of NF-κB, see section 1.3.2.1) were not altered by dexamethasone exposure of IL-1-stimulated FLSs.

1.3.3. Polymorphisms in the 5'-flanking region of IL-6

Three single nucleotide polymorphisms (SNPs) have been described in the 5'-flanking region of the human IL-6 gene; a G to C at position –174 (Fishman et al., 1998, Olomolaiye et al., 1998), a G to C at position –572 (Nakajima et al., 1999, Osiri et al., 1999) and a G to A at position –597 (Faulds et al., 1998, Jordanides et al., 2000). A variable length AT-tract polymorphism from –373 to –392 has also been described (Fishman et al., 1998, Nakajima et al., 1999, Terry et al., 2000). These polymorphisms had been identified prior to this thesis by the collaborative groups of Prof P Woo and Prof S Humphries at University College London.

1.3.3.1. SNPs in the 5'-flanking region of IL-6

The frequency of distribution of the –174, –572 and –597 alleles reported in this thesis for normal healthy individuals in various ethnic groups are in Hardy-Weinberg equilibrium (see table 1.2). There are clear ethnic differences between the frequency of distribution for these polymorphisms.

The –174C allele occurs significantly less frequently in Gujarati Indians, Southern Chinese, Afro-Carribeans and African-Americans compared to Caucasians. The lower frequency in retired Southern Chinese male coal miners is more difficult to interpret as a survival advantage of the –174G allele cannot be excluded. The –572 polymorphism has a similar reported frequency of distribution in Caucasians and African-Americas, though it is very interesting that in the Japanese population, the opposite allele frequency was reported with –572C being the most common allele. One should note that the Japanese study used PCR-RFLP with a different restriction enzyme, BsrBI, from the other studies. Though it recognises the same DNA sequence, it is possible that restriction digestion failure could have resulted in an over-estimation of the C-allele frequency for this SNP. In addition, the subjects in this study were all females selected as controls for a hypertension study. It would be of significant interest if the results were replicated in an independent Japanese population. The allele frequency for the –597 polymorphism is similar in each ethnic group to that of the –174 polymorphism. The –597A allele occurs in significantly lower frequency in African-Americans compared to Caucasians.

Ethnic group	Polymorphic site	n	Allele	Frequency	Reference
Caucasian	-174	383	G	0.597	Fishman et al., 1998
			C	0.403	
Caucasian	-174	73	G	0.555	Jordanides et al., 2000
			C	0.445	
Gujarati Indian	-174	115	G	0.850	Fishman et al., 1998
			C	0.150	
Southern Chinese	-174	259	G	0.998	ϒZhai et al., 2001
			C	0.002	
Korean	-174	53	G	0.994	Lim et al., 2002
			C	0.006	
Afro-Caribbean	-174	101	G	0.950	Fishman et al., 1998
			C	0.050	
African-American	-174	63	G	0.960	Osiri et al., 1999
			C	0.040	
Caucasian	-572	73	G	0.959	Jordanides et al., 2000
			C	0.041	
African-American	-572	63	G	0.905	Osiri et al., 1999
			C	0.095	
Japanese	-572	142	G	0.176	*Nakajima et al., 1999
			C	0.824	
Caucasian	-597	73	G	0.568	Jordanides et al., 2000
			A	0.432	
African-American	-597	63	G	0.952	Osiri et al., 1999
			A	0.048	

Table 1.2. The frequency of distribution of alleles at the –174, -572 and –597 SNPs of IL-6 in various ethnic groups.
n=number of individuals in the study group.
ϒRetired male coal miners only
*Females only

1.3.3.2. SNPs can influence transcription

Single nucleotide polymorphisms in the regulatory region of a gene can influence levels of transcription and expression of the gene. This has been demonstrated and characterised for two SNPs in the 5'-flanking region of the cytokine gene TNFα. The G to A SNP at position –376 allows allele-specific binding of the transcription factor OCT-1 to this site of multiple protein occupancy (Knight et al., 1999). The OCT-1 binding variant –376A was associated with higher TNFα-luciferase-reporter construct expression in primary human monocytes, Mono Mac cells. These *in vitro* findings appeared functionally significant as in a large case-control study of a West and East

African population, possession of the –376A allele (present in approximately 5% of the population) was associated with a significantly increased susceptibility to cerebral malaria. In addition, the C to A polymorphism at position –863 of TNFα has been shown to alter NF-κB binding (Udalova et al., 2000). The –863A allele reduces binding of the p50/p50 homodimer compared to the –863C allele while still permitting the same p50/p65 heterodimer binding. Reduced p50/p50 binding was associated with higher levels of TNFα expression in COS-7 cells. In Mono Mac cells, higher TNFα expression occurred with transfected A-allele rather than C-allele constructs, however this was dependent on the presence of the TNFα 3'-untranslated region, located down-stream of the reporter gene. This indicates that an allelic effect can be modified by factors influencing expression in other regions of the gene. Allelic associations can also be important. Within the same gene, this is illustrated by the effect of allelic association between the –863 polymorphism and another upstream SNP at position –1031. Concanavalin A stimulated peripheral blood monocuclear cells (PBMCs) from healthy donors possessing the –1031C–863A haplotype of TNFα produced 2-fold higher levels of TNFα expression than PBMCs from individuals possessing the dominant –1031T–863C haplotype (Higuchi et al., 1998). In contrast, transfection studies in the hepatocyte cell line HepG2, showed the –863A allele to be associated with lower levels of expression than –863C (Skoog et al., 1999). This corresponded with *in vivo* levels of expression in 254 healthy Swedish men in whom the –863A allele was associated with significantly lower levels of serum TNFα than the –863C allele. SNPs in the 5'-flanking region of a cytokine gene can influence transcription though the functional significance may vary depending on allelic associations and cellular context.

1.3.3.3. AT tract polymorphisms in the 5'-flanking region of IL-6

Several AT-tract polymorphisms between –373 and –392 have been described. The majority maintain the length of the AT-tract at 20 bases however polymorphisms varying the overall AT-tract length by one additional base have also been reported (Fishman et al., 1998, Nakajima et al., 1999, Terry et al., 2000). Table 1.3 shows these AT-tract variations and the frequency of distribution in the Caucasian and Japanese population.

Ethnic group	n	AT-tract allele	Frequency	Reference
Caucasian	57	A8/T12	0.421	*Fishman et al., 1998
Caucasian	78	A8/T12	0.370	Terry et al., 2000
Caucasian	57	A9/T11	0.211	*Fishman et al., 1998
Caucasian	78	A9/T11	0.190	Terry et al., 2000
Caucasian	57	A10/T10	0.175	*Fishman et al., 1998
Caucasian	78	A10/T10	0.180	Terry et al., 2000
Japanese	280	A10/T10	0.939	**Nakajima et al., 1999
Caucasian	57	A10/T11	0.123	*Fishman et al., 1998
Caucasian	57	A10/T11	0.250	Terry et al., 2000
Japanese	280	A10/T11	0.061	**Nakajima et al., 1999
Caucasian	57	A9/T10	0.053	*Fishman et al., 1998
Caucasian	57	A10/T9	0.017	*Fishman et al., 1998

Table 1.3. The frequency of distribution of alleles at the AT-tract of IL-6 in Caucasian and Japanese individuals.
n=number of individuals in the study group.
*normal controls and patients with SA
**females only

The frequency of distribution for each allele is similar in Caucasians between the two studies with A8/T12 the most common AT-allele. However, the frequency of alleles reported in the Japanese population is very different. Nakajima and co-workers (1999) used PCR-SSCP to identify the AT tract alleles, a technique that would not distinguish between allelic variations maintaining a constant length of AT-tract, but only variants of different lengths. The groups called 'A10T10' and 'A10T11' therefore probably represent a mixture of AT-alleles of 20 and 21bp lengths, respectively. The other two papers used sequencing and/or the method of Bowcock et al., (1989) to distinguish each allelic variant.

No transcription factors have been reported to bind to such AT-tracts. However, this sequence has implications in the tertiary structure of the DNA helix and may influence ease of strand opening, a process essential for transcription to occur (Siebenlist, 1979). AT rich regions have been shown to induce a cruciform extrusion *in vitro* under certain conditions (Bowater et al., 1994), a similar effect may occur *in vivo*.

1.3.4. Polymorphisms in other regions of the IL-6 gene

Variable region tandem repeats (VNTRs) of AT-rich sequences have been described in the 3'-flanking region of the IL-6 gene (Bowcock et al., 1989, Murray et al., 1997, Jordanides et al., 2000, Crilly et al., 2001). The functional relevance of these polymorphisms in the non-transcribed 3'-flanking region is unknown.

Single strand conformational polymorphism (SSCP) analysis revealed a G to A variant in exon 5 of IL-6 (Nakajima et al., 1999). Only heterozygotes for this variant were detected in 140 Japanese women with a frequency of 0.064. No other variants in the IL-6 intron or exon sequences have been reported.

1.3.5. Post-transcriptional regulation of IL-6 expression

Although the overall regulation of IL-6 expression is at the level of transcription, variations in mRNA stability and translation can modulate expression of the IL-6 protein. Deletion of N-terminal untranslated regions (UTRs) including AU-rich sequences of IL-6 mRNA has been shown to increase mRNA stability and result in higher IL-6 expression in transfected mouse NIH3T2 cells (Tonouchi et al., 1989). Sequence and position specific AU-rich regions in the 3'UTRs of the proto-oncogene c-Jun act as RNA-destabilising elements (Peng et al., 1996), in TNFα these regions have been shown to bind RNA binding proteins (AUBPs) involved in repression of translation (Hel et al., 1998). No variations of the 3'-UTR of IL-6 have been reported.

The half-life of IL-6 mRNA in fibroblasts and monocytes is approximately 1-hour (Elias and Lentz, 1990, Brach et al., 1990). IL-6 mRNA stability has been shown to be influenced by a number of inflammatory modulators. IL-1 and TNFα act synergistically in the up-regulation of IL-6 expression in fibroblasts by a mechanism involving increased transcriptional activation, but also increased mRNA stability (Elias and Lentz, 1990). IL-1β stabilises IL-6 mRNA induced by *c-kit* Ligand and IL-10 in mouse bone-marrow-derived mast cells via IL-1β inducible protein (Lu-kuo et al., 1996). In human fibroblast-like synoviocytes IL-1β stabilisation of IL-6 mRNA was via activation of the p38 MAPK pathway involving activation of MAPK-activated protein kinase 2 (MAPKAP kinase 2), (Miyazawa et al., 1998b, and see 1.3.2.10). The half-life of IL-6 was reduced by 10-fold in response to LPS, in MAPKAP kinase 2

deficient macrophages from knockout mice (Neininger et al., 2002). The effects of MAPKAP kinase 2 seemed to be mediated via the 3'-UTR with AU-rich regions, as MAPKAP kinase 2 could stabilise a mRNA reporter construct carrying the human or mouse IL-6 3'-UTR (there is high homology for this region between the two species). Deletion of the AU-rich element of the 3'-UTR in TNFα-mRNA abrogated the effects of MAPKAP kinase 2 (Neininger et al., 2002). In human monocyte cell lines, IL-10 stimulation was shown to reduce the half-life of IL-6 mRNA (Takeshita et al., 1996). Leukotriene B_4 can result in stabilisation of IL-6 mRNA, possibly via up-regulation of AUBPs through its activity as a calcium ionophore (Rola-Pleszczynski and Stankova, 1992). The effect of TNFβ (lymphotoxin) is contradictory. It has been reported to stabilise IL-6 mRNA in fibroblasts (Akashi et al., 1990), whereas to reduce IL-6 mRNA half-life in monocytes (Brach et al., 1990). In both cases, a mechanism requiring protein synthesis was shown to be necessary.

Despite influences on mRNA stability, the over-riding influence of transcriptional regulation over these post-transcriptional modifications in the expression of IL-6 is shown by the stimulation of PBMCs with IL-1 in the presence of histamine. Over all there was an increase in the expression of IL-6 through increased transcription, though IL-6 mRNA half-life was reduced (Vannier and Dinarello, 1994). Post-translational modification of the IL-6 protein also occurs and includes N- and O-linked glycosylations and phosphorylations (May et al., 1988, Santhanam et al., 1989), which in turn may influence the half-life, distribution, binding capacity or actions of the protein. At sites of inflammation, IL-6 has been shown to induce release of elastase, proteinase 3 and cathepsin G (serine proteases) from neutrophils and results in degradation and inactivation of IL-6 (Bank et al., 1999), though sIL-6R was protective against IL-6 inactivation by cathepsin G. This may represent a feedback mechanism to regulate the availability and biological actions of IL-6.

1.3.6. Hypothesis of this thesis

The hypothesis of this thesis was that over-expression of IL-6 contributes to disease susceptibility and phenotype of the systemic arthritis sub-type of JIA. As IL-6 is predominantly regulated at the level of transcription, genetic variations in the 5'-flanking region could influence IL-6 transcription and hence the pathophysiology of SA.

1.3.7. Aims of this thesis

The aims of this thesis were to:

i. Investigate the association of 5'-flanking region polymorphisms of the IL-6 gene with SA compared to healthy controls.

ii. Assess the effect of polymorphisms in the 5'-flanking region of IL-6 on the regulation of IL-6 transcription using IL-6 variant-reporter constructs in transfection studies.

iii. Identify alterations in transcription factor(s) binding due to different alleles that may explain functional differences in IL-6 transcription.

CHAPTER 2

MATERIALS AND METHODS

2.1. Source of patient and control genomic DNA samples

2.1.1. Patient samples

Fresh venous blood samples collected into sodium EDTA were obtained (with full patient and parental informed consent) from Caucasian patients attending paediatric rheumatology centres across the UK. This was facilitated through the British Paediatric Rheumatology Group. Blood was only taken from children when other blood samples were being collected for clinical reasons. Each patient had to have a confirmed diagnosis of juvenile idiopathic arthritis (JIA) by the International League against Rheumatism (ILAR) criteria (see section 1.2.10). Information was collected as to the age at onset of the disease, the sex of the patient, the classification and the pattern of the disease. Samples were sent for storage and HLA typing to the British Paediatric Rheumatology Group National DNA repository, Manchester University.

2.1.2. Control samples

Fresh venous blood samples collected into sodium EDTA were obtained from healthy individuals recruited from four independent sources as representative control samples of the UK Caucasian population. Healthy UK Caucasian adults aged 16-30 years, consecutively registered on a General Practice List from Nuneaton (Midlands) and North London, were invited to attend their general practitioner to donate a blood sample. There had to be no history of chronic illness or prior joint problems and the individual completely well at the time of sampling. Information on sex and age was collected. A third group was recruited from first time blood donors attending a blood-donor clinic in the West End of London. Individuals over the age of 18 years with no self-reported known illness were invited to allow an aliquot of blood to be taken for the study at the time of blood donation. Self-reported information on age, sex and ethnic origin was collected. Only samples from UK Caucasian individuals were used for the purposes of this study. First time donors were chosen to avoid sample duplication, as identification was anonymous. A fourth control group had been recruited prior to this thesis from North West London as UK healthy Caucasian men aged 50-61 years, as part of a study into cardiovascular risk factors (Miller et al., 1996). Permission was obtained to use these samples as a control group for the purposes of this study.

2.2. Purification of genomic DNA

2.2.1. Purification of genomic DNA from blood

Fresh venous blood in sodium EDTA (300-1000µl) was purified in one of two ways; by the Nucleon biosciences DNA extraction kit or by phenol: chloroform extraction.

2.2.1.1. Nucleon biosciences extraction kit

Blood in sodium EDTA (300-600µl) was purified using Nucleon biosciences DNA extraction kit for blood and cell cultures following the manufacturer's recommended instructions. In brief, the cells were lysed in SDS containing buffer and protein destroyed with sodium perchlorate (reagents supplied). The protein was extracted once with chloroform and once with Nucleon resin. The DNA was then precipitated with ethanol and re-suspended in 200µl of water or TE*.

2.2.1.2. Phenol: chloroform extraction

This method is based on that used by Kunkel et al. (1977).

Blood in sodium EDTA (1000-8000µl, best results with 6-7000µl) was diluted to 50ml with lysis buffer (320mM sucrose, 10mM tris-HCl, 5mM $MgCl_2$, 1% (v/v) triton) at 4°C and gently mixed. The lysed cells were spun at 2,500rpm (Sigma 4K15 refrigerated centrifuge) at 4°C for 10min. The supernatant was discarded and the pellet re-suspended in 4.5ml NaCl/EDTA buffer (75mM NaCl, 24mM EDTA pH8). 250µl of 10% SDS, 100µl of proteinase K (10µg/µl) and 150µl of sterile distilled water (SDW) were added and incubated at 37°C overnight. Protein was extracted with an equal volume of equilibrated phenol* (5ml), the phases separated by centrifugation at 2000rpm for 5min. The upper aqueous phase was transferred to a clean tube (the lower phenol phase discarded into phenol waste). A further extraction was carried out on the aqueous phase with 2.5ml phenol and 2.5ml SEVAQ (chloroform: isopropanol 24:1), spun as before (2000rpm for 5min), retaining the upper phase and then a final extraction with 5ml SEVAQ. The upper aqueous phase was transferred to a clean tube, 0.5ml of 3M sodium acetate was added followed by 12.5ml of ice-cold absolute ethanol and mixed by gentle inversion until the DNA threads could be seen to precipitate. For larger volumes of blood, the DNA could be hooked out with a glass pastette. For smaller volumes, the DNA was pelleted by centrifugation (13,000rpm for 1min). The DNA was air-dried before re-dissolving in 300-500µl of SDW or TE*.

2.2.2. Purification of genomic DNA from cell lines

Cells were grown to confluencey in culture (see 2.10), harvested with trypsin/EDTA neutralised by DMEM* containing FCS, washed twice with PBS* and the cell count determined (see section 2.10.3). A cell pellet of 1 x 10^6 cells was gently re-suspended in 700µl of genomic-DNA buffer (50mM Tris, 100mM EDTA pH8, 100mM NaCl and 1% SDS) using a 1000µl pipette tip with the end cut off. 35µl of Proteinase K (10mg/ml, Sigma) was added and the mix incubated overnight at 55°C. Protein was extracted using an equal volume of equilibrated phenol* which was mixed thoroughly, pulse centrifuged and the top aqueous phase containing the DNA removed into a fresh tube. This was repeated twice and followed by one extraction with an equal volume of chloroform: isopropanol (24:1). DNA was precipitated from the aqueous phase by adding an equal volume of cold propan-2-ol and gently mixing until threads of DNA precipitated. The DNA was either spooled out on a glass pastette or pelleted by centrifugation, washed twice in 70% ethanol, air dried and re-suspended in 300µl of TE*.

2.3. Electrophoretic separation of DNA molecules

2.3.1. Horizontal agarose gel electrophoresis

Typically a 1% (w/v) agarose suspension in 1x TAE* or TBE* buffer was boiled for 1min to dissolve the agarose, cooled to 40-50°C and 3µl of ethidium bromide (10mg/ml) was added per 100ml. The mix was then poured into a gel slab mould (BioRad) and allowed to set for 40min before use. For separation of small fragments of DNA (<200bp) or to distinguish fragments that differed in length by a small amount (≤50bp) separation was carried out on a 2-2.5% (w/v) agarose gel. Pre-loading, sample aliquots were mixed with 1/6^{th} volume 6x blue/orange loading dye (0.4% orange G, 0.03% bromophenol blue, 0.03% xylene cyanol FF, 15% Ficoll 400, 10mM Tris-HCl, 50mM EDTA). Gels were run from cathode to anode in 1x TAE or TBE (dependent on the buffer used to make up the gel), at 2-5 volts per cm, with a DNA molecular weight marker ladder (100bp ladder, Promega ± lambda DNA *Hind*III digest, see figure 2.1) in one lane. The DNA bands were viewed under ultraviolet light and a photographic record taken.

2.3.2. Vertical non-denaturing polyacrylamide gel electrophoresis

For a 100ml gel, 10ml of 10x TBE* and 40% sequencing grade acrylamide (National Diagnostics) plus water was mixed according to the percentage gel required (see table 2.1). Ammonium persulphate (AMPS, Sigma) was added and mixed, and then tetraethylmethylene diamine (TEMED, BDH) was added, thoroughly mixed and the gel solution immediately poured between glass plates (pre-washed and cleaned with ethanol). The gel was allowed to polymerise for 45min with 15% gel, to a minimum of 2hours with 4% gel, before pre-running in 1x TBE. Samples were loaded in 1x blue/orange loading dye (Promega).

Gel %	10x TBE	40% Acrylamide	H_2O	AMPS	TEMED	Use
4%	10ml	10ml	80ml	0.1g	40µl	EMSA
8%	10ml	20ml	69.6ml	350µl$^{\Upsilon}$	35µl	MADGE
15%	10ml	37.5ml	51.6ml	775µl$^{\Upsilon}$	77µl	Heteroduplex

Table 2.1. Polyacrylamide gel constituents.
$^{\Upsilon}$freshly prepared 10% (w/v) AMPS

2.4. Southern blotting and hybridisation

Typically, 20µg of purified genomic DNA (see sections 2.10.8 & 2.2.2) from stable cell transfectants was digested overnight with restriction enzyme (1U/µg of DNA). This was with *Hind*III or *Sph*I (see section 2.7) as these enzymes have only one cut site in the transfected plasmid construct. The digested products were separated by electrophoresis on a 0.8% horizontal slab agarose gel containing 0.3mg/ml ethidium bromide in 1xTBE* (section 2.3.1), for 16-20 hours at 2V/cm. Lambda DNA *Hind*III digest and 100bp marker ladders (figure 2.1) were run along side for size reference. This lane was removed before blotting, after a photographic record of the gel had been taken on an ultraviolet light-box with a ruler scale.

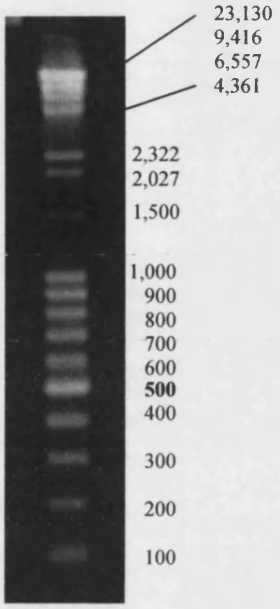

Figure 2.1. DNA molecular weight markers.
Combination of Lambda DNA digested with *Hind*III and 100bp ladder (Promega), run on a 1% agarose gel at 2.5v/cm for 45min, stained with ethidium bromide and viewed under UV light.

2.4.1. Southern blotting

The electrophoresed gel was denatured in 1.5M NaCl with 0.5N NaOH for 45min on a slow rotating platform. This was followed by a rinse in deionised water and neutralisation in 1M Tris (pH7.4) with 1.5M NaCl for 40min. The blot was then set up as shown in figure 2.2. The membrane used was nylon Hybond-N+ nucleic acid transfer membrane (Amersham), the buffer used was concentrated Salt Sodium Citrate (20xSSC*). Blotting was carried out for 16-24 hours. After blotting, the DNA was fixed to the membrane by baking between two pieces of Whatman 3MM paper for 2 hours at 80°C.

2.4.2. Hybridisation

The blotted membrane was prehybridised in hybridisation solution (6x SSC*, 5x Denhardt's reagent*, 0.5% SDS and 100mg/ml denatured, fragmented salmon sperm DNA*) for at least 2 hours at 68°C. This was carried out using roller bottles in a hybridisation oven (Hybaid) with 0.2ml hybridisation solution per cm^2 of membrane. 2-4ng of denatured radiolabelled probe (see 2.4.4) was added for hybridisation at 68°C for 12-18 hours.

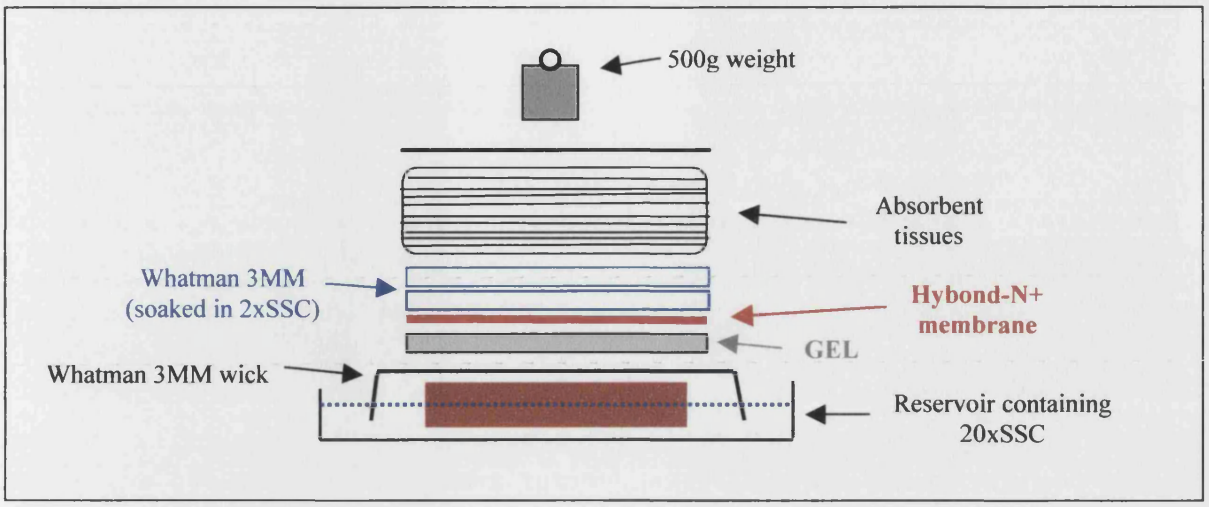

Figure 2.2. Southern blot set up.

2.4.3. Stringency washes

Following hybridisation, non-specifically bound probe was removed by stringency washes. This was carried out twice in 2x SSC* with 0.5% SDS, once in 2x SSC with 0.1% SDS, each for 15min at room temperature, once in 0.1x SSC with 0.5% SDS for 30min at 37°C and once in 0.1x SSC with 0.5% SDS for 60min at 65°C. The radioactive counts were read over the blot with a hand held monitor (Mini Instruments, Mini-Monitor GM Series 900) held 2cm above the blot, and if this was still above 10-20cps then the final wash was repeated. The blot was wrapped in Saran wrap (Dow Chemical Company) and exposed to x-ray film (X-OMAT, Kodak) for 16-24hours at –70°C. Longer exposures were carried out if required.

2.4.4. Preparation and random primer radiolabelling of DNA probe

For identification of the integration of IL-6-luciferase reporter constructs in the genomic DNA of stable transfectants, a 700bp fragment of the luciferase gene from PGL3 basic (Promega) was prepared. 15µg of plasmid DNA was digested with *Sph*I (see 2.7). The salt concentration of the reaction was then adjusted to high salt with NaCl for a second digestion with *Hind*III (section 2.7). The resultant fragment was separated by horizontal agarose gel electrophoresis (see 2.3.1), visualised under UV light and cut out in slices of agarose gel. The DNA fragment was isolated from the agarose using the Qiagen Qiaex II kit as out-lined in section 2.5.4.

The DNA was radiolabelled using the 'ready-to-go' system (Amersham). 100ng of DNA fragment in a final volume of 45µl deionised water, was denatured by boiling for 5min and then placed on ice. 5µl of α^{32}P-dCTP (3,000 Ci/mole) was added to the DNA and then this mix added to the lyophilised DNA polymerase and buffer mix from the kit. The labelling reaction was incubated for 30min at 37°C. Unincorporated radiolabel was removed by passing the incubated mix through a Sepharose 6CLB column (Clontech) to which ≤10bp fragments adhere and larger fragments pass through. The column was flushed with 150µl of TE. Labelled probes were required to have an activity of ≥100cps/ng (Mini-monitor GM series 900). Radiolabelled probe was denatured again immediately prior to hybridisation by boiling for 5min.

2.5. Polymerase chain reaction (PCR) amplification

2.5.1. Oligonucleotide primers

Oligonucleotide primers were synthesised to order by Genosys. The Tm value was calculated using the formula:

Tm in °C = 2(number of A+T residues) + 4(number of G+C residues)

This was used as a starting temperature for annealing. A series of PCR reactions was carried out to identify the optimum annealing temperature for each set of primers. Table 2.2 shows the identity of each primer pair, the sequence, the optimised annealing temperature and time, the product size and the PCR buffer conditions for all oligonucleotide primers used for PCR experiments. The PCR conditions for primers 9A/10A and 5bF/6R were optimised by G Faulds and L Luong.

2.5.2. Standard PCR conditions

Target DNA used per reaction was a colony stab, 10ng of plasmid DNA or 250ng of genomic DNA. 250ng of each oligonucleotide primer, 5µl of 10x PCR buffer (see table 2.2), the optimised concentration of $MgCl_2$ (see table 2.2), 0.2mM each dNTP, 2.5U *Thermus aquaticus* (*Taq*) DNA polymerase (Promega) and SDW to a total volume of 50µl were added. Reactions in individual PCR tubes were overlaid with 50µl of sterile mineral oil and run on a Perkin Elmer DNA Thermal Cycler 480 Machine. Reactions carried out in 96 well PCR plates were run on a Perkin Elmer (oil free) GeneAmp PCR System 9700 Machine.

	Annealing Temp/time	Product length	PCR buffer
Human IL-6			
–174 polymorphism / *Nla*III digestion 9A 5'-TGACTTCAGCTTTACTCTTTGT-3' 10A 5'-CTGATTGGAAACCTTATTAAG-3'	55°C/60s	190bp	NH_4 polmix $MgCl_2$ 1mM
–174 & –597 polymorphism / SSOP & *Sfa*NI digestion DF20^m 5'-AGTCACACACTCCACCTG-3' DF21 5'-GTGACTGACAGCACAGCT-3'	63°C/60s	858bp	Polmix $MgCl_2$ 3mM
–174 polymorphism / heteroduplex -174F 5'-GCTTCTTAGCGCTAGCCTCAATG-3' -174R 5'-TGGGGCTGATTGGAAACCTTATTA-3'	60°C/30s	116bp	Polmix $MgCl_2$ 2.5mM
–572/–597 polymorphism / *Mbi*I & *Fok*I digestion 5bF 5'-GGAGACGCCTTGAAGTAACTGC-3' 6R 5'-GAGTTTCCTCTGACTCCATCGCAG-3'	55°C/40s	163bp	Polmix $MgCl_2$ 1.5mM
–572 polymorphism / heteroduplex –572F 5'-CGCCTTGAAGTAACTGCACG-3' –572R 5'-GCCTGGGATTATGAAGAAGG-3'	54°C/45s	126bp	Polmix $MgCl_2$ 2.5mM
PGL3 basic plasmid Verification of IL-6 inserts in plasmid RV3 5'-CTAGCAAAATAGGCTGTCCC-3' GL2 5'-CTTTATGTTTTTGGCGTCTTCCA-3'	58°C/60s	147bp+ insert length	Polmix $MgCl_2$ 2mM
cDNA primers Actin PW229 5'-ATGGATGATGATATCGCCGC-3' PW230 5'-ATCTTCTCGCGGTTGGCCTT-3'	57°C/45s (x1), 55°C/45s (x29)	320bp (490bp gDNA)	Polmix $MgCl_2$ 2.5mM
IL-6 6-5' 5'-ATGAACTCCTTCTCCACAAGC-3' 6-3' 5'-CTACATTTGCCGAAGAGCCCTC... ...AGGCTGGACTG-3'	62°C/45s (x1), 60°C/45s (x29)	638bp (4311bp gDNA)	Polmix $MgCl_2$ 3mM

Table 2.2. Oligonucleotide primer pairs for PCR (made to order by Genosys).
Showing the sequences, annealing temperatures and time, product length, PCR buffer conditions and purpose for which PCR product was used.
Polmix = 10x *Taq* DNA polymerase buffer without $MgCl_2$ (Promega) containing 100mM Tris-HCl (pH9), 500mM KCl, 1.0% Triton X-100 (iso-Octylphenoxypoly-ethoxyethanol).
NH_4 polmix 10x contained 160mM $(NH_4)_2SO_4$, 670mM Tris (pH8.4), 0.001v/v Tween.

Reactions with genomic DNA template had a pre-cycling denaturation step of 4min at 95°C. All reactions underwent a post-cycling extension step of 10min at 72°C. Cycling was carried out at 95°C for 60sec, then the annealing temperature and length of time optimised for the individual primer set (see table 2.2), followed by 72°C for 90sec. Genomic DNA templates were cycled for 30-35 cycles, plasmid DNA templates for 25 cycles.

Two PCR buffers were used dependent on the subsequent use of the PCR product. The enzyme *NlaIII* was inhibited by KCl, therefore NH_4 polymix (see table 2.2) was utilised as PCR buffer for amplifications to be digested with *NlaIII*.

2.5.3. Conditions for reverse transcription PCR (RT-PCR)

To generate cDNA from RNA, 0.5µl of cDNA random hexamer primers (500µg/µl, Promega) were added on ice to 11µl of RNA preparation (section 2.6). These were annealed at 70°C for 10min then placed immediately on ice again. A cocktail of 4µl 5x First Strand Buffer (250Mm Tris-HCl pH8.3, 375mM KCl, 15mM $MgCl_2$, Gibco), 2µl 100mM DTT (Promega) and 2µl 5mM dNTP mix in nuclease free water was added to the primer annealed RNA. This was incubated at 42°C for 2min, then 1µl of Superscript II RNase H^- reverse transcriptase (200u/µl, Gibco) was added, gently mixed and incubation continued at 42°C for 50min. The enzyme was inactivated by incubation at 70°C for 10min and the final volume made up to 50µl with SDW. This sample preparation was then used in a standard PCR reaction (section 2.5.2). 1µl of cDNA preparation was used with 30 rounds of amplification using primers specific for exonic regions of IL-6 and actin (see table 2.2). These primers were chosen to be located in two separate exons so that any genomic DNA contamination could be identified as a longer product length. The first cycle was carried out at a slightly higher annealing temperature to increase specificity of binding and amplification for this round and reduce primer dimmer formation. Actin is a cell structure protein, expressed in similar levels in all cell types and not induced. The strength of the actin band allowed standardisation of the cDNA quantities used in RT-PCR (figure 2.3).

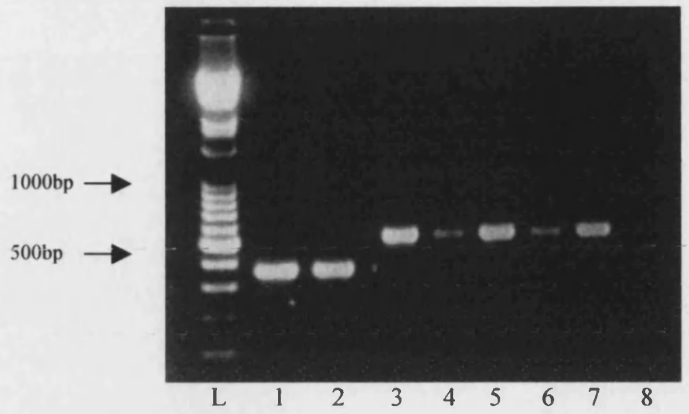

Figure 2.3. RT-PCR of HeLa cells for actin and IL-6.
cDNA was generated by RT-PCR using actin primers (PW229/230) and IL-6 primers (6-5'/6-3'), (see table 2.2). L=DNA marker ladder, 1&2=actin (320bp), 3, 5&7=IL-6 control (638bp), 4&6=IL-1-stimulated HeLa cells (638bp), 8=negative control.

2.5.4. PCR product and DNA fragment isolation

This was carried out using the Qiagen Qiaex II kit to isolate the DNA fragment from agarose gel. In brief, agarose slices containing the DNA fragment for purification were excised and placed in buffer QX1 (300µl buffer/100mg 0.8-1% gel), 20µl Qiaex suspension was added. The mix was incubated at 50°C for 5min to melt the agarose. Qiaex particles (to which the DNA binds) were pelleted by micro-centrifugation and washed once with QX1 buffer and twice with PE buffer. After air-drying the pellet, the DNA was eluted from the Qiaex particles with 40µl of water.

2.6. Purification of RNA

2.6.1. Purification of RNA from cell lines

Cell lines were grown over 48hours to 80% confluence in 6-well tissue culture plates seeded with 10^5 cells in 1ml DMEM/10%FCS (section 2.10). If required according to the experimental protocol, cells were stimulated with 100u/ml IL-1β for 3-6 hours pre-harvesting. Cells were harvested with trypsin/EDTA and pelleted (1200rpm at 4°C for 5min), then washed twice with cold PBS before re-suspension in 800µl RNAzol (Biogenesis). If not used immediately, the lysate was stored at –70°C.

RNAse-free tubes & pipette tips (Sarstedt), DEPC treated water* and sterile DEPC water washed glassware, baked at 120°C for 2hrs, were used throughout. To 800µl of

RNAzol/cell lysate, 80µl of RNAse free chloroform (BDH) was added, thoroughly mixed for 15sec and incubated on ice for 5min. The mix was then centrifuged at 12,000g for 15min at 4°C to separate the two phases. The upper aqueous phase containing the RNA was transferred to a clean tube, an equal volume of ice-cold isopropanol (RNAse free) was added and the mix incubated on ice for 15min. The precipitated RNA was pelleted by centrifugation at 12,000g at 4°C for 15min and then the supernatant discarded. The RNA pellet was washed once with 700µl of 70% ethanol (RNAse free) and re-pelleted at 7,500g at 4°C for 8min. The pellet was air-dried and re-dissolved in 10-20µl of nuclease free water. The RNA was kept on ice. If not used immediately it was stored at -70°C.

2.6.2. Quantification of RNA

A 1:50 dilution of the RNA preparation in RNAse-free water was quantified by optical density at 260nm in a UV spectrophotometer (Hitachi U-1100) in RNAse free cuvettes:

RNA concentration (µg/ml) = 40(constant for ssRNA) x dilution factor x OD_{260}

The quality of RNA was checked by running 5µl on a 1% agarose gel stained with ethidium bromide. Three distinct bands of ribosomal RNA (rRNA 28S, 18S and 5S) with a background smear of messenger RNA should be seen (figure 2.4).

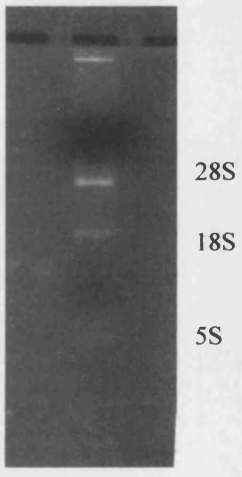

Figure 2.4. Electrophoretic separation of RNA on agarose gel.
RNA extracted from HeLa cells was separated on a 1% agarose gel by electrophoresis at 100v for 30min. Three bands of ribosomal RNA are produced (28S, 18S & 5S) with a background smear of mRNA.

2.7. Restriction enzyme digestion

To 1μg of PCR product (see section 2.5.2), 1-2U of restriction enzyme and 2.5μl of specific buffer (see table 2.3) were added to a total volume of 25μl made up with sterile distilled water. The reaction was incubated overnight at 37°C and then placed on ice. For digestion with *Sfa*NI however, the reaction was incubated for only 2 hours at 37°C, then heated to 65°C for 5min and placed on ice. For the micro-titre array diagonal gel electrophoresis (MADGE) high throughput method (section 2.8.1.2), this was carried out in a 96-well PCR plate.

1ug of plasmid DNA was digested in the same way. For double digests with enzymes requiring different salt conditions, digestion was carried out sequentially starting with the enzyme requiring the lowest salt concentration. The solution was then supplemented with additional salts and diluted as necessary to achieve the correct conditions for the second enzyme. For digestion of 1μg of genomic DNA, 1-4U of restriction enzyme was added and incubated for 16-20 hours.

To distinguish digested products of >50bp length difference, a 2% agarose gel was used. For product size differences ≤50bp an 8% polyacrylamide gel was used (see section 2.3.2). DNA standard size markers were run along side the product on each gel (*Hind*III digested lambda DNA for products >1000bp and 100bp DNA ladder, Promega, for products <1000bp).

2.7.1. Analysis of sequences for restriction enzyme sites

The sequence of interest was analysed automatically for >400 restriction enzyme recognition sequences using the 'Webcutter' on-line programme available at http://www.medkem.gu.se/cutter. The programme scanned both positive and negative DNA strands in both directions and sequence data could be entered from the GenBank sequence file to avoid errors.

Enzyme	Amount (per μg DNA)	Buffer (1x)	Manufacturer	Restriction sequence	Uses
*Aat*II	1U	J (50mM KCl, 10mM Tris-HCl, 7mM $MgCl_2$, 1mM DTT)	Promega	5'...GACGTˇC...3' 3'...CˇTGCAC...3'	Verification of IL-6 insert in pGL3 plasmid (no cut site in pGL3 basic)
*Bgl*II	1U	D (150mM NaCl, 6mM Tris-HCl, 6mM $MgCl_2$, 1mM DTT)	Promega	5'...AˇGATCT...3' 3'...TCTAGˇA...5'	Verification of IL-6 insert length in pGL3 plasmid (together with *Not*I cuts out insert + 203bp)
*BamH*I	0.5U	E (6mM Tris-HCl, 6mM $MgCl_2$, 100mM NaCl, 1mM DDT, pH7.5)	Promega	5'...GˇGATCC...3' 3'...CCTAGˇG...5'	Together with *Xho*I to shuttle the 1.17kb IL-6 fragment from pGEM to pBluescript
*Dpn*I	0.5U	Quikchange Site-directed mutagenesis kit buffer	Stratagene	5'...GAmˇTC...3' 3'...CTˇAmG...5'	Removal of parental template DNA after site-directed mutagenesis PCR
*Fok*I	2U	B (50mM NaCl, 6mM Tris-HCl, 6mM $MgCl_2$, 1mM DTT, 5μg BSA)	Promega	5'...GGATG$(N)_9$ˇ...3' 3'...CCTAC$(N)_{13}$ˇ...5'	Identification of IL-6 –597 genotype (cuts with –597A allele but not -597G)
*Hind*III	1U	E (6mM Tris-HCl, 6mM $MgCl_2$, 100mM NaCl, 1mM DDT, pH7.5)	Promega	5'...AˇAGCTT...3' 3'...TTCGAˇA...5'	Linearisation of IL-6/pGL3 constructs (one cut site in pGL3 basic vector, none in IL-6 insert)
*Kpn*I	0.5U	J (50mM KCl, 10mM Tris-HCl, 7mM $MgCl_2$, 1mM DTT)	Promega	5'...GGTACˇC...3' 3'...CˇCATGG...5'	Together with *Xba*I or *Nhe*I to allow direction specific cloning of IL-6 constructs into pGL3 basic
*Mbi*I	2U	Y+Tango (33mM Tris-acetate pH 7.9, 10mM Mg^{2+}acetate, 66mM K acetate, 0.1mg/ml BSA)	Fermentas	5'...CCGˇCTC...3' 3'...GGCˇGAG...5'	Identification of IL-6 –572 genotype (cuts with –572G allele but not -572C)
*Nhe*I	0.5U	B (50mM NaCl, 6mM Tris-HCl, 6mM $MgCl_2$, 1mM DTT, 5μg BSA)	Promega	5'...GˇCTAGC...3' 3'...CGATCˇG...5'	Together with *Kpn*I to allow direction specific cloning of IL-6 constructs into pGL3 basic
*Nla*III	1U	NEB4 (50mM KAc, 20mM Tris-acetate, 10mM Mg^{2+} acetate, 1mM DTT, pH7.9) supplemented with 100μg/ml BSA	New England Biolab	5'...CATGˇ...3' 3'...ˇGTAC...5'	Identification of IL-6 –174 genotype (cuts with –174C allele but not -174G)
*Not*I	1U	D (150mM NaCl, 6mM Tris-HCl, 6mM $MgCl_2$, 1mM DTT)	Promega	5'...GCˇGGCCGC...3' 3'...CGCCGGˇCG...5'	Verification of IL-6 insert length in PGL3 plasmid (together with *Bgl*II cuts out insert + 203bp)

Table 2.3. Restriction enzymes.....

Enzyme	Amount (per µg DNA)	Buffer (1x)	Manufacturer	Restriction sequence	Uses
*Sac*I	1U	J (50mM KCl, 10mM Tris-HCl, 7mM $MgCl_2$, 1mM DTT)	Promega	5'...GAGCTˇC...3' 3'...CˇTCGAG...5'	Together with *Xho*I, to shuttle the 1.17kb IL-6 insert from pBluescript into pGL3 basic
*Sal*I	5U	D (150mM NaCl, 6mM Tris-HCl, 6mM $MgCl_2$, 1mM DTT)	Promega	5'...GˇTCGAC...3' 3'...CAGCTˇG...5'	Distinguishing and linearising parental plasmid in transformer site-directed mutagenesis
*Sfa*NI	1U	NEB3 (100mM NaCl, 50mM Tris-HCl, 10mM $MgCl_2$, 1mM DTT)	New England Biolab	5'...GCATC$(N)_5$ˇ...3' 3'...CGTAG$(N)_9$ˇ...5'	Identification of IL-6 –174 genotype (cuts with –174G allele but not -174C)
*Sph*I	1U	K (10mM Tris-HCl, 10mM $MgCl_2$, 150mM KCl, pH7.4)	Promega	5'...GCATGˇC...3' 3'...CˇGTACG...5'	Linearisation of IL-6/PGL3 constructs (one cut site in PGL3 basic vector, none in IL-6 insert)
*Sst*II	5U	React 2 (50mM Tris-HCl, 10mM $MgCl_2$, 50mM NaCl, pH8)	Invitrogen	5'...CCGCˇGG...3' 3'...GGˇCGCC...5'	Distinguishing and selecting parental plasmid in transformer site-directed mutagenesis
*Xba*I	0.5U	D (150mM NaCl, 6mM Tris-HCl, 6mM $MgCl_2$, 1mM DTT)	Promega	5'...TˇCTAGA...3' 3'...AGATCˇT...5'	Together with *Kpn*I to allow direction specific cloning of ≤611bp IL-6 construct into pGL3 basic
*Xho*I	0.5U	D (150mM NaCl, 6mM Tris-HCl, 6mM $MgCl_2$, 1mM DTT)	Promega	5'...CˇTCGAG...3' 3'...GAGCTˇC...5'	Together with *BamH*I or *Sac*I to shuttle the 1.17kb IL-6 insert from pGEM to pBluescript and pGL3 basic

Table 2.3. Restriction enzymes, their buffers and uses.
ˇ indicates the cut site of the endonuclease.

2.8. Genotyping

2.8.1. Restriction fragment length polymorphism

This technique utilises restriction endonuclease digestion to distinguish between polymorphic sequences in a PCR amplified fragment of DNA containing the site of interest. It requires the base change of one allele to either form a restriction enzyme recognition site or abolish such a site, resulting in a different length of DNA fragment for each allele after exposure to the restriction enzyme.

2.8.1.1. MADGE high throughput method

This is based on the method used by Day and co-workers (1995).

1μg of PCR product containing the amplified IL-6 region around the polymorphisms – 174G/C (primers 9A & 10A), the -572G/C (primers 5bF & 6R) or the –597G/A (primers 5bF & 6R), (section 2.5.2) were digested in a 96 well PCR plate. A positive control for each genotype and a negative control were included per plate. The digest was carried out with 1-2U of restriction enzyme that would cut one allele but not the other, -174G/C (*Nla*III), -572 (*Mbi*I) and –597 (*Fok*I), (see section 2.7). After overnight digestion at 37°C, the products were resolved on 8% non-denaturing polyacrylamide gels (see section 2.3.2) pre-stained with ethidium bromide, using a matrix well lay out and 'diagonal' electrophoresis (as described by Day et al., 1995). The voltage, time of electrophoresis, and size of fragments obtained for each polymorphism are shown in table 2.4. A photographic record of the gel was made under UV light (see figure 2.5).

Polymorphism	Digestion product size	Electrophoresis voltage	Time of separation
-174	G allele 190bp C allele 143, 47bp	150V	45min
-572	G allele 101, 62bp C allele 163bp	150V	25min
-597	G allele 163bp A allele 116, 47bp	150V	35min

Table 2.4. Polyacrylamide gel electrophoresis conditions for MADGE genotype analysis of IL-6 polymorphisms.
Separation of restriction digest products was carried out by 'diagonal' electrophoresis on a horizontal 8% non-denaturing polyacrylamide gel.

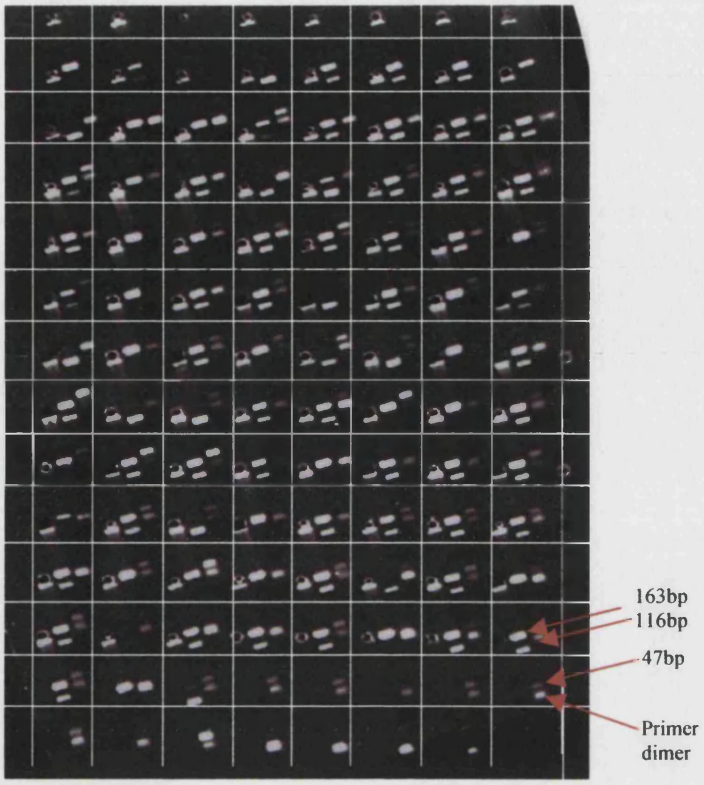

Figure 2.5. Micro-titre array diagonal gel electrophoresis for the –597 polymorphism of IL-6.

1μg of IL-6 PCR product using primers 5bF & 6R (table 2.2) was digested with 2u *Fok*I (see 2.7). *Fok*I cuts with the A allele at position –597 but not the G allele. The products were resolved on an 8% non-denaturing polyacrylamide gel (see 2.8.1). –597GG homozygotes produce a 163bp product, –597GA heterozygotes 163, 116 and 47bp products, and –597AA homozygotes produce 116 and 47bp products. The 163 & 116bp products can be seen within the centre of each grid.

2.8.2. Sequence specific oligonucleotide probing

The method was adapted from that of Turner et al. (1997).

Sequence specific oligonucleotide probing (SSOP) was used to determine the genotype of the –174 and –597 polymorphisms of IL-6. 1μg of PCR product (primers DF20^{m} & DF21, see 2.5.2) was dotted on to nylon nucleic acid transfer membrane (Hybond N+, Amersham), one membrane per allele to be probed. The double-stranded DNA was denatured by soaking the membrane for 5min in 0.5M NaOH with 1.5M NaCl, then neutralised for 1 min in 1.5M NaCl with 0.5M Tris. To cross-link the DNA to the membrane, the membrane was baked for 10min at 80°C and then treated for 30sec with 120,000μJ of ultraviolet energy (Stratagene UV Stratalinker 2400). The membrane was pre-hybridised in 15-25ml of hybridisation buffer (5x SSC*, 0.1% N-lauroylsarcosine, 0.02% SDS, 0.5% dried skimmed milk [Marvel]) for 60min at 42.5°C, using roller

bottles in a hybridisation oven (Hybaid). Biotinylated allele-specific oligonucleotide probe (see table 2.5) was added (20-40ng/ml of hybridisation buffer) and hybridised for 120min at 42.5°C. Following hybridisation, the membranes were washed in 5x SSC with 0.1% SDS for 5min at room temperature. Each membrane was stringency washed twice in 1x SSC with 0.1% SDS for 15min at the optimised stringency wash temperature the probe (table 2.5). All subsequent steps were carried out at room temperature. The membrane was then soaked for 1min in buffer 1 (0.15M NaCl, 0.1M Tris) before blocking for 30-45min in buffer 1 with 0.5% dried skimmed milk (Marvel), on a slow rotation platform. Streptavidin-horseradish peroxidase conjugate (Amersham) was diluted 1:10,000 with buffer 1 and the membrane soaked in this reagent for 30min on a slowly rotating platform. Streptavidin will bind with high affinity to the biotinylated probe. Washing was then performed twice in 0.4M NaCl with 0.1M Tris for 10min. The membranes were blotted dry and covered in LumiGLO Substrate Kit for chemiluminescent detection of horseradish peroxidase-labelled reagents (Kirkegaard & Perry Laboratories). Substrate A and substrate B (LumiGLO kit) were mixed in equal volumes. After 1min, the membranes were exposed to x-ray film (Kodak X-OMAT) for 10min and 2hour.

Oligo ID	Allele detected	Sequence	Tm	Stringency wash temp
DF11	-174G	5′-GTGTCTTGCGATGCTAAAG-3′	56°C	54°C
DF12	-174C	5′-CTTTAGCATGGCAAGACAC-3′	56°C	54°C
PW268	-597A	5′-ATTTGAGGATGGCCAGGC-3′	56°C	54°C
PW269	-597G	5′-CCTGGCCACCCTCAAATT-3′	56°C	54°C

Table 2.5. Sequence specific oligonucleotide probes for detection of –174 and –597 alleles of IL-6.
Oligonucleotides were synthesised to order with 5' biotinylated ends (Genosys).

2.8.3. Heteroduplex

This was carried out using a modified protocol of Morse et al., (1999).

Heteroduplex was used to genotype the –174 and –572 polymorphisms of IL-6. It involves amplification of a ~100bp region around the polymorphic site and then anneals the PCR product with a universal heteroduplex generator (UHG) that is the same sequence as the PCR product apart from 3-4 artificially inserted adenosine residues adjacent to the site of the polymorphism. This forms a loop in the DNA

structure at this site when PCR product is annealed, the exact conformation being influenced by the specific allele at the polymorphic site. With optimisation, the annealed products can be separated on a polyacrylamide gel to distinguish the alleles.

The sample DNA (200ng in 1µl) was amplified by PCR using primers –174F & R for the –174 heteroduplex and primers –572F & R for the –572 heteroduplex (section 2.5.2). Thirty-five cycles of PCR amplification were performed using an Applied Biosystems PE9700 thermal cycler. Specific UHG oligonucleotide for each heteroduplex (-174UHG, –572UHG, table 2.6) was amplified by PCR. 25pmol of UHG oligonucleotide was mixed with 5µl 10x *Taq* DNA polymerase buffer without $MgCl_2$ (100mM Tris pH9, 500mM KCl, 1.0% Triton X-100, Promega), 1.5mM $MgCl_2$, 0.2mM each dNTP, 250ng F & R primer, 0.5units *Taq* DNA polymerase (Promega), made up to 50µl with sterile distilled water. See table 2.6 for amplification cycle conditions for each UHG.

Oligo ID	Sequence, amplification primers and conditions
-174UHG	5′-TGGGGCTGATTGGAAACCTTATTAAGATTGTGCAATGTGAC... GTCCTTTAGCAT**C**AAAAGCAAGACACAACTAGGGGGAAAAGTGC... AGCTTAGGTCGTCATTGAGGCTAGCGCTAAGAAGC-3′ Primers: –174F & R (see table 2.2) Cycles: 95°C/5min (x1), 95°C/30sec, 60°C/30sec, 72°C/30sec (x25), 72°C/5min (x1)
-572UHG	5′-GCCTGGGATTATGAAGAAGGTAATACTACCAGTCATCTGAG... TTCTTCTGTGTTCTGGCTCTCCCTGTGAGAAAA**C**GGCTGTTGTA... GAACTGCCTGGCCACCCTCAAATTTCGTGCAGTTACTTCAAGGC... G-3′ Primers: –572F & R (see table 2.2) Cycles: 95°C/5min (x1), 95°C/45sec, 54°C/45sec, 72°C/45sec (x25), 72°C/5min (x1)

Table 2.6. Universal heteroduplex oligonucleotides for the –174 and –572 polymorphisms of IL-6.
Oligonucleotides were obtained synthesised to order by MWG Biotech (high purity salt free). The artificially added adenosine bases are indicated in blue lettering, the polymorphic site is underlined in bold.

PCR and UHG products were run on 2.5% agarose gel (see 2.3.1) to ensure equal concentrations of each. For induction of the heteroduplex, 8µl UHG was mixed with

8µl of PCR product, heated to 95°C for 5min and allowed to cool slowly to room temperature. 5µl of 6x blue/orange loading dye (Promega) was added and the samples loaded and run on a prepared 15% non-denaturing vertical polyacrylamide gel (37.5:1 ratio) in 1x TBE* (see 2.3.2). This was run using a Bio-Rad tank and gel plates at 200V for 5-6 hours. The gel was then stained with ethidium bromide and photographed under UV light (see figure 2.6).

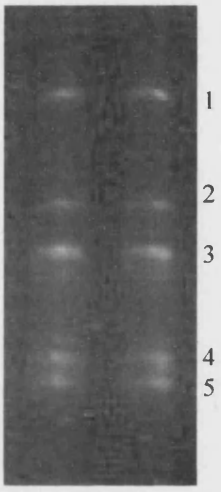

Figure 2.6. Optimised heteroduplex bands for the –174 polymorphism of IL-6.
-174UHG product (see text above) was mixed in equal volumes with PCR product using primers – 174F&R (see section 2.5.2). This was heated to 95°C for 5min and cooled slowly. Separation was on a 15% non-denaturing polyacrylamide gel (37.5:1 ratio), run in 1xTBE at 200V for 5hours.
Band 1= -174G (1 strand) annealed to UHG, 2= -174C (1 strand) annealed to UHG, 3= UHG annealed to UHG, 4=-174C (2nd strand) annealed to UHG, 5=-174 (2^{nd} strand) annealed to UHG.

2.8.4. DNA sequencing

2.8.4.1. Manual T7 sequenase sequencing

To confirm plasmid insert sequence and orientation in the PGL3 basic vector, manual sequencing was undertaken using the T7 Sequenase Sequencing Kit (Amersham Life Science). To prepare the DNA template, 2µg of test plasmid (from mini-prep or maxi-prep) in 16µl sterile distilled water was denatured with 4µl of 1mM EDTA & 1M NaOH mix, incubated for 5min at room temperature. The solution was neutralised with 2µl of 2M NH_4Ac (pH 5.4) and precipitated by the addition of 55µl absolute ethanol, incubated on dry ice for 15min, then pelleted by micro-centrifugation. The pellet was washed twice in 70% ethanol, dried and re-suspended in 5.5µl of distilled water.

For the annealing reaction, the re-suspended DNA was mixed with 5ng of sequencing primer (RV3 or GL2, table 2.2). 2µl of 5x T7 Sequenase Reaction Buffer was added and the mix incubated for at 65°C for 2min, then cooled slowly (over 20-30 min) to 35°C before placing on ice.

For the labelling reaction, 0.5µl of 1% Nonidet P40, 1µl of 0.1M DTT, 2µl of Labelling Mix (undiluted for >200bp sequencing, 1:5 dilution in water for shorter sequences), 0.5µl α^{35}S-dATP (1000Ci/mmol, Amersham) and 2µl of T7 sequenase polymerase (1:8 dilution in sequenase dilution buffer) were added to the primer annealed template. The reaction was mixed and incubated at room temperature for 2-5min (2min for sequences <200bp, 3min for sequences 200-300bp & 5min for sequences >300bp). 1µl of 0.1M $MnCl_2$ (in 0.15M sodium isocitrate) was added at the end of the incubation and 3.5µl of this mix was then added to each of four tubes containing 2.5µl of dideoxynucleotides ddGTP, ddATP, ddTTP and ddCTP respectively. This termination reaction was incubated at 37°C for 5min, after which 4µl of Stop Solution was added to each tube. Prior to running these on the sequencing gel, each mix was denatured by heating to 90°C for 2min.

The 'G', 'A', 'T' and 'C' reactions were run on a pre-prepared 6% polyacrylamide gel made with 40ml of SequaGel-6 acrylamide monomer (National Diagnostics) mixed with 10ml of SequaGel Complete Buffer Reagent (National Diagnostics). 400µl of fresh 10% ammonium persulphate (to initiate polymerisation) was added immediately prior to pouring the gel between glass plates (pre-washed with detergent and then ethanol) separated by 0.4mm spacers. The gel was allowed to polymerise for 45-90min, then pre-heated to 50°C by electrophoresis in 1x TBE* (1.5 volts per cm) on a Flowgen Sequencing Gel System, before the sequencing reactions were run. Longer sequencing reactions (>200bp) were loaded first and run for 4-6 hours compared to shorter sequencing reactions run for 2-4 hours. The gel was fixed for 5min in 40% glacial acetic acid with 40% ethanol, dried on a vacuum drier and exposed to x-ray film (X-OMAT, Kodak) for 1-2 days at room temperature. The sequence was read as a ladder produced by the random incorporation of termination dideoxynucleotides along the synthesised strand.

2.8.4.2. Automated thermocycle sequencing

The direct sequencing method of the Thermo Sequenase II Dye Terminator Cycle Sequencing Kit (Amersham Life Science) was used to sequence the IL-6 AT-tract from genomic DNA samples or plasmid constructs, and to sequence the 1.17kb insert of IL-6 in the pGEM vector and then in the pGL3 basic vector after site-directed mutagenesis. A list of the oligonucleotide primers used is shown in table 2.7.

800ng of plasmid DNA (mini- or maxi-prep) or 1μg of gel purified PCR product (from genomic DNA) in 8μl sterile distilled water was mixed with 2μl of reagent mix A (containing Thermo Sequenase II DNA polymerase) and 2μl of reagent mix B (containing dNTPs in excess, and dye-labelled termination ddNTPs). There was a different fluorescing colour label for ddATP, ddTTP, ddGTP and ddCTP. 5pM of primer in distilled water (2.5μl) was added (see table 2.7) and the total reaction volume was made up to 20μl with sterile distilled water. The reaction was pulse spun in a micro-centrifuge before thermal cycling for 25 cycles at 96°C for 30sec, 50°C for 15sec and 60°C for 60sec using an Applied Biosystems PE9700 thermal cycler. At the end of thermal cycling, 2μl of 1.5M NaAc pH>8 with 250mM EDTA was added and mixed to stop the reaction. 20μl of the mix was removed and DNA precipitated in 66μl of absolute ethanol on ice for 20min. Un-incorporated dNTPs and ddNTPs would remain in suspension. The DNA was pelleted by micro-centrifugation at 12,000rpm for 20min at 4°C. The pellet was washed twice in 250μl of cold 70% ethanol and re-pelleted at 12,000rpm for 10min before air-drying and re-suspended in 4μl of 90% (v/v) formamide and loading dye (Amersham). Before loading, the sequencing reaction was denatured by heating to 70°C for 2min and then immediately stored on ice. 1.5μl of sample was loaded onto a 6% polyacrylamide sequencing gel (see 2.8.4.1), pre-run in 1x TBE* using a Perkin-Elma ABI prism 377 DNA Sequencer. The samples were run over-night at 1V/cm (filter set A). As the incorporated termination ddNTPs from the DNA fragments passed the laser beam of the automated sequencer, the fluorescent dye emissions detected by the photodiode array detector were recorded. An example of the type of chromatogram that was generated by this method is shown in figure 2.7.

Primer ID	Sequence
Sequencing IL-6 insert from pGL3 basic vector	
RV3	5′-CTAGCAAAATAGGCTGTCCC-3′
GL2	5′-CTTTATGTTTTTGGCGTCTTCCA-3′
Sequencing 1.17kb IL-6 construct	
IL-6 Pro(1)F	5′- GGATCCTCCTGCAAGAGACACC-3′
IL-6 Pro(2)R	5′-CAGGGCAGAAAGGGGGAGATTAC-3′
IL-6 Pro(3)F	5′-CAAGGTCCTCCTTTGACATCCCC-3′
IL-6 Pro(4)R	5′-GTCTGCCATTTCTTCACCTGCTTC-3′
IL-6 Pro(5)F	5′-CCTACTGGAGATTCCAAGGGTCAC-3′
IL-6 Pro(6)R	5′-GAGTTTCCTCTGACTCCATCGCAG-3′
IL-6 Pro(7)F	5′-GAACTCAGATGACTGGTAGTATTACC-3′
IL-6 Pro(8)R	5′-CAGCACTTTGGCATGTCTTGAC-3′
IL-6 Pro(5b)F	5′-GGAGACGCCTTGAAGTAACTGC-3′
Sequencing IL-6 AT-tract	
AT1 F	5′-TCACAGGGAGAGCCAGAACA-3′
AT2 R	5′-TGCAGCTTAGGTCGTCATTG-3′

Table 2.7. Oligonucleotide primers used for sequencing.
Synthesised to order by Genosys. The F (forward) and R (reverse) suffix at the end of each primer ID indicates sequencing of the sense and anti-sense DNA strands respectively.

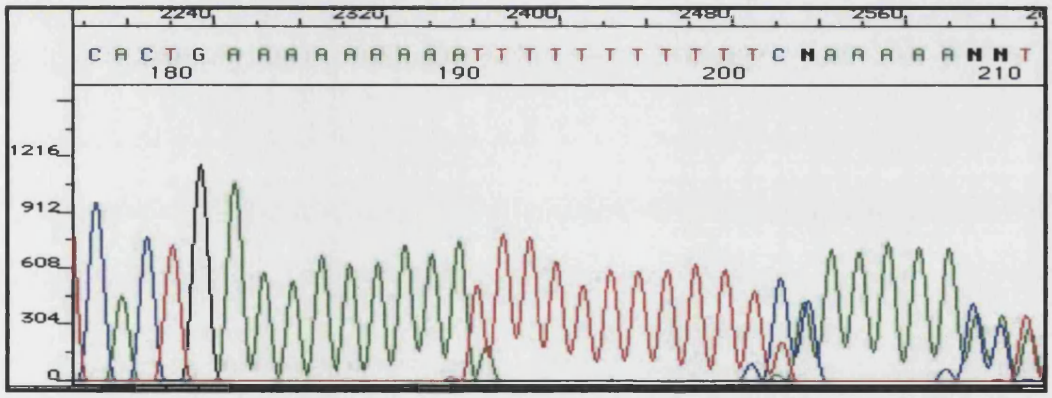

Figure 2.7. Automated sequencing chromatogram for the A9T11 allele of IL-6.
Sequencing was carried out using the Thermo Sequenase II Dye Terminator Cycle Sequencing Kit (Amersham Life Science) and run on a Perkin-Elma ABI prism 377 DNA Sequencer (6% polyacrylamide sequencing gel). See above text for details.

Later samples were sent for commercial sequencing by MWG Biotech.

2.9. Plasmid manipulation

2.9.1. Generation of 611bp and deletion mutant IL-6 reporter constructs

This had been carried out by D. Fishman prior to this study (Fishman et al., 1998). In brief, the IL-6 sequence from known –174GG and –174CC homozygous individuals (otherwise identical in IL-6 sequence from +70 to –560 as determined by automated sequencing) were amplified using PCR primers 5/2 (5'-CAGAAGAACTCAGATGAC

TGG-3') and 3/2 (5'-GCTGGGCTCCTGGAGGGG-3'). Fresh PCR product was sub-cloned into the pCRII vector (TA cloning kit, Invitrogen) utilising the single stranded deoxyadenosine residues at the 3'-end of the *Taq* polymerase synthesized PCR product and the single stranded deoxythymidine residue overhang in the linear vector. 4U of T4 DNA ligase was used with a 1:1 molar ratio of PCR product (1µl) to vector, 2µl 10x buffer L (500mM Tris pH7.8, 100mM $MgCl_2$, 200mM DTT), 4µl 10mM ATP and 3µl water, at 14°C overnight (~15hrs). Successful cloning was confirmed by X-gal and ampicillin selection on agar plates after transformation into 'One-Shot' *E. coli* (see sections 2.9.8.5&7). The clone was isolated and purified by mini-prep plasmid preparation (see 2.9.6.1) and provided a high quality PCR template for further manipulations. The inserted sequence was confirmed by automated sequencing.

In a second step, the IL-6 insert was amplified from pCRII containing the –174G or –174C allele using primers DF5/2D (5'-TATGCGAGGTAC˅CAGAAGAACTCAGAT GACTGG-3') and DF3/2D (5'-AGTTAAT˅CTAGATATGCTGGGCTCCTGGAGG GG-3'). This generated PCR fragment from +61 to –550 of the IL-6 sequence, constructs ΔG and ΔC (see figure 4.1). The primers had been designed to contain the restriction site sequence for *Kpn*I at the 5'-end (DF5/2D) and for *Xba*I at the 3'-end (DF3/2D), (extra sequence shown in purple, ˅ indicates cut site). This facilitated direction specific cloning into the PGL3 basic vector between the *Kpn*I and *Nhe*I cloning sites (figure 4.1). Ends generated by *Xba*I can be directly ligated to ends generated by *Nhe*I, though the recognition sites are lost in the product. The IL-6 PCR product was digested with *Kpn*I and *Xba*I, separated from the plasmid on a 1% agarose gel (see 2.3.1), isolated and purified using the Qiagen Qiaex II kit (see 2.5.4) and ligated with T4 DNA ligase as above into the PGL3 basic vector that had been linearised with *Kpn*I and *Nhe*I digestion.

For the shorter deletion mutant constructs, the same method was used with 3'-end primer DF3/2D and alternative 5'-end primers. For constructs ΔGD and ΔCD (IL-6 region +61 to –310) the 5'-end primer DFΔAT (5'-ACTGGTGGTAC˅CAAGACATG CCAAAGTG-3') was used, while for constructs ΔGDS and ΔCDS (IL-6 region +61 to –219) the 5'-end primer DF5/2DS (5'-GACCTGTAGGTAC˅CTCAATGACGACCT AAGCTG-3') was used. Each 5'-end primer contained the *Kpn*I recognition sequence (shown in purple, ˅ indicates the cut site).

2.9.2. Confirmation of successful cloning and plasmid construct identity

Clones were selected from agar plate colonies, isolated and purified by the mini-prep method (see 2.5.4). Confirmation of cloning success into PGL3 basic was carried out by insert removal and size determination with *Not*I and *Bgl*II digestion (cut sites on either side of where the insert should be), linearisation of the plasmid with *Aat*II digestion (cuts once only within the IL-6 insert) and by automated sequencing across the insert (figure 2.8a&b). The region was also amplified by PCR using primers RV3 and GL2 for regions of the pGL3 basic vector on either side of the insert (see section 2.5.2). This allowed digestion of the PCR product with *Nla*III or *SfaN*I to confirm the –174 allele (figure 2.8c&d), providing a quicker method than repeat sequencing after each amplification step. Large quantities of transfection grade plasmid were amplified using the standard alkaline-lysis maxi-prep method with caesium chloride purification (see 2.9.6.2 & 2.9.7) followed by repeat verification of the construct identity as outlined above.

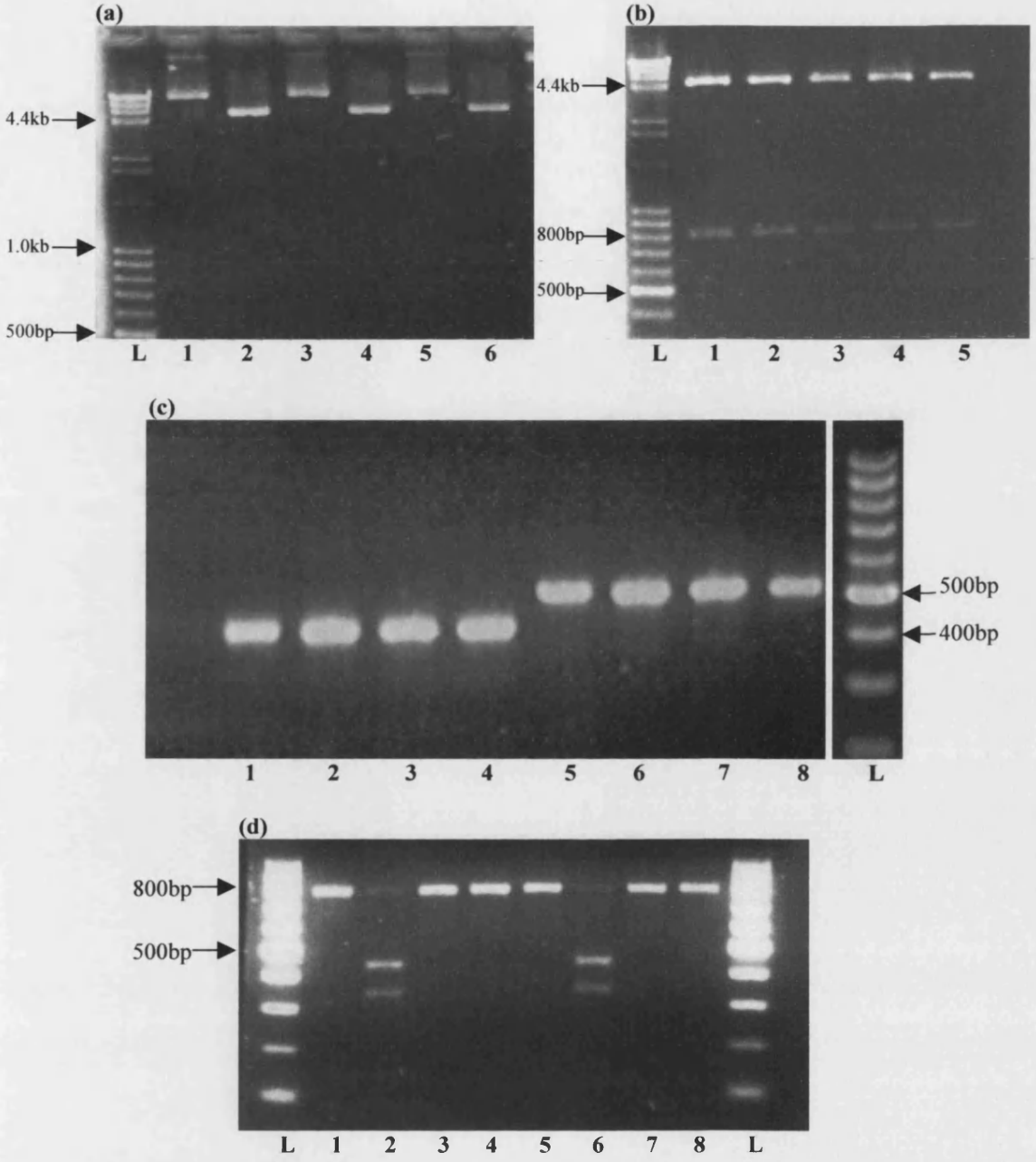

Figure 2.8. Confirmation of construct identity in PGL3 basic vector

(a) plasmid digested with *Aat*II (see 2.7).

Lane 1, 3 &5=undigested product; 2, 4 & 6=digested product (5.3kb, *Aat*II cuts only if IL-6 insert present).

(b) insert digested out with *Bgl*II & *Not*I restriction endonucleases (see section 2.7).

Lane 1, 3&5=ΔG, 2&4=ΔC (814bp).

(c) PCR amplification of insert using RV3 & GL2 primers (see section 2.5.2).

Lane 1&2=ΔGDS construct (427bp), 3&4=ΔCDS (427bp), 5&6=ΔGD (518bp), 7&8=ΔCD (518bp).

(d) PCR amplification of IL-6 insert in PGL3 basic vector, (primers RV3&GL2), followed by *SfaN*I digestion (see 2.7).

Lane 1&5=ΔG (undigested, 758bp), 2&6=ΔG (digested, 427&331bp), 3&7=ΔC (undigested, 758bp), 4&8=ΔC (digested, 758bp). L=100bp DNA ladder (Promega).

2.9.3. Quantification of plasmid DNA

The concentration of serial dilutions of purified plasmid DNA in water was determined by optical density at 260nm and 280nm (Hitachi U-1100 Tungsten UV spectrophotometer with 10mm path length quartz cuvettes) against a reference sample of diluted buffer. The concentration of nucleic acid can be calculated from the equation:

ds-DNA concentration (μg/ml) = 50(constant for dsDNA) x dilution factor x OD_{260}

That is, an OD_{260} of 1 is equal to approximately 50μg/ml for double-stranded DNA (40μg/ml for single-stranded DNA). The purity of the DNA sample can be calculated from the OD_{260}/OD_{280} ratio. A pure sample of DNA has an absorbance ratio of 1.8, while the absorbance ratio for pure RNA is 2.0. A purity ratio of 1.65-1.85 was required. Plasmid stocks were diluted to 1μg/μl with water and repeat spectrophotometry performed at 260nm. In addition, aliquots of diluted plasmid, and *Aat*II digested, linearised plasmid were run on a 0.8% agarose gel and photographed under UV light to ensure dilutions were equivalent. Diluted stocks were stored at –20°C.

2.9.4. Generation of the 1.17kb IL-6 reporter constructs

A 3kb IL-6 construct from +2000 to –1170 with flanking *BamH*I sites inserted into the pGEM vector (Promega, see figure 2.9) was a kind gift from S. Akira and T. Kishimoto of the Institute of Molecular and Cellular Biology, Osaka University, Japan. The sequence was verified by automated sequencing using the primers shown in table 2.7. A 1.17kb portion of the construct from +8 to –1170 was removed from pGEM by digestion with *BamH*I & *Xho*I and sub-cloned into pBluescript.SK phagemid (Stratagene). This allowed selection of the *Sac*I digestion site, not available from pGEM, for cloning into the pGL3basic vector (Promega). The construct was cut from pBluescript with restriction enzymes *Xho*I & *Sac*I and ligated into pGL3 basic between the *Xho*I & *Sac*I cloning sites (figure 2.9), using equal molar ratios of insert to vector with T4 DNA ligase as for the short constructs (see 2.9.1). Successful cloning was verified as outlined in section 2.9.2. PCR products were digested with *Mbi*I, *Fok*I, *Nla*III or *SfaN*I to confirm the allelic identities (see 2.7).

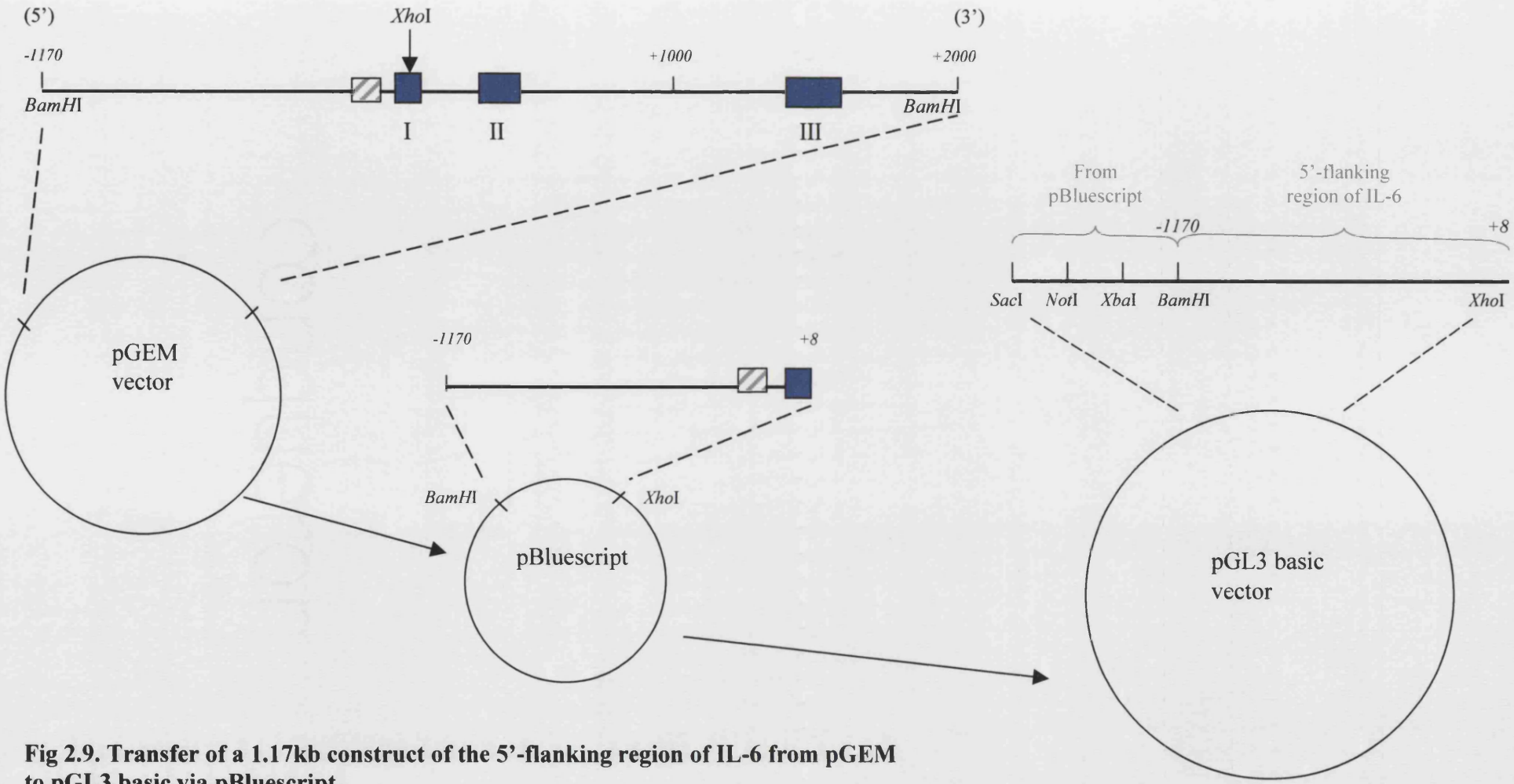

Fig 2.9. Transfer of a 1.17kb construct of the 5'-flanking region of IL-6 from pGEM to pGL3 basic via pBluescript.

A 1.17kb fragment of the 5'-flanking region of the IL-6 gene was cut from the 3kb construct in pGEM by digestion with *BamH*I & *Xho*I. This fragment was cloned into pBluescript between the *BamH*I and *Xho*I sites of the polycloning region. The fragment was removed from pBluescript by digestion with *Xho*I & *Sac*I and cloned into pGL3 basic between the *Xho*I & *Sac*I sites (for plasmid map see figure 4.1).

Automated sequencing across the insert was carried out to ensure no additional mutations had been introduced and to confirm orientation. Transfection-grade amplification and quantification of the plasmid was as for the short constructs.

2.9.5. Site-directed mutagenesis

To generate different –174/–572/–597 haplotypes from the 1.17kb clone obtained from S. Akira and T. Kishimoto, which was –174G[A9T11]–572G–597G, site-directed mutagenesis was carried out on the purified construct in pGL3 basic.

2.9.5.1. Quikchange

For the –174, -572 and –597 point mutations, the Quikchange site-directed mutagenesis kit (Stratagene) was used and is based on PCR with mutation primers to introduce the base change. Manufacturers instructions were followed and carried out directly on the supercoiled double-stranded DNA plasmid. Primers were designed to contain the desired base change for each site in the forward and reverse strand sequence (see table 2.8). The primers were incorporated in the PCR reaction one pair at a time, dependent on what haplotype combination was required. Extension of the primers was carried out with *Pfu* DNA polymerase. Following PCR, the parental DNA template was removed by digestion with *Dpn*1 endonuclease that is specific for methylated and hemi-methylated DNA. The parental DNA, isolated from *E. coli* would be dam methylated and susceptible to digestion whereas the freshly synthesised mutated DNA would not. The synthesised, mutated DNA was transformed into XL1-Blue supercompetent cells and selected on LB-plates containing ampicillin (see 2.9.8.6). Positive colonies were picked and the plasmid isolated and purified by mini-prep (see 2.9.6.1). Confirmation of successful mutation without introduction of other changes was carried out by automated sequencing across the region (see 2.4.8.2). Repeat PCR mutation steps were carried out for haplotypes requiring mutation at more than one site. This was carried out in collaboration with L. Luong in the department of Cardiovascular Genetics at University College London to obtain the three additional haplotypes, –174G–572G–597A, –174C–572G–597A and –174G–572C–597G. For some reason the haplotype –174C–572G–597G could not be generated on repeated attempts. The –174C–572G–597A haplotype was generated by first mutating the –597 allele and then mutating the –174 allele.

Primer ID	Sequence
IL-6 –174C MutF	5′-CTAGTTGTGTCTTGC**C**ATGCTAAAGGACGT-3′
IL-6 –174C MutR	5′-ACGTCCTTTAGCAT**G**GCAAGACACAACTAG-3′
IL-6 –572C MutF	5′-GTTCTACAACAGCC**C**CTCACAGGGAGAGCC-3′
IL-6 –572C MutR	5′-GGCTCTCCCTGTGAG**G**GGCTGTTGTAGAAC-3′
IL-6 –597A MutF	5′-ACTGCACGAAATTTGAGG**A**TGGCCAGGCAGTTCTAC-3′
IL-6 –597A MutR	5′-GTAGAACTGCCTGGCCA**T**CCTCAAATTTCGTGCAGT-3′

Table 2.8. Site-directed mutagenesis primer pairs for the -174, -572 and –597 polymorphisms.
Primers were synthesised to order by Genosys. The introduced mutagenic nucleotide bases are underlined in bold.

2.9.5.2. Transformer site-directed mutagenesis

Site-directed mutagenesis and amplification based on the Quikchange PCR technique could not be used for single base changes in the AT-tract because this low GC residue region did not allow for a primer design with a high enough Tm to allow cyclical annealing and extension. A transformer site-directed mutagenesis system was therefore designed based on the Clontech Transformer Site-Directed Mutagenesis kit using a protocol adapted from Deng and Nickoloff (1992). In this method, two oligonucleotide primers were simultaneously annealed to denatured plasmid construct DNA. The mutagenic primer (AT601F) contained the desired AT-tract mutation, while the selection primer (PGB1F) introduced a mutation to a unique restriction site in the plasmid, (see table 2.9 for primer sequences). A 200-fold excess molar ratio of primer to plasmid was used, with the amounts required calculated from the equation:

pmoles DNA = (μg DNAx10^6)/(330 x primer length in bp)

Mutation of the restriction site from *Sal*I to *Sst*II allowed selection of the mutated plasmid strand. A series of transformations and digestions allowed selection and isolation of mutated plasmid. Transformation efficiency is lost with linearised parental plasmid on digestion with *Sal*I. The primer/plasmid mix was denatured by boiling in annealing buffer (20mM Tris-HCl pH7.5, 10mM $MgCl_2$, 50mM NaCl) then annealed on ice. Synthesis of the mutant strand was as per manufacturers instructions (Clontech Transformer Site-Directed Mutagenesis kit), 2-4U T4 DNA polymerase and 4-6U T4 DNA ligase were used. The synthesis reaction contained a mixture of parental homozygous plasmid and heterozygous parental/mutant synthesised plasmid. This was in a 30μl volume of ≥6mM Tris-HCl, 6.7mM $MgCl_2$ and 33.3mM NaCl. 3.1μl of 10 x buffer D (see table 2.3), 6.4μl water and 5U *Sal*I were added and digestion allowed to

proceed for 2 hours at 37°C. This would linearise the parental DNA and reduce efficiency of transformation to <1% of the non-linearised plasmid (pre-determined). Transformation was into BMH 71-18 mutS cells (see section 2.9.8.4). Transformed plasmid was then isolated and purified by mini-prep (see 2.9.6.1). The synthesis step was repeated using the complementary mutation and selection primers (AT601R & PGB1R, table 2.9) and then a second *Sal*I digestion with 10U of endonuclease was carried out to yield homozygous mutant plasmids and nicked or linearised parental DNA. This was transformed into 'One Shot' competent *E. coli* and selected on ampicillin-containing agar plates (see 2.9.8.5). Mini-preps of isolated colonies were digested with *Sst*II and successful mutation to incorporate this new restriction site was detected on 1% agarose gel separation. Preparations that were identified as successfully mutated for the *Sst*II selection site were sequenced for the AT-tract using automated sequencing (see 2.4.8.2).

Primer ID	Sequence 5' to 3'	Desired change
AT601F	P-ATCTGGTCACTGAAAAAAAA**T**TT... ...TTTTTTTTTCAAAAAACATAGC	A9T11 to A8T12
AT601R	P-GCTATGTTTTTTGAAAAAAAAAA... ...A**A**TTTTTTTTCAGTGACCAGAT	Generation of second strand for A8T12 mutated strands
PGB1F	P-GATAAGGATCCG**CG**GACCGATGCCCT	*Sal*I site (GTCGAC) to *Sst*II site (CCGCGG)
PGB1R	P-AGGGCATCGGTC**CG**CGGATCCTTATC	Generation of second strand for *Sst*II mutated strand

Table 2.9. Mutation and selection primers for AT-tract site-directed mutagenesis.
Primers were synthesised to order by Genosys with phosphorylated 5'-ends. The introduced mutated nucleotide bases are underlined in bold.

2.9.6. Isolation of plasmid DNA by the alkaline lysis method

These methods were modified from the procedure of Birnboim and Doly (1979).

2.9.6.1. Small scale purification of plasmid DNA (mini-prep)

Small scale sequencing grade plasmid DNA was prepared using the Wizard plus mini-prep DNA purification system (Promega) according to Manufacturer's instructions. A single transformed bacterial colony was picked and inoculated into 5ml of LB media* containing 100μg/ml ampicillin* and incubated (at 37°C), whilst shaking for 6-8 hours to a cell density of ~ 1 x 10^9 cells/ml (determined by optical density at 600nm, see section 2.9.8.3). 1.5ml of this culture was transferred to an eppendorf tube and pelleted by centrifugation at 1,200g for 5min at room temperature. This was re-suspended in 200μl of re-suspension solution (50mM Tris-HCl pH8.0, 10mM EDTA pH8.0 & 100μl/ml RNAse A) then 200μl of alkaline cell lysis solution (200mM NaOH, 1% SDS) was added and thoroughly mixed until the solution became clear. 200μl of neutralisation solution (3M KAc pH5.5) was added, precipitating the bacterial cell debris that was then pelleted by centrifugation at 10,000g for 5min. The resultant supernatant was applied to a Wizard mini-prep column containing 1ml of DNA binding resin (Promega kit). The solution was drawn through the column by means of a vacuum pump and washed with 2ml of ethanol based column wash (200mM NaCl, 20mM Tris-HCl pH7.5, 5mM EDTA & 55% ethanol) to remove RNA, proteins and low molecular weight impurities. The plasmid DNA was eluted from the column with 50μl of TE buffer pre-heated to 70°C and collected into a fresh eppendorf tube by centrifugation of the column at 10,000g for 20sec.

2.9.6.2. Large scale purification of plasmid DNA (maxi-prep)

Large scale, transfection grade (endotoxin-free) plasmid DNA was prepared using an in-house protocol. Transformed *E. coli* from a glycerol stock or a single bacterial colony grown on LB agar* containing 50μg/ml ampicillin (± X-gal/IPTG if blue/white selection was required, see 2.9.8.7) were inoculated into 7-10ml of LB media containing 100μg/ml ampicillin and incubated (at 37°C), shaking for 8-10 hours (until turbid). This starter culture was transferred to 500ml of Terrific-broth* containing 100μg/ml ampicillin, in a 2 litre conical flask. This was cultured for 12-16 hours at 37°C in the shaking incubator.

The 500ml culture was transferred to a 500ml centrifuge bottle and centrifuged in GS3 rotor (Sorvall) at 8000rpm for 5min at 4°C to pellet the bacteria. The supernatant was decanted and the bacterial pellet re-suspended and washed in 100ml cold STE (100mM NaCl, 10mM Tris pH8.0 & 1mM EDTA pH8.0). The suspension was re-centrifuged at 8000rpm for 5min at 4°C. The bacterial pellet was re-suspended in 18ml cold solution I (50mM glucose, 25mM Tris pH8.0 & 10mM EDTA pH8.0), gently mixed using a 5ml disposable pipette and transferred to a 250ml centrifuge bottle. 36ml of freshly made solution II (0.2M NaOH, 1% SDS) was added and after thorough mixing, was incubated for 10min at room temperature. Next 20ml cold solution III (3M KAc & 11.5% acetic acid) was added, vigorously mixed and incubated for 20min on ice. These steps lyse the bacterial cells and release the DNA plasmid into suspension. The flocculant suspension of plasmid and precipitated cell debris was centrifuged in SLA-1500 rotor (Sorvall) at 8000rpm for 15min at 4°C. The supernatant was carefully removed, filtered into clean 250ml centrifuge bottles, through fine nylon mesh to remove any remaining cellular debris. To the filtered plasmid suspension 0.6 volumes of propan-2-ol was added and incubated for 10min at room temperature. The mix was centrifuged at 10,000rpm for 15min at room temperature. The pellet of plasmid DNA was carefully rinsed twice with 70% ethanol and then air-dried before re-suspending in 8ml cold TE (10mM Tris pH8.0, 1mM EDTA pH8.0) overnight at 4°C. For transfection grade plasmid, very low in RNase and LPS content, the plasmid DNA was purified twice by caesium chloride gradient (see below).

2.9.7. Caesium chloride purification of plasmid DNA

8g of caesium chloride (CsCl, 1g/ml) was dissolved in the 8ml plasmid-DNA in TE buffer preparation, prepared by maxi-prep (see above). 150ml of ethidium bromide (10mg/ml) was added to label the DNA and complex with remaining bacterial proteins. The solution was gently transferred to Quickseal centrifuge tubes (Beckman) using a syringe (no plunger) and wide bore needle to avoid shearing of the plasmid DNA. The tubes were precision balanced and heat-sealed before ultracentrifugation in a 70.1Vti rotor (Beckman) at 60,000rpm for 20 hours at 20°C. Normally after centrifugation, two bands were visible under normal light. The thinner, upper band consisted of nicked circular plasmid DNA and linear bacterial (chromosomal) DNA, while the lower band consisted of closed circular plasmid DNA. A red pellet along the side or bottom of the tube consisted of ethidium bromide-RNA/protein precipitates. A 21-guage hypodermic

needle was inserted into the top of the tube to allow air to enter and then the lower band of circularised plasmid was removed with a 21-guage hypodermic needle and 1ml syringe (figure 2.10). This DNA was transferred to a clean Quickseal tube, made up with 1mg/ml CsCl in TE and ultracentrifuged for a second time as above. Often after this second purification, only one band of DNA (circularised) would be visible. The double purified, circularised plasmid DNA was removed from the Quickseal tube as before and the ethidium bromide extracted using TE-saturated butanol. 6-8 times volume of TE-saturated butanol was added to the DNA solution, the two phases mixed and the organic phase removed from the top. This was repeated ≥6 times until the pink colour had disappeared completely from the aqueous and organic phases. To precipitate the DNA from the CsCl solution, an equal volume of water was added followed by 2 volumes of 4M ammonium acetate (pH5.4) and cold ethanol to a volume of 70%. The DNA was precipitated on ice for at least 15min and then recovered by centrifugation in a Corex tube using the HB4 rotor (Sorvall) at 10,000rpm for 1hour at 4°C. The pellet was washed twice with cold 70% ethanol and air-dried before re-suspension in TE* and the DNA concentration determined by optical density at 260nm (see 2.9.3). Plasmid identity was verified by PCR and restriction enzyme digestion (see 2.9.2). Purified plasmid was stored at –20°C.

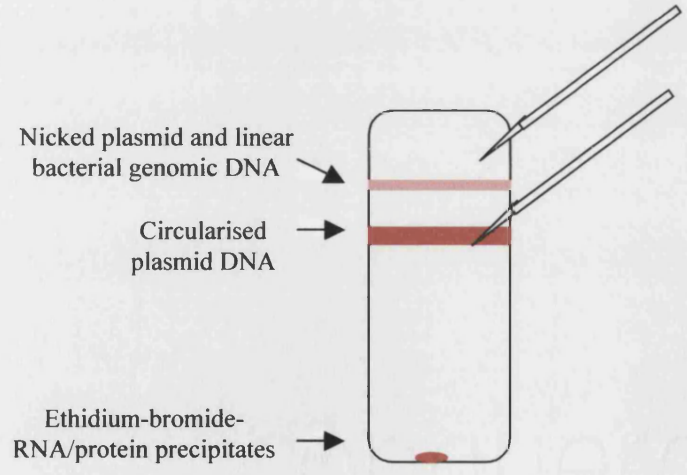

Figure 2.10. Isolating purified circularised plasmid DNA by CsCl ultra-centrifugation.
The plasmid prep in 1mg/ml CsCl/TE was ultra-centrifuged at 60,000rpm for 20hours at 20°C. The circularised plasmid DNA band was carefully aspirated using a 21-guage hypodermic needle.

2.9.8. Bacterial cell culture and transformation

2.9.8.1. *Escherichia coli* strains

Three strains of *E. coli* were used for transformations involved in genetic manipulation experiments. BMH 71-18 mutS *E. coli* (Clontech) were used for the transformer site-directed mutagenesis of the AT-tract. This strain has a Tn10 transposon carrying a tetracycline resistance gene inserted in its DNA mismatch repair gene, rendering it recombinase deficient so that induced mis-match mutations in the plasmid are not 'repaired' during transformation. These cells were received as non-competent and were made competent before transformation. The other two strains of *E. coli* were obtained already competent. The INVαF' *E. coli* strain (OneShot cells, Invitrogen) was used for sub-cloning and the XL-1 Blue *E. coli* strain (Stratagene) was used following PCR-based site-directed mutagenesis.

2.9.8.2. Culture medium and plates

Luria-Bertani (LB) medium (10g/l bactotryptone, 5g/l bacto-yeast extract, 10g/l NaCl in water, pH7.0, autoclaved to sterilise) was used to culture all three strains except for the maxi-prep method where high yield was required and Terrific-broth (48g/l EzMix Terrific broth base [Sigma], 0.8% glycerol in water, autoclaved to sterilise) was used. To culture single colonies, 20g/l of agar was added to the LB medium and autoclaved to sterilise. Approximately 25ml per 100mm petri dish was poured. For plasmid selection, once the mix had cooled to 50°C before pouring, the appropriate antibiotic (ampicillin 50μg/ml, tetracycline 50μg/ml, filter sterilised) was added, and X-gal plus IPTG (see 2.9.8.7) were added where blue/white selection was required. Bacterial cultures were streaked on to the agar plate and grown overnight, incubated at 37°C.

2.9.8.3. Preparation of competent BMH 71-18 mutS cells

BMH 71-18 mutS *E. coli* cells were made competent using a modified protocol of Chung and co-workers (1989). The supplied cells (Clontech) were cultured on an agar plate containing tetracycline (see above) to obtain single colonies. A single colony was picked and inoculated into 5ml LB* media containing tetracycline* (50μg/ml) and grown overnight at 37°C, shaking at 220rpm. 1ml of the overnight culture was transferred to 100ml LB media in a 500ml flask and incubated at 37°C for 2-3hours, whilst shaking. Serial aliquots were removed from 2 hours incubation and the optic

density determined at 600nm (Hitachi U-1100 Spectrophotometer). When the OD_{600} reached 0.45-0.50 (indicating optimal exponential cell growth), the culture was chilled on ice for 20min. The cells were then pelleted by centrifugation at 1,200g for 5min, at 4°C and the pellet re-suspended in 10ml cold transformation and storage solution (85% LB medium, 10% polyethylene glycol, 5% dimethyl sulphoxide and 50mM $MgCl_2$, filter sterilised). Aliquots of competent cells were stored at –80°C or used immediately for chemical transformation.

2.9.8.4. Transformation of competent BMH 71-18 mutS *E.coli*

10µl of plasmid DNA was gently mixed with 100µl of competent BMH 71-18 mutS cells (see above) and incubated on ice for 20min. This was followed by incubation at 42°C for 60sec before storage back on ice. 1ml of LB medium was added and cultured for 1hour at 37°C in the shaking incubator (220rpm) to allow expression of the antibiotic resistance gene. Transformation was confirmed by culture on LB-agar plate containing ampicillin (see 2.9.8.2) as the transformed plasmids contained an ampicillin resistance gene.

2.9.8.5. Transformation of INVαF' competent *E. coli*

2µl of 0.5M β-mercaptoethanol was added and gently mixed with a 50µl vial of OneShot (INVαF' *E. coli*, Invitrogen) cells thawed on ice. Plasmid DNA (1-25ng) was added and gently mixed, followed by incubation on ice for 30min, incubation at 42°C for 30sec and then incubation on ice again for 2min. 450ml of SOC medium (LB* media plus freshly added 1/100th volume 1M $MgSO_4$, 1M $MgCl_2$ & 2M glucose, filter sterilised) at room temperature was added and incubated at 37°C for 1hour, whilst shaking. Controls were included to estimate the transformation efficiency (0.1ng of supercoiled pUC test plasmid, supplied with the competent cells) and negative controls to check for contamination ('no DNA'). 1x, 0.1x and 0.01x dilutions were plated onto LB-agar plates containing ampicillin (see 2.9.8.2) and cultured overnight, up side down at 37°C to confirm transformation. The cells had a transformation efficiency of $>10^8$ transformants per µg of supercoiled plasmid. The transformed cells were stored as glycerol stocks (see 2.9.8.8), plasmid DNA was isolated and purified by one of the alkaline lysis methods (see 2.9.6).

2.9.8.6. Transformation of XL-1 Blue competent *E. coli*

1µl of *Dpn*1-treated DNA from the Quikchange Site-Directed Mutagenesis protocol (see 2.9.5.1) was added and gently mixed with 50µl of XL-1 Blue Supercompetent *E. coli* cells (Stratagene), thawed and incubated on ice for 30min. Transformation efficiency was determined by adding 0.1ng of pUC18 to a 50µl aliquot of cells. The reaction was heated to 42°C for 45secs and then incubated on ice for 2min. 500ml of NZY broth (5g/l bacto-yeast extract, 10g/l NZ amine (casein hydrolysate), freshly added 12.5ml 1M $MgCl_2$, 12.5ml 1M $MgSO_4$ & 20ml/l 20% glucose (w/v), pH7.5) was added and incubated for 1hour at 37°C, shaking (220rpm). Transformation was confirmed by plating 250µl of the transformation culture on an LB-agar plate containing ampicillin (see 2.9.8.2). Transformation efficiency was $>10^8$ cfu/µg of pUC18 (5µl of transformation culture was applied to the agar plate) with >98% blue phenotype colonies when plated on agar plates containing X-gal and IPTG (see below).

2.9.8.7. Blue/white colony selection with X-gal and IPTG

For plasmid selection, where cloning resulted in disruption of the *LacZ* gene and promoter association (such as construct ligation into the multi-cloning site of pCRII, see 2.9.1) loss of β-galactosidase activity from the plasmid indicated successful cloning. This was detected on LB-agar plates (see 2.9.8.2) containing X-gal (20µl of 10% (w/v) 5-bromo-4-chloro-3-indolyl-β-D-galactopyranoside in dimethylformamide) and IPTG (20µl of 100mM isopropyl-β-thiogalactopyranoside in water), filter sterilised. Colonies of bacteria that contain successful construct insertion appear white.

2.9.8.8. Glycerol stocks

For long-term storage of manipulated plasmids, glycerol stocks were made by addition of 20% sterile glycerol to transformed bacteria stock and stored at –80°C.

2.10. Mammalian cell culture and transfection

Mammalian cell culture used full sterile technique in a dedicated class I tissue culture hood. Cells were grown in Falcon tissue culture flasks (T25, T75 or T175) at 37°C under 5% CO_2: 95% air, in high humidity in a humidified incubator dedicated to mycoplasma-free tissue culture. HeLa cells (human cervical epithelioid carcinoma cell line) and Huh7 cells (human hepatoma cell line) were obtained from the European cell

bank and stocks maintained at fewer than 30 passages for transfection. Cells were maintained in Dulbecco's Modified Eagle's Medium (DMEM – high glucose, Gibco) supplemented with 10% (v/v) heat inactivated foetal calf serum (FCS, Globepharm), 2mM glutamine, 100IU/ml penicillin V, 100μg/ml streptomycin & gentamicin (Gibco), and 1mM non-essential amino acids (Sigma). Each additive was filter sterilised. When near confluent, the adherent cells were passaged by washing with warmed Hanks' balanced salt solution (0.185g/l $CaCl_2$, 0.4g/l KCl, 0.06g/l KH_2PO_4, 0.1g/l $MgCl_2$, 0.1g/l $MgSO_4$, 8g/l NaCl, 0.35g/l $NaHCO_3$, 0.048g/l Na_2HPO_4, 1g/l D-glucose, pH7.4 from Gibco) to remove the media. The cells were then covered with 3-5ml trypsin-EDTA (2.5g/l trypsin in Versene [0.015% phenol red, 140mM NaCl, 2.6mM KCl, 1.5mM KH_2PO_4, 9mM Na_2HPO_4, 600μM EDTA & 20mM HEPES, pH7.2] from Gibco) and incubated for 2-3min until the cells de-adhered. The cells were transferred to a 50ml Falcon tube, 2x volume of DMEM media containing FCS was added to neutralise the trypsin and the cells harvested by centrifugation at 1200rpm for 5min. The cell pellet was re-suspended in the required volume of warmed media and seeded into fresh culture flasks. A one in five cell split was usually required every 3-4 days to prevent cell overgrowth.

Frozen stocks were regularly prepared to ensure availability of low passage cells for transfection studies. The cells were grown to 80% confluency and harvested as described above. The cell pellet was then re-suspended in cold DMEM media containing 20% heat inactivated FCS and 10% dimethyl sulphoxide (DMSO, Sigma). 1ml aliquots were transferred to cryotubes (NUNC) and slowly cooled to –80°C over propan-2-ol. After 24 hours, these were transferred to liquid nitrogen for long-term storage. To revive cells, a vial was removed from liquid nitrogen storage, warmed for 1min at room temperature and then a further 1min at 37°C in a water bath after loosening and re-tightening the lid to prevent explosion of the vial on warming. The thawed contents were mixed with 10ml of pre-warmed DMEM media containing 10% FCS in a falcon tube, pelleted at 1200rpm for 5min, re-suspended in media and seeded into a $80cm^2$ culture flask. The cells were grown at 37°C, 5% CO_2: 95% air, high humidity in a dedicated tissue culture incubator.

2.10.1. Transfection of HeLa and Huh7 cells

Cultured cells, of less than 30 passage, grown to 80-90% confluence in 80cm^2 flasks, were detached by trypsin-EDTA, pelleted, washed once with media and re-suspended in DMEM with 10% FCS to achieve a concentration of 10^5 viable cells per ml (see 2.10.3 for trypan blue stain for viability). The cells were seeded into 6-well (1ml per well) or 24-well (0.5ml per well) tissue culture plates (NUNC) and grown for 48hrs until ~80% confluent. The media was removed and replaced with fresh DMEM media containing 10% FCS. 2-3 hours later, the DNA-calcium phosphate precipitate in Hepes buffered saline (see 2.10.1.1) was applied drop-wise to each well. Incubation was continued for 18hrs. At this time, the media was removed and the adherent cells washed twice with warmed Hanks buffered salt solution (Gibco) to remove remaining precipitate debris and non-dead adherent cells. Fresh DMEM media containing 2% FCS was applied, this was considered as time zero for stimulation (where stripped FCS was used see preparation protocol section 2.10.2). If cytokine stimulation or dexamethasone inhibition was required, it was added in this change of media. The cytokines used were recombinant human IL-1β (800units/μl in sterile PBS with 0.1% BSA stabiliser; specific activity 2 x 10^8units/mg, Genzyme) and recombinant human TNFα (lyophilised from sterile PBS with BSA, reconstituted in sterile distilled water to 1.1 x 10^3units/μl; specific activity 1.1 x 10^8units/mg, R & D Systems). Cytokine aliquots were stored at –80°C for ≤6 months (with only one freeze-thaw). Dexamethasone was obtained in crystalline form (Sigma) and dissolved in ethanol to a 10^{-3}M stock solution (stored at –20°C for ≤1 month in aliquots used only once). In experiments with ethanol-dissolved dexamethasone, the presence of ethanol was controlled for by adding the equivalent volume of 100% ethanol to the media of cells in other wells.

After addition of media ± cytokine/dexamethasone, the cells were incubated for set lengths of time, variant from 2-24hrs. For time point zero samples, wells were harvested without the addition of media. At the set time point, cells were washed twice with cold Hank's buffered salt solution and harvested into 1 x lysis buffer (100μl, Promega), then stored at –80°C. Prior to assaying the lysed cellular contents for luciferase and β-galactosidase levels (see 2.10.4&5), the plates were thawed (freezing helped to ensure 100% cell lysis was achieved), cells scraped from the bottom of each

well, transferred to an eppendorf tube and cellular debris pelleted by pulse micro-centrifugation. The supernatant was assayed immediately.

2.10.1.1. Calcium phosphate precipitation of DNA for transfection

The technique was based on a modified protocol from Graham and van de Eb (1973) and Wigler et al. (1977).

8μg (1μg/μl stock) of test plasmid DNA and 2μg (1μg/μl stock) of RSV-β-gal plasmid was dissolved in 165μl TE (1mM Tris, 0.1mM EDTA) pH8.0. 25ml of 2M $CaCl_2$ was added, mixed thoroughly and this solution added drop-wise into 200μl of 2 x Hepes buffered saline (HBS, pH7.12) diluted from a stock of 10x HBS*, pH adjusted with NaOH. Precipitate formation and mixing was assisted by bubbling air through the solution. A fine opaque suspension should be obtained rather than large clumps of precipitate forming out of suspension. This was incubated for 30min at room temperature before applying drop-wise to the cells (250μl per well for 6-well plates, 120μl per well for 24-well plates).

2.10.2. Preparation of stripped FCS

This method used a protocol described by Fenske (1991).

For 500ml of heat inactivated FCS (Globepharm, from the same batch as the unstripped FCS) 500mg of activated charcoal and 50mg of dextran T70 were added, stirred for 30min, centrifuged at 1,500g for 15min to pellet the charcoal with bound dextran and the supernatant filter sterilised through a 0.22μm filter before use. Aliquots of the stripped FCS were stored at –20°C.

2.10.3. Determining cell viability

0.2% trypan blue solution was mixed in a 1:2 ratio with cells in media (up to 10^6 cells per ml), incubated at room temperature for 5min and then the number of cells counted in an improved Neubauer cell counting chamber (Hausser Scientific) under light microscope. Only dead cells take up the trypan blue dye over 5min incubation, so the ratio of dead (blue stained cells) to total cells can be determined. Only cell stocks ≥95% viable were used in experiments. The concentration of viable cells was

calculated as the average number of unstained cells per square of the counting chamber x dilution x 10^4 per ml.

2.10.4. Assay for luciferase expression

Luciferase levels were measured using luciferase assay system (Promega). 20µl of transfected cell lysate (section 2.10.1) was mixed with 100µl of luciferase assay substrate (reconstituted in luciferase assay buffer) and the luminescence produced was measured over 15sec intervals in a luminometer (BioOrbit 1253) using Stingray software (DazDaq) to record the results. This produced results in luminescent emission units for luciferase. The results were controlled for variation in transfection efficiency by dividing the luciferase luminescent emission units for luciferase by the β-galactosidase luminescent emission units (see below) for each sample. An average of these ratios was then calculated for replica wells and the standard deviation was determined (using Microsoft Excel). Results more than 2 standard deviations from the mean were excluded.

2.10.5. Assay for β-galactosidase expression

β-galactosidase expression from co-transfected plasmid was used as an internal control for transfection efficiency and level of cell activity. The background level of β-gal expression in un-transfected cells was negligible. β-galactosidase activity was assayed using Galacto-light Plus reporter gene assay for β-gal (Tropix). 20µl of cell lysate (2.10.1) was incubated for 1 hour at room temperature with 200µl of Galacton-Plus reagent (diluted 1:100 in Galacton reaction buffer diluent). 300µl of accelerator II was then added and the luminescence produced measured over 5sec intervals in a luminometer (BioOrbit 1253) with Stingray software (DazDaq). This produced luminescent emission units for β-galactosidase that were used to control luciferase luminescent emission units as described above.

2.10.6. In situ β-galactosidase activity assay

The efficiency of transfection was calculated by determination of the proportion of cells positive for β-galactosidase activity post-transfection with the plasmid RSV-β-gal (see 2.10.1). After transfection by calcium phosphate precipitation, the cells were washed 5x with phosphate buffered saline (PBS*) to remove untransfected precipitate.

The cells were then covered with 2% gluteraldehyde and fixed for 40min. The fix solution was removed and the cells covered with fresh stain solution (0.2% X-gal, 10mM sodium phosphate pH7.0, 1mM $MgCl_2$, 150mM NaCl, 3.3mM $K_4Fe(CN)_63H_2O$ and 3.3mM $K_4Fe(CN)_6$). The cells were incubated for 1hour at 37°C, the stain removed and the cells covered in 70% glycerol solution. The number of stained (β-galactosidase positive) cells per 100 cells present was counted under light microscope.

2.10.7. Fluorescence-activated cell sorter (FACS)

2.10.7.1. Carboxyfluorescein succinimidyl ester (CFSE) staining

To determine the rate of cell division of cell lines and to ensure that the cells were in log phase when being transfected, cells were stained with CFSE. 5-(and-6)-carboxyfluorescein diacetate, succinimidyl ester (CFDA SE) is colourless and nonfluorescent and diffuses passively into cells. Once in the cell, CFDA SE forms an amine-reactive carboxyfluorescein succinimidyl ester (CFSE) as its acetate groups are cleaved by intra-cellular esterases. The succinimidyl ester group of CFSE reacts with intracellular amines, to form a fluorescent conjugate that is well retained (up to 8 weeks in lymphocytes and for at least 20 days in hepatocytes). The label is inherited in a 1:1 ratio by daughter cells on division. The time for each division can therefore be calculated from the time taken for mean cell fluorescent intensity to halve (Lyons and Parish, 1994, Graziano et al., 1998).

CFDA SE (Molecular Probes) was reconstituted to a concentration of 5mM in DMSO. Adherent HeLa cells cultured in 6-well or 24-well plates were washed 3x in warmed PBS* to remove any traces of FCS remaining from the media. 2.5μM CFDA SE in warmed PBS (5μl of 5mM stock in DMSO per 10ml PBS) was applied to cover the cells and incubated at 37°C for 15min. The CFDA SE solution was removed and the cells washed 3x in warmed DMEM media containing 10% FCS. Incubation was then continued in DMEM media with 10% FCS. At the required time point post-staining, cells were harvested with trypsin/EDTA, pelleted by centrifugation at 1200rpm at 4°C for 5min and washed 2x in 5ml FACS buffer (1x PBS, 0.1% azide, 1% FCS). The cells were re-suspended in 100μl of fix buffer (FACS buffer with 0.1% formaldehyde). It had previously been established that cell fluorescence was not affected by fix buffer compared to FACS buffer and that fix buffer allowed the cells to be stored for up to

72hours at 4°C. Detection and analysis of percentage stained cells was carried out using a fluorescence-activated cell sorter (see 2.10.7.3).

2.10.7.2. Surface labelling of IL-1RI on HeLa and Huh7 cells

IL-1RI (CD121a) is the signal transduction molecule of the IL-1 receptor complex. HeLa and Huh7 cells were seeded into 24-well culture plates and grown to ~80% confluence as for transfection (see 2.10.1). The DMEM media was changed at 0hrs and contained either 2% FCS (unstripped) or 2% stripped FCS (see 2.10.2) ± IL-1β (100units/ml) ± dexamethasone (10^{-7}M) and incubation continued to the set time point. At this time, cells were washed with cold Hanks buffered salt solution to remove residual media and harvested into 1ml cold 0.2% EDTA with 10min incubation at 4°C. Cells were transferred to 15ml falcon tubes, pelleted at 1000rpm for 5min at 4°C and washed once in cold FACS buffer*. They were then transferred to the wells of a microtitre plate (~10^6cells per well) and pelleted at 1500rpm for 4min at 4°C. The cells were re-suspended in 100µl FACS buffer containing a 1:1, 1:2, 1:5 or 1:10 dilution of biotinylated rat anti-human IL-1R1 monoclonal antibody (anti-CD121a, Pharmingen) and were then incubated on ice for 30min. For secondary labelling with quantum red (QR) for fluorescent detection, the cells were pelleted again by centrifugation, washed 3x with FACS buffer and re-suspended in 100µl of FACS buffer containing a 1:40 dilution of QR-labelled avidin (Pharmingen), then incubated for 30min on ice (with light excluded). Cells were pelleted and washed 3x with FACS buffer, then re-suspended in 100µl of fix buffer (FACS buffer with 0.1% formaldehyde). Freshly isolated B-cells and monocytes from peripheral blood of healthy volunteers, with or without LPS stimulation (1µg/ml in RPMI media), were used as positive controls with anti-CD19PE (Phycoerythrin, Pharmingen) labelling of B-cells and anti-CD14FITC (Fluorescein isothiocynate, Pharmingen) labelling of monocytes/macrophages carried out (as above) before IL-1RI staining. Unstimulated T-cells, freshly isolated from the peripheral blood of healthy volunteers were used as 'negative' (low expressing) controls and were labelled with anti-CD3FITC (Pharmingen). Detection and analysis of percentage stained cells was carried out using a flow analyser cell sorter (figure 2.11 and section 2.10.7.3).

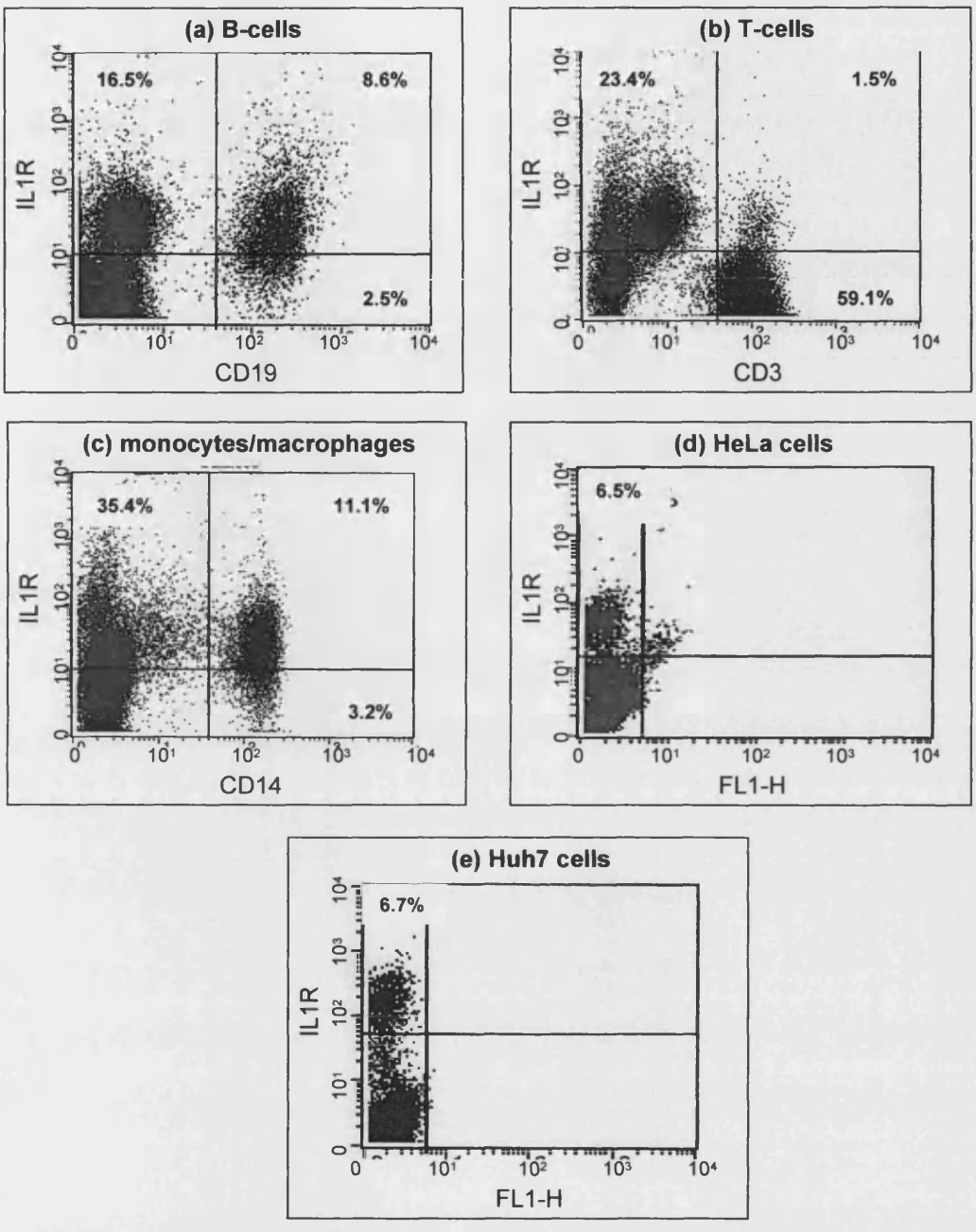

Figure 2.11. Constitutive levels of IL-1RI expression on freshly isolated peripheral blood (a) B-cells, (b) T-cells and (c) monocytes/macrophages compared to (d) HeLa and (e) Huh7 cells.

B-cells were labelled with anti-CD19PE, T-cells with anti-CD3FITC and monocytes/macrophages with anti-CD14FITC. All cells were labelled with biotin-conjugated rat anti-human IL-1RI (CD121a) mAb and avidin-quantum red (see 2.10.7.2). The cells were analysed by FACS (see 2.10.7.3). The percentage of gated cells positive for IL-1RI (quantum red) is shown on dot plot graph. The proportion of cells constitutively expressing IL-1RI was similar for cultured HeLa and Huh7 cells, 6.5% and 6.7% respectively. The proportion of B-cells and monocytes/macrophages constitutively expressing IL-1RI was 77.5% and 77.6% respectively. Only 0.03% of T-cells constitutively expressed detectable levels of IL-1RI.

2.10.7.3. FACS acquisition and analysis

Cell analysis and fluorescence detection of CFSE (see 2.10.7.1) and quantum red-tagged IL-1RI (see 2.10.7.2) labelled cells was carried out on a Becton-Dickinson FACSCAN with CellQuest software. The cells were analysed for size versus granularity (forward and side scatter properties) and the main cell population gated, this gate being maintained throughout the acquisition and analysis. The detector/amplifier settings were optimised for unstained HeLa cells and 0hr stained cells, and kept constant throughout. Up to 50,000 events were collected for each time point. Cells labelled in the same way, but finally re-suspended in FACS buffer* rather than fix, were incubated with a 1:20 ratio of propidium iodide (500μg/ml) to cell suspension for 5min at room temperature. This enabled confirmation that the gated cells were all viable and that the majority of outliers were dead cells as propidium iodide is taken up by dead cells.

2.10.8. Generation of stable transfected cell lines

Transfections were set up for HeLa cells as described in section 2.10.1. 10μg of test plasmid DNA and 0.5μg of antibiotic resistance expressing plasmid PSVneo (gift of Dr Fellowes, UCL) conferring resistance to G418 (a neomycin analogue) to allow selection of transfected cells, were transfected using the calcium phosphate precipitation method (2.10.1.1). The cells were transfected for 24 hours, washed with Hanks buffered salt solution and fresh DMEM media with 10% FCS applied. Incubation was continued for 12-18 hours to allow expression of the G418 resistance gene. The media was then changed to contain 800μg/μl G418, the optimum concentration determined to ensure 100% killing of HeLa cells without PSVneo transfection. The transfected HeLa cells were cultured in this G418 selection media until individual colonies started to re-appear. Individual colonies were picked using a pipette tip, transferred to individual wells and grown up in G418 selection media. Once adequate cell numbers from each colony were obtained, a sample of cells was tested for luciferase expression using the luciferase assay system (2.10.4) to ensure that the test plasmid and not just the antibiotic resistance plasmid had inserted into the cell line genome. Once established, stable transfectants were maintained in media containing 400μg/ml G418 or stored frozen in liquid nitrogen (see 2.10). Genomic DNA was isolated (see 2.2.2) from a sample of each luciferase-expressing colony and Southern

blot analysis was carried out (see 2.4). This allowed determination of the copy number of luciferase genes (and hence test construct) inserted into the genome of each clone.

For experiments with stable transfectants, an individual clone or 'pool' of clones (combined equal quantities of individual clones for one plasmid-construct type) were seeded at 10^5 cells/ml into 6-well tissue culture plates and grown in maintenance media (DMEM with 10% FCS and 400μg/ml G418). These were incubated over 48hrs to 80-90% confluence and then harvested or stimulated with cytokines or dexamethasone for set time-periods before harvesting into trypsin/EDTA as for transient transfections (see 2.10.1). The cytokines used were recombinant human IL-1β and TNFα (see 2.10.1), and recombinant human IL-6 up to 1000u/ml (obtained as lyophilised product from sterile PBS with BSA, reconstituted in sterile distilled water to 1.25 x 10^3 units/μl; specific activity 1.1 x 10^8 units/mg, R & D Systems). Lipopolysaccharide up to 10μg/ml (from 1mg/ml reconstituted in sterile DMEM, Sigma) and crystalline dexamethasone 10^{-7}M (see 2.10.1) were used.

2.11. Electrophoretic mobility shift assays

This technique was based on the methods of Fried and Crothers (1981), Garner and Revzin (1981).

2.11.1. Preparation of protein nuclear extracts

This used a method adapted from Dignam et al., (1983). HeLa cells were grown to 80% confluence in 175cm^2 tissue culture flasks (Gibco), washed twice with PBS* (calcium/magnesium free), then gently scraped from the flask with a rubber scrapper into ice cold PBS. The cells were pelleted by centrifugation at 1,200 rpm for 5 min at 4°C (Heraeus Instruments, Megafuge 2.0R) followed by a second wash in cold PBS. The pelleted cells were re-suspended in 5 times volume of ice cold buffer A containing freshly added protease inhibitors (10mM Hepes pH 7.8, 1.5mM $MgCl_2$, 60mM KCl, 10mM NaCl, 0.5mM EDTA, 0.5mM DTT, 50μg/ml AEBSF (4-[2-aminoethyl]benzenesulfonylfluoride HCl, CalBioChem), 1 tablet/50ml Complete Protease Inhibitor Cocktail (EDTA-free, Boehringer)), incubated for 10min on ice and then re-pelleted at 2,000rpm for 5 min at 4°C. The pelleted cells were re-suspended in 3 times volume of buffer A/protease inhibitors with 0.05% TritonX-100 (iso-

octylphenoxy polyethoxyethanol molecular biology grade, BDH) and kept on ice, while mechanically lysed using a Dounce A homogeniser (tight fitting pestle, Wheaton, USA). 90% cell lysis without nucleosome rupture was required (approximately 80-100 strokes), and checked for under light microscopy. The nuclear fraction of lysed cells was separated from the cytosol by centrifugation at 2,000rpm for 10min at 4°C. The nuclear pellet was re-suspended in an equal volume of buffer B containing freshly added protease inhibitors (40mM Hepes pH 7.8, 3mM $MgCl_2$, 0.5mM EDTA, 50% glycerol, 1mM DTT, 50µg/ml AEBSF, 1 tablet/50ml Complete Protease Inhibitor Cocktail). NaCl from a 5M stock was added to the desired final concentration (low salt extracts 10mM NaCl, medium salt extracts 150mM NaCl, high salt extracts 300mM NaCl). This was gently mixed on a rotary mixer at 4°C for 30min, then cellular debris removed by centrifugation at 14,000 rpm for 30min at 4°C in a bench-microfuge (eppendorf 5415C). The supernatant containing the nuclear proteins was carefully removed, snap frozen in liquid nitrogen in small aliquots and stored at -70°C. Each aliquot was only thawed once for use. Protein concentration was determined by BCA/copper sulphate reaction, read by spectrophotometer with a BSA standard (see 2.12.2).

2.11.2. Preparation of radiolabelled DNA probes

2.11.2.1. 5'-end labelling DNA probes

Sequence complementary, single-strand oligonucleotide probes were synthesised to order (see table 2.10). 40pM of single-stranded oligonucleotide was dissolved in 29µl of water, and mixed with 4µl of 10x kinase buffer (Promega; 700mM Tris-HCl pH 7.6, 100mM $MgCl_2$, 50mM DTT), 4µl of T4 polynucleotide kinase (Promega), and 3µl of $^{\gamma-32}$P-ATP (3000 Ci/mmol specific activity, Amersham). The mix was incubated for 40 min at 37°C, for 5 min at 65°C and stored on ice. 40µl of each complementary, end-labelled oligonucleotide was mixed with 20µl of SDW in an eppendorf, sealed and floated in a beaker of water pre-heated to 95°C, allowed slowly to cool to room temperature overnight to promote DNA annealing into double-stranded probes. Unincorporated radiolabel was removed by passing the annealed probe mix through a Sepharose 6CLB column-10 (Clontech) that retards ≤10bp particles. Purified probe was collected by centrifugation of the loaded column (3,000g for 3min). A specific activity of >500cpm/µl of probe was required.

2.11.2.2. Integrated second-strand labelling of DNA probes

DNA probes >30bp in length were radiolabelled by Klenow synthesis of a second strand to a DNA template sequence to obtain adequate specific activity for EMSA. 64pmol of single-stranded DNA template was annealed with 180pmol of a short complementary primer sequence (see table 2.10) by boiling together in a sealed tube for 3min, then cooling slowly to room temperature to allow annealing. In a microtube on ice, a mix was prepared of 2µl 20mM DTT, 5µl 2mM dATP/dTTP/dGTP mix, 2µl 10x RP buffer (900mM Hepes pH 6.6, 100mM $MgCl_2$), 3.5µl SDW and 5µl $^{\alpha 32}$P-dCTP (>3000Ci/mmol specific activity, Amersham). 1.5µl (64pmol) of annealed template/primer was added, followed by 1µl (5 units) of DNA polymerase I large (Klenow) fragment (Promega) and incubated at room temperature for 16 hours. 2.5µl of 2mM unlabelled-dCTP was subsequently added as a cold chase and incubated for 2 hours to ensure complete double-strand synthesis. The Klenow was deactivated by heating to 75°C for 10min before storing on ice. The probe mix was diluted in 100µl of TE* and purified by TE-30 Sepharose spin column (Clontech) to remove unincorporated primer and dNTPs, centrifugation at 3,000g for 3min.

Cold probes for competition studies were generated using the same method. In the initial incubation mix, 5µl of 2mM unlabelled dCTP was substituted for the radiolabelled dCTP and incubated as above. No cold chase was required but otherwise preparation was the same as for hot probes. Pre-purification, unlabelled probes were diluted in TE to obtain 3.33x concentration of radiolabelled probe.

2.11.3. Binding reaction

The binding reaction was carried out with 10µg of nuclear extract pre-incubated for 10mins at room temperature with 10µg of poly dI.dC (Amersham, 10µg/µl in dI.dC buffer*) in 10µl 2x Parker Buffer (16% Ficoll, 40mM Hepes pH 7.9, 100mM KCl, 2mM EDTA pH 8, 1mM DTT) made up to 19.5µl with SDW. 5pmol of radiolabelled probe in 0.5µl TE was added and incubated with the nuclear extract mix for 20min at 21°C. The binding reaction temperature was initially room temperature but as this was found to vary over a range of 5°C with effects on non-specific protein binding to the probe (see 5.2.1), the temperature was subsequently fixed at 21°C in a water bath.

Probe identity	Region of IL-6 gene / length	Allele(s)
1G	**-189 to –164 / 26bp**	**-174G**
5′-CTAGTTGTGTCTTGCGATGCTAAAGG-3′		
3′-GATCAACACAGAACGCTACGATTTCC-5′		
1C	**-189 to –164 / 26bp**	**-174C**
5′-CTAGTTGTGTCTTGCCATGCTAAAGG-3′		
3′-GATCAACACAGAACGGTACGATTTCC-5′		
2G	**-184 to –134 / 51bp**	**-174G**
5′-TGTGTCTTGCGATGCTAAAGGACGTCACATTGCACAATCTTAATAAGGTTT-3′		
3′-ACACAGAACGCTACGATTTCCTGCAGTGTAACGTGTTAGAATTATTCCAAA-5′		
2C	**-184 to –134 / 51bp**	**-174C**
5′-TGTGTCTTGCCATGCTAAAGGACGTCACATTGCACAATCTTAATAAGGTTT-3′		
3′-ACACAGAACGGTACGATTTCCTGCAGTGTAACGTGTTAGAATTATTCCAAA-5′		
3G	**-235 to –161 / 75bp**	**-174G**
5′-CTTCTTAGCGCTAGCCTCAATGACGACCTAAGCTGCACTTTT...		
3′-GAAGAATCGCGATCGGAGTTACTGCTGGATTCGACCTGAAAA...		
	...CCCCCTAGTTGTGTCTTGCGATGCTAAAGGACG-3′	
	...GGGGGATCAACACAGAACGCTACGATTTCCTGC-5′	
3C	**-235 to –161 / 75bp**	**-174C**
5′-CTTCTTAGCGCTAGCCTCAATGACGACCTAAGCTGCACTTTT...		
3′-GAAGAATCGCGATCGGAGTTACTGCTGGATTCGACCTGAAAA...		
	...CCCCCTAGTTGTGTCTTGCCATGCTAAAGGACG-3′	
	...GGGGGATCAACACAGAACGGTACGATTTCCTGC-5′	
4G	**-613 to –539 / 71bp**	**-597G/-572G**
5′-GCACGAAATTTGAGGGTGGCCAGGCAGTTCTACAACAGCCGC...		
3′-CGTGCTTTAAACTCCCACCGGTCCGTCAAGATGTTGTCGGCG...		
	...TCACAGGGAGAGCCAGAACACAGAAGAAC-3′	
	...AGTGTCCCTCTCGGTCTTGTGTCTTCTTG-5′	
4A	**-613 to –539 / 71bp**	**-597A/-572G**
5′-GCACGAAATTTGAGGATGGCCAGGCAGTTCTACAACAGCCGC...		
3′-CGTGCTTTAAACTCCTACCGGTCCGTCAAGATGTTGTCGGCG...		
	...TCACAGGGAGAGCCAGAACACAGAAGAAC-3′	
	...AGTGTCCCTCTCGGTCTTGTGTCTTCTTG-5′	

Table 2.10. The IL-6 5'-flanking region probes used for EMSA studies.
Red lettering = polymorphic alleles. Blue lettering = oligonucleotide primer sequences used for second strand synthesis. Underlined lettering = synthesised second strand.
Single-strand oligonucleotides and primers were synthesised to order by Genosys.

In the optimization process, different concentrations of poly (dI.dC).poly (dI.dC) were tried by varying the quantity at pre-incubation. Poly (dI.dC).poly (dI.dC) is a synthetic double-stranded polymer of inosine and cytosine (abbreviated to poly dI.dC, obtained from Amersham as a sodium salt) and will bind non-specifically to nuclear proteins such as histones. For probes 1G and 1C (table 2.10), an NF1 specific binding buffer

(final concentration 10% glycerol, 10mM Tris HCl, 0.5mM EDTA, 5mM $MgCl_2$, 50mM NaCl) was used in place of Parker buffer.

2.11.4. Cold competition and supershift studies

For cold-competition studies, unlabelled probe (see section 2.11.2.2) was used at 3.33x concentration of radiolabelled probe. Double-stranded, purified oligonucleotides of transcription factor consensus binding site sequences were obtained to order from Santa Cruz (20ng/µl) or MWG Biotech (1µg/µl), (table 2.11). These were used unlabelled in competition studies. 5pmol (0.5µl) of radiolabelled probe was mixed with unlabelled probe/oligonucleotide in TE to the required ratio, total volume 8µl. The ratios used were 1:0, 1:2, 1:5, 1:10, 1:20 and 1:50 radiolabelled (hot) to unlabelled (cold) probe. This mix was added in place of radiolabelled probe alone in the binding reaction (see 2.11.3) and incubated at 21°C for 20min. The total volume of the pre-incubation reaction was 20µl.

For supershift studies, 1.5µl of specific antibody (2µg/µl in PBS containing 0.1% sodium azide, Santa Cruz, see table 2.12) was added either 'before' or 'after' the binding reaction (total volume 20µl, see 2.11.3). If added 'before', it was added to the pre-incubation mix after the 10min incubation of nuclear extracts with polydI.dC and incubated at 21°C for 20min before addition of the radiolabelled probe. If antibody was added 'after', it was added after the addition and incubation of radiolabelled probe with nuclear extracts, and incubated for a further 20min at 21°C. The volume of SDW was altered to keep the total volume of the reaction at 20µl. During optimization antibody concentrations of 100-300ng/µl of reaction, an incubation temperature of 4°C instead of 21°C and lengths of incubation up to 60mins were also tried.

Probe identity	Transcription factor identified to bind	Probe length
C/EBP$^{\perp}$	**C/EBP family members**	**20bp**
5′-TGCAGATTGCGCAATCTGCA-3′		
3′-ACGTCTAACGCGTTAGACGT-5′		
CREB$^{\perp}$	**CREB/ATF family members**	**27bp**
5′-AGAGATTGCCTGACCTCAGAGAGCTAG-3′		
3′-TCTCTAACGGACTGGAGTCTCTCGATC-5′		
Glucocorticoid receptor$^{\perp}$	**GR**	**27bp**
5′-AGAGGATCTGTACAGGATGTTCTAGAT-3′		
3′-GCTCCTAGACATGTCCTACAAGATCTA-5′		
NF1 control$^{\Upsilon}$	**NF1**	**26bp**
5′-AAGGGATGGCTGCCAGCCAAGCATGA-3′		
3′-TTCCCTACCGACGGTCGGTTCGTACT-5′		
NF1 consensus 1 (NF1-1)$^{\perp}$	**NF1 family members**	**25bp**
5′-TTTTGGATTGAAGCCAATATGATAA-3′		
3′-AAAACCTAACTTCGGTTATACTATT-5′		
NF1 consensus 2 (NF1-2)$^{\Upsilon}$	**NF1 family members**	**25bp**
5′-TTTTGGATTGATGCCATTATGATAA-3′		
3′-AAAACCTAACTACGGTAATACTATT-5′		
NF1mut1$^{\perp}$	not NF1	**25bp**
5′-TTTTGGATTGAATAAAATATGATAA-3′		
3′-AAAACCTAACTTATTTTATACTATT-5′		
NF1mut2$^{\Upsilon}$	not NF1	**25bp**
5′-TTTTGGATTGATTAAATTATGATAA-3′		
3′-AAAACCTAACTAATTTAATACTATT-5′		
NF-κB$^{\perp}$	**NF-κB family members**	**22bp**
5′-AGTTGAGGGGACTTTCCCAGGC-3′		
3′-TCAACTCCCCTGAAAGGGTCCG-5′		
Random probe$^{\Upsilon}$	(a universal heteroduplex generator for an exonic portion of the IL-4 receptor gene around Q 576)	**93bp**
5′-CAGCTGCAGCCCCCGTCTCGGCCCCCACCAGTGGCTATCATTTGTACA...		
3′-GTCGACGTCGGGGGCAGAGCCGGGGGTGGTCACCGTATGTAAACATGT...		
...TGCGGTGGAGCAGGGTGGCACCCAGGCCAGTGCGGTGGTGGGCTT-3′		
...ACGCCACCTCGTCCCACCGTGGGTCCGGTCACGCCTCCACCCGAA-5′		
Sp1$^{\perp}$	**Sp1**	**22bp**
5′-ATTCGATCGGGGCGGGGCGAGC-3′		
3′-TAAGCTAGCCCCGCCCCGCTCG-5′		
YY1$^{\perp}$	**YY1**	**27bp**
5′-CGCTCCGCGGCCATCTTGGCGGCTGGT-3′		
3′-GCGAGGCGCCGGTAGAACCGCCGACCA-5′		

Table 2.11. The transcription factor consensus site and mutant oligonucleotide sequences used as competitors and controls for EMSA studies.

Purple lettering denotes binding bases in sequence. Underlined lettering denotes mutated bases.

$^{\perp}$ oligonucleotides obtained from Santa Cruz Biotechnology.

$^{\Upsilon}$ oligonucleotides designed in this study and obtained pre-synthesised from MWG Biotech.

Identity	Specificity	Epitope	Cross-reactivity	Species raised in
sc-150X	α-C/EBPβ	C-terminus rat CEBPβ	human reactive non cross-reactive with other C/EBP members	Rabbit (polyclonal IgG)
sc-746X	α-C/EBP	C-terminus human C/EBPβ	cross-reactive with C/EBPα, δ and ε	Rabbit (polyclonal IgG)
sc-186X	α-CREB-1[i]	C-terminus human CREB-1	cross-reactive with CREB-1p43, ATF-1 and CREM-1	Rabbit (polyclonal IgG)
sc-271X	α-CREB-1[ii]	DNA binding/ dimerisation domain human CREB-1	specific for CREB-1p43	Mouse (monoclonal IgG_{2b})
sc-1002X	α-GRα	C-terminus human GRα	non cross-reactive GRβ	Rabbit (polyclonal IgG)
sc-1003X	α-GR	N-terminus human GRα	cross-reactive GRβ, not other steroid receptors	Rabbit (polyclonal IgG)
sc-870X	α-NF1	N-terminus human NF1	reactive with all NF1 isoforms	Rabbit (polyclonal IgG)
sc-281X	α-YY1	C-terminus human YY1	specific	Rabbit (polyclonal IgG)
sc-7341X	α-YY1	human YY1 αα 1-414	specific	Mouse (monoclonal IgG1)

Table 2.12. Specific antibodies used for EMSA supershift studies and as primary detection antibodies for Western blots, obtained from Santa Cruz Biotechnology (2mg/ml).

2.11.5. Gel resolution of EMSA bands

EMSA bands were resolved after the binding reaction on a 4% non-denaturing polyacrylamide gel with 0.5x TBE* (see section 2.3.2); gel plates were 12cm long, separated by 1mm spacers with a 14 x 1cm well comb. The gel was pre-run in 0.5x TBE at 10volts/cm until the current and temperature stabilised (about 4 hours). The full 20µl of binding reaction was loaded per well and could be seen to sink into the well because of the glycerol in the binding buffer. Loading dye* was used only in an empty or probe only lane. The gel was run at 10volts/cm until unbound radiolabelled probe began to come off into the lower reservoir, 2.5-4.5 hours dependent on the probe size. For each set of probes, the length of run was kept constant. The gel was transferred to Whatman 3MM paper and dried for 1 hour at 80°C on a vacuum pump gel drier. The bands were then detected on x-ray film (BIOMAX, Kodak) and put down for 4 - 8 hours at –80°C (see figure 2.12).

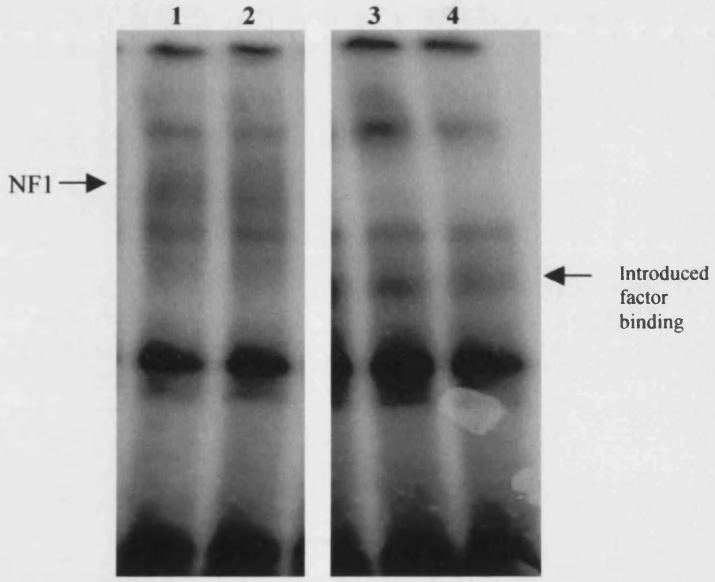

Figure 2.12. EMSA for NF1 consensus probe and NF1 mutant probe with HeLa cell nuclear extracts.

5pmol of NF1 consensus 1 (NF1-1) or NF1 mutant 1 (NF1-mut1) probe (see table 2.11) was 5'-end labelled (see 2.11.2.1) and incubated with 10µg of unstimulated HeLa cell nuclear extracts in a binding reaction containing Parker buffer (see 2.11.3). The products were separated by electrophoresis on a 4% non-denaturing polyacrylamide gel run for 2.5hrs at 4°C. Lanes 1&2=NF1-1 probe, lanes 3&4=NF1-mut1 probe. The NF1-mut1 sequence abolished NF1 binding but permitted another nuclear factor to bind.

2.12. Protein detection and quantification

2.12.1. Enzyme-linked immunosorbent assays (ELISA)

Standardised ELISA kits from R & D Systems were used to detect IL-1α, IL-1β, TNFα and IL-6 in culture media and serum. These were used according to manufacturers instructions. 50µl of cell culture medium or serum was added to the microtitre-plate wells pre-coated with antibody and then incubated at 37°C for 1hr. All samples and standards were loaded in duplicate. Unbound protein was washed away using 1x PBS* with 0.05% Tween (polyoxyethelenesorbitan monolaurate, Sigma). A second antibody, conjugated to horseradish peroxidase, was added to each well. This was incubated at 37°C for 1hr before unbound antibody was washed away (PBS/Tween) and detection substrate added to produce the chemiluminescent reaction when hydrolysed by the horseradish peroxidase. The plates were read at an absorbance of 450nm (Anthos II plate reader, Stingray (DazDaq) software package). A standard curve was plotted from which the cytokine concentration of the sample was calculated.

2.12.2. Determining total protein concentration

Total protein concentrations from cell lysates or nuclear extracts were determined using a Bicinchoninic acid (BCA) protein assay system. 10µl aliquots of cell or nuclear extracts (diluted 1:0, 1:5, 1:10) were loaded onto a micro-titre plate (NUNC) in duplicate alongside 10µl aliquots of bovine serum albumin (BSA) standards covering the range 0.1, 0.2, 0.5, 0.8 & 1mg/ml. Samples and standards were loaded in duplicate together with two control reference samples containing water or cell lysis buffer. 200µl of BCA reagent (196µl BCA and 4µl copper(II) sulphate solution mixed immediately prior to use) was added to each well. The plate was covered and incubated for 30min at 37°C, before cooling to room temperature again for 5min. The alkaline medium allows the proteins to reduce Cu^{2+} to Cu^{+} resulting in a colour change that was read at an absorbance of 562nm, using an Anthos II plate reader. Using Stingray (DazDaq) software, a standard curve was plotted from which the protein concentration of the samples could be calculated.

2.12.3. Polyacrylamide gel electrophoresis (PAGE)

SDS-PAGE gels were used based on the method of Laemmli (1970) and run using the Mini-PROTAN II gel electrophoresis system (BioRad). A 6cm x 8cm x 1mm gel cell

was assembled according to manufacturer's instructions. A 4cm resolving gel of 12% polyacrylamide was poured (for 10ml, 4.85ml SDW, 3ml 37.5:1 acrylamide:bisacrylamide at 40% [National Diagnostics], 2ml 1.5M Tris-HCl pH 8.8, 100µl 10% (w/v) SDS, 6µl TEMED (electrophoresis grade, BDH), 60µl 10% (w/v) AMPS (Sigma) and allowed to polymerise for 30min over-layed with a few drops of water. The over-layed water was poured off and a 1.5cm stacking gel of 3% polyacrylamide poured on top with an 8 x 0.5cm well comb inserted (for 2.5ml, 1.4ml SDW, 750µl 37.5:1 acrylamide:bisacrylamide at 40%, 300µl 1M Tris-HCl pH 6.8, 25µl 10% (w/v) SDS, 2µl TEMED, 20µl 10% AMPS) and allowed to polymerise for 30min. 100ng of pure protein or 10µg of nuclear extract was mixed with equal volumes of 2x Novex Tris-Glycine SDS Sample Buffer (Gibco), boiled for 2min to denature the protein, microcentrifuged at 13,000rpm for 1min to remove insoluble debris and loaded into the wells set in the gel. Electrophoresis was carried out in SDS running buffer (25mM Tris pH8.3, 200mM glycine (electrophoresis grade, pH8.3), 0.1% (w/v) SDS) from cathode to anode at a constant 150V (~35mA) for 1 hour, until the bromophenol blue tracking dye reached the bottom of the gel. In all cases, 5µl of Benchmark Pre-stained Protein Ladder (Gibco) was run alongside the protein sample to enable estimation of the molecular weights of protein bands detected by Western blotting (figure 2.13).

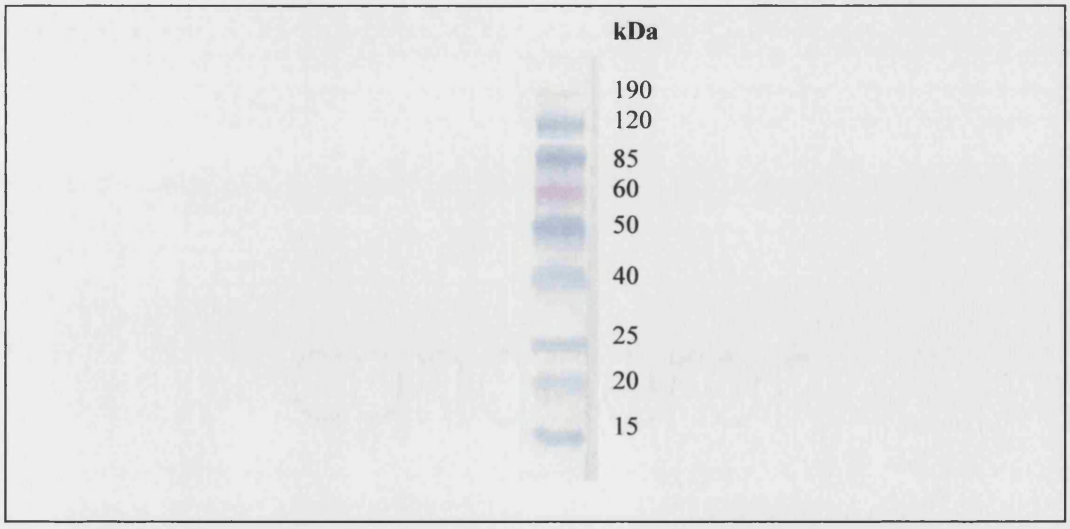

Figure 2.13. Pre-stained Protein Molecular Weight Marker (Benchmark, Gibco). Approximate molecular weights (kDa) shown on SDS-PAGE denaturing gel (3% polyacrylamide stacking gel, 12% polyacrylamide resolving gel, see above).

2.12.3.1. Western blotting

This is a based on a modified method of Towbin et al., (1979). Proteins were transferred from the polyacrylamide gel by wet transfer to a polyvinylidene difluoride (PVDF) membrane (Hybond P membrane, Amersham). A 6.5cm x 8.5cm PVDF membrane was cut with a notch in one corner to identify lane 1 of the gel. The membrane was pre-soaked briefly in methanol (Sigma) followed by a rinse in SDW, before soaking for 2min in transfer buffer (25mM Tris pH 8.3, 200mM glycine, 5% (v/v) methanol). Whatman 3MM paper cut to size and the blotting cassette porous nylon pads were also soaked in transfer buffer. The pre-soaked PVDF membrane was placed over the polyacrylamide gel with the exclusion of air bubbles and sandwiched between 4 pieces of pre-soaked Whatman 3MM paper, 2 nylon pads and 2 plastic supports, before immersion in the blotting tank filled with transfer buffer (BioRad Minitransblot System, figure 2.14). Ensuring that the membrane was on the anode side, transfer was carried out with a constant 60V (195mA) for 45min.

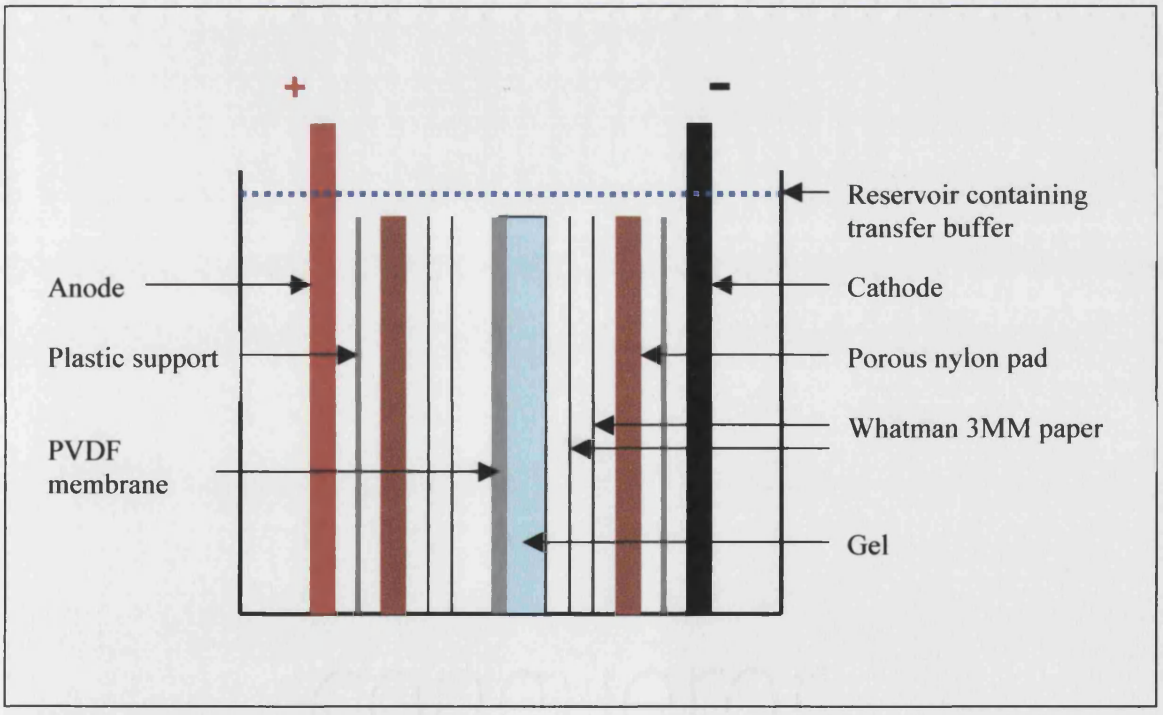

Figure 2.14. Western blot set up.

2.12.3.2. Immunological detection of proteins following transfer

The nitrocellulose membrane was 'blocked' with 5% (w/v) Marvel milk (Premier Brands) in PBS* for 45min at room temperature on a slow rotating platform. This was to prevent non-specific binding of antibodies to protein-free sites. The membrane was then incubated with the primary detection antibody (1:2000 dilution, see table 2.12) in PBS containing 0.1% (v/v) Tween overnight at 4°C on a slow rotating platform. This was followed by five washes in PBS/0.1% Tween for 5min each at room temperature. The membrane was then incubated for 2 hours at room temperature with secondary detection horseradish peroxidase (HRP)-conjugated antibody specific to the species of the primary antibody (1:1000 dilution, see table 2.13). This was also followed by 5x 5min washes in PBS/Tween at room temperature.

Immunoglobulin specificity (peroxidase-conjugated)	**Conc./ dilution used**	**Supplier**	**Primary antibodies** (table 2.12)
Swine anti-rabbit immunoglobulin (polyclonal, mainly to IgG)	1.3mg/ml 1:1000	DAKO	α-C/EBPβ sc-150 α-C/EBP sc-746 α-CREB-1^{i} sc-186 α-GRα sc-1002 α-GR sc-1003 α-NF1 sc-870 α-YY1 sc-281
Sheep anti-mouse immunoglobulin (polyclonal, whole antibody)	1:1000	Amersham	α-CREB-1^{ii} sc-271 α-YY1 sc-7341

Table 2.13. Secondary detection horseradish peroxidase (HRP)-conjugated antibodies used for immunological detection of Western blots.

The membranes were developed using enhanced chemiluminescence (ECL) Western Blotting Detection Reagents (ECL Plus, Amersham), according to manufacturers instructions. In brief, 5ml of substrate A (supplied) was mixed with 125µl of substrate B (supplied). This was poured onto the membrane and incubated at room temperature for 5min. Membrane bound HRP and added H_2O_2 (in applied reagents) catalyse the oxidation of an acridan-based substrate in the applied reagent to release a high level, sustained output of light, detectable on film. Excess reagent was drained off and the

membrane wrapped in transparent cling-film with air bubbles excluded, placed protein side up in an autoradiograph cassette and exposed to X-ray film (BIOMAX, Kodak) for 5-60sec (figure 2.15). Longer exposures were carried out so that the edges of the membrane could be clearly seen and marked on the developed radiograph. This enabled the positions of the protein molecular weight marker bands to be traced onto the radiograph for estimation of the molecular weight of detected sample bands.

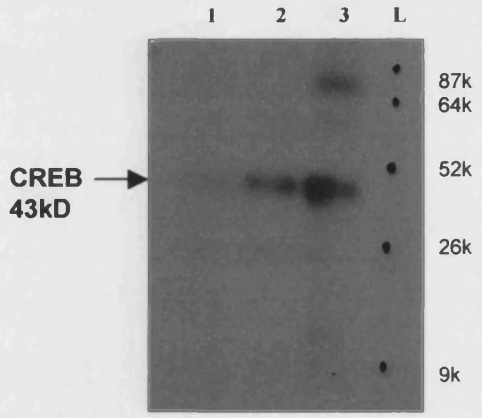

Figure 2.15. Western blot for CREB in HeLa cell nuclear extracts.
CREB was detected using Sc-271 mouse monoclonal anti-CREB antibody (table 2.11) followed by HRP-conjugated rabbit anti-mouse polyclonal antibody (table 2.12), (see 2.12.3 for method).
Lane 1=unstimulated HeLa cell nuclear extracts, lanes 2&3=IL-1β-stimulated HeLa cell nuclear extracts, L=protein size marker ladder.

2.13. Statistical methodology

Advice on statistical analysis was obtained from Dr Cathryn Lewis, Lecturer in Statistics, Guy's, Kings and St. Thomas' School of Medicine, London, UK. All methods except the EH programme were carried out in Microsoft Excel (for PC) and used raw data.

2.13.1. Power calculations

Calculation of the power of the study and numbers needed to achieve a pre-determined level of significance were calculated using the formula

$$n > 4[p_1(1-p_1)+p_2(1-p_2)]/e^2$$

p_1 and p_2 are the proportions in the two groups being studied, e is the estimate of what would be considered a significant difference (Fleiss et al., 1980).

2.13.2. Determination of genotype association

The chi-square test was used to compare genotype distribution between cases and controls and to confirm populations were in Hardy Weinberg Equilibrium. This test determines whether an observed distribution differs from an expected distribution.

$$\chi^2 = (O_i - E_i)^2 / E_i$$

O_i is the observed frequency distribution and E_i is the expected frequency distribution. From χ^2 the probability value (p) was determined from χ^2 tables, a p-value <0.05 (95% confidence) was considered significant.

The Hardy Weinberg equilibrium equation tests for stability of a mutation or allele within the gene pool of a population.

$$p^2 + 2pq + q^2 = 1$$

p is the frequency of the dominant allele in the population and q is the frequency of the recessive allele.

The Fisher Exact test was used to compare genotype distribution between cases and controls where there was a small expectation value due to the rarity of the –572 CC homozygote genotype of IL-6. The exact method calculates the probability of the contingency table for the genotype frequency distribution found in cases and controls with that of similar tables.

To investigate association between allelic carriage and disease, the odds ratio (OR) was determined from a 2 x 2 cross-classification table (see below) comparing distribution in cases and controls.

		Disease	
		+	-
Allelic carriage	+	a	b
	-	c	d

OR = ad / bc

2.13.3. Estimation of haplotype frequency and association

Haplotype frequencies were estimated from the genotype frequencies in controls and cases using the estimation of haplotype (EH) programme available through the human genome mapping project (www.hgmp.mrc.ac.uk). This programme was also used to compare haplotype frequency distribution between cases and controls using the chi-square test. It calculated the log likelihood values for the null hypothesis and determined the linkage disequilibrium measure Delta (Δ) between loci.

2.13.4. Comparing transfection results

The standard deviation was calculated for each set of experiments as a measure of the spread around the mean. This is the square root of the variance, where variance is

$$s^2 = \Sigma (X - M)^2 / N-1$$

X is the individual sample value, M is the mean of the sample values and N is the number of samples.

The T-test was used to compare transfection results. This uses the formula

$$t = (X_1 - X_2) / \sqrt{A \times B}$$

$$A = (n_1 + n_2) / n_1 n_2$$

$$B = [(n_1 - 1)s_1^2 + (n_2 - 1)s_2^2] / [n_1 + n_2 - 2]$$

X is the sample mean, s is the standard deviation and n is the number of values within the sample. The denominator is a measure of experimental error, thus the higher the value of t, the greater the confidence that there is a difference between the samples. From t, the probability value (p) was determined from tables, a p-value <0.05 (95% confidence) was considered significant.

Methods appendix

Antibiotics	These were added to media just prior to use from stock solutions that had been filter sterilised Ampicillin: 100mg/ml in water Tetracycline: 12.5mg/ml in 50% ethanol (stored in dark)
50x Denhardt's Solution	1%(w/v) BSA, 1%(w/v) Ficoll, 2%(w/v) polyvinyl-pyrollidine
DEPC treated water	0.1% DEPC left over-night and then sterilised by autoclave
dI.dC buffer	1mM EDTA, 40mM KCl, 5mM $MgCl_2$, 5mM $MgCl_2$, 2.5mM DTT (lyophilised poly.(dI-dC).(dI-dC) added and heated to 65°C for 5min)
DMEM media	Dulbecco's modified essential media (high glucose, Gibco) supplemented with FCS, 2mM glutamine, 100IU/ml penicillin, 100µg/ml streptomycin & gentamicin, 1mM non-essential amino acids
FACS buffer	1x PBS, 0.1% azide, 1% FCS
10x HBS	8.18% NaCl, 5.94% HEPES, 0.2% Na_2HPO_4
LB agar	1.5g agar per 100ml LB media
LB media	1% bacto-tryptone, 0.5% bacto-yeast extract, 170mM NaCl, pH7.5
Loading dye	
10x blue	0.25% bromophenol blue, 0.25% xylene cyanol FF, 15% Ficoll, 10mM Tris-HCl, 50mM EDTA
6x blue/orange	0.4% orange G, 0.03% bromophenol blue, 0.03% xylene cyanol FF, 15% Ficoll 400, 10mM Tris-HCl, 50mM EDTA
PBS	0.01M Phosphate buffer, 2.7M KCl, 137mM NaCl
Equilibrated phenol	Phenol solution with 0.1%(w/v) 8-hydroxyquinoline, equilibrated x1 with equal volume 1M Tris-HCl (pH8.0), x2 with equal volume 100mM Tris-HCl (pH8.0)
Fragmented salmon sperm	10mg/ml dH_2O, sheared using an 18 gauge needle and boiled for 10min
20x SSC	3M NaCl, 0.3M Na_3citrate, pH7.0
50x TAE	2M Tris, 1M Acetic acid, 50mM EDTA (pH8.0)
10x TBE	0.89M Tris, 0.89M Boric acid, 25mM EDTA (pH8.0)
TE	10mM Tris-HCl pH8.0, 1mM EDTA, pH7.5 (1:10 dilution was used for transfection calcium phosphate precipitation protocol)
Terrific broth	48g EzMix terrific broth base (Sigma), 8ml glycerol per 1000ml dH_2O

Solutions and media were sterilised by autoclaving or filtration through a Supore® Acrodisc™ 13 (0.2µm) syringe filter.

CHAPTER 3

RESULTS:

The association of 5'-flanking region polymorphisms of IL-6 with SA

3.1 Recruitment of case and control populations

At the start of this study, power calculations were carried out to determine the numbers of samples needed for control and patient groups. The calculation was based on the formula $n > 4[p_1(1-p_1)+p_2(1-p_2)]/e^2$, where p_1 and p_2 are the proportions in the two groups and e is the estimate of what would be considered a significant difference (Fleiss et al., 1980). To have 80% power for determining allelic, genotype or haplotype frequency in a control population with 95% confidence limits, a minimum of 385, 113 and 381 individuals would be required for the –174, -572 and –597 polymorphisms respectively (based on the estimated common-allele frequency for each polymorphism from preliminary studies 0.55, 0.95 and 0.56 respectively). As the systemic arthritis (SA) from of juvenile idiopathic arthritis (JIA) has a relatively low incidence (1:100,000 in the UK), it was considered feasible to obtain approximately 100 SA patient samples, therefore unequal group size comparison with controls was going to be necessary to achieve a power of 80%. For detection of a 10% difference in common-allele carriers between cases and controls it was calculated that numbers needed for the –174 polymorphism were 129 cases and 774 controls, for the –572 polymorphism 65 cases and 388 controls and for the –597 polymorphism 121 cases and 728 controls. These numbers were considered feasible to recruit.

Independent representative groups (control samples) were recruited from the healthy adult Caucasian population of the UK. Two groups were recruited from consecutively registered individuals on a General Practice List, one from Nuneaton in the Midlands, the Nuneaton samples (n=225), and one from North London, the Goodinge samples (n=238). Individuals were UK Caucasians, had no known illness and specifically had no history of joint problems. They were aged 16-30 years for the Nuneaton Group and ≥16 years for the Goodinge group. A third group, the WEDC samples (n=253) were recruited from first time blood donors attending a blood-donor clinic in the West End of London. These individuals were Caucasian, ≥18 years and had no know illnesses or joint problems as self-reported. A fourth group, the NPH samples (n=385) had been recruited prior to this study from North West London, through Northwick Park Hospital, as healthy Caucasian males with no history of medical or joint problems, aged 50-61 years, for a prospective study of cardiovascular risk factors (Miller et al., 1996). Permission was obtained to use these samples for this study. Control sample groups were chosen from London and the Midlands, as the majority of patients with

JIA were recruited from these areas (see below). A fresh venous blood sample was obtained in EDTA from each recruit (with informed consent & ethical approval) and genomic DNA isolated (see section 2.2.1). Samples from the Northwick Park Hospital controls were kindly provided as aliquots of pre-isolated genomic DNA (stored at –20°C) by our collaborator S. Humphries.

UK Caucasian patients with JIA were recruited through the British Paediatric Rheumatology Group (BPRG). A national DNA repository has been set up at Manchester University to store these samples (under the supervision of W. Thompson, R. Donn and P. Woo). Patients attending paediatric and adolescent rheumatology units across the UK were asked to donate a fresh venous blood sample (with full patient and parental informed consent) at the time of a blood test for clinical reasons. The patients had a confirmed diagnosis and sub-classified type of JIA by ILAR criteria (see table 1.1). Information was collected as to the age at onset of disease, gender of patient and pattern of disease. One hundred and eighteen Caucasian patients with SA were recruited, 75% through our own hospitals and tertiary referral centres in London (Great Ormond Street and University College London hospitals), 10% from Birmingham, 8% from Manchester and the remainder from other UK centres. Genomic DNA was isolated from each fresh blood sample (see 2.2.1).

3.2. Genotype analysis

There are many techniques for genotype analysis. The methods chosen need to be accurate, fast and allow high-throughput if large numbers of samples are to be analysed in a population study. Three techniques were chosen and compared for this thesis, restriction fragment length polymorphism (RFLP), sequence specific oligonucleotide probing (SSOP) and heteroduplex analysis. All three techniques require the prior knowledge of polymorphisms of interest and of the surrounding DNA sequences of the gene, and depend on successful generation of a PCR product, but are then amenable to large-scale sample analysis.

Prior to this thesis, single-strand conformational polymorphism (SSCP) analysis had been carried out for 1.2kb of the 5'-flanking region, the five exons and four introns of the IL-6 gene (D Fishman, L Luong, personal communication). This had identified four SNPs and a variable AT-tract length polymorphism in the 5'-flanking region and a

single SNP in exon 5. The SNP in exon 5, a base transition from T to C, was a silent polymorphism (TTT>TTC), conserving the phenylalanine residue at position 201 of the IL-6 protein. The C to A SNP at position –627 was found to occur in <1% of the Caucasian population (preliminary studies, L. Luong, personal communication). The G to C SNP at position –174, G to C SNP at position –572, G to A SNP at position –597 and variable AT-tract length polymorphisms between –373 and -392 occurred more frequently (Fishman et al., 1998, Nakajima et al., 1999, Osiri et al., 1999, Jordanides et al., 2000, Terry et al., 2000).

IL-6 plays an important pathogenic role in SA (see section 1.2.10). It is predominantly regulated at the level of transcription. The 5'-flanking region polymorphisms of IL-6 occur within the main regulatory region for IL-6 transcription and so their possible association with SA was investigated. The distribution of the SNPs –174G/C, -572G/C and –597G/A was determined in the healthy Caucasian population and compared to SA.

RFLP analysis relies on a restriction endonuclease that will recognise the DNA sequence of one allele but not the other. Cleaved products of one allele can be distinguished from uncleaved products of the other allele by electrophoretic resolution on an agarose or acrylamide gel. This is a quick and relatively cost efficient method, widely used in genotyping (Holloway et al., 1999). It can be carried out in a 96-well micro-titre plate allowing reasonably high throughput. The technique is generally considered 95-96% accurate for genotype determination when appropriate positive and negative controls are used. A very low or very high frequency of the allele that will cut, is more likely to result in skewing of results if there is a problem with the efficiency of the digestion stage of the technique and RFLP conditions have to be carefully optimised to minimise over- or under-digestion with appropriate controls for each experiment. The cut site in the PCR product needs to generate sufficiently different product lengths to enable clear size distinction by gel electrophoresis. Micro-titre array diagonal gel electrophoresis (MADGE) employs acrylamide gel electrophoresis from 96-wells to allow digestion products differing by only a few bases to be clearly distinguished (Day et al., 1995). RFLP was optimised for three 5'-flanking region polymorphisms of IL-6, the –174 G/C polymorphism, the –572 G/C

polymorphism and the –597 G/A polymorphism. The restriction enzyme *Nla*III (*Hsp*92II) will recognise and digest the sequence 5'...CATGˇ...3'

3'...ˇGTAC...5' from –171 to –174

of IL-6 when the –174 C allele is present but not the G allele (see figure 1.9). *Mbi*I will recognise and digest the sequence 5'...CCGˇCTC...3'

3'...GGCˇGAG...5' from –569 to –574 of IL-6

when the –572 G allele is present but not the C allele, and *Fok*I will recognise and digest the IL-6 sequence 5'...GGATG$(N)_9$ˇ...3'

3'...CCTAC$(N)_{13}$ˇ...5' from –582 to -599 with the A allele at –597 but not the G allele (figure 1.9).

Figure 3.1 shows the optimised products separated on 8% polyacrylamide gels for a 190bp PCR product from –128 to –318 of IL-6 for the –174 polymorphism and a 163bp PCR product from –468 to –632 for the –572 and –597 polymorphisms (see 2.8.1.1 for the methods).

SSOP uses a variant of the Southern blot technique. PCR product of the region of interest is applied to nylon nucleic acid transfer membrane (Hybond N+), denatured and probed by complementary single-stranded allelic probes for the polymorphism to be detected. The probe was biotinylated to allow detection with streptavidin-bound-horseradish peroxidase and substrate addition to produce a chemiluminescent reaction detected on radiograph (see 2.8.2 for the method and allelic probe sequences). The method allows a relatively high throughput, though the procedure is more labour intensive than for RFLP. The technique is very sensitive to the temperature and salt concentration of stringency washes, which need to be carefully optimised for each set of probes. Even with optimisation, one allelic probe will often bind more efficiently, resulting in potential false positives. Inclusion of positive and negative controls on each membrane is essential.

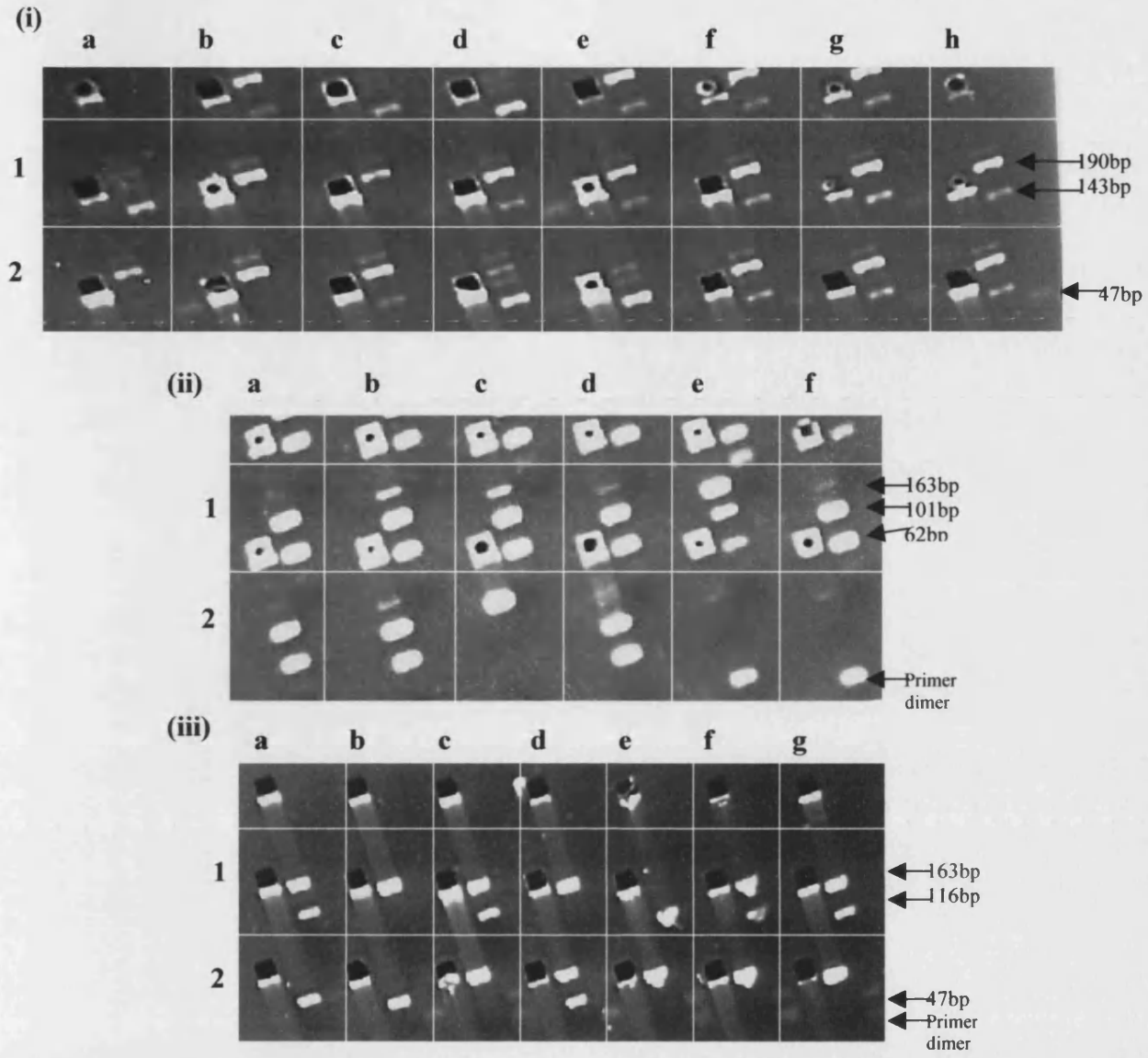

Figure 3.1. RFLP-MADGE of the (i) –174 G/C, (ii) -572 G/C and (iii) –597 G/A polymorphisms of IL-6.

200ng of genomic DNA, amplified by PCR for the IL-6 5'-flanking region (primers IL-6 9A&10A for –174 region, primers IL-6 5bF&6R for –572&-597), made up to a volume of 25µl with specific restriction endonuclease buffer was digested over-night with (i) 1U *Nla*III, (ii) 2U *Mbi*I or (iii) 1U *Fok*I, then resolved by electrophoresis on an 8% polyacrylamide gel pre-stained with ethidium bromide and visualised under UV light (see 2.8.1.1. for methods and PCR primers).

(i) -174: *Nla*III digestion of 190bp PCR product cuts the –174 C allele (143/47bp) but not the G allele (190bp). Genotype results: sample 1a=CC, 1b=GG, 1c=GG, 1d=GC, 1e=GC, 1f=GC, 1g=GC, 1h=GC, 2a=GG, 2b=GG, 2c=GC, 2d=CC, 2e=CC, 2f=GC, 2g=GC, 2h=GC.

(ii) -572:*Mbi*I digestion of 163bp PCR product cuts the –572 G allele (101/62bp) but not the C allele (163bp). Genotype results: sample 1a=GG, 1b=GG, 1c=GG, 1d=GG, 1e=GC, 1f=GG, 2a=GG, 2b=GG, 2C=CC, 2d=GG, 2e&2f=inadequate PCR product.

(iii) -597*Fok*I digestion of 163bp PCR product cuts the –597 A allele (116/47bp) but not the G allele (163bp). Genotype results: sample 1a=GA, 1b=GG, 1c=GA, 1d=GG, 1e=AA, 1f=GA, 1g=GA, 2a=AA, 2b=AA, 2c=GG, 2d=GA, 2e=GG, 2f=GG, 2g=GG.

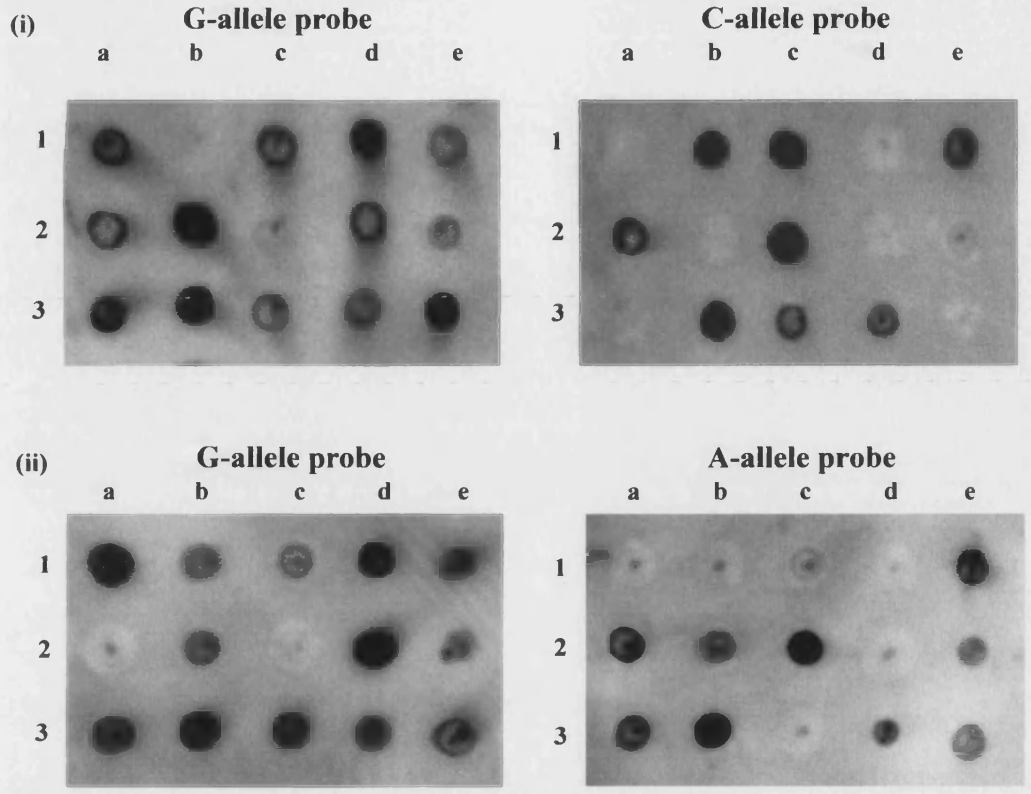

Figure 3.2. SSOP of the (i) –174 G/C and (ii) –597 G/A polymorphisms of IL-6.
1μg of IL-6 5'-flanking region PCR product (primers IL-6 DF20mod&DF21) was applied to nylon nucleic acid transfer membrane (Hybond N+, Amersham), denatured with 0.5M NaOH/1.5M NaCl, baked for 10min at 80°C before probing with biotinylated allele specific probe (i) –174G probe DF11, –174C probe DF12, stringency wash temp. 54°C or (ii) –597G probe PW269, –597A probe PW268, stringency wash temp. 54°C (see 2.8.2 for methods, primer and probe sequences). The probes were detected with streptavidin-horseradish peroxidase and substrate addition to produce a chemiluminescent reaction exposed to radiograph.
(i) -174: Sample 1a=GG, 1b=CC, 1c=GC, 1d=GG, 1e=GC, 2a=GC, 2b=GG, 2c=CC, 2d=GG, 2e=GC, 3a=GG, 3b=GC, 3c=GC, 3d=GC, 3e=GG.
(ii) -597: Sample 1a=GG, 1b=GG, 1c=GA, 1d=GG, 1e=GA, 2a=AA, 2b=GA, 2c=AA, 2d=GG, 2e=GA, 3a=GA, 3b=GA, 3c=GG, 3d=GA, 3e=GA.

Heteroduplex analysis uses PCR product of the region of interest to anneal a universal heteroduplex generator (UHG) specific for each polymorphism. A UHG is a complementary sequence of the full length of the PCR product (usually 100-125bp in length) with several base insertions adjacent to the polymorphic site to produce a structural loop that varies with the allele. These structural variants can be separated by electrophoresis on a high-percentage polyacrylamide gel. Heteroduplex is generally considered the most accurate of the three techniques. However, it is dependent on the quality of the PCR product obtained and the design of the UHG to achieve clear separation of the allelic bands. The UHG itself can form homodimers that need to be

optimised to run separately from the heteroduplex bands. Compared to RFLP or SSOP, heteroduplex is more expensive and more labour intensive, allowing only moderate throughput of samples (20-40 per gel). It has the advantage however that PCR products can be multiplexed for more than one polymorphism per lane, if the UHG design is such that the different allelic bands run in different positions on the gel.

Figure 3.3 shows the optimised heteroduplex banding patterns using a 116bp PCR product & 120bp UHG for the –174 G/C polymorphism, and a 126bp PCR product & 130bp UHG for the –572 G/C polymorphism, separated by electrophoresis on a 15% polyacrylamide gel (see section 2.8.3. for the method and UHG sequences).

All samples were analysed by RFLP for each genotype. All SA samples and 50% of control samples were additionally genotyped by a second method. Each result was analysed by two independent observers. If there was observer disagreement for any results, these were repeated until agreement was reached. If there were disagreements in results between techniques, then samples were analysed by a third method if available, or by automated sequencing (commercially by MWG Biotech). If none of these options were possible, the sample was discounted. Direct sequencing is considered the gold standard for genotype analysis with modern automated sequencing techniques allowing increased speed and throughput of samples, however it is expensive and labour intensive to do on a large scale, and considered unnecessary for every sample.

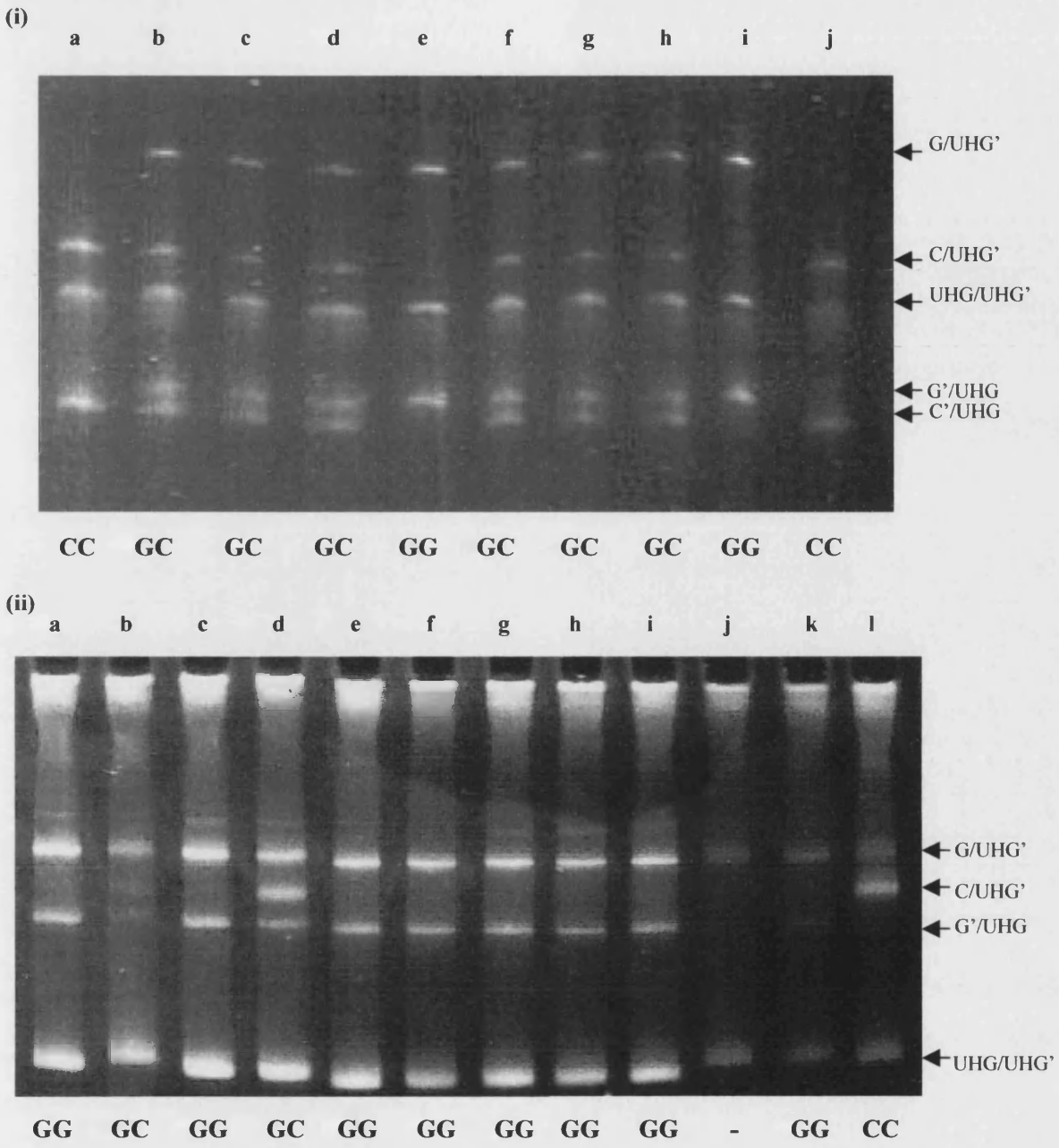

Figure 3.3. Heteroduplex of the (i) –174 G/C and (ii) –572 G/C polymorphisms of IL-6.

200ng of genomic DNA was amplified by PCR (i) primers IL-6 –174F&R or (ii) primers IL-6 –572F&R and UHG for each sequence was amplified in the same way. Equal amounts of PCR product and UHG were mixed, melted at 95°C and cooled to anneal, products were resolved on a 15% polyarcylamide gel, stained with ethidium bromide and visualised under UV light (see 2.8.3. for method, primer and UHG sequences).

G/UHG'= one strand of the G allele PCR product annealed to the complementary UHG strand, C/UHG'= one strand of the C allele PCR product annealed to the complementary UHG strand. G'/UHG and C'/UHG= the other strand of the gene PCR product annealed to the complementary strand of UHG. UHG/UHG'= the two UHG strands annealed to each other. G/G' and C/C' products had a higher electrophoretic mobility and ran faster through the gel.

3.2.1. Comparison of techniques

For samples that were genotyped by more than one method, comparisons could be made as to the accuracy and efficiency of each technique for determining the IL-6 polymorphisms. Table 3.1 shows the number of samples from those analysed that were considered to be correctly genotyped by a technique, that is to say, those results that agreed between two techniques, or agreed with the automated sequence result. This allowed the positive predictive value for the technique to be determined. The table also shows the number of samples that could not be genotyped by that technique, indicating the efficiency of the method, the negative predictive value. For both the –174 and –572 polymorphisms, heteroduplex analysis was 100% accurate in genotype determination. The accuracy of RFLP for these polymorphisms was 96%, within the accepted level of accuracy for this technique. For the –174 polymorphism, the efficiency of RFLP was higher than for heteroduplex (90% compared to 79%). This resulted in statistically better results overall by RFLP than heteroduplex, a trade-off of the efficiency of RFLP for the accuracy of heteroduplex. For the –572 polymorphism, there was no significant difference between the efficiency or overall statistical results obtained by RFLP or heteroduplex, though heteroduplex gave no incorrectly identified genotypes. Despite the higher accuracy of heteroduplex, it is possible for this technique to skew results if it fails to produce results for one genotype more frequently than for another. RFLP may produce an over-representation of one genotype by over- or under-enzyme digestion. The incorrectly genotyped samples in this study were generally due to under-cutting of the enzyme despite careful optimization and the presence of control samples. The accuracy of both techniques may have been over-estimated if both techniques incorrectly identified the genotype in the same way. If both techniques agreed on the genotype of a sample, further analysis such as sequencing was rarely carried out, however, when it was, the sequencing genotype agreed with the genotype determined by the other two methods. For the –597 polymorphism, RFLP and SSOP appeared equally accurate at 98% (table 3.1). Again, this may have been an over-estimation for the same reasons as above. A number of randomly chosen samples were sequenced and agreed with the genotypes determined by RFLP/SSOP. Taking into consideration accuracy and efficiency of RFLP and SSOP for this polymorphism, there was no significant difference between the two techniques. Based on these results, RFLP was considered the most appropriate technique in this study for large-scale genotype determination, with heteroduplex analysis to confirm the results where

possible. This was considered particularly important for the patient groups where the smaller number of samples compared to controls would result in a more significant skewing of results if even a few genotypes were incorrectly identified.

(a) –174 G/C polymorphism	Heteroduplex	RFLP
Number of samples genotyped	262	262
Number of samples clear results obtained	206	246
Number of samples results obtained which agreed with finally determined genotype	206	237
Positive predictive value	1.0	0.96

Observed difference 0.12, p-value <0.002, 95% confidence limits 0.061, 0.179

(b) –572 G/C polymorphism	Heteroduplex	RFLP
Number of samples genotyped	181	181
Number of samples clear results obtained	167	166
Number of samples results obtained which agreed with finally determined genotype	167	159
Positive predictive value	1.0	0.96

Observed difference 0.04, p-value $0.1 < p < 0.2$, 95% confidence limits -0.019, 0.099

(c) –597 G/A polymorphism	RFLP	SSOP
Number of samples genotyped	263	263
Number of samples clear results obtained	256	250
Number of samples results obtained which agreed with finally determined genotype	251	244
Positive predictive value	0.98	0.98

Observed difference 0.03, p-value $0.1 < p < 0.2$, 95% confidence limits -0.003, 0.069

Table 3.1. Comparison of the accuracy & efficiency of genotyping techniques for the –174, -572 and –597 SNPs of IL-6.
The techniques for each polymorphism were compared by proportions testing to 95% confidence (shown under each table).

3.3. The –174 polymorphism of IL-6

3.3.1. The –174 genotype is associated with susceptibility to SA

Genomic DNA was isolated from venous blood samples donated by each control subject. Each sample was genotyped for the –174 polymorphism using RFLP with *Nla*III (see 2.8.1.1). The NPH controls were genotyped in S. Humphries laboratory by G. Faulds, using the same RFLP technique (*Nla*III MADGE). Twelve of these samples and 80 other samples were genotyped by both laboratories for comparison and no differences were obtained (no further NPH DNA was available for complete repetition of the genotype analysis). The WEDC and Nuneaton controls were also genotyped by heteroduplex (see 2.8.3). Table 3.2 shows the –174 genotype distribution analysed using the chi-square test. All four control-groups were in Hardy-Weinberg (H-W) equilibrium and there was no significant difference between the genotype distributions (95% confidence, 2 degrees of freedom, df). The results were therefore combined to give a representative genotype distribution for the UK Caucasian population. GC was the most common genotype with a frequency of 0.470. GG had a frequency of 0.363 and CC was the least common genotype with a frequency of 0.168. The C allele frequency was 0.402.

Genotyping for the –174 polymorphism was carried out on the SA samples by RFLP with *Nla*III and heteroduplex. Genotype results could only be obtained for 107 of the 118 SA samples, mainly because PCR products could not be generated, despite attempts with different PCR primers. The 11 patients for which –174 genotype results could not be obtained were not significantly different in terms of distribution of gender ($p=0.82$) or age at onset ($p=0.09$) from those for which –174 genotype results could be obtained (chi-square test, 95% confidence, 2df). The genotyping success rate of 91% for the SA samples was equivalent to the overall success rate for the control groups, 90%. Different methods of DNA preparation were employed during the course of sample collection. The first samples collected were prepared using the Nucleon resin kit (see section 2.2.1.1). This method yielded genomic DNA of poor quality and reduced stability than conventional phenol-extraction methods, and phenol-extraction was soon adopted as the preferred method of preparation for the rest of the samples.

Control group	GG	GC	CC	n	C-allele frequency
Nuneaton	0.364	0.461	0.175	206	0.405
Goodinge	0.387	0.464	0.149	194	0.381
WEDC	0.321	0.527	0.152	237	0.416
NPH	0.376	0.441	0.183	383	0.403
Combined NUN/GOOD/WEDC/NPH	0.363	0.470	0.168	1020	0.402

Table 3.2. The genotype distribution for the –174 polymorphism of IL-6 in healthy UK Caucasian controls.
Each group is in H-W equilibrium by chi-square test (with 95% confidence, 1df), with no significant difference between the groups (chi-square test, 95% confidence, 2df, $p>0.1$). n=number of samples.

In the SA group, the GC genotype was most common with frequency 0.598. The GG frequency was 0.280 and the CC frequency 0.121 (C-allele frequency 0.421). These results were not in H-W equilibrium ($p=0.019$) and comparison with the control population using the chi-square test (95% confidence, 2 df) revealed a significant difference in genotype distribution ($\chi^2=6.435$, $p=0.040$), (figure 3.4). There were significantly fewer CC homozygous individuals in the SA group and significantly more GC heterozygotes than the control population. The allele frequency was not statistically significantly different between the two groups, probably due to the relatively small numbers in the SA group. However, the magnitude of the association between allele carriage and disease can be seen from the odds ratio (OR, see 2.13.2 for method). This indicates the 'odds' of having disease with carriage of one allele, compared to the 'odds' with carriage of the other allele. If there was no association between allele carriage and disease then OR would be 1.0. The OR for SA with carriage of the G-allele was 1.46, indicating a significant association.

To ensure that the –174 genotype association was specific for SA and not just associated with JIA, other sub-types of JIA were compared. These UK Caucasian patients had been recruited in the same way as the SA patients, though recruitment started after SA recruitment and consequently fewer samples were available; oligoarticular (n=64), extended-oligoarticular (n=69), polyarticular (n=60), (see table 1.1 for classification). Genotyping was carried out by RFLP with *Nla*III and heteroduplex. The results confirmed a specific association with SA, but not other sub-types of JIA (table 3.3). There was no significant difference between oligoarticular,

extended-oligoarticular or polyarticular JIA compared to the control population ($p>0.08$).

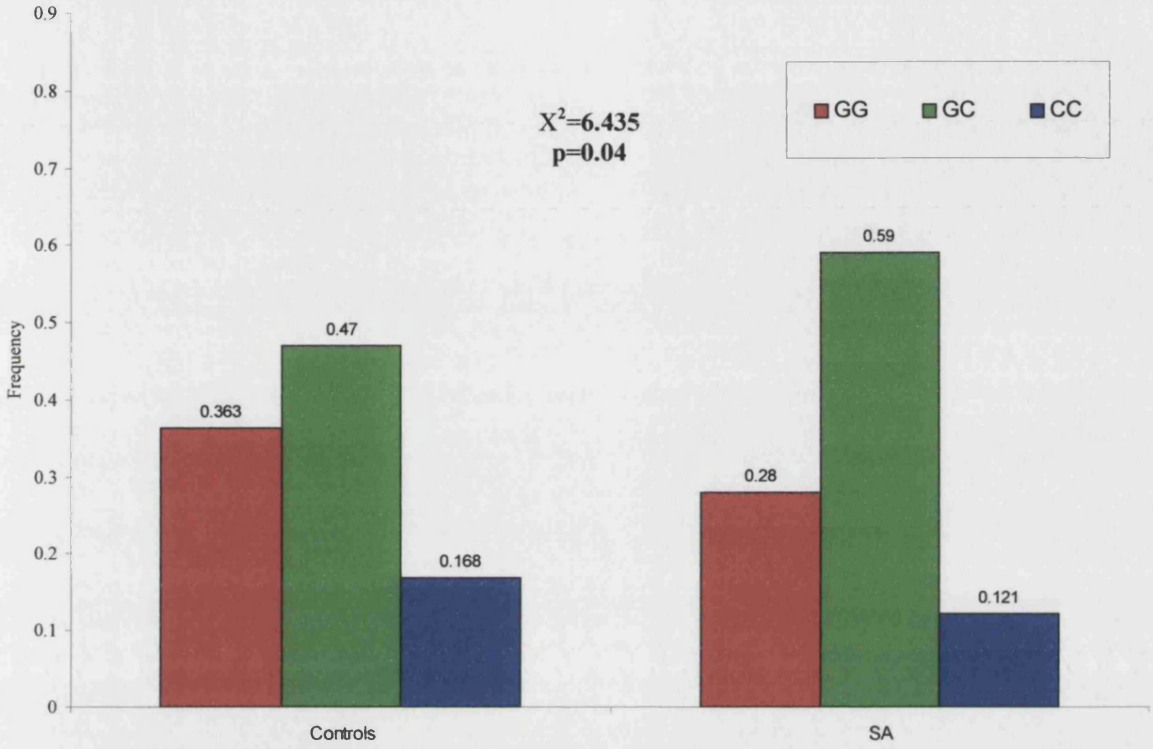

Figure 3.4. The genotype distribution for the –174 polymorphism of IL-6 in SA compared to controls.
The –174 genotype was determined by RFLP with *Nla*III and heteroduplex analysis (see 2.8.1.1&2.8.3) for 1020 UK Caucasian healthy controls and 107 UK Caucasian SA patients (data values shown). The control but not the SA group was in H-W equilibrium (chi-square test). Controls were compared to SA by chi-square test and were significantly different (95% confidence, 2df), X^2 and p-value shown.

JIA sub-type	GG	GC	CC	n	χ^2	p-value
SA	0.280	0.598	0.121	107	6.435	*0.040
Oligoarticular	0.263	0.526	0.211	57	2.449	0.294
Extended-oligoarticular	0.339	0.500	0.161	62	0.222	0.895
Polyarticular	0.232	0.518	0.250	56	4.900	0.086
Control population	0.363	0.470	0.168	1020	-	-

Table 3.3. The genotype distribution for the –174 polymorphism of IL-6 in different sub-types of JIA compared to healthy controls.
All except the SA group were in H-W equilibrium by chi-square test (95% confidence, 1 df). Each JIA sub-type was compared to the healthy Caucasian control population using the chi-square test, results shown (95% confidence, 2df). *denotes statistical significance within these limits. n=number of samples.

3.3.2. The –174 genotype is associated with early-onset SA

The peak age at onset for SA is 2-4 years of age. Children with early onset disease (≤5 years of age) tend to have more severe disease with a poorer prognosis (Modesto et al., 2001). Figure 3.5 shows the distribution of age at onset for 96 of the 107-SA patients for which age at disease-onset information was available.

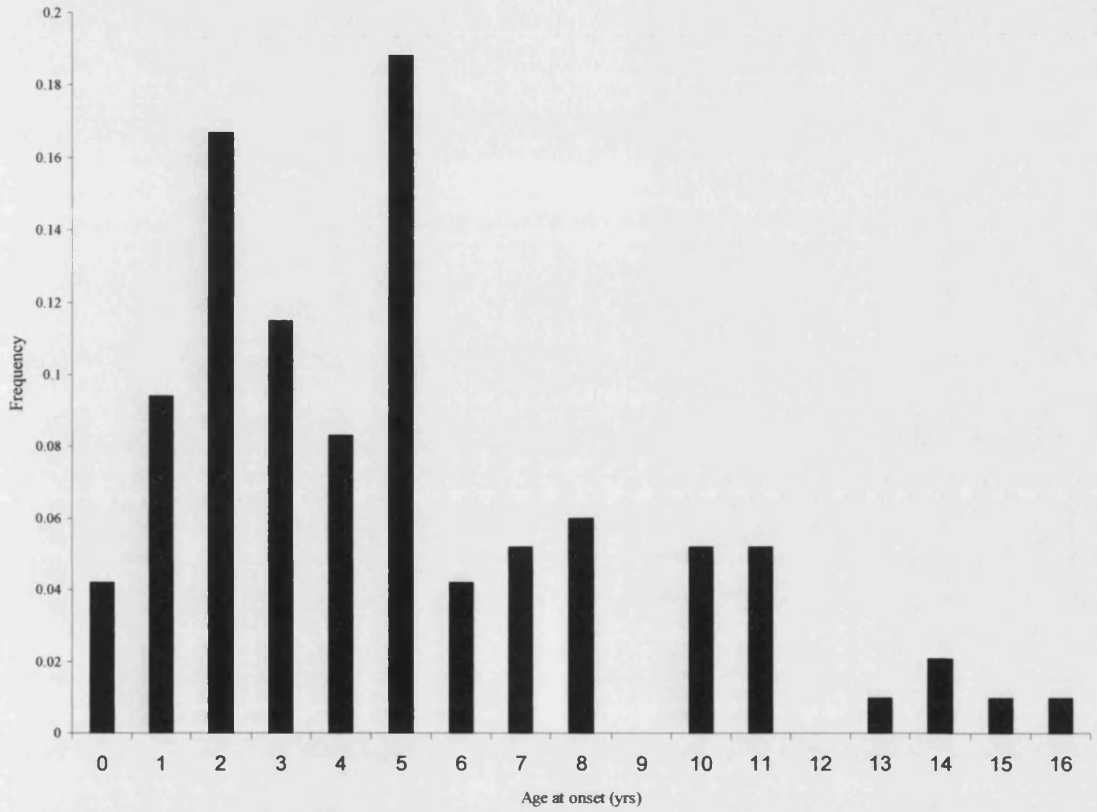

Figure 3.5. The distribution of age at onset for SA in 96 patients.
Age at onset was known for 96 of the 107 SA patients that were genotyped for the –174 polymorphism of IL-6. The median age at onset was 4.5 years, modal age at onset 5 years.

This sub-group of patients was not significantly different from the total group of SA patients when compared by chi-square analysis (95% confidence, 2df, p=0.102). The median age at onset was 4.5 years, modal age at onset 5 years, with 69% of patients ≤5 years at onset. The –174 genotype distribution was compared to the control population for early onset SA (≤5 years at onset) and late onset SA (>6 years at onset). The differences in genotype distribution in the total SA group were attributable to differences in genotype distribution in children with disease onset ≤5 years of age and not in the older age at onset group (table 3.4).

SA group	GG	GC	CC	n	χ^2	p-value
Any age at onset	0.292	0.594	0.115	96	4.901	*0.027
≤ 5 years at onset	0.258	0.652	0.091	66	8.431	*0.015
≥ 6 years at onset	0.367	0.467	0.167	30	0.002	0.999

Table 3.4. The genotype distribution for the –174 polymorphism of IL-6 in SA by age of onset.

Only the late age at onset group (≥ 6 years) was in H-W equilibrium by chi-square test (95% confidence, 1df). Each group was compared to the healthy Caucasian control population using the chi-square test, results shown (95% confidence, 2df). *denotes statistical significance within these limits. n=number of samples.

The CC genotype was under-represented in the early-onset group raising the possibility that the CC genotype may be protective against SA, or at least against the more severe, early-onset form of the disease. Indeed, the odds ratio (OR) for SA in individuals carrying the –174 G-allele was 2.01 for onset of disease ≤5 years of age, compared to 1.46 for SA onset at all ages, and 1.01 for onset of disease ≥6 years of age. This suggests that the –174 polymorphism may be a severity as well as a susceptibility marker for SA.

The course of SA can be heterogeneous despite the unifying ILAR classification criteria (table 1.1). The predominant disease course following onset can be sub-divided into persistent or relapsing arthritis, or persistent or relapsing systemic features, though these may overlap and vary with time for each individual making clear sub-classification difficult. Of those patients for which information on disease course was available, only 41, 78% had persistent arthritis and 22% on-going systemic features (12% of relapsing, 10% persisting). Though the group with disease course information was small, the chi-square test showed no significant difference between this group and the total SA group (95% confidence, 2df, p=0.292). Comparison of the –174 genotype distribution between the group with ongoing arthritis and the group with ongoing systemic features revealed no significant difference (chi-square test, 95% confidence, 2df, p=0.219). It is difficult to draw any conclusion however with small numbers and resultant low power.

3.3.3. The –174 genotype distribution is not influenced by gender

The gender distribution for 106 of the SA patients for which information was available was 54% female. This reflects the equal susceptibility for SA of males and females. Sixty percent of controls were female. There was no significant difference between the –174 genotype distribution in males and females for SA ($p=0.320$) or controls ($p=0.233$) by the chi-square test (95% confidence, 2df).

3.3.4. HLA association studies with the -174 genotype

No HLA associations have been consistently reported for SA. Those that have been reported have been with Class II genes but data are either conflicting or restricted to limited numbers of patients. HLA-DR4 was reported to be associated with SA in a UK study of 51 and a US study of 81 Caucasian patients respectively (Bedford et al., 1992, Miller et al., 1985). However, a larger European study (including 108 SA patients) found no association with HLA-DR4, nor any other Class II loci (Desaymard et al., 1996). More recently, a UK based study of 521 JIA patients found association of DRB1*11 and DQA1*05 with SA (Thomson et al., 2002). R. Donn (Manchester University) kindly provided HLA typing information on the SA patients in this study, from the National BPRG project on HLA associations with childhood arthritides (Arthritis Research Campaign funded). The number of individuals in each HLA sub-group was small (DR4 and DR11 14-18%, other sub-types <10%). No statistically significant association between the –174 and HLA genotypes could be identified but the power was low and so no conclusions could be drawn.

3.4. The –572 polymorphism of IL-6

3.4.1. The –572 genotype is not associated with SA

Samples from the Nuneaton, Goodinge and WEDC control groups were genotyped for the –572 polymorphism of IL-6 using RFLP with *Mbi*I, the Nuneaton and WEDC controls were also analysed by heteroduplex (see 2.8.1.1 & 2.8.3). No samples from the NPH control group were available for –572 genotyping. The Nuneaton, Goodinge and WEDC control groups were in H-W equilibrium for the –572 polymorphism, with no significant difference in genotype distribution between the groups (Fisher's exact test, $p \geq 0.7$), (table 3.5). An exact test was used because of small 'expected' numbers with the rare allele making the chi-square test formulation inappropriate (Weir, 1996). The groups were combined as a representative UK Caucasian control population. The

GG genotype was by far the most common genotype with a frequency of 0.856. The GC genotype occurred at a frequency of 0.137, the CC genotype extremely rare at frequency of 0.007. C allele frequency was 0.076.

Control group	GG	GC	CC	n	C-allele frequency
Nuneaton	0.836	0.154	0.010	201	0.087
Goodinge	0.852	0.143	0.004	230	0.076
WEDC	0.876	0.116	0.008	241	0.066
Combined Nun/Good/WEDC	0.856	0.137	0.007	672	0.076

Table 3.5. The genotype distribution for the –572 polymorphism of IL-6 in healthy UK Caucasian controls.
Each group is in H-W equilibrium by Fisher's exact test, with no significant difference between groups (Fisher's exact test, p≥0.7). n=number of samples.

Genotyping for the –572 polymorphism was similarly carried out on the SA samples by RFLP with *Mbi*I and by heteroduplex. PCR product for the region surrounding the –572 and –597 polymorphisms of IL-6 could only be generated for 85 of the 118 stored samples and genotype results for the –572 polymorphism could only be obtained for 52. This low success rate reflected the quality of the samples for which genomic DNA had been prepared using the Nucleon resin extraction method rather than phenol-extraction (see 2.2.1). Nucleases must have remained in the samples as many of them had become degraded with time. It was not possible to obtain fresh samples. The PCR technique was proven effective on the samples isolated by phenol-extraction from the control subjects (94% success rate). Comparison of the distribution of gender and age at onset for the SA patients with and without –572 genotype results, revealed no significant difference (chi-square test, 95% confidence, 2df, p=0.945 and 0.994 respectively). The genotype results obtained were in H-W equilibrium by Fisher's exact test. The GG genotype was most frequent at 0.904, with GC frequency 0.096 and CC genotype frequency 0.000 (reflecting the small sample number and the low frequency of this genotype in the Caucasian population), (figure 3.6). There was no significant difference between the –572 genotype distribution for SA and controls (Fisher's exact test, p=0.675), though the power of the study was reduced by only obtaining genotype results for 44% of the SA samples.

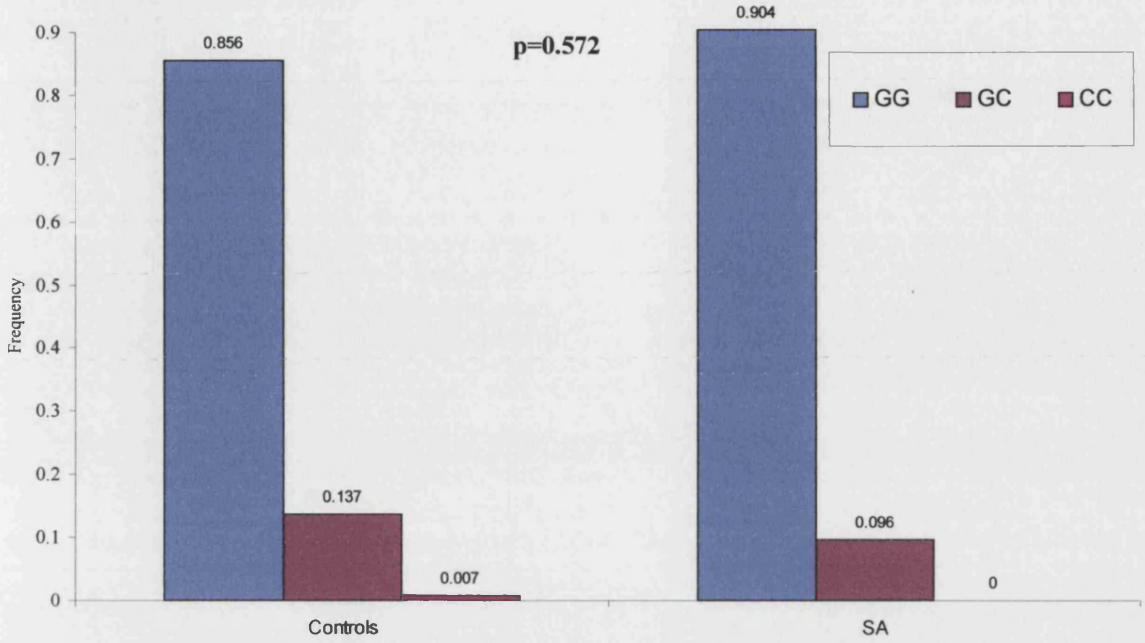

Figure 3.6. The genotype distribution for the –572 polymorphism of IL-6 in SA and controls.

The –572 genotype was determined by RFLP with *Mbi*I and heteroduplex analysis (see 2.8.1.1 & 2.8.3) for 672 UK Caucasian healthy controls and 52 UK Caucasian SA patients (data values shown). Both the control and SA group were in H-W equilibrium (exact test). Controls were compared to SA by exact test and were not significantly different, p-value shown.

3.5 The –597 polymorphism of IL-6

3.5.1 The –597 genotype is not associated with SA

The Nuneaton, Goodinge and WEDC controls were genotyped for the –597 polymorphism using RFLP with *Fok*I, the Nuneaton and WEDC samples were also genotyped by SSOP (see 2.8.1.1 & 2.8.2). The Nuneaton and Goodinge controls were in H-W equilibrium using the chi-squared test (95% confidence), (table 3.6). However, the WEDC control group was just out-with H-W equilibrium for 95% confidence limits (p=0.043), but well within H-W equilibrium for 90% confidence limits (chi-square test) and there was no significant difference between the Nuneaton, Goodinge or WEDC groups (chi-square test, 95% confidence, 2df, p≥0.1). The groups were therefore combined as a representative control population. The combined group was in H-W equilibrium (chi-square test, 95% confidence). The GA genotype was most common (frequency 0.471), with the GG homozygote genotype (frequency 0.374) more common that the AA genotype (frequency 0.156). The A allele frequency was 0.391.

Control group	GG	GA	AA	n	A-allele frequency
Nuneaton	0.374	0.455	0.171	211	0.398
Goodinge	0.422	0.409	0.168	232	0.373
WEDC	0.325	0.544	0.131	237	0.403
Combined Nun/Good/WEDC	0.374	0.471	0.156	680	0.391

Table 3.6. The genotype distribution for the –597 polymorphism of IL-6 in healthy UK Caucasian controls.

The Nuneaton and Goodinge groups, but not the WEDC group, were in H-W equilibrium by chi-square test (95% confidence). The WEDC group was in H-W equilibrium by chi-square test for 90% confidence limits. There was no significant difference between the Nuneaton, Goodinge or WEDC groups (chi-square test, 95% confidence, $p \geq 0.1$). n=number of samples.

Genotyping the –597 polymorphism by RFLP with *Fok*I and SSOP obtained results for 85 of the 118 SA samples. Incomplete typing was again due to problems generating PCR product from many stored genomic DNA samples. Comparison of distribution of gender and age at onset was not significantly different ($p=0.998$ and 0.443 respectively by chi-square test, 95% confidence, 2df) for the group for which –597 genotyping was obtained and for those genotyping could not be done. The genotype distribution was in H-W equilibrium (chi-square test, 95% confidence), GA frequency 0.471, GG genotype frequency 0.412 and AA genotype frequency 0.118 (figure 3.7). There was no significant difference between this distribution and that of the control population (chi-square test, 95% confidence, 2df, $p=0.600$). This was also the case if the WEDC control group was omitted ($p=0.431$). It should be remembered that the power of the study to exclude an association with SA is lowered by the reduced number of samples for which genotyping results were obtained.

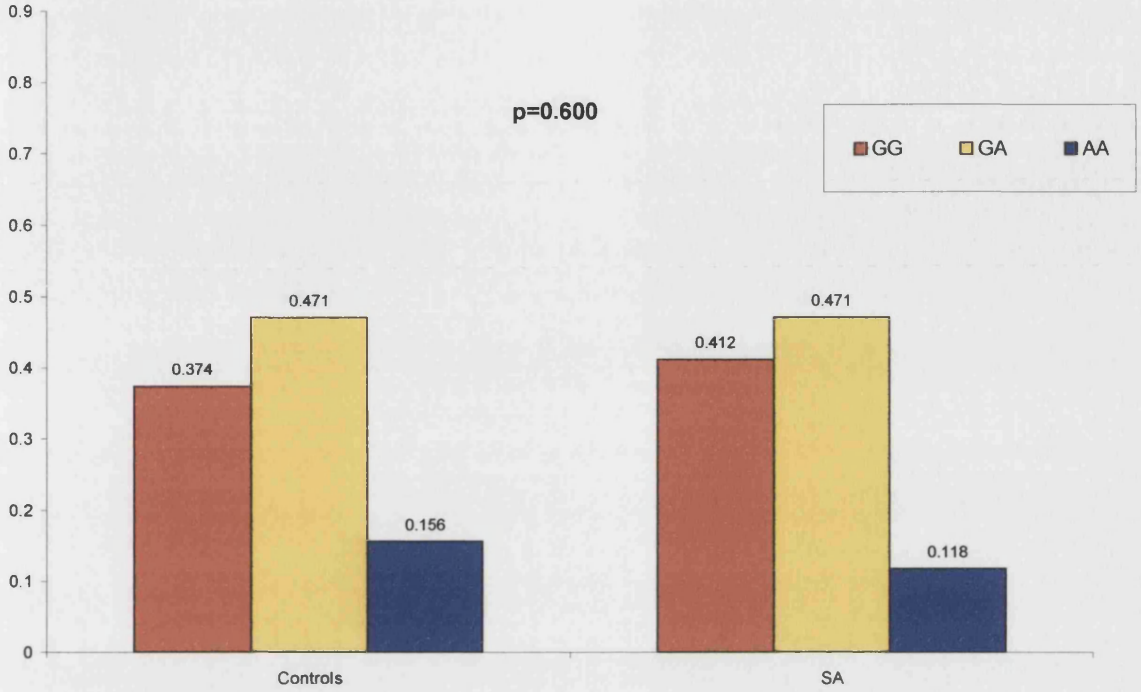

Figure 3.7. The genotype distribution for the –597 polymorphism of IL-6 in SA and controls.

The –597 genotype was determined by RFLP with *Fok*I and SSOP (see 2.8.1.1 & 2.8.2) for 680 UK Caucasian healthy controls and 85 UK Caucasian SA patients (data values shown). Results were compared by chi-square test (2df), with p-value shown.

3.6. Allelic associations with the –174 polymorphism

3.6.1. The –174 polymorphism is in strong allelic association with –597 and weak allelic association with -572

To investigate whether allelic association occurred between the –174, -572 and –597 SNPs, the genotype information for 600 controls with 2- or 3-loci genotype information was analysed using the EH linkage-utility program (available through HGMP, www.hgmp.mrc.ac.uk). This programme calculated the gene frequency from the genotype data for cases and controls, and then estimated the 2- and 3-loci haplotype frequencies under the assumption of either allelic association (associated model) or of no allelic association (independent model), (Terwilliger and Ott, 1994). The EH program uses the Expectation-maximisation algorithm to obtain accurate and fast estimates of haplotype frequencies from genotype data and can be used to test differences between haplotype frequencies. By performing the analysis on cases,

controls and the combined cases and controls, a likelihood ratio test can be used to test for a difference in haplotype frequencies between cases and controls. The chi-square test for the independent inheritance model (assumption of no allelic association) versus the associated inheritance model (assumption of allelic association), for each set of loci, revealed a significant difference ($p<0.0001$, table 3.7). This indicated that there was allelic association between the SNPs. Allelic frequency tables generated from these estimated haplotype frequencies allowed determination of the linkage disequilibrium co-efficient Δ for the –174 & –572 alleles, and the –174 & –597 alleles.

(a) n=617

		Haplotype frequency	
-174 allele	**–597 allele**	**Independent model**	**Associated model**
G	G	0.366	0.595
G	A	0.232	0.003
C	G	0.246	0.018
C	A	0.156	0.384

$\chi^2 = 1022.76$, $p<0.00001$, Ln(L) = -732.11
Δ=0.956

(b) n=612

		Haplotype frequency	
-174 allele	**-572 allele**	**Independent model**	**Associated model**
G	G	0.555	0.531
G	C	0.045	0.069
C	G	0.369	0.394
C	C	0.030	0.006

$\chi^2 = 31.19$, $p<0.0001$, Ln(L) = -871.78
Δ=0.188

(c) n=660

		Haplotype frequency	
-572 allele	**-597 allele**	**Independent model**	**Associated model**
G	G	0.561	0.539
G	A	0.363	0.386
C	G	0.046	0.068
C	A	0.030	0.007

$\chi^2 = 29.57$, $p<0.0001$, Ln(L) = -945.99
Δ=0.176

Table 3.7. Estimated 2-loci haplotype frequencies for the SNPs (a) –174/–597, (b) –174/–572, (c) –572/–597 of IL-6 in healthy UK Caucasian controls.
Haplotype frequencies were estimated from the genotype frequency using the EH linkage-utility program for independent (assumption of no allelic association) and associated (assumption of allelic association) models of inheritance. If alleles were not associated then the results from the two models would be similar. The likelihood of the models was compared by chi-square test (95% confidence, 1df). Ln(L)=log likelihood of allelic association, Δ=linkage disequilibrium co-efficient, n=number of samples.

The –174G was in strong allelic association with -597G, -174C with –597A (Δ=0.956). The –174G was in weak allelic association with –572C, -174C with –572G (Δ=0.188). Consistent with the strong allelic association between the –174 and –597 SNPs, the –597G was in weak allelic association with –572C, –597A with –572G (Δ=0.176).

3.6.2. The –174/-597 haplotype frequency was significantly different in SA

Interestingly, when the estimated haplotype frequencies for the –174 and –597 SNPs were determined for the SA group, the allelic association between these polymorphisms was significantly less (Δ=0.871) than for the healthy control group (Δ=0.956), ($p<0.02$, table 3.8).

(a) n=81

		Haplotype frequency	
-174 allele	**-597 allele**	**Independent model**	**Associated model**
G	G	0.381	0.585
G	A	0.249	0.044
C	G	0.224	0.019
C	A	0.146	0.351

$\chi^2 = 90.18$, $p<0.0001$, Ln(L) = -110.78
Δ=0.871

(b)

Ln(L) SA	Ln(L) controls	Ln(L) all	Difference	χ^2	p-value
-110.78	-732.11	-847.11	4.22	8.44	$0.02<p<0.05$

Table 3.8. Estimated 2-loci haplotype frequencies for the SNPs –174 and –597 of IL-6 in (a) Caucasian SA patients, (b) compared to healthy Caucasian controls.
(a) Haplotype frequencies were estimated from the genotype frequency using the EH linkage-utility program for independent (assumption of no allelic association) and associated (assumption of allelic association) models of inheritance. The likelihood of the models was compared by chi-square test (95% confidence, 1df). Ln(L)=log likelihood of allelic association, Δ=linkage disequilibrium co-efficient, n=number of samples. (b) the Ln(L) was compared for the genotype distribution in SA and healthy controls (see table 3.7) by chi-square test (95% confidence, 3df).

The difference was due to a significantly higher frequency of –597A–174G individuals and lower frequency of –597A–174C individuals in the SA group, suggesting that carriage of the –174G allele was associated with an increased susceptibility to SA, independent of the allele at position –597.

3.6.3. The –597G–572G–174G and –597A–572G–174C haplotypes were most common

In the same way, using the EH linkage-utility program, the 3-loci haplotype frequencies for the –174, –572 and –597 polymorphisms could be estimated and compared for the control and SA group. This showed that the most common naturally occurring haplotype was the –597G–572G–174G with a frequency of 0.524, followed by the –597A–572G–174C with a frequency of 0.372 (table 3.9). The –597G–572C–174G haplotype was the next common with a frequency of 0.070, while other haplotypes occurred more rarely with a frequency of ≤0.018. The order of haplotype frequency was similar for the SA group though 3-loci haplotype data could only be calculated on 35 of the SA patients.

			Haplotype frequency	
-597 allele	**-572 allele**	**-174 allele**	**Controls** (n=610)	**SA** (n=35)
G	G	G	0.524	0.570
A	G	C	0.374	0.313
G	C	G	0.070	0.057
G	G	C	0.018	0.030
A	C	C	0.007	<0.001
A	G	G	0.005	0.030
A	C	G	0.001	0.000
G	C	C	<0.001	0.000
			χ^2=1005.06 p<0.00001 Ln(L)=-1003.13	χ^2=37.46 p<0.0001 Ln(L)=-56.11

Table 3.9. Estimated 3-loci haplotype frequencies for the SNPs –597, –572 and –174 of IL-6 in Caucasian controls and SA patients.
Haplotype frequencies were estimated from the genotype frequency using the EH linkage-utility program for independent (assumption of no allelic association) and associated (assumption of allelic association) models of inheritance. The values for the associated model are shown as the results showed a high significance of allelic association when compared by chi-square test (95% confidence, 7df), shown under the table. Ln(L)=log likelihood of allelic association, n=number of samples.

3.7. Power calculations

Retrospectively, the observed difference in the frequency of G-allele carriers between controls and cases was less than the estimated 10% taken at the start of this study. The observed differences were 4.7% for the –174, 2.8% for the –572 and 3.8% for the –597 polymorphism. The power of this study to exclude a polymorphic association with

disease was therefore significantly less than 80%. Given this low power it is fortunate that the –174 polymorphism association with SA was detected. Four independently recruited control groups of adequate numbers to have 80% power in comparing groups of equal sizes were not significantly different from one another. It is therefore unlikely that population stratification was present, making it less likely that the difference seen between the controls and SA group for the –174 polymorphism occurred by chance alone.

3.8. Summary of genotype results

The –174 polymorphism of IL-6 was associated with SA, with the CC genotype occurring in significantly lower frequency in SA compared to healthy controls. The –174 polymorphism appeared to be a severity, as well as susceptibility marker, with the lower frequency of –174CC occurring in the early disease onset group (≤5 years of age) who tend to have a poorer disease prognosis. The odds ratio for SA was higher for carriers of the –174G-allele and from the allelic association studies this appeared to be independent of the allele at position –597. The –597 polymorphism was in strong allelic association with –174 and the –572 polymorphism in weak allelic association with –174 and –597. The haplotype –597G–572G–174G was the most common, followed by –597A–572G–174C and –597G–572C–174G, other haplotypes were rare.

CHAPTER 4

RESULTS:

The influence of IL-6 5'-flanking region polymorphisms on transcriptional activity

4.1. Transfection studies

Transient and stable transfection studies were used to investigate the potential influence of the 5'-flanking region polymorphisms of IL-6 on the levels of IL-6 gene transcription. This was first carried out in HeLa cells, a transformed human epithelial cell line derived from a cervical carcinoma. These epithelial cells are robust, relatively easy to culture and transfect efficiently. They express endogenous IL-6 (confirmed by RT-PCR) that is inducible with pro-inflammatory cytokine stimulation (IL-1β & TNFα), and therefore have constitutive and induced expression of relevant transcription factors required for IL-6 transcription. The HeLa cells provided an *ex vivo* model of human cells for comparison of the allelic effects of IL-6 polymorphisms. Huh7 cells, a transformed human hepatocyte cell line derived from a hepatocellular carcinoma, were chosen as a second cell type for investigation. In terms of volume of IL-6 production *in vivo* and responsiveness to acute inflammatory stimuli, hepatocytes were considered the largest producers of IL-6. RT-PCR studies confirmed that Huh 7 cells expressed endogenous IL-6 and that the gene was inducible with IL-1 stimulation.

Luciferase was chosen as the reporter gene as it fulfilled the criteria for an ideal reporter, not undergoing any post-transcriptional or post-translational modification, remaining intra-cellular and producing a gene product easily detectable on assay. In addition, the intracellular half-life of luciferase is three hours making it a sensitive indicator to changing levels of promoter activity over time (Bronstein et al., 1994). The β-galactosidase (β-gal) gene driven by the respiratory syncytial virus (RSV) promoter was chosen as a control plasmid as this gene has a long half-life, does not undergo post-transcriptional or post-translational modification and the RSV promoter is non-responsive to cytokine stimulation with IL-1 and TNFα (confirmed in transfection studies). β-gal remains as an intra-cellular protein and is easily detected with substrate assay. Transfected β-gal was expressed in HeLa and Huh7 cells with negligible endogenous levels detected. The pro-inflammatory cytokines IL-1β and TNFα were chosen as inducers of IL-6 transcription to model an acute inflammatory response. These cytokines, particularly IL-1, are the main inducers of IL-6 and act via the NF-κB and C/EBP transcription factor sites, with a lesser involvement of the cAMP response element (see section 1.3.2). Glucocorticoids were investigated as a known repressor of IL-6 transcription (see 1.3.2.5).

4.1.1. Generation of plasmid constructs

The genotype associations identified between the –174 G/C polymorphism of IL-6 and systemic arthritis (SA, see chapter 3), were examined. Constructs of 611bp of the 5'-regulatory region of IL-6 from +61 to –550 were initially used to investigate the –174 allelic effects. These constructs were generated by PCR of individuals of known sequence, with either the homozygote G or the C allele at position –174. The fragment was cloned into the luciferase-reporter plasmid PGL3-basic between the *Kpn*I and *Nhe*I restriction sites (figure 4.1 & section 2.9.1). The constructs were named ΔG for the –174G allele and ΔC for the –174C allele. Automated sequencing confirmed that the constructs differed only by the allele at position –174. The AT-tract sequence between –373 and –392 was a constant A8/T12 for both constructs. To investigate the influence of IL-6 5'-flanking regions up-stream of the –174 polymorphism, including the AT-tract and surrounding region, deletion mutants of constructs ΔG and ΔC (611bp) were generated by PCR and cloned into the same sites of PGL3-basic (see section 2.9.1). Constructs designated ΔGD (-174G) & ΔCD (-174C) were 371bp in length from +61 to –310 (figure 4.1). Constructs designated ΔGDS (-174G) & ΔCDS (-174C) were 280bp in length from +61 to –219 (figure 4.1). ΔGD/ΔCD lacked the AT-tract and surrounding regions from –311 to –550 and ΔGDS/ΔCDS in addition lacked the AP1 site and surrounding regions from –220 to –310. To investigate the potential influence of AT-tract polymorphisms on IL-6 transcription, construct ΔG9/11 (-174G) was generated by PCR of genomic DNA from an individual with known AT-tract sequence A9T11 instead of A8T12. This construct was otherwise identical to ΔG as confirmed by automated sequencing. Each construct was checked for correct orientation and sequence of the insert by manual and automated-sequencing (see section 2.8.4). The length of each insert was verified by agarose gel electrophoresis of *Not*I and *Bgl*II restriction digest products or by PCR amplification (see section 2.9.2). The PCR product was digested with *Sfa*NI (cuts –174G sequence but not –174C) to allow quick verification of the allele at position –174 (see 2.9.2 & 2.7).

The PGL3-basic plasmid vector was selected for this study as it does not contain any other promoter sequences. The 5'-flanking region of IL-6 therefore directly regulates all cellular levels of luciferase in this system.

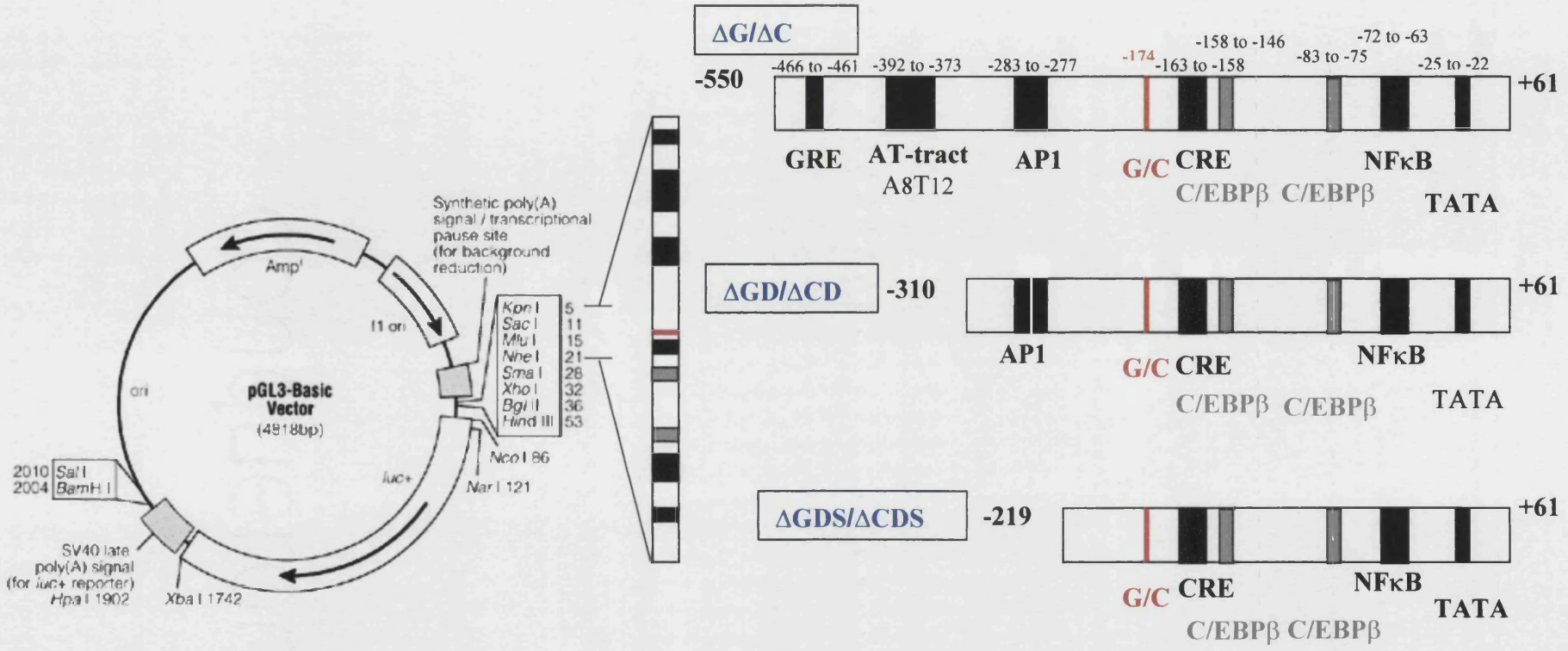

Figure 4.1. The ΔG/ΔC (611bp), ΔGD/ΔCD (371bp) and ΔGDS/ΔCDS (280bp) IL-6 5'-flanking region constructs cloned into PGL3-basic.
Known 5'-flanking region sequences of IL-6 were amplified by PCR and cloned into the PGL3-basic luciferase reporter vector (Promega) between restriction sites *Kpn*I and *Nhe*I (see section 2.9.1 for method). The –174G/C polymorphism site and main transcription factor sites are indicated (see 1.3.2 for more detail).
Luc+=luciferase gene (arrow indicates direction of read frame), Amp'=ampicillin resistance gene.

To investigate the influence of the –174 polymorphism in the context of naturally occurring haplotypes of the 5'-flanking region polymorphisms, a 1.17kb IL-6 construct from +8 to –1170 (in pGEM) was kindly provided by S. Akira and T. Kishimoto (Institute of Molecular and Cellular Biology, Osaka University, Japan). Automated sequencing confirmed the sequence to have the common allele at each polymorphic site corresponding to Yasukawa et al. (1987), GenBank accession number Y00081 (–174G^{-373}A9/T11^{-392}–572G–597G–627C). The 1.17kb IL-6 sequence was sub-cloned from the pGEM vector into pBluescript phagemid (Stratagene) and then cloned into the PGL3-basic plasmid between *Sac*I and *Xho*I (see 2.9.4). Confirmation of orientation of the insert was established by automated sequencing. This construct was designated GGG (–597G–572G–174G). The –627 polymorphism was kept constant at –627C as the frequency of the other allele had been shown to be extremely rare in the UK Caucasian population (frequency <0.010, see 3.2). Genotype studies in the healthy UK Caucasian population revealed the most common naturally occurring haplotype to be –597G–572G–174G at frequency 0.524, the next most common haplotype was –597A–572G–174C at frequency 0.372, followed by –597G–572C–174G at frequency 0.070 (section 3.6.3). The additional haplotypes were generated by site-directed mutagenesis from the GGG construct and designated AGC (–597A–572G–174C) and GCG (–597G–572C–174) respectively. The GCG construct allowed comparison with GGG to investigate the effect of the –572 polymorphism on transcription. To determine if the –597 polymorphism had an independent functional influence on transcription despite strong allelic association with –174 a fourth construct was generated with –597A–572G–174G, designated AGG. This haplotype occurred only rarely in the UK Caucasian population with a frequency of 0.005 (section 3.6.3). Successful mutation for each allele was preliminarily confirmed by PCR and RFLP with *Sfa*NI for the –174 polymorphism, *Mbi*I for the –572 polymorphism and *Fok*I for the –597 polymorphism (see 2.7). Each haplotype construct was then sequenced by automated sequencing (MWG Biotech) to verify the haplotype and to ensure no other mutations had been introduced. The AT-tract was kept constant at A9/T11.

A sequence identical to the GGG construct from Akira and Kishimoto but with an AT-tract of A8T12 instead of A9T11 was not available. Attempts to mutate the A9T11 AT-tract of the 1.17kb construct by transformer site-directed mutagenesis (see 2.9.5.2) were repeatedly unsuccessful. This was probably because of A to T binding within the

AT-tract of the mutation primer to form a hairpin-like structure and thereby preventing binding to the template DNA. This occurred despite high annealing temperatures and extended end sequences on the primers. Mutation of a restriction digest site (*SalI*) within the plasmid vector to allow selection was successful by this technique (see 2.9.5.2). The potential influence of the AT-tract polymorphism was therefore only investigated in the 611bp constructs.

The IL-6 plasmid DNA constructs were purified for transfection by double caesium chloride gradients (see 2.9.7). This ensured a high level of purity, with negligible levels of endotoxin or nicked, degraded or truncated plasmid. PCR and RFLP were used to verify the polymorphism of each preparation. The concentration of plasmid DNA was determined by optical density at 260nm; 1μg/μl stocks were then prepared and the OD_{260} rechecked (see 2.9.3).

4.1.2. Optimization of transfection conditions

Transfection was carried out in 24 well plates. $5x10^4$ viable cells were seeded per well and grown for 48 hours until 80-90% confluence was reached. The IL-6 constructs were co-transfected by the calcium phosphate precipitation method with RSV-β-gal control plasmid (see 2.10.1 for method). Transfection efficiency was found to be 70-75% by β-galactosidase staining (see 2.10.6). Cell viability post-transfection was reduced by 20%. After 18 hours of transfection in media containing 10% foetal calf serum (FCS), the cells were washed and stimulated with fresh media (2% FCS) with or without added cytokine. The IL-6 promoter but not the RSV-promoter was sensitive to cell exposure to FCS or IL-1. The optimal concentration of FCS to maintain cell viability but with minimal IL-6 stimulation was found to be 2%. Enzyme-linked immunosorbent assay (ELISA, see 2.12.1) was used to confirm the absence of cytokines IL-1, TNF, and IL-6 from the media or heat inactivated FCS batches used. A commercial assay for lipopolysaccaride (LPS) confirmed <0.1units/ml of LPS in the media or FCS. After the required stimulation time, cells were washed, harvested, and light emission units for luciferase and β-galactosidase were determined (see 2.10.5&6).

The results presented in this chapter represent repeat experiments with at least two separate preparations of construct DNA. Any individual results greater than two

standard deviations from the mean were excluded. Luciferase light-emission units were corrected for β-galactosidase activity to standardise for variation in transfection efficiency between experiments.

$$\text{Standardised result} = \frac{\text{luciferase light emission units (units/min)}}{\beta\text{-galactosidase light emission units (units/min)}}$$

The results are presented as fold-change compared to baseline (0hrs) unless stated otherwise and shown graphically as the mean ± standard deviation. Statistical significance was determined using the paired T-test with 95% confidence limits.

4.1.3. The –174 polymorphism influences levels of IL-6 transcription

Basal and IL-1β-induced levels of IL-6 transcription were compared for the 611bp constructs ΔG (–174G) and ΔC (–174C) co-transfected with RSV-β-gal into HeLa cells for 18 hours. The cells were washed and stimulated with fresh media (2% FCS) alone or containing 100units/ml of IL-1β (Genzyme Diagnostics). At set time intervals post stimulation, the cells were harvested and assayed for levels of luciferase and β-galactosidase.

There was a small, but significant increase in levels of IL-6 transcription from baseline with media change alone (ΔG 2.8-fold, $p=0.028$, ΔC 2.2-fold, $p=0.012$) but no significant difference between ΔG and ΔC in unstimulated cells ($p>0.1$, figure 4.2). IL-1β stimulation resulted in increased IL-6 transcription for both ΔG and ΔC with maximum expression occurring within 6 hours of IL-1 stimulation. There was a significant difference in the magnitude of response to IL-1β for ΔG (32-fold) and ΔC (18-fold) with –174G resulting in an approximately 2-fold higher level of expression than –174C at maximal stimulation ($p=0.002$, figure 4.2).

A dose response curve was determined for the constructs with 6-hours of IL-1β stimulation. Maximum stimulation for both alleles was reached at 100units/ml IL-1β above which the dose response reached a plateau (figure 4.3). The G-allele reached a significantly higher level of expression than the C-allele at 100units/ml IL-1β stimulation ($p=0.024$). 100units/ml IL-1β was chosen for subsequent experiments as the optimal dose to achieve maximal stimulation of both alleles. This equates to 2.9nM of IL-1β; within the physiological pico- to nano-molar range of IL-1 *in vivo*.

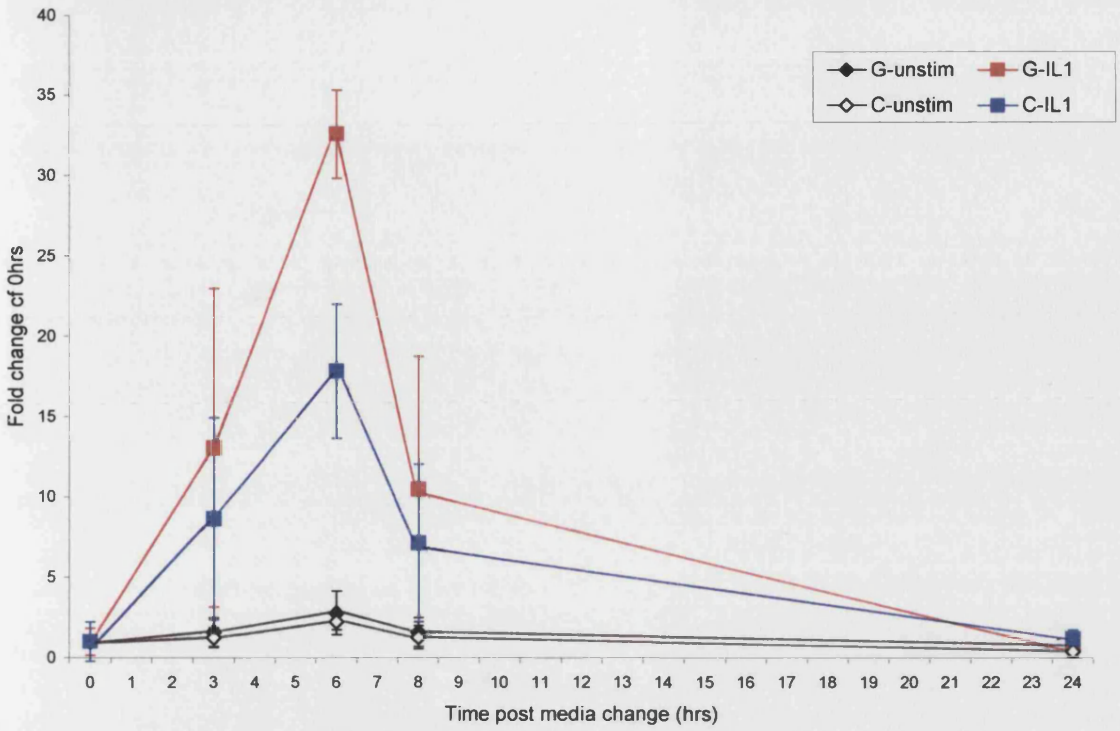

ΔG compared to ΔC

	UNSTIMULATED		IL-1β-STIMULATED	
Time post media change (hrs)	mean difference	p-value	mean difference	p-value
3	0.346	0.111	4.409	0.060
6	0.546	0.242	14.744	0.002*
8	0.309	0.123	3.345	0.074
24	0.057	0.244	0.234	0.187

Figure 4.2. Time course for ΔG and ΔC constructs transfected into HeLa cells, unstimulated and with IL-1β stimulation.

HeLa cells in 24-well plates were co-transfected with the IL-6-luciferase constructs ΔG or ΔC and control plasmid RSV-β-gal. After 18hrs, cells were washed with PBS and 1ml of 2%FCS medium ± 100U IL-1β was added to each well. At the allocated time point, cells were harvested and luciferase and β-galactosidase assays carried out (see section 2.10.1). Luciferase light-emission units were standardised for β-gal levels. Results show fold change in levels of expression compared to baseline (0hrs). Results represent eight repeat experiments with duplicate wells, y-error bars= standard deviation. The table shows comparison of values by paired T-test, *denotes a significant difference within 95% confidence limits.

ΔG produced approximately 2-fold higher levels of reporter gene expression than ΔC at maximal stimulation. At all time points, IL-1β significantly increased the level of expression for ΔG and ΔC ($p<0.04$). 2% FCS medium alone (unstimulated conditions) significantly increased ΔG and ΔC expression at 6-hours only ($p<0.03$).

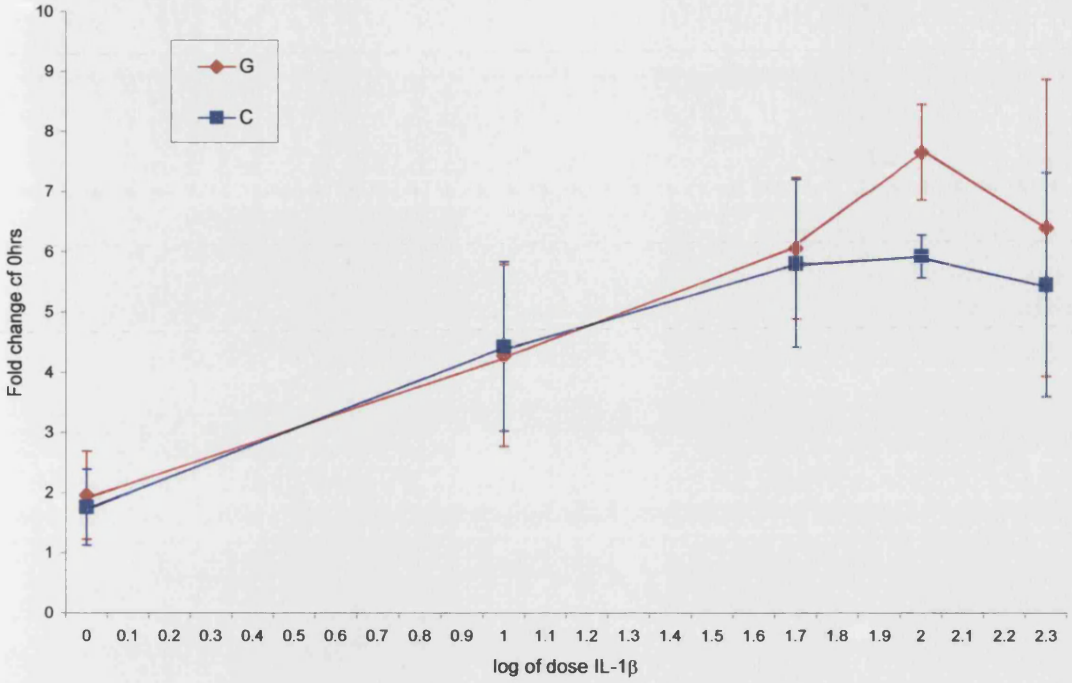

ΔG compared to ΔC

Dose IL-1β (units/ml)	mean difference	p-value
1	0.199	0.076
10	0.149	0.423
50	0.252	0.061
100	1.73	0.024*
200	0.950	0.066

Figure 4.3. Dose response curve for IL-1β stimulation of ΔG and ΔC constructs transfected into HeLa cells.

HeLa cells in 24-well plates were co-transfected with the IL-6-luciferase constructs ΔG or ΔC and control plasmid RSV-β-gal. After 18hrs, cells were washed with PBS and 1ml of 2%FCS medium + 1, 10, 50, 100 or 200U of IL-1β (shown as log of the dose) was added to each well. After 6 hours, the cells were harvested and luciferase and β-galactosidase assays carried out (see section 2.10.1). Luciferase light-emission units were standardised for β-gal levels. Results show fold change in levels of expression compared to baseline (0hrs), representing two repeat experiments with duplicate wells, y-error bars= standard deviation. The table shows comparison of values by paired T-test, *denotes a significant difference within 95% confidence limits.

Maximal stimulation for ΔG and ΔC occurred with 100U/ml IL-1β with ΔG showing significantly higher levels of expression.

4.1.4. Regions up-stream of the –174 polymorphism modulate the –174 allelic effect

Deletion mutants of constructs ΔG and ΔC were used to investigate the possible influence of up-stream regions of IL-6 on the –174 allelic effect in HeLa cells. Specific AT-tract polymorphisms at –373 to –392 have been reported to be associated with the –174 G and C alleles (Fishman et al., 1998). Deletion mutants lacking the AT-tract and surrounding region to –310 (ΔGD and ΔCD) were studied as well as mutants lacking the AP1 site (–277 to –283) and surrounding regions to –219 (ΔGDS and ΔCDS), (figure 4.1). A time course of IL-1β stimulation (100U/ml) for the deletion mutants in HeLa cells revealed maximal stimulation of transcription to occur at 6-hours, as for the 611bp constructs ΔG and ΔC. The constructs were therefore compared in unstimulated and IL-1β-stimulated conditions at this time point.

Significantly higher expression was obtained for ΔG compared to ΔC with IL-1β stimulation ($p=0.018$), but not when unstimulated ($p=0.051$), (figure 4.4). Constructs ΔGD and ΔCD resulted in significantly lower levels of unstimulated and IL-1β-stimulated expression (2.8-fold reduction, $p<0.001$) indicating that the deleted region from –311 to –550 contains an enhancer element(s) for constitutive and IL-1β-induced IL-6 transcription.

ΔGD showed significantly higher levels of transcription than ΔCD with IL-1β stimulation ($p=0.032$), but not when unstimulated ($p=0.077$). Constructs ΔGDS and ΔCDS resulted in a further small, but significant reduction in the level of unstimulated and IL-1-stimulated transcription, with the reduction being least for ΔGDS when stimulated with IL-1β (1.13-fold, $p=0.045$) compared to unstimulated ΔGDS (reduction 1.52-fold, $p=0.0002$), unstimulated ΔCDS (reduction 1.36-fold, $p<0.0001$) and IL-1-stimulated ΔCDS (reduction 1.42-fold, $p<0.0001$). This indicated that the deleted region from –220 to -310 also acts as an enhancer for constitutive and IL-1β induced expression of IL-6. However, the fact that the G-allele is able to partially over-come the effect of removal of this enhancer region when stimulated with IL-1β suggests that an element in this region may be interacting with the –174 polymorphism.

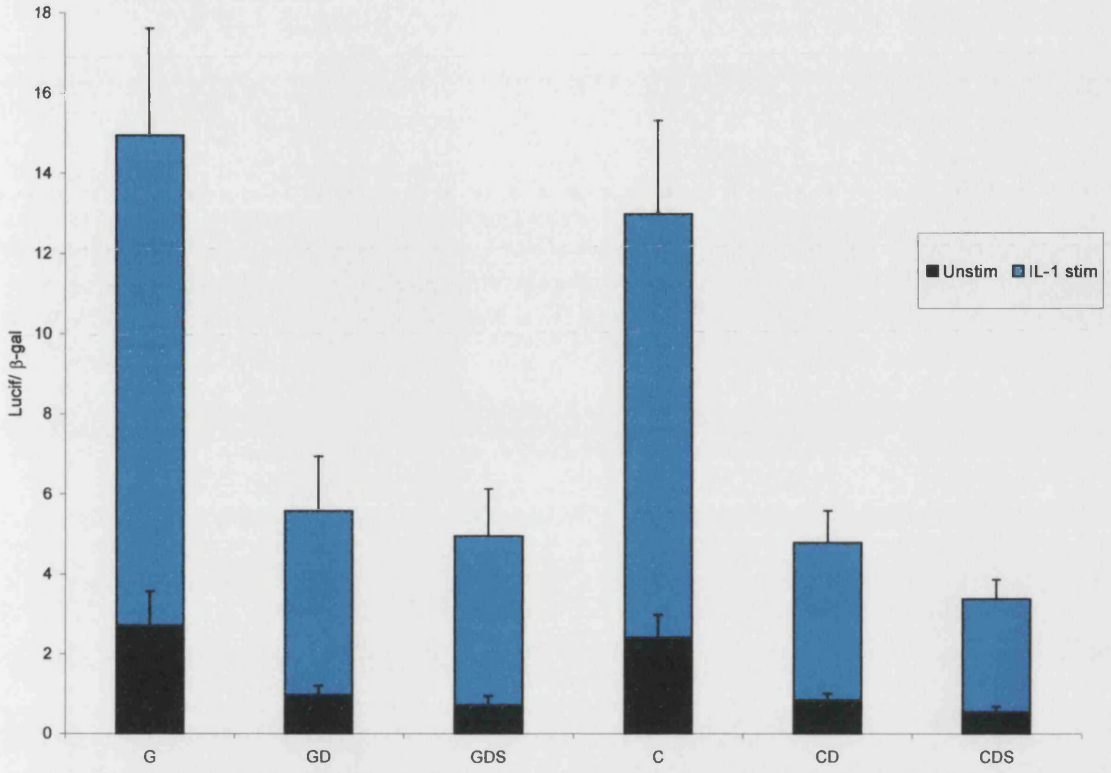

Comparison of constructs

		UNSTIMULATED		IL-1β-INDUCED	
Construct 1	Construct 2	mean difference	p-value	mean difference	p-value
ΔG	ΔC	0.310	0.051	1.958	0.018*
ΔG	ΔGD	1.745	<0.001*	9.323	<0.001*
ΔGD	ΔGDS	0.252	<0.001*	0.623	0.045*
ΔC	ΔCD	1.568	<0.001*	8.196	<0.001*
ΔCD	ΔCDS	0.285	<0.001*	1.411	<0.001*
ΔGD	ΔCD	0.133	0.077	0.791	0.032*
ΔGDS	ΔCDS	0.165	0.007*	1.582	<0.001*

Figure 4.4. Comparison of deletion mutant constructs ΔG/ΔC, ΔGD/ΔCD and ΔGDS/ΔCDS transfected into HeLa cells.

HeLa cells in 24-well plates were co-transfected with the IL-6-luciferase constructs ΔG or ΔC, ΔGD or ΔCD, ΔGDS or ΔCDS and control plasmid RSV-β-gal. After 18hrs, cells were washed with PBS and 1ml of 2%FCS medium ± 100U of IL-1β was added to each well. After 6 hours, the cells were harvested and luciferase and β-galactosidase assays carried out (see section 2.10.1). Luciferase light-emission units were standardised for β-gal levels. Results show fold change in levels of expression compared to baseline (0hrs), representing three repeat experiments with 8 replica wells, y-error bars= standard deviation. The table shows comparison of values by paired T-test, *denotes a significant difference within 95% confidence limits.

Deletion of region –311 to –550 (ΔGD & ΔCD) and –220 to –310 (ΔGDS & ΔCDS) resulted in sequential reductions in the level of transcription with both alleles. Deletion of region –220 to –310 had differential effects on ΔGDS compared to ΔCDS.

This could be an enhancer element facilitating down-stream factor binding when the –174C allele is present, or an inhibitory element facilitating down-stream factor binding when the –174G allele is present. Either way, it suggests that factor(s) bound around the –174 site are differentially stabilized or facilitated by a factor(s) in the region –220 to –310. Interestingly, ΔGDS showed significantly higher levels of transcription than ΔCDS when unstimulated ($p=0.007$) as well as with IL-1β stimulation ($p<0.001$), which had not been seen with the longer constructs ΔGD/ΔCD and ΔG/ΔC. Again this supports an interaction between factor(s) in the region –220 to –310 with factor(s) binding around the –174 polymorphism, with differential modulation for the G and the C allele. This could be an inhibitory element acting more strongly on –174G or an enhancer element acting more strongly on –174C.

4.1.5. AT-tract polymorphisms influence levels of IL-6 transcription

A number of AT-tract polymorphisms have been described (see section 1.3.3.3). In the Caucasian population, the most common polymorphism has been shown to be A8T12 with a frequency of 0.370 (Terry et al., 2000) to 0.421 (Fishman et al., 1998). The next most common polymorphism that maintains the total length of the AT-tract was A9T11 with a frequency of 0.190 (Terry et al., 2000) to 0.211 (Fishman et al., 1998). A8T12 was in strong allelic association with –174C and A9T11 with –174G (Twine et al., 2003). Other polymorphisms identified were A10T9, A10T10, A10T11, A9T10, A9T12 and A11T9. To investigate the possible influence of AT-tract polymorphisms on levels of IL-6 transcription, the 611bp ΔG construct with AT-tract A8T12 ($\Delta G_{8/12}$) was compared to a ΔG construct with AT-tract A9T11 ($\Delta G_{9/11}$), but otherwise identical. These constructs were transfected into HeLa cells and compared for unstimulated and IL-1β-stimulated expression at 6 hours (the time of maximum stimulation). $\Delta G_{8/12}$ resulted in 1.2-fold higher levels of IL-6 transcription than $\Delta G_{9/11}$, both for unstimulated ($p=0.029$) and IL-1β-stimulated expression ($p=0.007$), (figure 4.5). These results indicate that the AT-tract has functional significance in IL-6 transcription and that AT-tract polymorphisms influence levels of expression in HeLa cells. It is possible that the reduced level of transcription seen with deletion mutants ΔGD and ΔCD was at least in part due to removal of the AT-tract.

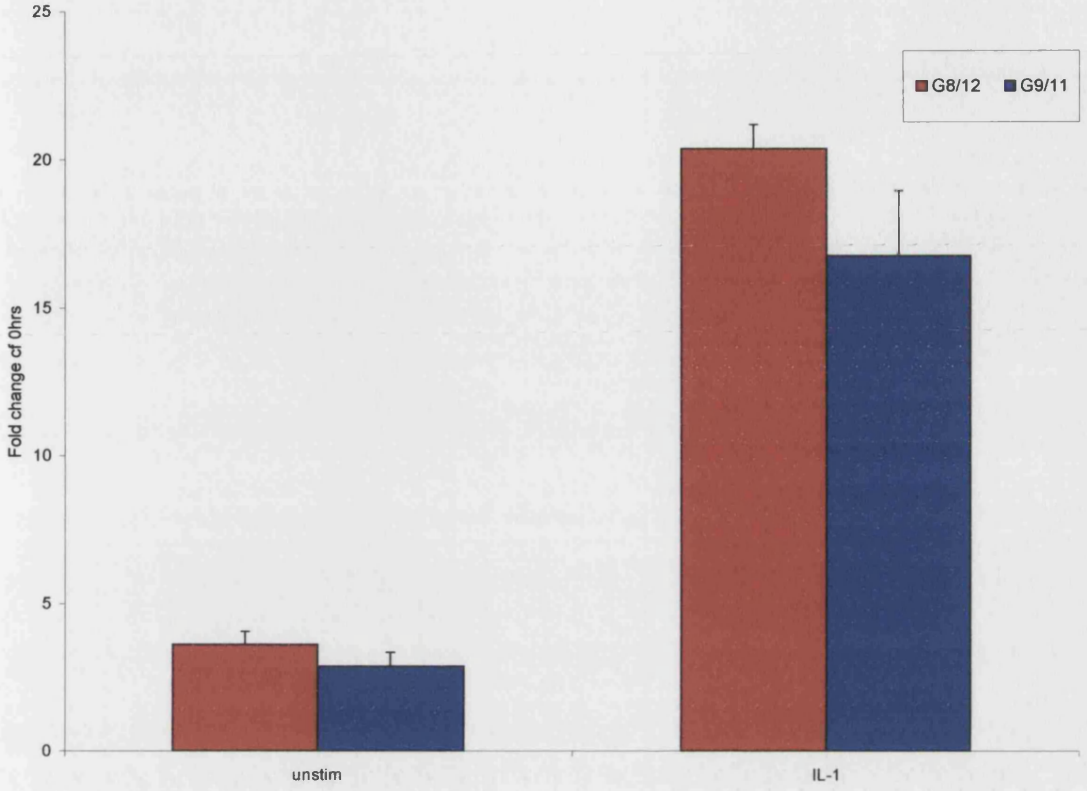

Comparison of constructs

		UNSTIMULATED		IL-1β-INDUCED	
Construct 1	Construct 2	mean difference	p-value	mean difference	p-value
ΔG8/12	ΔG9/11	0.759	0.029*	3.611	0.007*

Figure 4.5. Comparison of ΔG8/12 and ΔG9/11 constructs transfected into HeLa cells.

HeLa cells in 24-well plates were co-transfected with the IL-6-luciferase constructs ΔG8/12 or ΔG9/11 and control plasmid RSV-β-gal. After 18hrs, cells were washed with PBS and 1ml of 2%FCS medium ± 100U of IL-1β was added to each well. After 6 hours, the cells were harvested and luciferase and β-galactosidase assays carried out (see section 2.10.1). Luciferase light-emission units were standardised for β-gal levels. Results show fold change in levels of expression compared to baseline (0hrs), representing three repeat experiments with 4 replica wells, y-error bars= standard deviation. The table shows comparison of values by paired T-test, *denotes a significant difference within 95% confidence limits.

ΔG8/12 produced significantly higher levels of reporter gene expression than ΔG9/11 in unstimulated and IL-1β stimulated conditions.

4.1.6. The –572 but not the –597 polymorphism has an independent functional effect on IL-6 transcription

Constructs of the most common naturally occurring haplotypes of the –174, -572 and –597 polymorphisms of IL-6 were used to investigate the influence of the up-stream polymorphisms on the –174 allelic effect. It was of particular interest to determine whether the –597 polymorphism had any independent or modifying functional effect with respect to the –174 polymorphism as strong allelic association had been shown between –174G and –597G, –174C and –597A (see section 3.6.1). 1.17kb constructs GGG (–597G–572G–174G), AGG (–597A–572G–174G), AGC (–597A–572G–174C) and GCG (–597G–572C–174G) were transfected into HeLa cells by calcium phosphate precipitation, for 18-hours as for the shorter constructs (see 2.10.1). All constructs had a constant A9T11 AT-tract. Although the AGG construct was not one of the common haplotypes, it was used to provide information regarding the functional significance of the –174 and –597 polymorphisms, in comparison to the AGC and GGG constructs.

A time course for IL-1β stimulation (100U/ml) confirmed maximal stimulation to be at 6 hours for the 1.17kb constructs as for the 611bp constructs, shown in figure 4.6 for GGG and ΔG (6-fold, $p \leq 0.0001$). Although a change of media alone (unstimulated conditions, 2% FCS) resulted in a small increase in transcription with the short construct (2-fold, $p=0.004$), this change did not induce a significant increase in transcription with the long construct ($p=0.069$) suggesting that the longer construct was less sensitive to cellular changes induced by exposure to serum factors. The 1.17kb haplotype constructs were compared at the 6-hour time point.

Comparing levels of transcription between the four haplotype constructs, there was no significant difference with unstimulated IL-6 transcription ($p>0.06$), (figure 4.7). However, with IL-1β-stimulated transcription, the GGG haplotype construct (most common naturally occurring haplotype) was associated with a significantly higher level of expression than the AGC haplotype construct (the other common naturally occurring haplotype), ($p=0.016$, figure 4.7). This was consistent with the –174 allelic effect seen with the short constructs ΔG and ΔC (section 4.1.3).

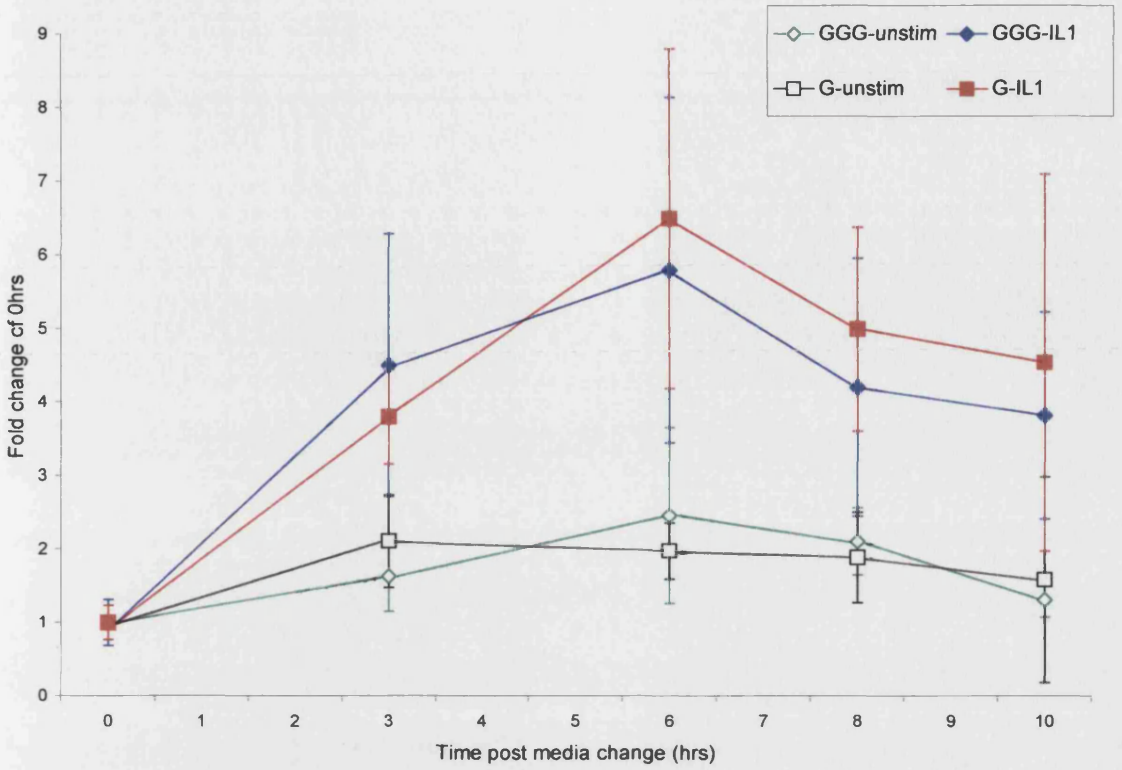

Comparison of conditions for each construct

Condition 1	Condition 2	mean difference	p-value
GGG-unstim 0hrs	GGG-unstim 6hrs	2.458	0.069
G-unstim 0hrs	G-unstim 6hrs	1.973	0.004*
GGG-unstim 6hrs	GGG-IL1 6hrs	3.334	0.0001*
G-unstim 6hrs	G-IL1 6hrs	4.519	0.0004*

Figure 4.6. Time course for GGG and ΔG constructs transfected into HeLa cells, unstimulated and IL-1β stimulated.

HeLa cells in 24-well plates were co-transfected with the IL-6-luciferase constructs GGG or ΔG and control plasmid RSV-β-gal. After 18hrs, cells were washed with PBS and 1ml of 2%FCS medium ± 100U IL-1β was added to each well. At the allocated time point, cells were harvested and luciferase and β-galactosidase assays carried out (see section 2.10.1). Luciferase light-emission units were standardised for β-gal levels. Results show fold change in levels of expression compared to baseline (0hrs). Results represent duplicate experiments with 4 replica wells, y-error bars= standard deviation. The table shows comparison of values by paired T-test, *denotes a significant difference within 95% confidence limits.

Maximal stimulation with IL-1β occurred at 6 hours for GGG and ΔG in HeLa cells. ΔG but not GGG transcription was induced by 2 % FCS medium change alone (unstimulated conditions).

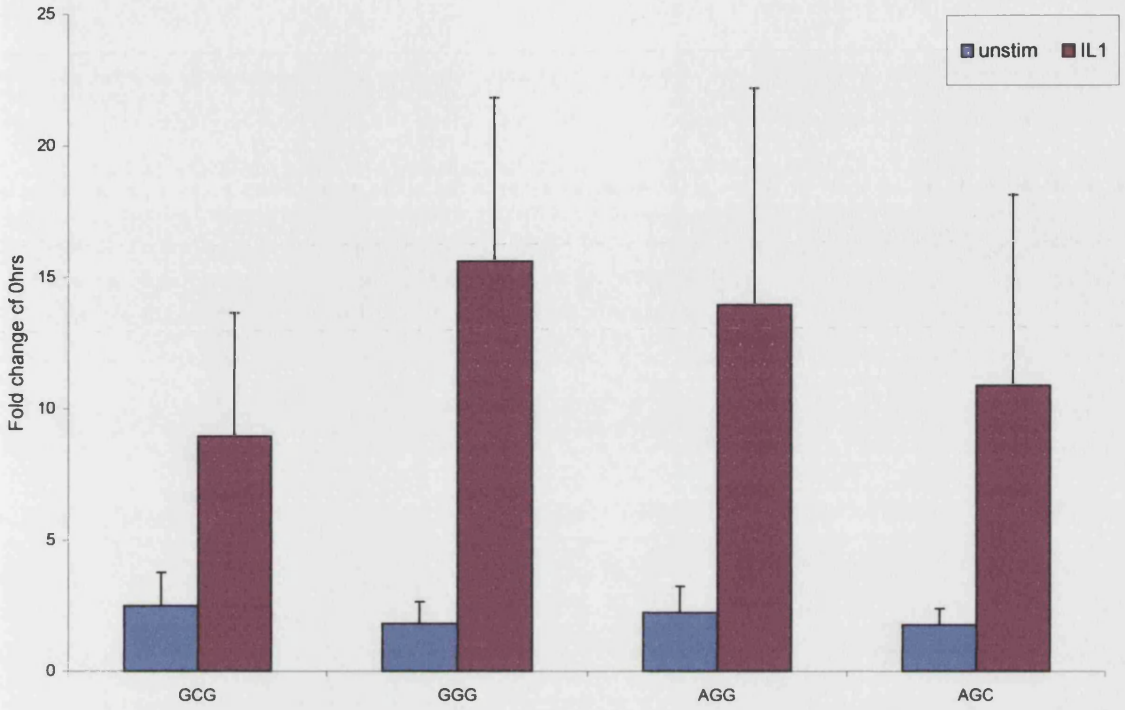

Comparison of constructs

		UNSTIMULATED		IL-1β-INDUCED	
Construct 1	Construct 2	mean difference	p-value	mean difference	p-value
GGG	AGG	0.426	0.070	1.658	0.240
GGG	AGC	0.038	0.434	4.711	0.016*
GGG	GCG	0.690	0.063	6.637	0.019*
AGG	AGC	0.728	0.101	3.053	0.054

Figure 4.7. Comparison of haplotype constructs GCG, GGG, AGG and AGC transfected into HeLa cells.

HeLa cells in 24-well plates were co-transfected with the IL-6-luciferase constructs GCG, GGG, AGG or AGC and control plasmid RSV-β-gal. After 18hrs, cells were washed with PBS and 1ml of 2%FCS medium ± 100U of IL-1β was added to each well. After 6 hours, the cells were harvested and luciferase and β-galactosidase assays carried out (see section 2.10.1). Luciferase light-emission units were standardised for β-gal levels. Results show fold change in levels of expression compared to baseline (0hrs), representing five repeat experiments with 4 replica wells, y-error bars= standard deviation. The table shows comparison of values by paired T-test, *denotes a significant difference within 95% confidence limits.

With IL-1β stimulation, GGG was associated with higher levels of expression than AGC, with no significant difference between GGG and AGG. GCG was associated with significantly lower levels of expression than GGG. There was no significant difference between haplotypes in unstimulated conditions.

The –597 polymorphism did not appear to have an independent functional effect on IL-6 expression as there was no significant difference between the GGG and AGG construct with IL-1β stimulation (p=0.240, figure 4.7). The –572 polymorphism in contrast appeared to have an independent functional effect on IL-1β-induced IL-6 transcription, with the GGG construct associated with significantly higher levels of expression than the GCG construct (p=0.019, figure 4.7).

4.1.7. IL-6 polymorphic effects are cell specific

To investigate whether the haplotype effect seen in HeLa cells may be cell-specific, comparative transfection studies were carried out in Huh7 cells. The haplotype constructs GGG, AGG, AGC and GCG were transfected by calcium phosphate precipitation into Huh7 cells for 18 hours as for HeLa cell transfections. A time course for IL-1β stimulation (100U/ml) for the 1.17kb and 611bp constructs established that the time of maximal stimulation of transcription for these constructs in Huh7 cells was at 9 hours rather than 6 hours as in HeLa cells (shown for GGG and ΔG, figure 4.8). The fold induction was generally lower in Huh7 cells (3.5-fold, $p<0.003$) than for HeLa cells. Doses of IL-1β greater than 100U/ml did not result in any higher levels of stimulation. In Huh7 cells, change of medium alone (containing 2% FCS) resulted in a small but significant increase in the levels of transcription for both the long (1.3-fold, p=0.033) and short construct (1.4-fold, $p<0.001$), (figure 4.8). These differences compared to transfections in HeLa cells probably reflect different kinetics and transcription factor responses between the two cells to serum factors and IL-1β. The constructs were therefore compared at the 9-hour time point in Huh7 cells.

Levels of transcription in Huh7 cells were not significantly different between haplotype constructs whether unstimulated or IL-1β-stimulated ($p>0.05$, figure 4.9), though there was a trend towards the opposite effect to that seen in HeLa cells with GGG producing lower levels of transcription with IL-1 stimulation than AGC (p=0.06). This suggests that the 5'-flanking region polymorphisms of IL-6 have a cell-specific effect on IL-6 transcription, with differences in expression seen in HeLa cells but not Huh7 cells reflecting possible differences in transcription factor(s) expressed between these cell types.

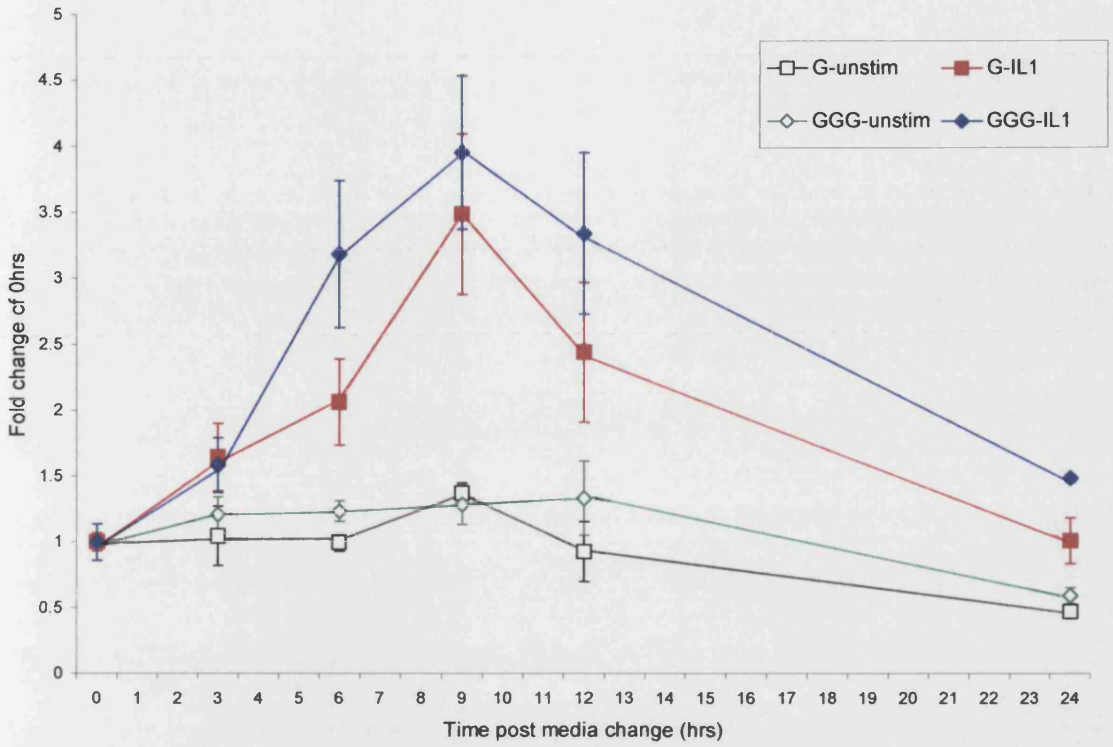

Comparison of conditions for each construct

Condition 1	Condition 2	mean difference	p-value
GGG-unstim 0hrs	GGG-unstim 9hrs	1.288	0.033*
G-unstim 0hrs	G-unstim 9hrs	1.370	<0.001*
GGG-unstim 9hrs	GGG-IL1 9hrs	2.667	0.001*
G-unstim 9hrs	G-IL1 9hrs	2.116	0.003*

Figure 4.8. Time course for GGG and ΔG constructs transfected into Huh7 cells, unstimulated and IL-1β stimulated.

Huh7 cells in 24-well plates were co-transfected with the IL-6-luciferase constructs GGG or ΔG and control plasmid RSV-β-gal. After 18hrs, cells were washed with PBS and 1ml of 2%FCS medium ± 100U IL-1β was added to each well. At the allocated time point, cells were harvested and luciferase and β-galactosidase assays carried out (see section 2.10.1). Luciferase light-emission units were standardised for β-gal levels. Results show fold change in levels of expression compared to baseline (0hrs). Results represent duplicate experiments with 4 replica wells, y-error bars= standard deviation. The table shows comparison of values by paired T-test, *denotes a significant difference within 95% confidence limits.

Maximal stimulation with IL-1β occurred at 9 hours for GGG and ΔG in Huh7 cells. Both ΔG and GGG transcription was induced by 2 % FCS medium change alone (unstimulated conditions).

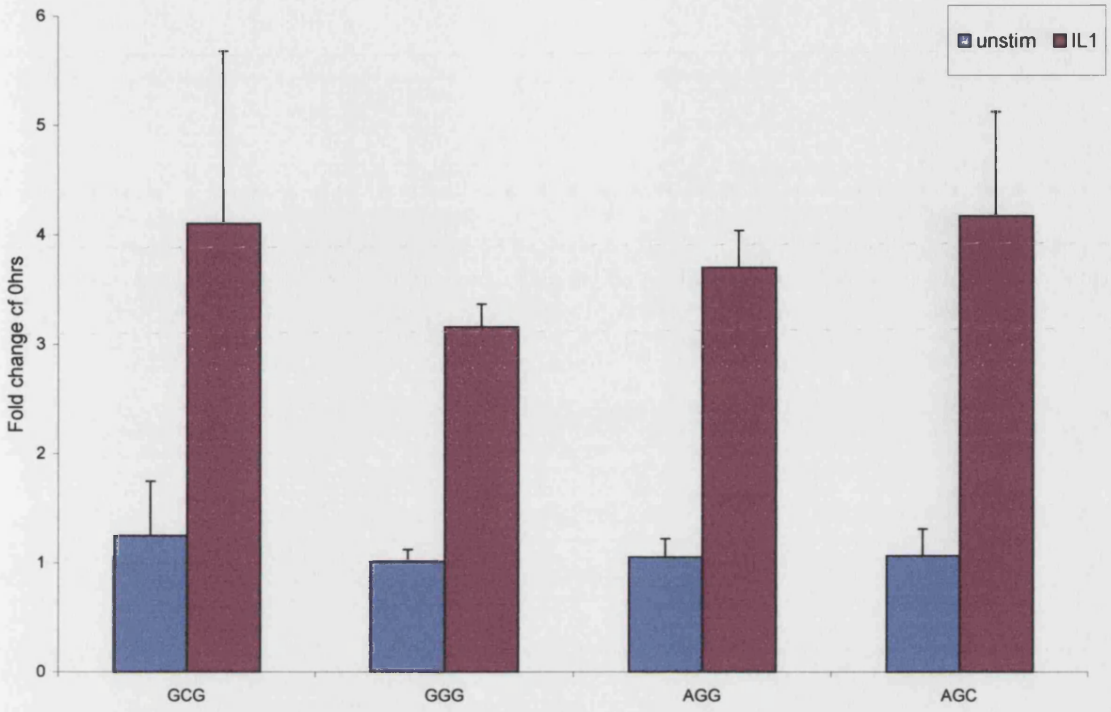

Comparison of constructs

		UNSTIMULATED		IL-1β-INDUCED	
Construct 1	Construct 2	mean difference	p-value	mean difference	p-value
GGG	AGG	0.040	0.367	0.542	0.109
GGG	AGC	0.047	0.384	1.012	0.060
GGG	GCG	0.238	0.232	0.943	0.180
AGG	AGC	0.007	0.479	0.470	0.223

Figure 4.9. Comparison of haplotype constructs GCG, GGG, AGG and AGC transfected into Huh7 cells.

Huh7 cells in 24-well plates were co-transfected with the IL-6-luciferase constructs GCG, GGG, AGG or AGC and control plasmid RSV-β-gal. After 18hrs, cells were washed with PBS and 1ml of 2%FCS medium ± 100U of IL-1β was added to each well. After 9 hours, the cells were harvested and luciferase and β-galactosidase assays carried out (see section 2.10.1). Luciferase light-emission units were standardised for β-gal levels. Results show fold change in levels of expression compared to baseline (0hrs), representing duplicate experiments with triplicate wells, y-error bars= standard deviation. The table shows comparison of values by paired T-test, *denotes a significant difference within 95% confidence limits.

There was no significant difference between haplotypes in unstimulated or IL-1β stimulated conditions in Huh7 cells.

4.1.8 The –174 allelic effects are altered by glucocorticoid inhibition

Acute flare-ups of systemic arthritis respond quickly to treatment with glucocorticosteroids, which is the mainstay of initial therapy. Glucocorticoids, including dexamethasone, are known to inhibit IL-6 transcription (see section 1.3.2.5). A known glucocorticoid-receptor element (GRE) is located at –210 to –214 of the IL-6 5'-flanking region, close to the –174 polymorphism. Two putative GRE sites are located just downstream of the –572 and –597 polymorphisms (-461 to –466 & –552 to –557). The possible influence of the 5'-flanking region polymorphisms on dexamethasone inhibition of IL-6 transcription was investigated.

1.17kb and 611bp constructs were transfected into HeLa for 18 hours as before (section 2.10.1) and stimulated with IL-1β (100U/ml) with or without the presence of dexamethasone (dissolved in ethanol). An equivalent amount of ethanol (4μl, 217nm) was added as a control to non-dexamethasone containing media. Ethanol can have inhibitory effects on transcription, however, the concentrations required to produce such an effect on other genes that have been studied was in the μM range (Mandrekar et al., 1999). A dose response curve was plotted for the 6-hour time point, shown for ΔG and ΔC (figure 4.10). The optimal dose of dexamethasone, for inhibition of reporter transcription was 10^{-7}M. Of note, the –174 G/C allelic effect with IL-1β stimulation is lost in the presence of maximal inhibitory concentrations of dexamethasone.

A time course for dexamethasone inhibition (10^{-7}M) confirmed maximal inhibition of IL-1β-induced transcription of the constructs to occur at 6-hours (shown for GGG and ΔG, figure 4.11a). A similar time course in Huh7 cells showed no significant inhibition of IL-1β-induced transcription of the constructs (figure 4.11b). Further investigations on the effect of dexamethasone inhibition were therefore confined to HeLa cells and compared at the 6-hour time point.

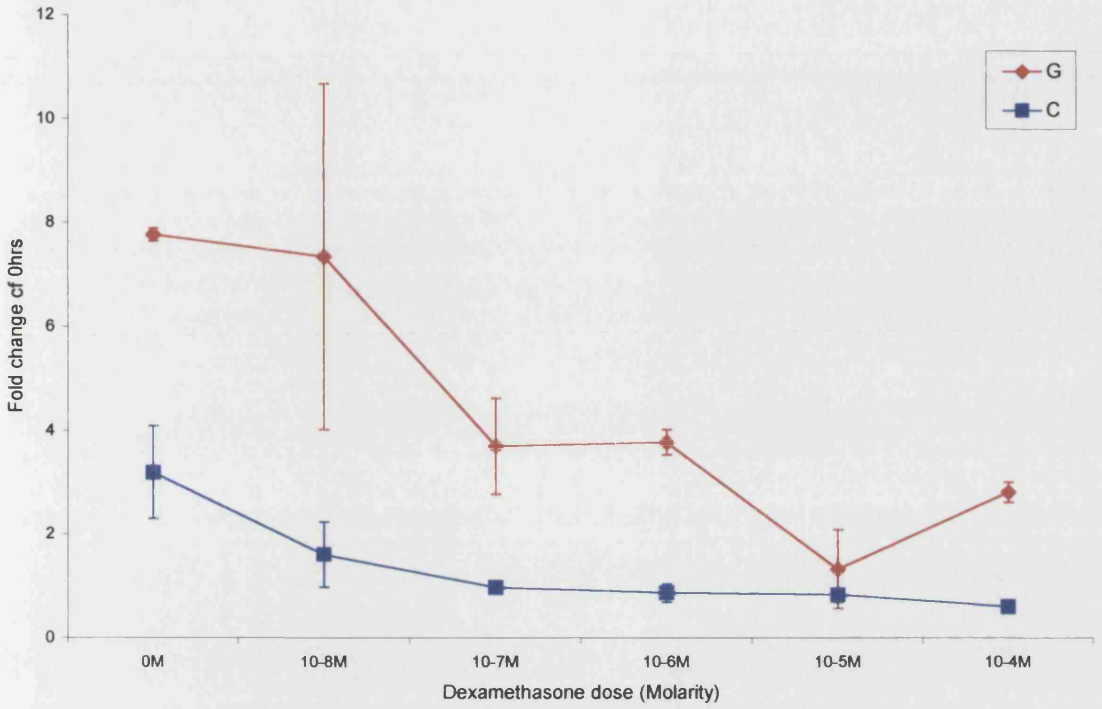

Comparison of conditions for each construct

Condition 1	Condition 2	mean difference	p-value
G-0M dex	C-0M dex	4.573	0.038*
G-10^{-7}M dex	C-10^{-7}M dex	2.722	0.067
G-0M dex	G-10^{-7}M dex	4.070	0.044*
C-0M dex	C-10^{-7}M dex	2.219	0.079

Figure 4.10. Dose response curve for dexamethasone inhibition of IL-1β-induced expression of ΔG and ΔC constructs transfected into HeLa cells.

HeLa cells in 24-well plates were co-transfected with the IL-6-luciferase constructs ΔG or ΔC and control plasmid RSV-β-gal. After 18hrs, cells were washed with PBS and 1ml of 2%FCS medium + 100U IL-1β and 0, 10^{-8}, 10^{-7}, 10^{-6}, 10^{-5} or 10^{-4} Molar Dexamethasone (with 4μl ethanol) was added to each well. After 6 hours, the cells were harvested and luciferase and β-galactosidase assays carried out (see section 2.10.1). Luciferase light-emission units were standardised for β-gal levels. Results show fold change in levels of expression compared to baseline (0hrs), representing duplicate experiments with duplicate wells, y-error bars= standard deviation. The table shows comparison of values by paired T-test, *denotes a significant difference within 95% confidence limits.

Optimal inhibition of IL-1β-induced transcription of ΔG and ΔC occurred with 10^{-7}M dexamethasone. In the presence of dexamethasone the –174G/C allelic difference is lost.

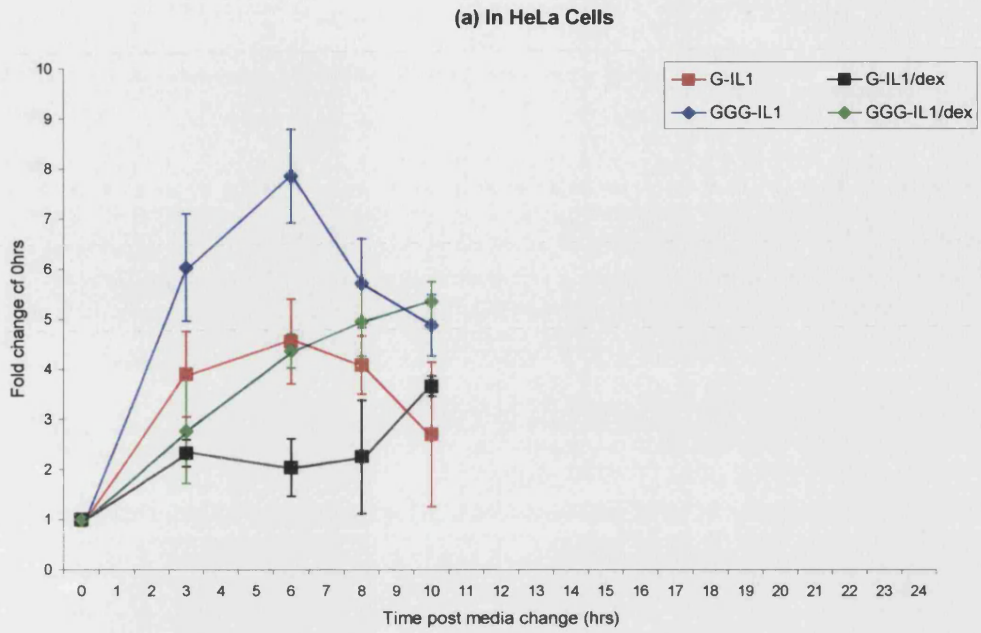

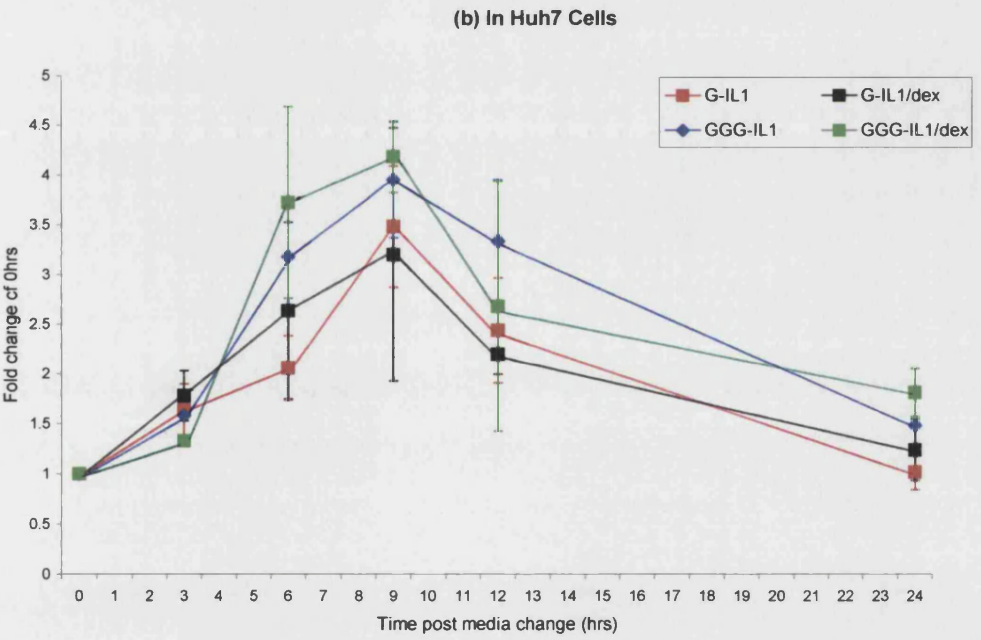

IL-1 compared to IL-1/dex	mean difference in HeLa	p-value	mean difference in Huh7	p-value
G 3hrs	1.580	0.010*	0.134	0.261
GGG 3hrs	3.262	0.018*	0.256	0.174
G 6hrs	2.529	0.001*	0.573	0.067
GGG 6hrs	3.493	0.006*	0.542	0.239
G 8/9hrs	1.843	0.023*	0.285	0.134
GGG 8/9hrs	0.766	0.098	0.230	0.288

Figure 4.11. Time course for dexamethasone inhibition of IL-1β-induced expression of GGG and ΔG constructs transfected into (a) HeLa cells and (b) Huh7 cells.

Figure 4.11(cont.)
(a) HeLa cells or (b) Huh7 cells, in 24-well plates were co-transfected with the IL-6-luciferase constructs GGG or ΔG and control plasmid RSV-β-gal. After 18hrs, cells were washed with PBS and 1ml of 2%FCS medium + 100U IL-1β ± 10^{-7}M dexamethasone was added to each well. At the allocated time point, cells were harvested and luciferase and β-galactosidase assays carried out (see section 2.10.1). Luciferase light-emission units were standardised for β-gal levels. Results show fold change in levels of expression compared to baseline (0hrs). Results represent duplicate experiments with 4 replica wells, y-error bars= standard deviation. The table shows comparison of values by paired T-test, *denotes a significant difference within 95% confidence limits.
Maximal inhibition of IL-1β-induced transcription by dexamethasone occurred at 6 hours in HeLa cells for GGG and ΔG. No inhibition of IL-1β-induced transcription was seen by dexamethasone in Huh7 cells.

The 611bp ΔG and ΔC constructs were compared in HeLa cells with dexamethasone inhibition (10^{-7}M), for unstimulated and IL-1β-stimulated (100U/ml) expression. Dexamethasone resulted in significant inhibition of unstimulated expression ($p<0.01$) and of IL-1β-stimulated expression ($p<0.05$), (figure 4.12). The reduction in IL-1β-stimulated expression was significantly greater ($p=0.042$) for ΔG (2.0-fold, $p<0.001$) compared to ΔC (1.7-fold, $p=0.023$) resulting in loss of the -174G/C allelic difference. Although the IL-1β-induced –174 allelic effect was lost with dexamethasone inhibition, dexamethasone produced a difference in the levels of unstimulated transcription between the two alleles. The ΔG construct was associated with a higher level of expression than ΔC under these conditions ($p=0.016$), with less constitutive inhibition of the –174 G than C allele ($p<0.05$), (figure 4.12).

Glucocorticoids can influence transcriptional activity via direct mechanisms involving glucocorticoid receptor binding to glucocorticoid-response elements in the gene, or via indirect mechanisms by inhibition of other transcription factors or co-factors (either through gene inhibition or protein-protein interactions), (discussed in section 1.3.2.5). Many mechanisms may be relevant in the context of the IL-6 gene and glucocorticoids are clearly involved in modulation of the –174 allelic effect. The different influences of dexamethasone on the –174 alleles for unstimulated and IL-1-stimulated transcription may reflect the different transactivation mechanisms operative in basal and induced expression.

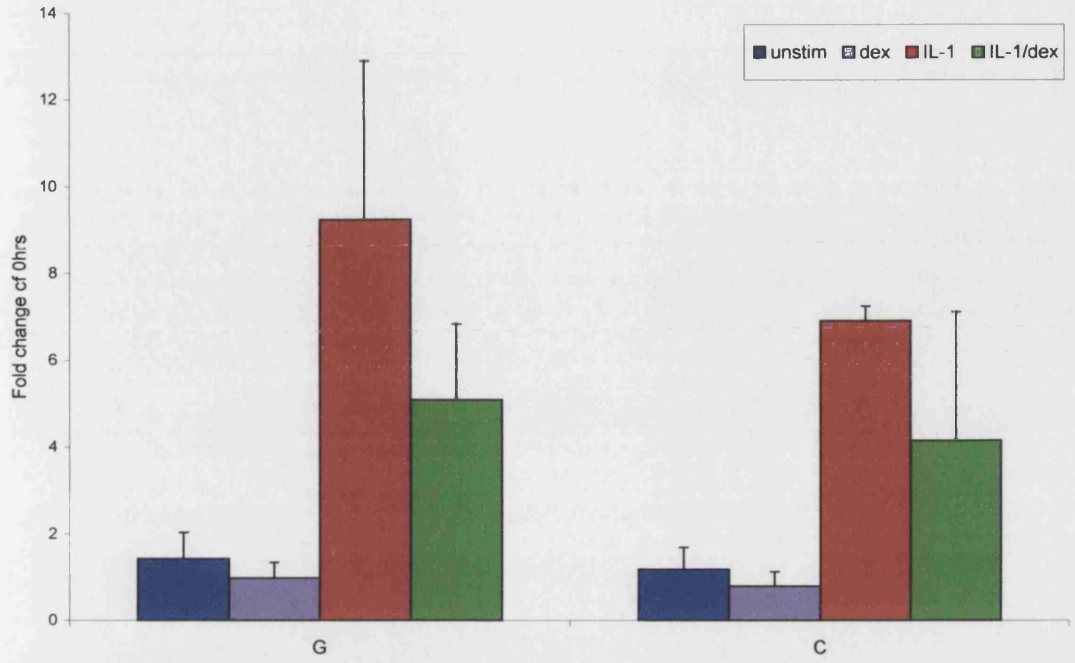

Comparison of conditions and constructs

Condition 1	Condition 2	mean difference	p-value
G-unstim	G-dex	0.447	0.007*
C-unstim	C-dex	0.382	<0.001*
G-IL1	G-IL1/dex	4.147	<0.001*
C-IL1	C-IL1/dex	2.756	0.023*
G-unstim	C-unstim	0.252	0.092
G-dex	C-dex	0.192	0.016*
G-IL1	C-IL1	2.332	0.044*
G-IL1/dex	C-IL1/dex	0.941	0.189
G-0hr (baseline)	G-unstim (6hr)	1.481	<0.001*
C-0hr (baseline)	C-unstim (6hr)	1.325	<0.001*

Figure 4.12. Comparison of dexamethasone inhibition of ΔG and ΔC constructs transfected into HeLa cells.

HeLa cells in 24-well plates were co-transfected with the IL-6-luciferase constructs ΔG or ΔC and control plasmid RSV-β-gal. After 18hrs, cells were washed with PBS and 1ml of 2%FCS medium ± 100U of IL-1β ± 10^{-7}M dexamethasone was added to each well. After 6 hours, the cells were harvested and luciferase and β-galactosidase assays carried out (see section 2.10.1). Luciferase light-emission units were standardised for β-gal levels. Results show fold change in levels of expression compared to baseline (0hrs), representing six repeat experiments with duplicate wells, y-error bars= standard deviation. The table shows comparison of values by paired T-test, *denotes a significant difference within 95% confidence limits.

Dexamethasone significantly inhibited levels of ΔG and ΔC transcription whether unstimulated or IL-1β-stimulated. With IL-1β stimulation, ΔG was inhibited significantly more by dexamethasone than ΔC (p=0.042) resulting in loss of the –174 allelic effect. In unstimulated conditions, ΔC was inhibited significantly more by dexamethasone than ΔG resulting in a –174 allelic effect.

The effect of Dexamethasone inhibition (10^{-7}M) on the 1.17kb haplotype constructs was compared in HeLa cells under the same conditions. Dexamethasone inhibition of IL-1β-induced expression of the haplotype constructs in HeLa cells revealed significant inhibition of GGG (1.6-fold reduction, p=0.002) and AGG (1.3-fold reduction, p=0.011), but not of AGC (1.1-fold reduction, p=0.324), (figure 4.13a). This mirrors the effects seen for the short constructs. In both cases the glucocorticoid inhibition occurred more strongly for IL-1β-induced expression with the –174 G rather than C allele, and resulted in loss of the –174 associated allelic differences between haplotypes.

4.1.9. The –572 polymorphism alters inhibition by glucocorticoids

Dexamethasone did not significantly inhibit IL-1β-induced expression of GCG in HeLa cells (1.2-fold reduction, p=0.066), although GGG was significantly inhibited (1.6-fold reduction, p=0.002), (figure 4.13a). This may reflect alteration of glucocorticoid binding to a site(s) adjacent to the –572 polymorphism that the –572G allele may facilitate but the –572C allele inhibit. According to consensus sequence comparisons, there are two putative glucocorticoid receptor binding sites down-stream of –572 (-461 to –466 & -552 to –557) that the –572 polymorphism may influence.

4.1.10. Stripped FCS alters levels of transcription

FCS is necessary for cell viability and for IL-1β induction of IL-6 transcription. A series of transfection experiments were carried out in serum deplete medium (D-MEM without supplemented FCS or A-MEM, Gibco). Although the effect of medium change, containing 2% FCS (unstimulated conditions, see 4.1.3), on levels of IL-6 construct expression were abolished by using FCS deplete medium, no induction of IL-6 transcription with addition of IL-1β was seen without the presence of FCS. FCS can contain varying amounts of hormone and steroid compounds such as oestrogens, growth factors and cortisol (Nakama et al., 1995), which despite heat inactivation could be influencing levels of transcription in the transfection system. A treatment shown to bind and remove (strip) hormone and steroid compounds from FCS was described by Fenske (1991). This method, using activated charcoal and dextran, was adapted to produce stripped FCS for transfection studies (see 2.10.2).

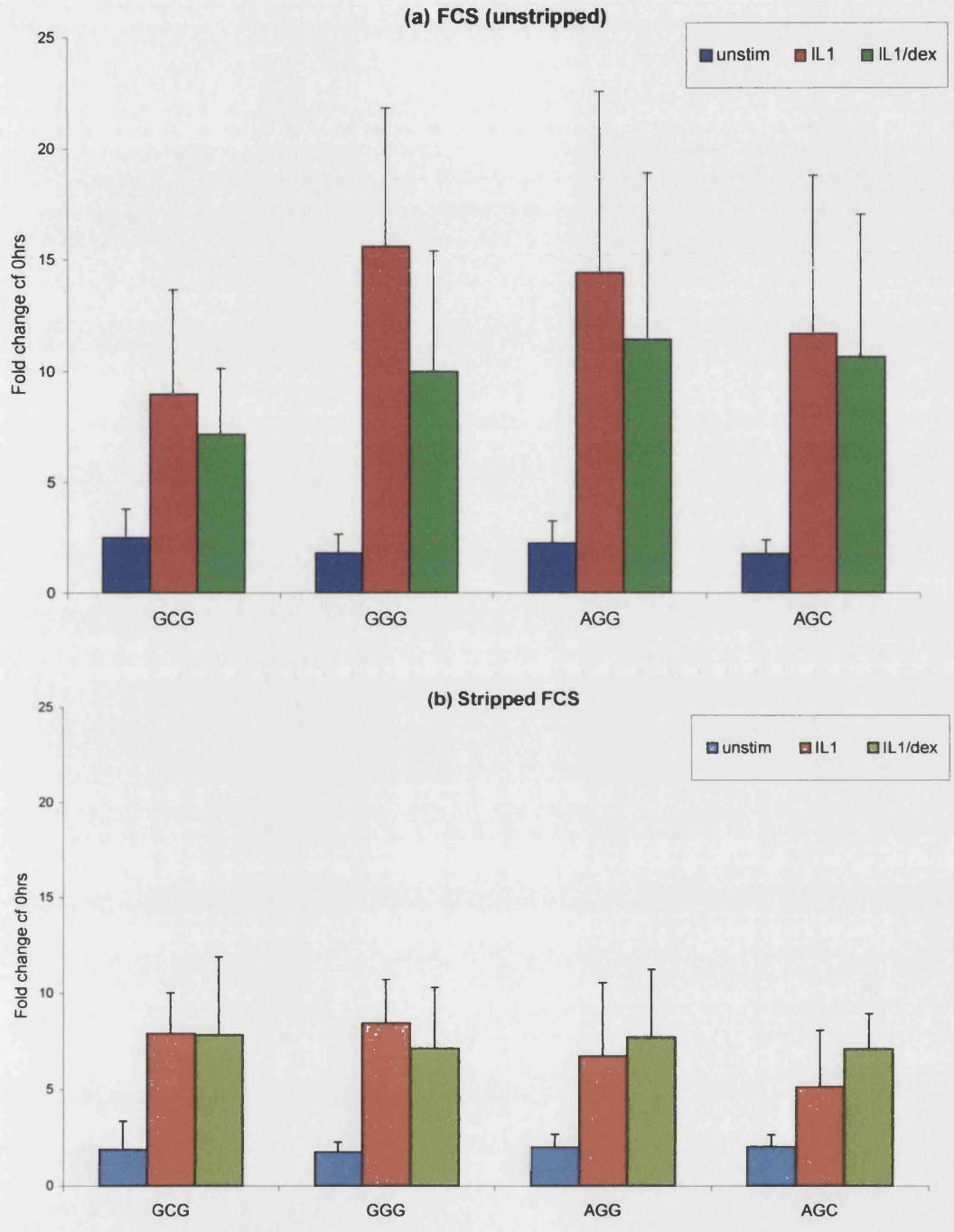
(a) FCS (unstripped)
unstim
IL1
IL1/dex
Fold change cf 0hrs
25
20
15
10
5
0
GCG
GGG
AGG
AGC
(b) Stripped FCS
unstim
IL1
IL1/dex
Fold change cf 0hrs
25
20
15
10
5
0
GCG
GGG
AGG
AGC

Figure 4.13...

Comparison of conditions for each construct

		FCS (unstripped)		Stripped FCS	
Condition 1	Condition 2	mean difference	p-value	mean difference	p-value
GGG-unstim	AGG-unstim	0.427	0.070	0.239	0.156
GGG-unstim	AGC-unstim	0.037	0.433	0.280	0.101
GGG-unstim	GCG-unstim	0.691	0.062	0.142	0.385
GGG-IL1	AGG-IL1	1.186	0.307	1.714	0.073
GGG-IL1	AGC-IL1	3.930	0.037*	3.297	0.003*
GGG-IL1	GCG-IL1	6.635	0.019*	0.535	0.326
GGG-IL1/dex	AGG-IL1/dex	1.457	0.238	0.575	0.318
GGG-IL1/dex	AGC-IL1/dex	0.649	0.366	0.046	0.482
GGG-IL1/dex	GCG-IL1/dex	2.815	0.102	0.695	0.338
GGG-IL1	GGG-IL1/dex	5.630	0.002*	1.299	0.102
AGG-IL1	AGG-IL1/dex	2.987	0.011*	0.990	0.231
AGC-IL1	AGC-IL1/dex	1.051	0.324	1.952	0.096
GCG-IL1	GCG-IL1/dex	1.810	0.066	0.069	0.487

Figure 4.13. Comparison of dexamethasone inhibition of haplotype constructs GCG, GGG, AGG and AGC transfected into HeLa cells with medium containing (a) FCS (unstripped) and (b) stripped FCS.

HeLa cells in 24-well plates were co-transfected with the IL-6-luciferase constructs GCG, GGG, AGG or AGC and control plasmid RSV-β-gal. After 18hrs, cells were washed with PBS and 1ml of (a) 2%FCS (unstripped) or (b) 2% stripped FCS (str-FCS, activated charcoal and dextran treated, see 2.10.2) media ± 100U of IL-1β ± 10^{-7}M dexamethasone was added to each well. After 6 hours, the cells were harvested and luciferase and β-galactosidase assays carried out (see section 2.10.1). Luciferase light-emission units were standardised for β-gal levels. Results show fold change in levels of expression compared to baseline (0hrs), representing six repeat experiments with triplicate wells, y-error bars= standard deviation. The table shows comparison of values by paired T-test, *denotes a significant difference within 95% confidence limits.

Dexamethasone inhibited IL-1β-induced transcription of GGG significantly more than AGC, resulting in loss of the –174 allelic associated difference between haplotypes. GCG was not inhibited by Dexamethasone. Str-FCS reduced the level of IL-1β stimulation of GGG, AGG and AGC but not of GCG. Str-FCS also abolished the effect of dexamethasone inhibition.

The presence of 2% stripped FCS (str-FCS) in the media instead of 2% unstripped FCS, from the same serum batch, was compared in unstimulated, IL-1β–stimulated and dexamethasone inhibited transfections of the IL-6 haplotype constructs. Unstimulated levels of transcription for the four haplotype-constructs were not altered by the presence of str-FCS in the media ($p>0.07$, figure 4.13b). However, the levels of Il-1β-stimulated transcription were significantly reduced by str-FCS for the GGG, AGG and AGC constructs ($p<0.001$) but not the GCG construct ($p=0.328$). GGG was still associated with significantly higher levels of expression than AGC ($p=0.003$), with no significant difference between GGG and AGG ($p=0.073$). GCG on the other hand, showed no significant difference in levels of transcription from GGG ($p=0.326$). This would be consistent with the –572 allelic differences acting via glucocorticoid effects that are lost with stripping of the FCS. Str-FCS completely removed the inhibitory effect of dexamethasone on IL-1-induced transcription of the constructs ($p>0.09$). Several explanations for the effect of stripped FCS are possible. Stripping of the FCS may remove a co-stimulatory factor required for maximal IL-1β stimulation or introduce an inhibitory factor to IL-1 stimulation. It would appear to remove a factor necessary for dexamethasone inhibition or add a factor that inhibits dexamethasone activity. Dextran is a highly soluble compound that may not be completely removed in association with activated charcoal on filtration of the FCS after stripping. This could account for inhibitory effects seen. It is also possible that the str-FCS alters the expression of IL-1 receptors (IL-1R) on the cell surface either directly or by removal of factors that up-regulate IL-1R expression.

Interestingly, a similar comparison of the effect of str-FCS (same str-FCS as used for HeLa cell studies) on IL-1β induction of IL-6 haplotype constructs in Huh7 cells produced no significant differences in the levels of transcription compared to unstripped FCS. This could reflect different cell-specific mechanisms involved in IL-6 transcription.

4.2. Stable transfections

With stable transfectants, the plasmid construct is integrated into the genomic DNA of the host cell, histone bound and condensed into the chromatin structure. Cells derived from an individual clone will be identical for the number of copies of construct integrated and the position at which the plasmid is located within the genome. However, this will differ between cell colonies as integration of the plasmid into the genome occurs randomly. Stable transfectants represent the *in vivo* packaging and presentation of DNA more closely than transient transfections (Smith and Hager, 1997). With random integration, or even with targeted integration, strong host genomic sequences near the integrated construct may influence the level of reporter expression. The majority of randomly integrated constructs are likely to insert into the extensive non-coding regions of the genome and are therefore less likely to be influenced by surrounding host sequences. However, it is important to remember that enhancers and repressors can act over many kilobases. Another genomic influence on the levels of construct expression may be the tightness of chromatin condensation at the site of integration and therefore the accessibility of the DNA sequence to transcription initiation factors. Despite these caveats, stable transfectants were generated in HeLa cells to enable the specific effect of various inducers and repressors of IL-6 transcription to be investigated with reduced experiment-experiment variability. Comparison of several stable clones and pooled stable clones would help confirm that an observed effect between construct clones was a feature of the construct variant.

Stable transfectants were generated in HeLa cells using the 611bp ΔG & ΔC reporter constructs and the 1.17kb GGG, AGG and AGC haplotype reporter constructs (see section 2.10.8). Plasmids coding for G418 antibiotic resistance were co-transfected to enable selection for successful integration. Individual colonies were harvested and grown up for screening. Genomic DNA was isolated from those clones that expressed luciferase (approximately 50% of the G418 resistant clones). The genomic DNA was digested with the endonuclease *Sph*I that has only one restriction site in the IL-6-PGL3-basic construct (see figure 4.1). Southern Blot analysis was performed using a 750bp probe, generated by *Hind*III and *Sph*I restriction digestion of the PGL3-basic plasmid, isolated, purified and radiolabelled (see section 2.4.4). This allowed determination of the number of copies of construct inserted into each stable clone (figure 4.14).

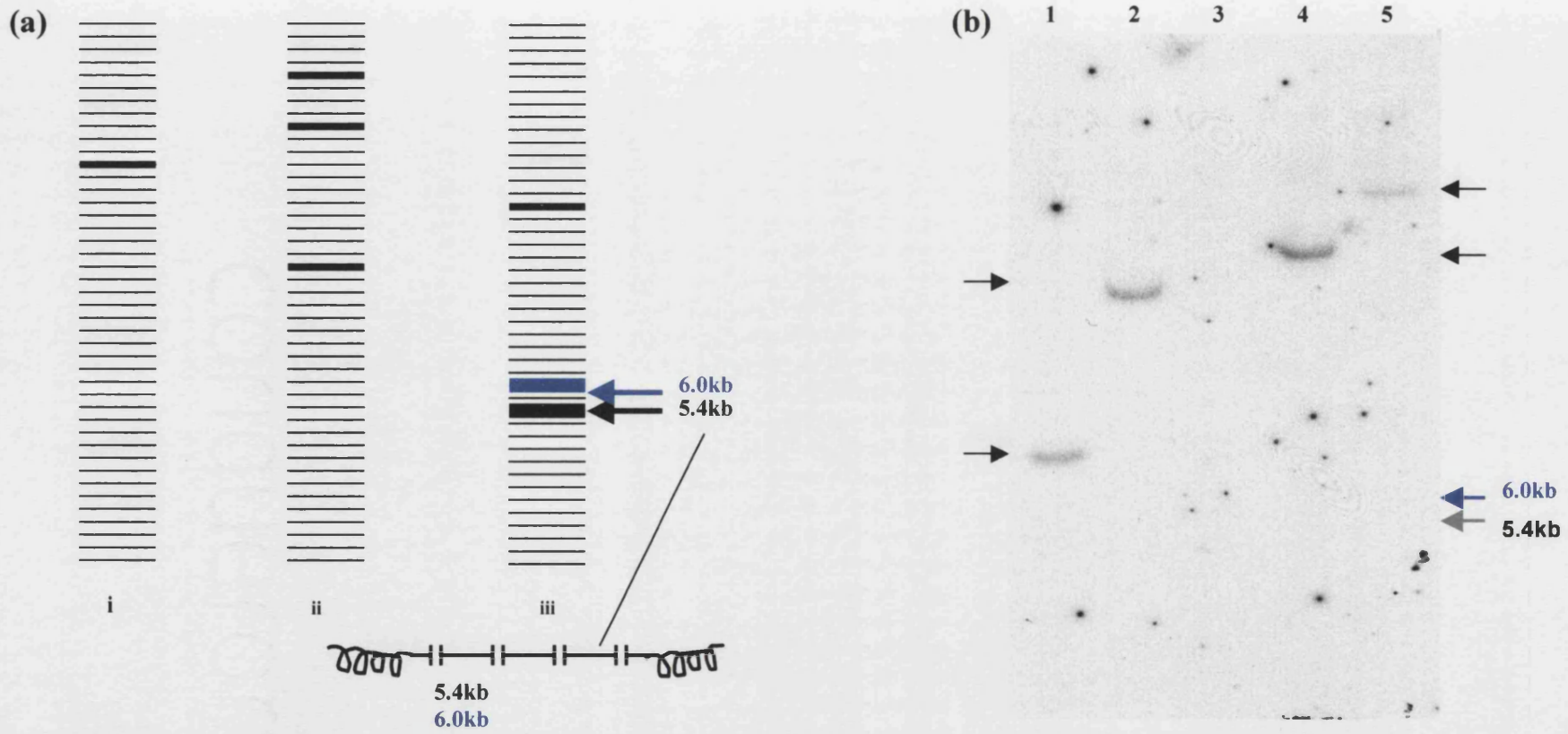

Figure 4.14. Southern blot analysis of IL-6-lucifearse constructs as stable transfectants in HeLa cells

(a) schematic representation (b) autoradiograph of probed blot.

20μg of purified genomic DNA was digested overnight with 20U of *Sph*I, the products were separated on a 0.8% agarose slab gel with a DNA size ladder and transferred by electrophoresis onto nylon Hybond-N+ nucleic acid transfer membrane. The probe was prepared from PGL3-basic vector digested with *Hind*III and *Sph*I, the fragment isolated, purified and end labelled with $^{\alpha 32}$-P (see section 2.4 for method). (a) The dark bands represent putative locations of inserted constructs detected on probing (i) for a single inserted copy with band location dependent on where the construct has integrated into the genome, (ii) for multiple copies integrated at different sites, (iii) for multiple copies integrated at the same site. The length of the PGL3-basic vector plus construct is ~5.4kb for the 611bp constructs and ~6.0kb for the 1.17kb constructs, band thickness will relate to the number of copies inserted at the site. (b) Lane 1=ΔG clone, 2=ΔC clone, 3=untransfected HeLa, 4=GGG clone, 5=AGG clone. Black arrows indicate bands detected on probing, the blue and grey arrows indicate the expected position of bands due to multiple copies integrated at one site.

Only one copy of the IL-6-luciferase construct had randomly inserted into each clone.

4.2.1. The –174 polymorphism has similar effects in stable transfections as transient transfections

Pooled stable transfectants for each construct were used to minimize the influences of host genomic factors on results. The stable transfectants were seeded into 24-well plates at the same concentration as HeLa cells for transient transfection ($5x10^{-6}$ viable cells/ml) and grown to approximately 80% confluency before change of media (2% FCS) and IL-1β stimulation. The cells were harvested after stimulation as for transient transfections and assayed for luciferase expression (see 2.10.4). Luciferase light emission units were normalised for any variations in cell numbers between wells by total protein content (see 2.12.2). A time course for IL-1β-stimulation (100U/ml) showed the time of maximal stimulation for IL-1β to be 8 hours with stable transfectants rather than 6 hours as for the transient transfectants (shown for ΔG & ΔC, figure 4.15). With the stable transfectants, media change with 2% FCS had no significant effect on levels of construct transcription over 12 hours ($p>0.06$) though these constructs in transient transfections had been sensitive (section 4.1.3). These differences may reflect the more compacted and packaged nature of the integrated construct within the host DNA. With stable transfectants, ΔG produce significantly higher levels of transcription than ΔC with IL-1β-stimulated ($p<0.001$) but not unstimulated ($p>0.9$) conditions, as had been found for transient transfections (figures 4.15 & 16). The effect of dexamethasone inhibition was also similar with dexamethasone producing more inhibition of IL-1β-induced transcription for ΔG than ΔC (2.3-fold reduction compared to 1.8-fold, $p=0.01$), (figure 4.16). However unlike with transient transfections, the –174 allelic difference was maintained despite the differences in dexamethasone inhibition ($p=0.002$). The effect of dexamethasone inhibition on unstimulated transcription was out-with statistical significance though it showed a trend towards more inhibition for ΔC than ΔG (1.3-fold reduction compared to 1.1-fold, $p=0.07$), (figure 4.16). Dexamethasone in unstimulated conditions did not induce a –174 G/C allelic difference of statistical significance ($p=0.066$). However, as with transient transfections, the conclusion remains that glucocorticoids have a modulatory effect on the –174 allelic differences.

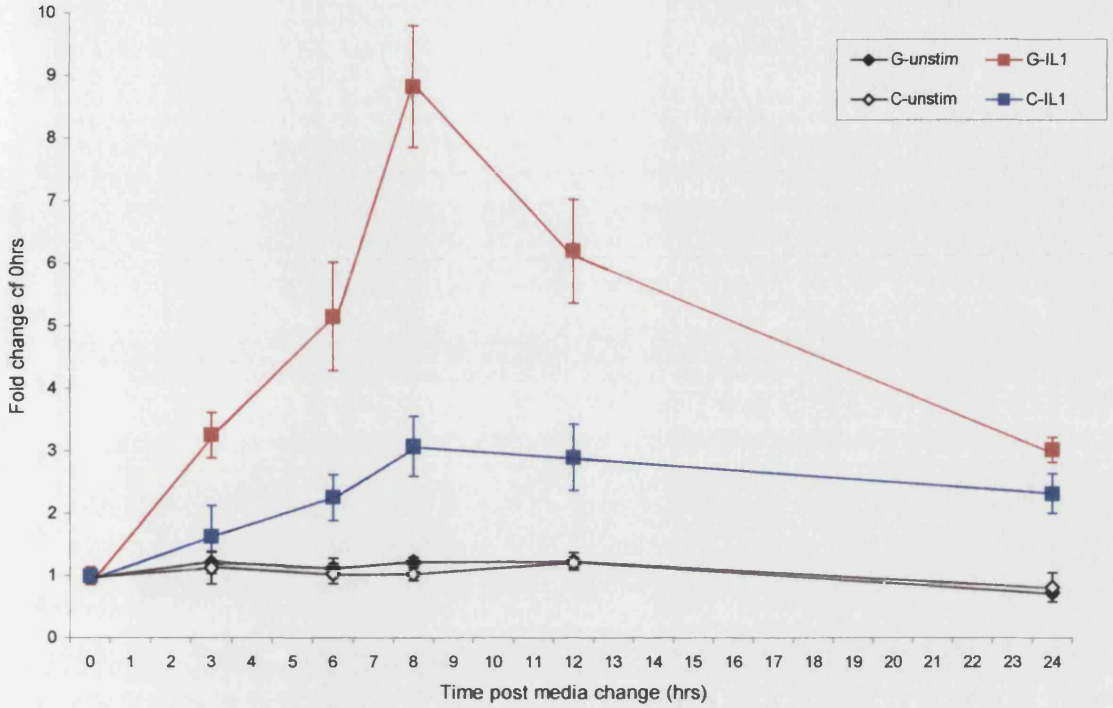

ΔG compared to ΔC

	UNSTIMULATED		IL-1β-STIMULATED	
Time post media change (hrs)	mean difference	p-value	mean difference	p-value
3	0.082	0.116	2.130	<0.001*
6	0.086	0.174	2.897	0.002*
8	0.201	0.162	5.749	<0.001*
12	0.022	0.341	3.299	<0.001*
24	0.083	0.240	0.699	0.011*

Figure 4.15. Time course for ΔG and ΔC pooled HeLa cell stable transfectants, unstimulated and IL-1β stimulated.

Pooled HeLa stable transfectants for IL-6-luciferase constructs ΔG or ΔC in 24-well plates were grown to ~80% confluence, washed with PBS and 1ml of 2%FCS medium ± 100U IL-1β added to each well. At the allocated time point, cells were harvested and luciferase and total protein content assays carried out (see section 2.10.8). Luciferase light-emission units were normalised for total protein content. Results show fold change in levels of expression compared to baseline (0hrs). Results represent duplicate experiments with 4 replica wells, y-error bars= standard deviation. The table shows comparison of values by paired T-test, *denotes a significant difference within 95% confidence limits.

Maximal stimulation with IL-1β occurred at 8 hours for stable transfectants. With IL-1β stimulation, ΔG clones produced significantly higher levels of expression than ΔC.

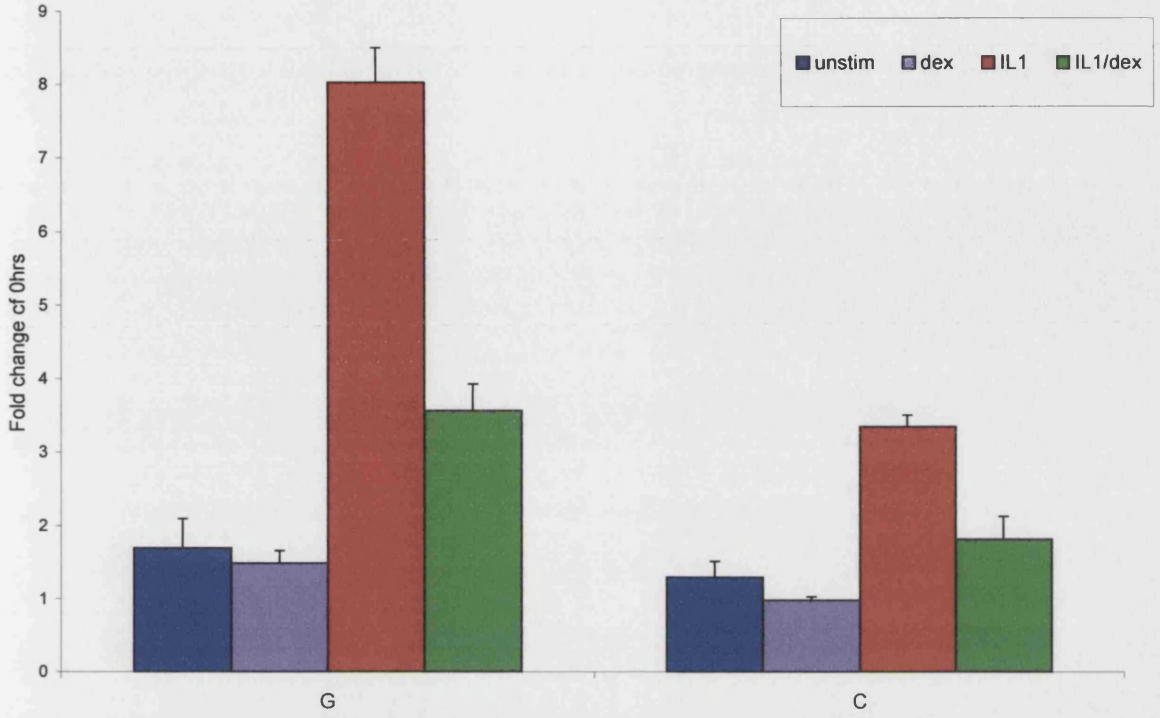

Comparison of conditions for each construct

Condition 1	Condition 2	mean difference	p-value
G-unstim	G-dex	0.200	0.219
C-unstim	C-dex	0.325	0.074
G-IL1	G-IL1/dex	4.650	0.005*
C-IL1	C-IL1/dex	0.531	<0.001*

Comparison of constructs

Construct 1	Construct 2	mean difference	p-value
G-unstim	C-unstim	0.395	0.096
G-dex	C-dex	0.536	0.066
G-IL1	C-IL1	4.685	0.003*
G-IL1/dex	C-IL1/dex	1.751	0.002*

Figure 4.16. Comparison of dexamethasone inhibition of ΔG and ΔC pooled HeLa cell stable transfectants.

Pooled HeLa stable transfectants for IL-6-luciferase constructs ΔG or ΔC in 24-well plates were grown to ~80% confluence, washed with PBS and 1ml of 2%FCS medium ± 100U IL-1β ± 10^{-7}M dexamethasone added to each well. After 8 hours, cells were harvested and luciferase and total protein content assays carried out (see section 2.10.8). Luciferase light-emission units were normalised for total protein content. Results show fold change in levels of expression compared to baseline (0hrs). Results represent duplicate experiments with 4 replica wells, y-error bars= standard deviation. The table shows comparison of values by paired T-test, *denotes a significant difference within 95% confidence limits.

Dexamethasone significantly inhibited levels of IL-1β-induced ΔG and ΔC transcription. With IL-1β stimulation, ΔG was significantly more inhibited by dexamethasone than ΔC (p=0.01) though the –174 allelic difference was not lost. In unstimulated conditions, there was a trend towards ΔC being more inhibited by dexamethasone than ΔG (p=0.07).

4.2.2. The –174 allelic effect is similar with TNFα and IL-1β induced transcription

The potential effect of the –174 polymorphism on IL-6 transcription with pro-inflammatory stimuli other than IL-1 was investigated using the pooled stable transfectants. Like IL-1, tumour necrosis factor (TNF) is another major mediator of inflammation and can induce IL-6 expression *in vivo* and *in vitro*. Signal transduction via the TNF-specific receptor, TNFR1, can activate several protein kinases in common to IL-1 transduction via IL-1R though the predominance of different pathways will vary between cell-types. This includes mitogen-activated protein kinase, MAPK (particularly dominant in fibroblasts), the NF-κB inhibitor, IκB kinase and the TNF-/IL-1-activated β-casein kinase. In addition, TNF can activate apoptotic cell signaling. It has been shown that cultured cells can display a broader spectrum of IL-1-induced kinase activation than tissues *in vivo*, probably related to cells undergoing proliferation connecting receptors with more signaling pathways than resting or differentiated cells (Saklatvala et al., 1999). It was therefore important to confirm the results with a different inducer of IL-6. Pooled HeLa cell stable transfectants were seeded out and grown up as before. A dose response curve for TNFα stimulation showed 1000U/ml to be within the range producing maximal stimulation of IL-6 construct expression (shown for ΔG stable transfectants in figure 4.17). A time course for stimulation with TNFα (1000U/ml) showed maximal stimulated expression of the constructs to be at 6-8 hours. Even with maximal stimulation, TNFα was approximately two-fold weaker at inducing construct transcription than IL-1β (3.7-fold compared to 8.0, $p<0.001$, figure 4.17). This may reflect a feature of the cells (for example fewer surface TNFR than IL-1R) or may reflect a feature of the TNF-signaling pathway and its effects on the IL-6 gene.

The levels of construct transcription with TNFα were compared between pooled HeLa cell stable transfectants for the 1.17kb constructs GGG, AGG & AGC and the 611bp constructs ΔG & ΔC. The results mirrored those for IL-1 (figure 4.18). GGG showed significantly higher levels of transcription than AGC with IL-1 ($p=0.04$) or TNFα ($p=0.019$) stimulation. This was due to the –174 allelic effect as there was no significant difference between GGG and AGG ($p>0.1$) and ΔG produced significantly higher levels of transcription than ΔC.

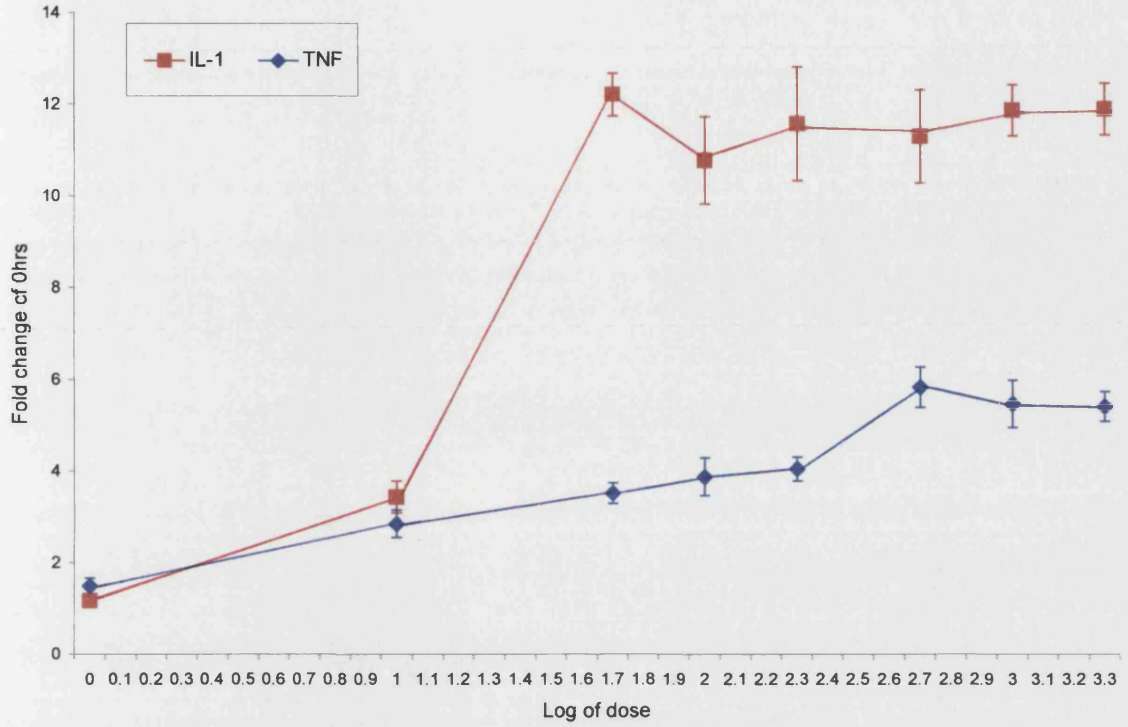

TNFα compared to IL-1β

Dose IL-1β (units/ml)	mean difference	p-value
1	0.321	0.017*
10	0.586	0.079*
50	8.69	<0.001*
100	6.895	<0.001*
200	7.523	<0.001*
500	5.458	0.002*
1000	6.392	<0.001*
2000	6.475	<0.001*

Figure 4.17. Dose response curve for TNFα and IL-1β stimulation of pooled ΔG HeLa cell stable transfectants.

Pooled HeLa stable transfectants for IL-6-luciferase construct ΔG in 24-well plates were grown to ~80% confluence, washed with PBS and 1ml of 2%FCS medium + 1, 10, 50, 100, 200, 500, 1000 or 2000U of TNFα or IL-1β (shown as log of the dose) were added to each well. After 8 hours, cells were harvested and luciferase and total protein content assays carried out (see section 2.10.8). Luciferase light-emission units were normalised for total protein content. Results show fold change in levels of expression compared to baseline (0hrs). Results represent duplicate experiments with duplicate wells, y-error bars= standard deviation. The table shows comparison of values by paired T-test, *denotes a significant difference within 95% confidence limits.

Maximal stimulation occurred with ≥500U/ml TNFα and ≥50U/ml IL-1β with TNFα showing a lower maximal induction of expression than IL-1β.

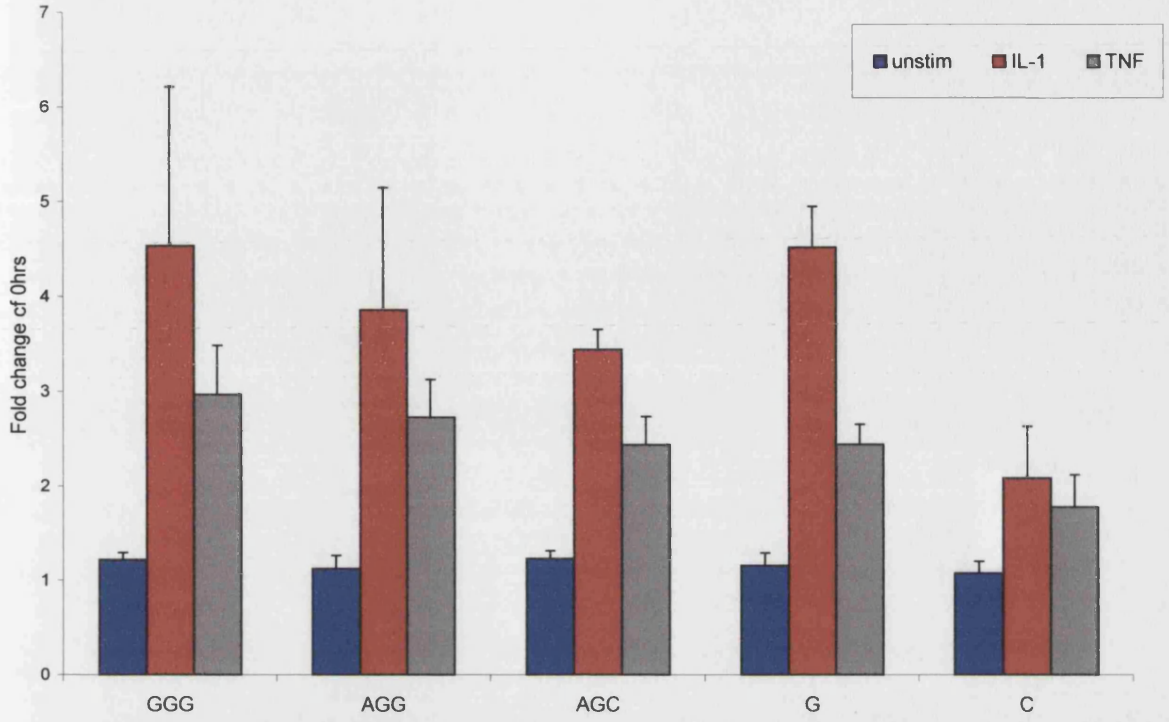

Comparison of constructs

Construct 1	Construct 2	mean difference	p-value
GGG-unstim	AGG-unstim	0.092	0.069
GGG-unstim	AGC-unstim	0.012	0.378
G-unstim	C-unstim	0.081	0.081
GGG-IL1	AGG-IL1	0.680	0.112
GGG-IL1	AGC-IL1	1.096	0.040*
G-IL1	C-IL1	2.437	<0.001*
GGG-TNF	AGG-TNF	0.240	0.183
GGG-TNF	AGC-TNF	0.527	0.019*
G-TNF	C-TNF	0.665	0.002*
AGG-IL-1/TNF	AGC-IL-1/TNF	0.300	0.005*

Comparison of IL-1β and TNFα stimulation

Construct	mean difference	p-value
GGG	1.574	0.002*
AGG	1.134	<0.001*
AGC	1.005	<0.001*
G	2.078	<0.001*
C	0.306	0.134

Figure 4.18. Comparison of TNFα and IL-1β stimulation of GGG, AGG, AGC, ΔG and ΔC pooled HeLa cell stable transfectants.

Pooled HeLa stable transfectants for IL-6-luciferase constructs GGG, AGG, AGC, ΔG or ΔC in 24-well plates were grown to ~80% confluence, washed with PBS and 1ml of 2%FCS medium ± 1000U TNFα ± 100U IL-1β were added to each well. After 8 hours, cells were harvested and luciferase and total protein content assays carried out (see section 2.10.8). Luciferase light-emission units were normalised for total protein content. Results show fold change in levels of expression compared to baseline (0hrs). Results represent duplicate experiments with 4 replica wells, y-error bars= standard deviation. The table shows comparison of values by paired T-test, *denotes a significant difference within 95% confidence limits.

GGG and AGG were significantly higher expressers than AGC, and DG than DC, with IL-1β or TNFα stimulation. There were no differences in unstimulated conditions.

Of interest, with ΔC there was no significant difference in the levels of expression of IL-1β- and TNFα-stimulated transcription ($p=0.134$) although IL-1β-stimulated transcription was significantly higher for ΔG, GGG, AGG and AGC ($p\leq0.002$). It is possible that this reflects the difference in mechanisms of activation between the –174 G and C alleles. There were no significant differences in the levels of transcription between constructs in unstimulated conditions ($p\geq0.07$).

Lipopolysaccharide (LPS) has been shown to be an inducer of IL-6 transcription in some cell types and IL-6 can induce C/EBPβ expression, which could act as an auto-regulatory feed-back-loop for IL-6 expression (see section 1.3.2.2). Time course and dose response experiments were carried out using the pooled HeLa cell stable transfectants for IL-6 (up to 2000 U/ml) and LPS (up to 100μg/ml) but did not produce any significant stimulation of construct transcription ($p\geq0.1$). IL-6 and LPS were biologically active with IL-6 (1000units/ml) strongly inducing serum amyloid A-reporter gene constructs in HeLa cells and LPS (10μg/ml) inducing IL-10-reporter gene constructs in cultured monocytes (S Cole, R Fellowes, personal communication).

4.3. Summary of transfection results

The results from the transient and stable transfections show that the –174G allele of IL-6 is associated with higher levels of transcription than –174C in the context of naturally occurring haplotypes in HeLa cells but not Huh7 cells, when induced by IL-1β or TNFα. An up-stream region between –220 and –310 has modulatory effects on the –174 polymorphism as does inhibition by glucocorticoids. In addition, the –572 and AT-tract polymorphisms have independent functional effects on IL-6 transcription with –572G associated with significantly higher levels of transcription than –572C, and A8T12 with higher levels than A9T11.

CHAPTER 5
RESULTS:

The influence of 5'-flanking region polymorphisms of IL-6 on transcription factor binding

5.1. Electrophoretic mobility shift assays

Following identification of DNA polymorphisms that alter the transcription of a gene, definition of protein factors that bind to these sequences is necessary to understand the mechanisms causing the effect of the DNA polymorphism. The first step to defining these interactions can be carried out by DNA electrophoretic mobility shift assay (EMSA). This technique involves incubation of a radiolabelled DNA probe with cell nuclear extracts to form DNA-protein complexes that can be resolved by electrophoresis on a non-denaturing polyacrylamide gel (see section 2.11 for method). The probe with no protein bound to it will have a high electrophoretic mobility and will be located at the bottom of the gel, while the probe with a protein or complex of proteins bound to it will migrate more slowly through the gel. The decreased electrophoretic mobility of the DNA-protein complex is influenced by the size, shape and charge of the complex and results in a location nearer the top of the gel (figure 5.1). The position of the radiolabelled DNA on the polyacrylamide gel can be visualised on an autoradiograph. To confirm the specificity of the protein binding to the radiolabelled DNA sequence, a large excess of an unlabelled DNA competitor sequence can be added to the binding reaction. If the unlabelled competitor sequence also binds the same protein(s), then this will occur preferentially as the unlabelled competitor is in excess. This will result in the reduction or loss of the radiolabelled DNA band. Addition in excess of a random, unrelated or artificial DNA sequence can also be used to confirm the specificity of protein binding. This should not alter the intensity of the radiolabelled DNA band. By using competitor DNA sequences containing previously established DNA binding sites for specific transcription factors (available through programmes such as Sigscan, see below), it can be established whether protein(s) bound to the DNA sequence under investigation are likely to be the same or related factors. Similarly, by using competitor DNA sequences that differ by one base (such as different polymorphic alleles) or a few bases to alter the transcription factor binding site, the effect on transcription factor binding efficiency can be compared. Once the presence of transcription factor(s) has been identified by EMSA competition studies, an antibody supershift can be carried out to provide further evidence that the specific transcription factor is involved in binding to the radiolabelled DNA probe. An excess of specific antibody when added to the binding reaction can result in one of three possible changes to the radiolabelled DNA band if the factor is involved in the DNA-protein complex (figure 5.1).

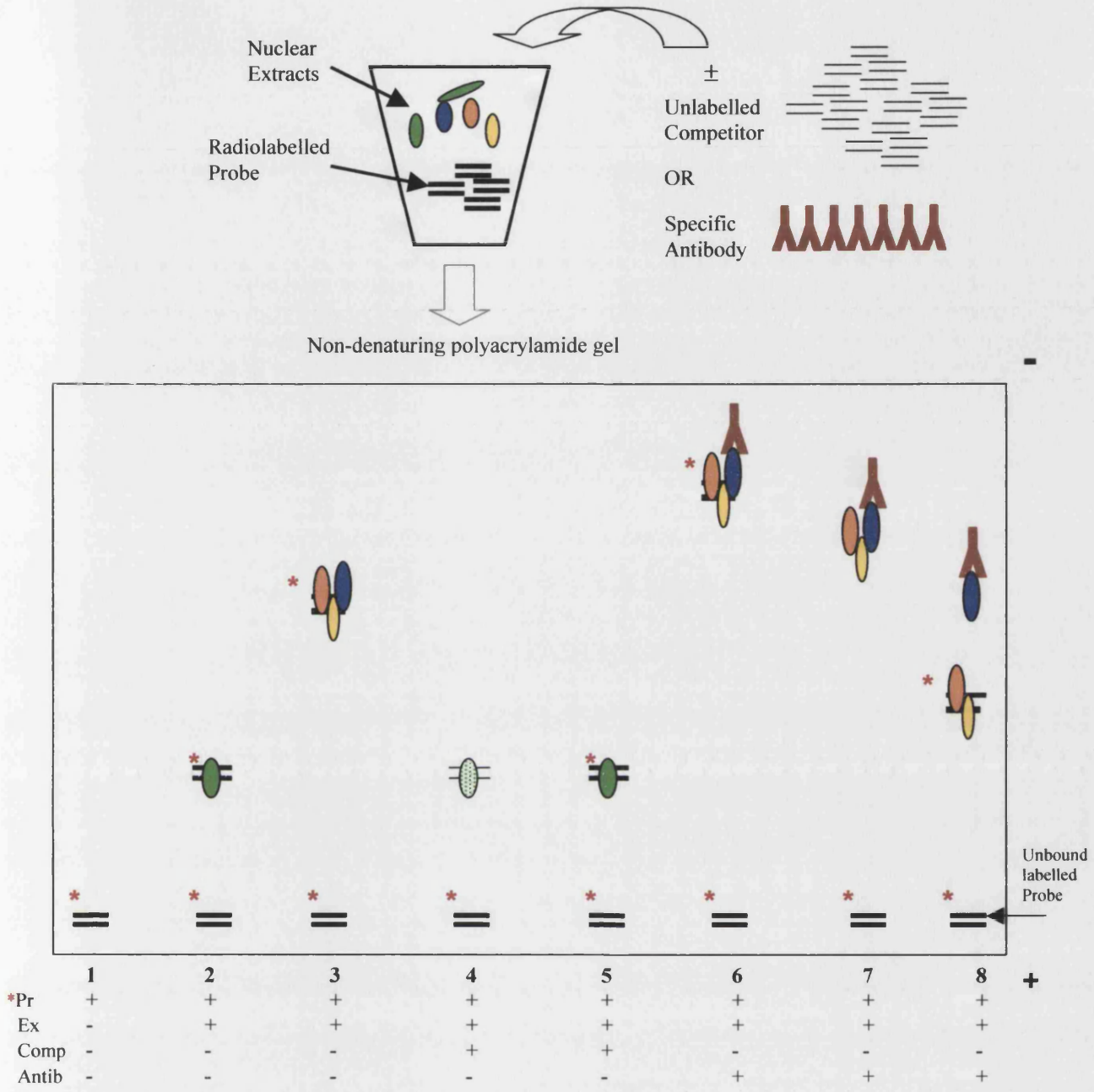

Figure 5.1. Schematic representation of DNA EMSA.

Nuclear protein extracts are mixed with radiolabelled DNA probe and resolved by electrophoresis on a non-denaturing polyacrylamide gel (see 2.11 for method). Only bands marked by * contain radiolabelled probe and will be detected on an autoradiograph. *Pr=radiolabelled probe, Ex=nuclear extract, Comp=unlabelled competitor, Antib=specific antibody.

Lane 1= probe only, no protein binding

Lane 2= probe bound by one nuclear protein

Lane 3= probe bound by nuclear protein complex

Lane 4= nuclear protein binding to probe competed out by specific unlabelled competitor sequence, resulting in loss of radiolabelled band (compare with lane 2)

Lane 5= nuclear protein binding to probe not competed by unlabelled non-specific DNA sequence, resulting in no influence on radiolabelled band

Lane 6= radiolabelled band classically supershifted by specific antibody to a nuclear protein binding to the probe (compare with lane 3)

Lane 7= radiolabelled band is absent after specific antibody competition binding to a nuclear protein necessary for a complex of factors to bind (compare with lane 3)

Lane 8= radiolabelled band shifted downwards by specific antibody binding a nuclear protein and removing it from a complex of factors that bind (compare with lane 3)

Firstly, if the antibody binds to the transcription factor, which in turn binds to the DNA probe, this will cause a decreased electrophoretic mobility of the complex resulting in a band position nearer the top of the gel (classic supershift). Secondly, if the antibody binds to the transcription factor in such a way that the interaction with the probe is abolished, the radiolabelled band may be reduced or absent (antibody competition). This could happen if the antibody binds to or masks the binding site of the protein for the DNA probe or the binding site for other proteins essential as a complex for binding of the factor to the DNA sequence. Thirdly, the band may be shifted down the gel resulting from increased electrophoretic mobility, if the antibody binds to the transcription factor and removes it from a complex of proteins bound to the DNA probe.

EMSA and supershift studies were used to identify proteins that could bind to the specific DNA sequences at and around the polymorphic sites in the 5'-flanking region of IL-6 and to compare protein binding between allelic variants. Three probes were used to investigate the effect of the –174 polymorphism, a 26bp probe from base –164 to –189 (designated probe 1), a 51bp probe from base –134 to –184 (designated probe 2) and a 75bp probe from base –161 to –235 (designated probe 3), (figure 5.2). A 75bp probe from base –539 to –613 (designated probe 4) was used to investigate transcription factor binding around the –597 polymorphism (figure 5.2). Nuclear protein extracts were prepared from HeLa cells, the cell type that in transfection studies showed functional differences for the –174 polymorphism on the levels of IL-6 transcription (see chapter 4).

A number of computer programs have been developed that search for the presence of potential transcription factor binding sites in DNA sequences. The HGMP GCG Sigscan program (Prestridge, 1991) was used to analyse regions of the IL-6 gene around each polymorphic site with the different allelic sequences. This provided a starting point for investigation of potential binding factors at these sites. However, it is not exhaustive. The programme is limited by the comprehensiveness of the associated database, which lists consensus sequences and specific published sequences for transcription factors, but does not allow for degeneracy.

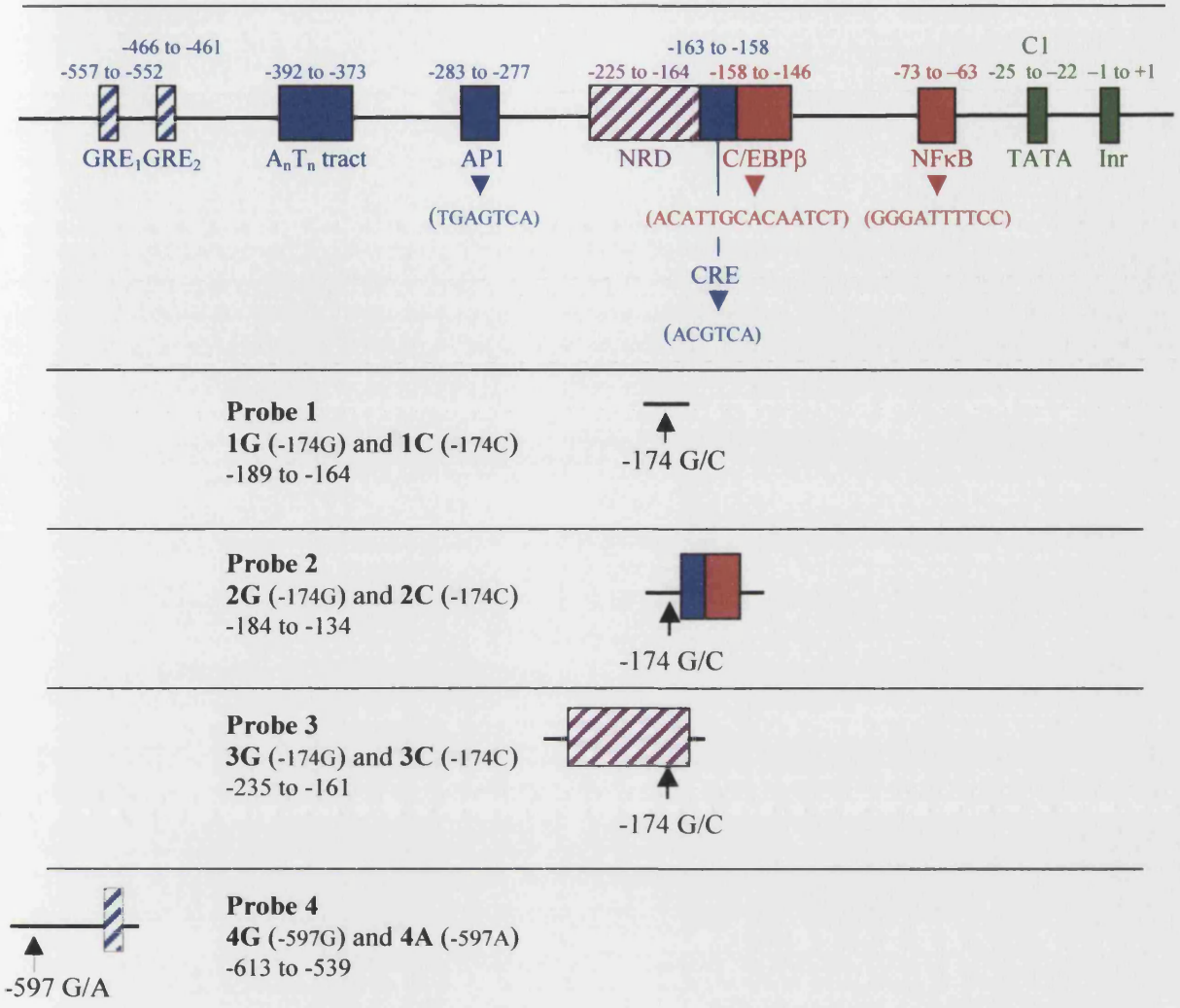

Figure 5.2. EMSA probes of the 5'-flanking region of IL-6 used for transcription factor binding studies.

The 26bp probes (1G&1C) were obtained as complementary single-strand sequences to order from Gensosys. These were 5'-end radiolabelled and annealed (see 2.11.2.1). The longer probes (2G&2C, 3G&3C and 4G&4A) were obtained as a single-strand DNA sequence to order from Genosys and the second strand was synthesised with integrated radiolabelled dCTP using Klenow (see 2.11.2.1). The DNA sequences of the probes is shown in table 2.10.

Even if transcription factor binding-site homology is identified, this does not determine whether the factor (or co-factor) is present in a specific cell type or whether the factor will actually bind to the gene in question. Binding to a consensus sequence is influenced by surrounding flanking sequences.

5.1.1. EMSA probes and nuclear extracts

Double-stranded DNA probes of various lengths of the IL-6 gene sequence surrounding the –174 polymorphism were generated with either a G or a C allele at position –174 (figure 5.2). Short probes (≤ 30bp) were obtained as custom-made complementary single-stranded sequences that were end-labelled with γ-^{32}P-ATP using T4 polynucleotide kinase and then annealed. Longer probes were generated using Klenow to synthesise a second-strand containing α-^{32}P-dCTP from single-stranded sequences and a short primer (see 2.11.2.2). This produced long probes of high specific activity as required in EMSA. Attempts using Taq or Pfu DNA polymerase in a PCR reaction to generate double-stranded, radiolabelled probes, either failed to synthesise a second-strand (probably due to the relatively low molar ratio of α-^{32}P-dCTP compared to other dNTPs) or generated probes of only low radioactive specificity. The relative specific activity of each of the labelled probes was measured by applying 0.5µl of 1:0, 1:10 and 1:20 dilutions of the purified working stock to a disc of 3MM Whatman paper and determining the counts per second (cps) at a distance of 1cm using a calibrated Mini-Monitor Geiger counter (GM Series 900, Mini-Instruments Ltd). Probes of ≥200cps/µl, were considered hot enough to use for EMSA studies.

Nuclear extracts were prepared from HeLa cells (section 2.11.1) that were either unstimulated (exposed only to media with 2% or 10% FCS) or stimulated for varying lengths of time with IL-1β (100units/ml in media containing 2% FCS). The extracts were prepared in a range of salt concentrations, high salt (300mM NaCl), medium salt (150mM NaCl) or low salt (10mM NaCl). This covered the range of salt concentrations in which most nuclear proteins are stable.

5.1.2. Optimization of EMSA conditions

For each set of EMSA probes used, EMSA conditions were initially optimized (see 2.11.3). Varying concentrations of poly dI.dC were pre-incubated with the extracts to

determine the optimum concentration (10μg) to reduce non-specific protein binding. A range of salt concentrations in the binding reaction buffer (0-65mM NaCl, 0-100mM KCl) were compared, with little effect on the EMSA bands produced for two consensus probes (NF1 control and NF-κB, see table 2.11). These factors were chosen because they have known or putative binding sites in the IL-6 5'-flanking region sequence around the –174 site (see figure 5.5 and section 1.3.2). Two binding reaction buffers were compared; a specific nuclear factor 1 (NF1) buffer (glycerol based with NaCl, from Chodosh et al., 1988) and a universal Parker Buffer (ficoll based with KCl, see section 2.11.3). There was no difference between NF1 control EMSAs with the two buffers, however the NF-κB consensus EMSA was clearer with universal Parker buffer. Parker buffer also produced clear EMSA bands for a C/EBPβ consensus probe from the serum amyloid A gene, as seen by Xia and co-workers (1997). Parker buffer was therefore used as the binding reaction buffer of choice.

EMSAs were carried out with unstimulated and IL-1β stimulated HeLa nuclear extracts (300mM NaCl) with the NF-κB consensus probe to confirm that IL-1β-inducible transcription factors were indeed up regulated in the stimulated extracts. Figure 5.3 shows this EMSA, with only one weak but specific band (d, competed out by cold probe) binding with unstimulated extracts and three additional bands binding with IL-1-stimulated extracts (a, b, c), with an increased intensity of band d. This is consistent with different isoforms of NF-κB being activated by IL-1 and translocating to the nucleus to be available for DNA consensus site binding (see section 1.3.2.1).

The EMSA for the NF1 control probe with HeLa cell extracts in Parker buffer (figure 5.4) showed one specific band (A) that competed out with cold probe at 10-fold excess and one non-specific lower band (B) that did not compete out with cold probe at 50-fold excess. This was consistent with previously published results using this NF1 consensus sequence (Chodosh et al., 1988). Band A was stronger with unstimulated HeLa cell extracts than after IL-1 stimulation suggesting that IL-1 may down-regulate nuclear NF1.

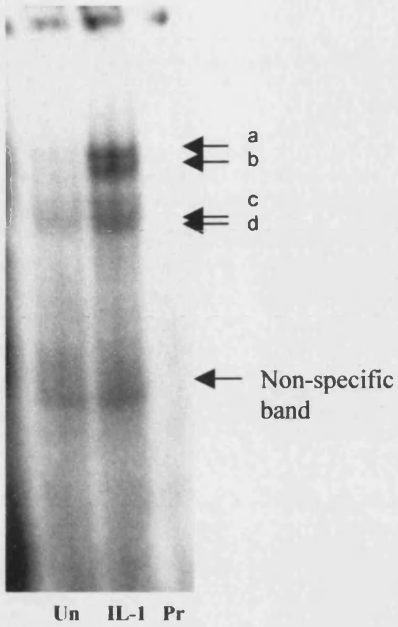

Figure 5.3. EMSA of NF-κB consensus probe incubated with unstimulated and IL-1β-stimulated HeLa cell nuclear extracts.

5pmol radio-labelled NF-κB consensus probe (see table 2.11 for sequence) was incubated with 10μg of 300mM NaCl HeLa nuclear extracts in Parker buffer, run on a 4% non-denaturing polyacrylamide gel at 4°C for 3.5 hours (see 2.11). Un=unstimulated extracts, IL-1= 2-hour IL-1β-stimulated extracts, Pr=probe only.

One specific band d that competed out with cold probe was seen with unstimulated extracts. Three additional specific bands a-c were seen with IL-1-stimulated extracts. The lower band was considered non-specific as it did not compete out with excess unlabelled probe.

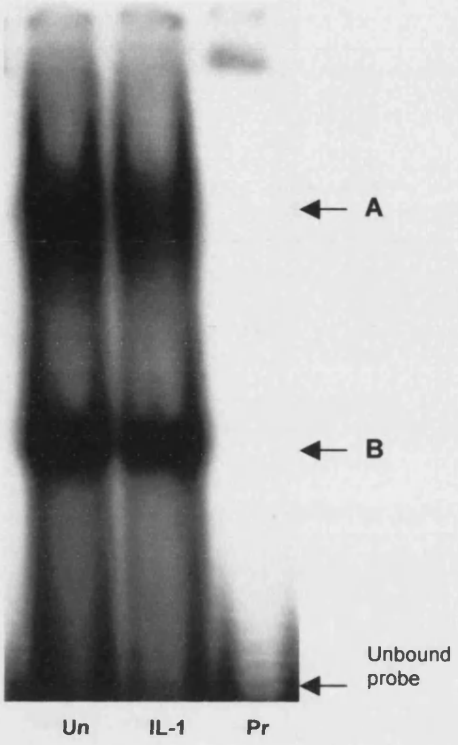

Figure 5.4. EMSA of NF1 control probe incubated with unstimulated and IL-1β-stimulated HeLa cell nuclear extracts.

5pmol radio-labelled NF1 control probe (see table 2.11) was incubated with 10μg of 300mM NaCl HeLa nuclear extracts pre-incubated with 10μg poly dI.dC, run on a 4% non-denaturing polyacrylamide gel at 4°C for 4 hours (see 2.11). Un=unstimulated extracts, IL-1= 2-hour IL-1β-stimulated extracts, Pr=probe only.

Band A is stronger with unstimulated than IL-1 stimulated extracts. It was shown that Band A could be competed out by 10-fold excess cold probe, while band B did not compete out with 50-fold excess cold probe.

5.2. The effect of the –174 polymorphism on transcription factor binding

Comparison of the –174G and –174C allelic sequences of IL-6 using Sigscan identified only one difference between the two alleles in transcription factor binding site homologous sequences (figure 5.5). The –174C allele created a possible NF-1 transcription factor binding site of sequence TGGCA (bases –173 to –177), which was not present with the –174G allele.

Two known and several possible transcription factor binding-sites were also identified around the –174 polymorphic site (figure 5.5). Although these factors do not directly bind to the bases at position –174, allelic changes may alter their steric binding to nearby sequences. Further NF1 protein family binding-sequence comparisons revealed an alternative degenerate site for NF1. The –174C allele of IL-6 differed from the canonical NF1 consensus sequence by two bases, whereas the –174G allele differed by three bases (figure 5.6). NF1 was considered a potential regulatory transcription factor that could differentially bind to the –174 alleles and alter levels of transcription.

5.2.1. The –174 polymorphism does not alter transcription factor binding to a 26bp probe of the 5'-flanking region of IL-6

A 26bp probe of the 5'-flanking region of IL-6 from –164 to –189 was generated containing either the G-allele or the C-allele at position –174 (see figure 5.5), these were designated probes 1G and 1C respectively. The sequences for probes 1 are shown in table 2.10. Sigscan identified the presence of two common consensus sequences with either allele at position –174, a glucocorticoid receptor (GR) consensus sequence GACACA (Chan et al., 1991) from –179 to –184 and a c-Myb consensus sequence CAACT (Sureau et al., 1992) from –183 to –187. c-Myb was unlikely to be a candidate transcription factor in HeLa cells as it is a proto-oncogene almost exclusively expressed in immature haematopoietic cells and involved in their differentiation. The C-allele probe (1C) contained the putative NF1 consensus binding-site TGGCA (Paonessa et al., 1988) from –173 to –177, with this site being degenerate by one base with the G-allele probe. Both the C and the G allele probes were degenerate by two and three bases respectively for the canonical NF1 consensus binding sequence (figure 5.6).

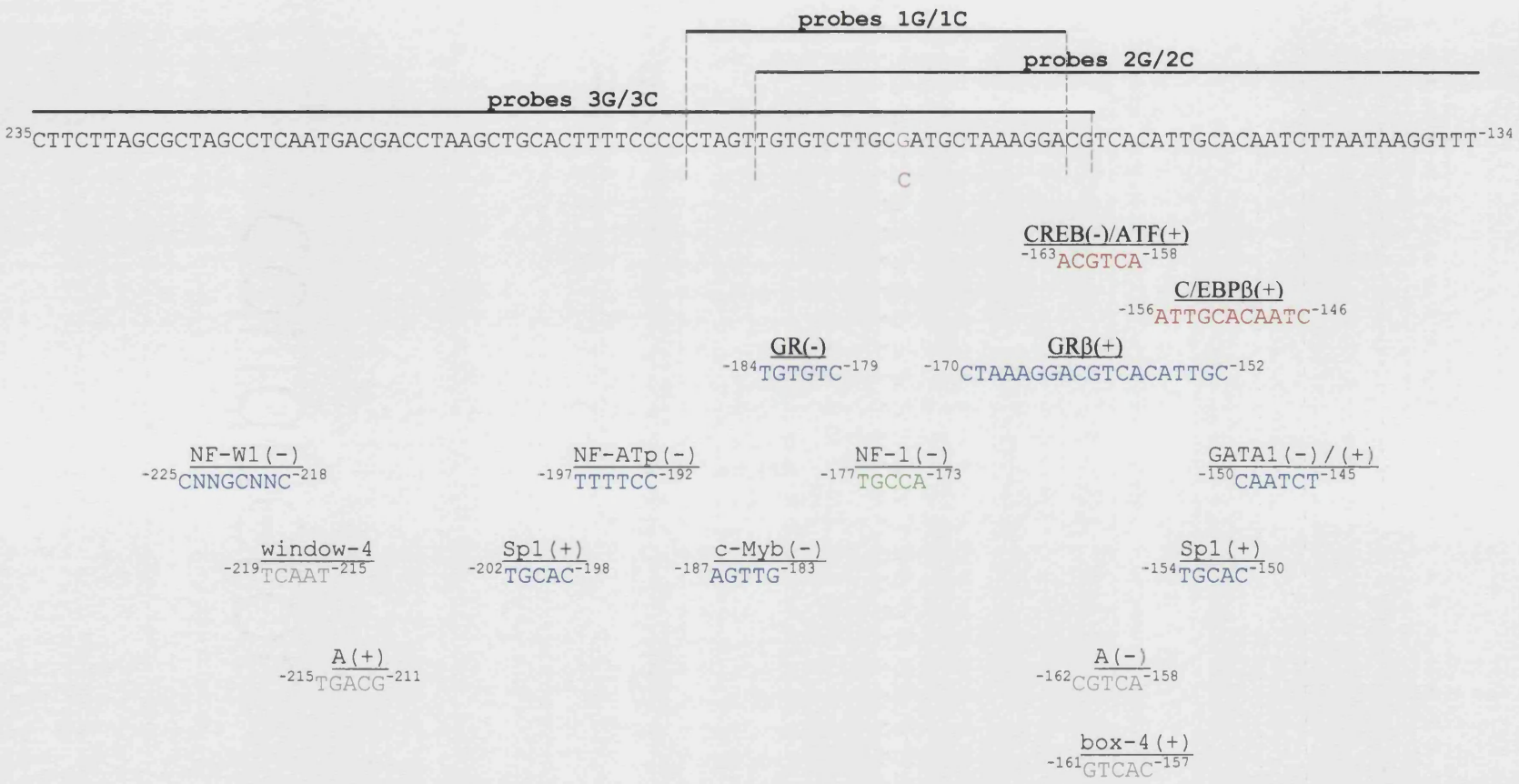

Figure 5.5. Results of HGMP Sigscan search for transcription factor binding-site homology in the 5'-flanking region of IL-6 from –134 to –235, with either the G or the C allele at position –174.

Purple lettering= –174 polymorphism, red lettering= known transcription factor binding-site, blue lettering= possible transcription factor binding-site, green lettering= possible transcription factor binding-site with the –174C allele but not with –174G, grey lettering= possible binding-site for unknown transcription factor, (+)/(-)= direction of binding-site consensus sequence.

NNTGGNNNNNNGCCAAN **(NF1 consensus)**

CTAGTTGTGTCTTGCCATGCTAAAGG **(IL-6 C-174)**

CTAGTTGTGTCTTGCGATGCTAAAGG **(IL-6 G-174)**

Figure 5.6. Comparison of the canonical NF1 consensus binding-site to the IL-6 gene sequence from –171 to –186.
The –174C allele differs from the consensus sequence by two bases, whereas the –174G allele differs by three bases.
Underlined lettering=NF1 consensus binding-site sequence (Chodosh et al., 1988; Jones et al., 1987).
Red lettering=mis-matched base in the IL-6 sequence

Figure 5.7 shows the EMSA with probes 1G and 1C with HeLa cell nuclear extracts. Although several bands are produced with either probe and a lower band Z appears with probe 1C but not probe 1G, these bands were not competed out by excess cold probe up to 50 times the concentration of radio-labelled probe and were therefore unlikely to be specific bands. Probes 1G and 1C may have been too short to allow protein binding. Protein binding to specific DNA sites is not only dependent on the DNA base sequence of the consensus site but also in the context of adjacent DNA sequences. These will influence the tertiary structure of DNA helical turns, the exposure of specific DNA bases, hydrophobic, steric and electrophysiological forces, and co-factor binding.

5.2.2. The –174 polymorphism alters transcription factor binding to a 51bp probe of the 5'-flanking region of IL-6

Longer probes of the IL-6 sequence surrounding the –174 polymorphism were generated to investigate whether the –174 alleles altered transcription factor binding to adjacent transcription factor sites. A 51bp probe from –134 to –184 with either a G or a C allele at position –174 were designated 2G and 2C respectively (see figure 5.5 and table 2.10 for sequence). These included the known down-stream transcription factor binding-sites of IL-6, the cAMP response element TGACGT from –158 to –163, the C/EBPβ site ACATTGCACAATCT from –146 to –158 and a GR binding site between –145 and -173. The probe also contained part of the negative regulatory region from –73 to –181 with an Sp1 transcription factor consensus site TGCAC between –150 and –154. In THP-1 cells, Sp1 has been shown to be part of a negative regulatory complex interacting with this region of the IL-6 gene.

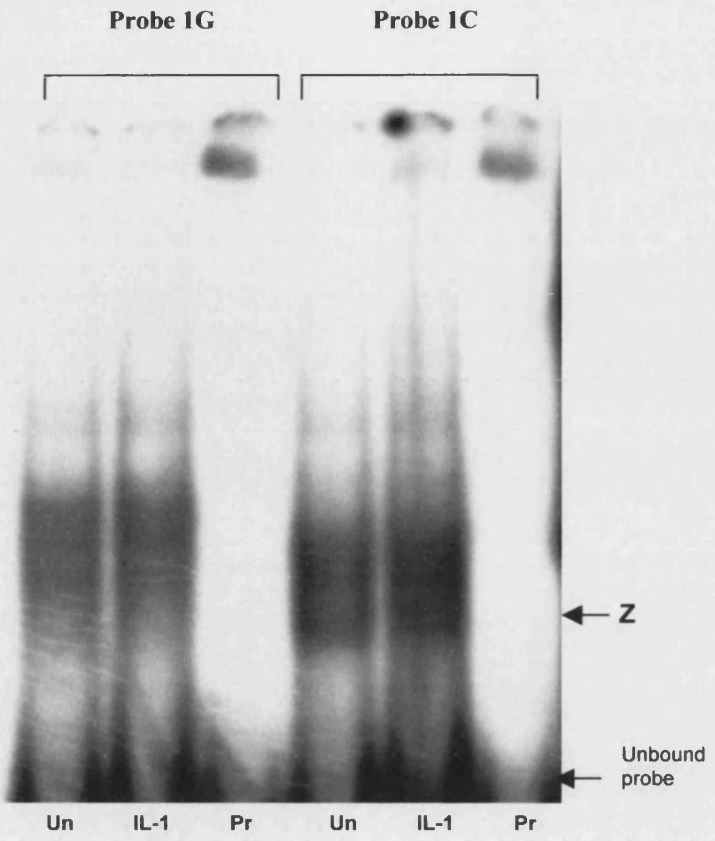

Figure 5.7. EMSA of IL-6 probes 1G and 1C incubated with unstimulated and IL-1β-stimulated HeLa cell nuclear extracts.

5pmol radio-labelled probe was incubated with 10μg of 300mM NaCl extracts pre-incubated with 10μg poly dI.dC, run on a 4% non-denaturing polyacrylamide gel at 4°C for 4 hours (see 2.11). Un= unstimulated extracts, IL-1= 2-hour IL-1β-stimulated extracts, Pr= probe only.
Band Z was only seen with probe 1C, however, neither this band nor the upper two bands common to both probes competed out with 50-fold excess cold probe.

A time course for unstimulated and IL-1β-stimulated HeLa extracts (300mM NaCl) binding to probes 2G and 2C, revealed maximal up-regulation of transcription factor binding to these probes with 30min IL-1β-stimulated extracts (figure 5.8). HeLa nuclear cell extracts stimulated by IL-1β for 30min were therefore used in subsequent experiments to compare the banding pattern and specificity of transcription factor binding to the G and C allele probes. This was carried out with HeLa cell nuclear extracts at three salt concentrations, 10mM, 150mM and 300mM NaCl (see methods 2.11.1). In all three salt concentrations, probe 2G had two distinct upper bands C and D, whereas probe 2C produced only one distinct upper band that was equivalent in position to band C with probe 2G (figure 5.9). There were also two lower bands G and H with both probes.

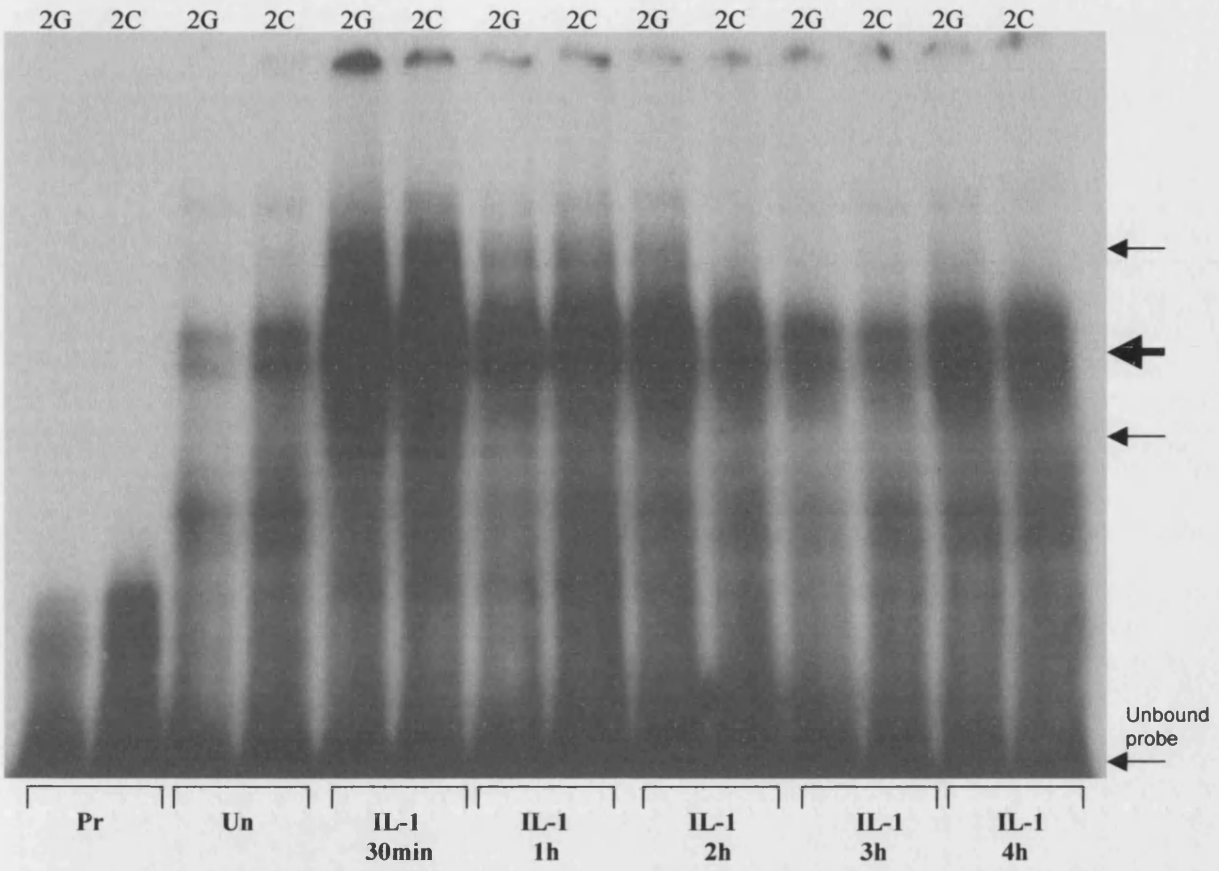

Figure 5.8. EMSA of IL-6 probes 2G and 2C incubated with unstimulated and increasing times of IL-1β-stimulated HeLa cell nuclear extracts.

5pmol radio-labelled 2G or 2C probe was incubated with 12μg of 300mM NaCl extracts pre-incubated with 10μg poly dI.dC and run on a 4% non-denaturing polyacrylamide gel at 4°C for 4 hours (see 2.11). Un= unstimulated extracts, IL-1= IL-1β-stimulated extracts for given length of time, Pr= probe only, unlabelled arrows indicate bands induced or up-regulated by IL-1β.

Transcription factor binding was maximally up regulated with IL-1 stimulation for 30mins.

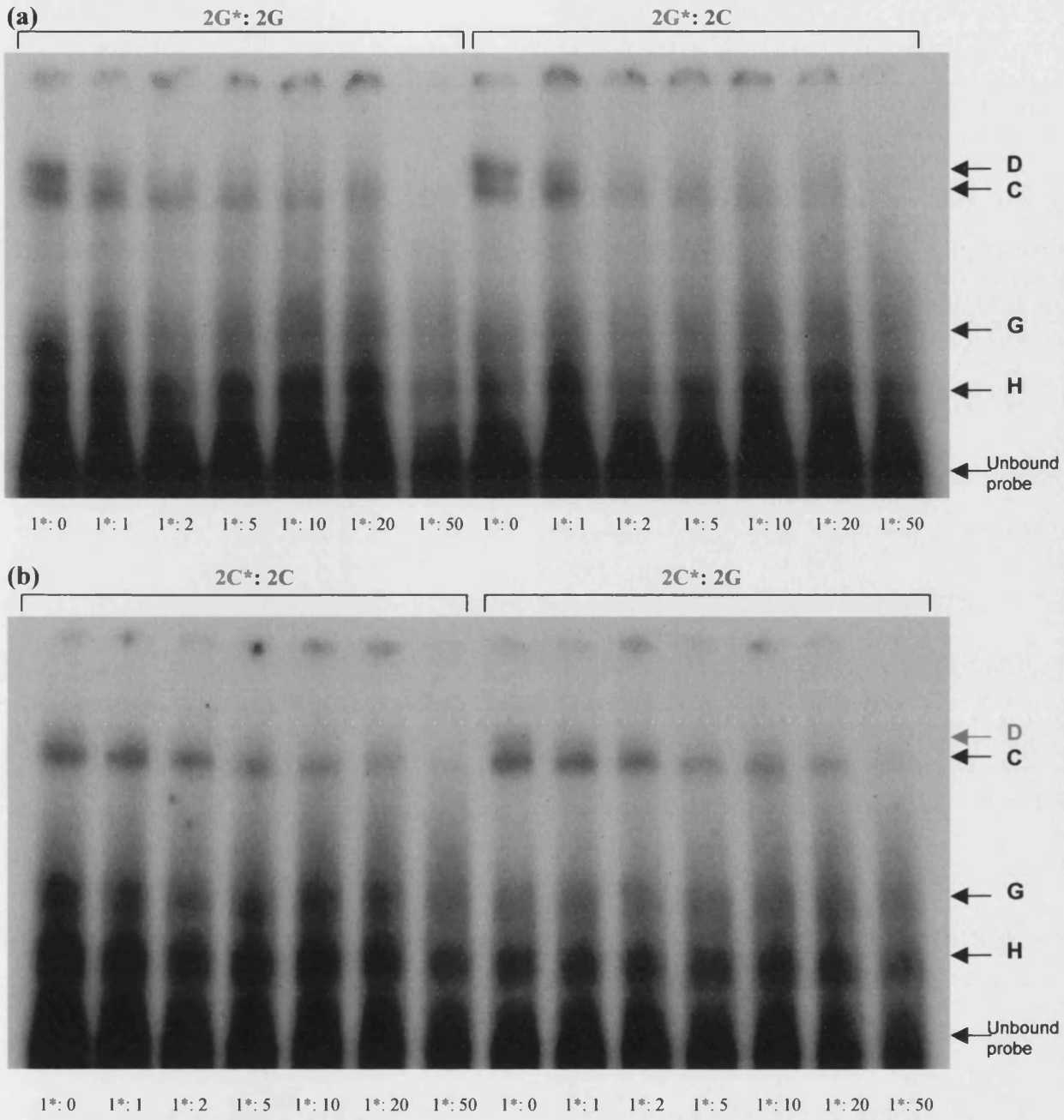

Figure 5.9. EMSA of IL-6 probes (a) 2G and (b) 2C incubated with 30min IL-1β-stimulated HeLa cell nuclear extracts (10mM NaCl) with competition from unlabelled 2G or 2C probe.

Radiolabelled probe* (5pmol) was mixed with the indicated ratio of unlabelled probe, incubated with 10μg of 10mM NaCl extracts pre-incubated with poly dI.dC (10μg) and run on 4% non-denaturing polyacrylamide gels at 4°C for 4 hours (see 2.11 for method). Unbound probe was run to the bottom of the gel. Red lettering= radio-labelled probe, blue lettering= unlabelled competitor probe. The ratio of radiolabelled to unlabelled probe is shown at the bottom of each lane.

Band C was common to both probes. With probe 2G, a lower ratio of unlabelled probe 2C was required to compete out band C than unlabelled probe 2G. Band D occurred with probe 2G and only required low ratios of unlabelled probe 2G or 2C to compete it out. Bands G and H were common to both probes.

Band D was competed out at very low ratios of cold competition by either cold probe 2G or 2C, despite probe 2C not producing this band. This suggested that band D was a non-specific band forming when the G allele was present and this was confirmed by cold competition with random probe (a universal heteroduplex generator for an exonic sequence of IL-4 receptor, see table 2.11). Random probe competed out band D but not the specific band C (figure 5.10). With 150mM NaCl HeLa extracts there was an additional lower band (I) produced on EMSA (figure 5.10), both this and band G were non-specific bands as they were competed out with random probe.

Band C appeared to be stronger with probe 2C than 2G. With radiolabelled probe 2G, lower ratios of the C allele competitor probe (20-fold of 2C) than the G allele competitor probe (50-fold of 2G) were required to compete out band C (figure 5.9). Similarly, in figure 5.10, a 20-fold excess of the C allele competitor probe (2C) was able to compete out band C for the 2G probe, but a 20-fold excess of the G allele competitor probe (2G) failed to do so. In an attempt to reduce non-specific protein binding, the EMSA binding reaction was carried out at the higher temperature of 21°C instead of 16°C (figure 5.11). Band D was no longer seen to form with probe 2G. However, band C remained stronger with probe 2C and higher ratios of unlabelled probe 2G than 2C were required to compete out band C.

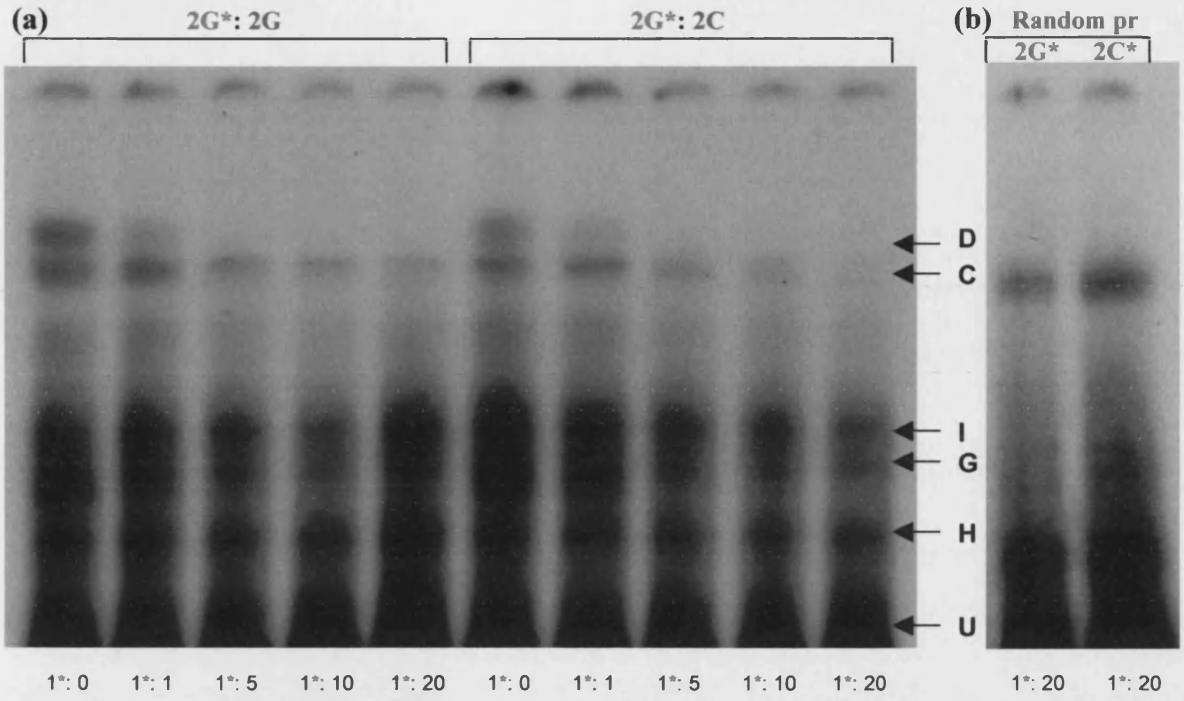

Figure 5.10. EMSA of IL-6 probe 2G with 30min IL-1β-stimulated HeLa cell nuclear extracts (150mM NaCl).

(a) specific competition with increasing amounts of unlabelled 2G and 2C probe, (b) random competition with 20-fold random probe on radiolabelled probe 2G and 2C.

Radiolabelled probe* (5pmol) with the indicated ratio of unlabelled probe was incubated with 10μg of 150mM NaCl HeLa extracts pre-incubated with poly dI.dC (10μg) and run on a 4% non-denaturing polyacrylamide gel at 4°C for 4 hours (see 2.11 for method). U= unbound probe, R= random probe (a universal heteroduplex generator for an exonic sequence of IL-4 receptor, table 2.11), red lettering= radiolabelled probe, blue lettering= unlabelled competitor probe. The ratio of radiolabelled to unlabelled probe is shown at the bottom of each lane.

Non-specific bands D, G and I are competed out by random probe. Specific band C is not competed out by random probe. Band C is stronger with probe 2C than 2G. 20-fold unlabelled probe 2C competes out band C completely from radiolabelled probe 2G, whereas band C is still seen with competition from 20-fold of unlabelled probe 2G.

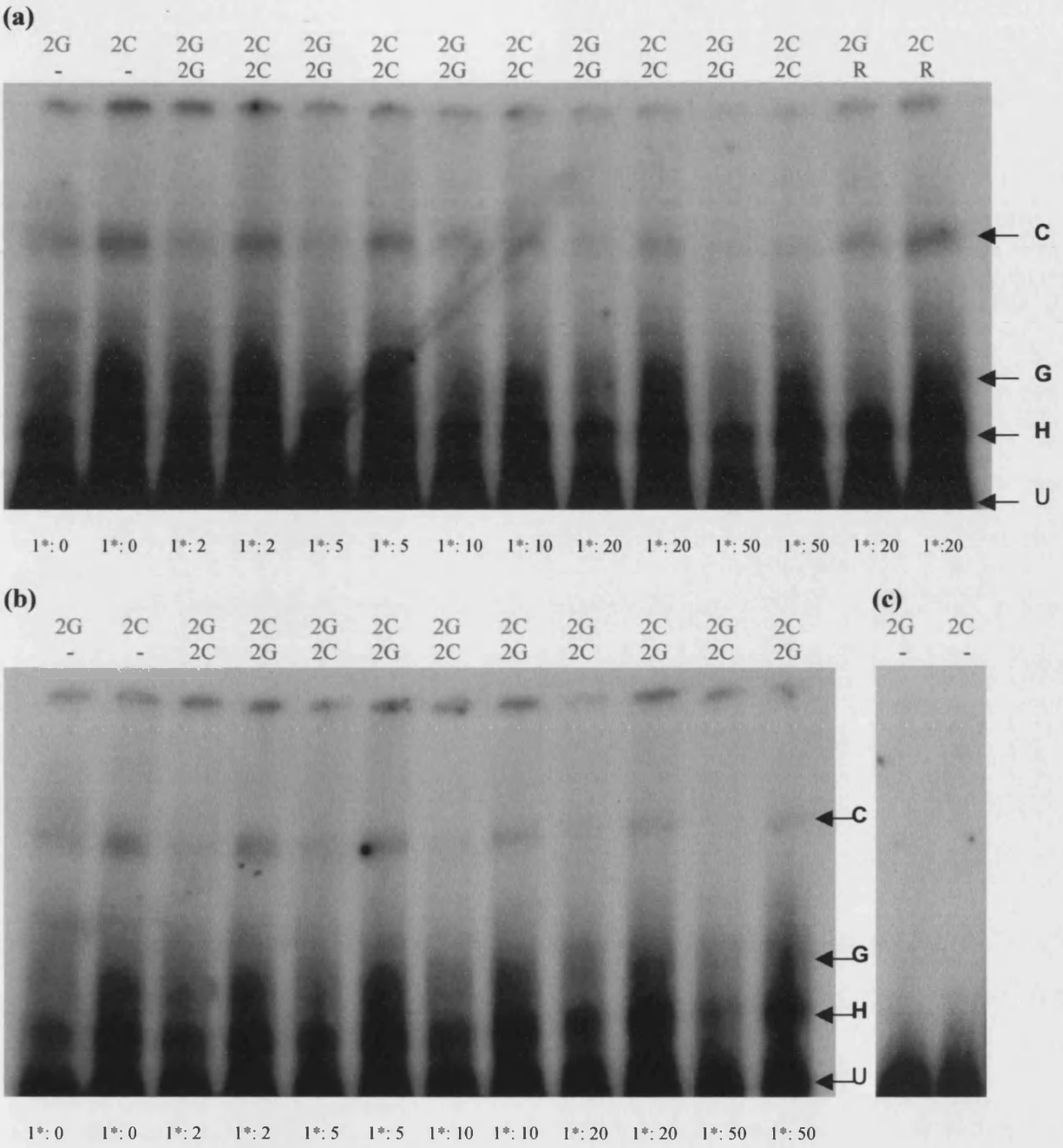

Figure 5.11. EMSA of IL-6 probes 2G and 2C incubated with 30min IL-1β-stimulated HeLa cell nuclear extracts at 21°C with specific competition,

(a) increasing amounts of unlabelled probe of the same allele as the radiolabelled probe, (b) increasing amounts of unlabelled probe of the other allele from radiolabelled probe, (c) probe only, with no nuclear extracts or competition.

Radio-labelled probe* (5pmol) was mixed with the indicated ratio of unlabelled probe, incubated with 10μg of 300mM NaCl extracts pre-incubated with poly dI.dC (10μg) and run on 4% non-denaturing polyacrylamide gels at 4°C for 4 hours (see 2.11 for method). R= random probe (see table 2.11), U= unbound probe, red lettering= radiolabelled probe, blue lettering= unlabelled competitor probe. The ratio of radiolabelled to unlabelled probe is shown underneath each lane.

Band C is consistently stronger with probe 2C than 2G. Competition of radiolabelled probe 2C with 50-fold excess unlabelled probe 2C but not probe 2G competed out band C. Competition of radiolabelled probe 2G with 10-fold excess unlabelled probe 2C but not probe 2G competed out band C. Band G was non-specific.

Cold competition with unlabelled probe 2C or 2G added *after* the initial 20min binding reaction with radiolabelled probe also resulted in competition of band C from both probe (figure 5.12). This supports band C being a probe specific band, and the results support probe 2C being a stronger competitor than probe 2G. There was complete loss of band C for radiolabelled probe 2G with addition of 20-fold of the C allele competitor probe (2C), however band C was still faintly visible with addition of 20-fold of the G allele competitor probe (2G), (figure 5.12). With the radiolabelled probe 2C, band C was stronger after addition of 20-fold of the G allele competitor probe than after addition of 20-fold of the C allele competitor probe.

The results shown are representative of five separate preparations of labelled and unlabelled probes, and three separate preparations of nuclear extracts at three different salt concentrations. They show that a nuclear factor, or complex of factors, binds to the IL-6 sequence between –134 and –184 producing band C on EMSA under a range of conditions. The –174C allele appears to bind this factor(s) more strongly than the –174G allele. Since the C allele was found to be associated with lower levels of expression with IL-1β-stimulation than the G allele in HeLa cell transfection studies (see chapter 4), it was hypothesised that the factor(s) binding more strongly to the C allele sequence would have an inhibitory influence on transcription. Since band C was present in unstimulated as well as IL-1β-stimulated extracts, the transcription factor must be constitutively expressed in HeLa cells. To account for the transfection study results, the factor(s) would have to be down regulated in the nucleus by IL-1β-stimulation, but removed less effectively from the C allele sequence than from the G allele sequence due to stronger binding to the C allele sequence.

There was one lower band H produced consistently on EMSA that was not competed out by random probe. It was however, also not competed out by unlabelled specific competitor probe up to 50-fold excess, suggesting that this band was probably non-specific.

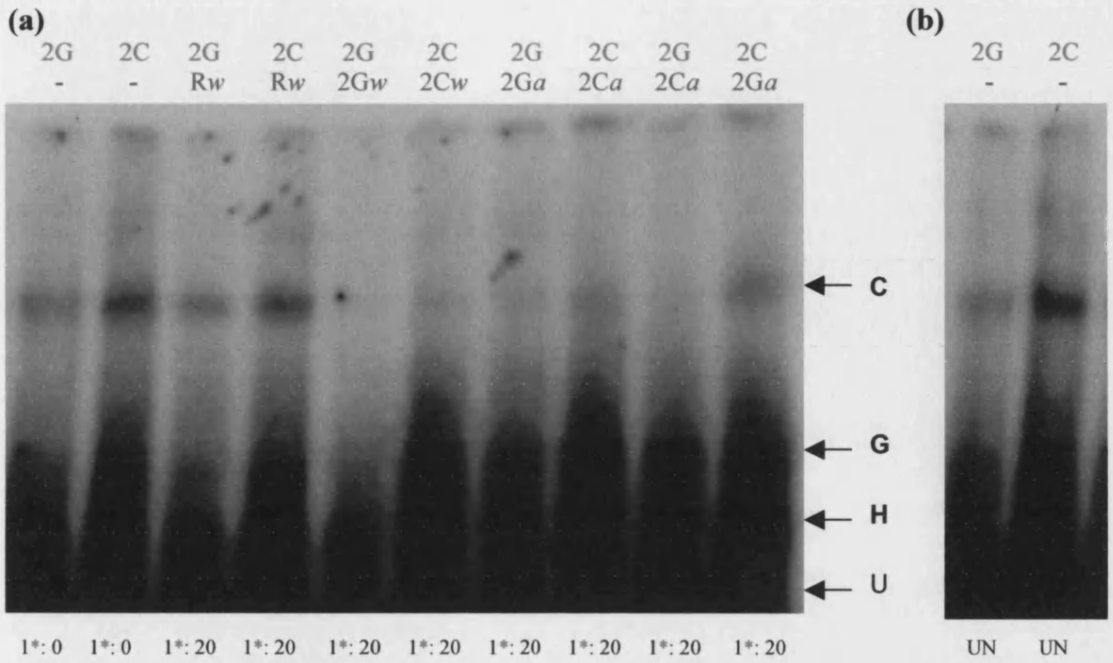

Figure 5.12. EMSA of IL-6 probes 2G and 2C incubated with (a) 30min IL-1β-stimulated HeLa cell nuclear extracts or (b) unstimulated (UN) HeLa cell nuclear extracts.

Competition in (a) was with 20-fold unlabelled competitor probe either added with (*w*) or after (*a*) the radiolabelled probe binding reaction.

5pmol of radio-labelled probe* was used for each reaction. A 20min incubation with 10μg of 150mM NaCl HeLa extracts, pre-incubated with poly dI.dC (10μg) was carried out at 21°C with either 20-fold unlabelled competitor for 'with' reactions, or no competitor for 'after' reactions. For 'after' reactions 20-fold unlabelled competitor was added after the initial binding reaction and incubated for a further 20min at 21°C before running on a 4% non-denaturing polyacrylamide gel at 4°C for 4hrs (see 2.11). Red lettering= radiolabelled probe, blue lettering= unlabelled competitor. The ratio of radiolabelled probe to unlabelled competitor is shown underneath each lane. U= unbound probe. R= random probe (see table 2.11).

Band C is stronger for probe 2C than 2G, with IL-1-stimulated and unstimulated HeLa extracts. Band C is not competed out by random probe but is competed out by unlabelled probe 2G or 2C, added 'with' or 'after' radiolabelled probe. With 20-fold excess of the 2C competitor probe added 'after' radiolabelled probe 2G, band C is no longer seen. However, with 20-fold excess of the 2G competitor probe added 'after' radiolabelled probe 2G, band C is still faintly visible. With 20-fold competitor probe 2C added 'after' radiolabelled probe 2G band C is weaker than when 20-fold competitor probe 2G was added. Band G is a non-specific band.

5.2.3. The possible role of NF1 in altered transcription factor binding between –174 alleles in a 51bp probe of IL-6

The possibility that the factor, or one of a complex of factors, producing band C on EMSA with probes 2G and 2C (see above) could be NF1 was investigated. Dependent on the gene they act on, members of the NF1 family of transcription factors have been shown to display both transcription repressor and activator function. In the human metallothionein IIA gene, NF1 has been shown to act as a transcriptional repressor (Osada et al., 1997b), which was also the case with rat hepatic aldehyde dehydrogenase 3 (Lindahl et al., 1999). However, in the rat α_{1b} adrenergic receptor gene, NF1 has been shown to act as a transcriptional activator (Gao et al., 1996), as with adenoviral RNA polymerase II (Jones et al., 1987). The –174C allele contains an NF1 consensus binding-site. It was plausible that NF1 could bind preferentially to the C allele producing a stronger band on EMSA. As the C allele resulted in lower levels of IL-1-induced IL-6 transcription in HeLa cell transfection studies, the hypothesis was that if NF1 was involved it was likely to have inhibitory influences on transcription in the context of the human IL-6 gene. Western blot analysis of unstimulated and IL-1-stimulated HeLa nuclear cell extracts confirmed the presence of NF1 in these extracts (figure 5.13), although there were also some lower molecular-weight proteins detected. These were probably degraded NF1 protein fragments resulting from the method of preparation of nuclear extracts. The samples were dounce homogenised to rupture the cellular membrane and although this was carried out on ice, the friction generated may have resulted in heat production causing fragmentation of some nuclear proteins. Alternatively, proteolytic cleavage may have resulted in some fragmentation of the protein products, despite the presence of protease inhibitors in the buffers. Several species of C/EBPβ have been found to arise from proteolytic degradation during extract preparation (Vales and Friedl, 2002). Protein fragments are less likely to bind specifically to DNA or form complexes with other bound proteins. As these fragments are smaller, they would be expected to have a higher electrophoretic mobility if they bound to DNA and to pass faster through the gel (it is possible that this accounts for some of the non-specific lower bands seen on EMSA). The salt concentration of the extracts may additionally influence protein stability.

Equal quantities of total nuclear protein extracts were applied to the Western blot for unstimulated and IL-1β-stimulated extracts. NF1 formed a smaller proportion of the total protein in IL-1β-stimulated extracts compared to unstimulated extracts. This would suggest that NF1 levels are not significantly up regulated by IL-1-stimulation and may be inhibited.

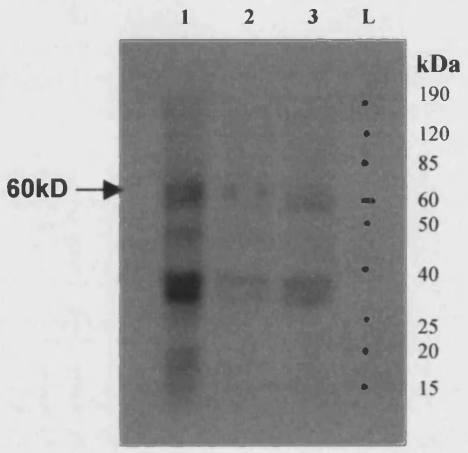

Figure 5.13. Western blot for NF1 in unstimulated and IL-1β-stimulated HeLa cell nuclear extracts.

5μg of nuclear extract was applied per lane. NF1 was detected using primary antibody Sc-870 rabbit polyclonal anti-NF1 antibody (table 2.12), secondary antibody HRP-conjugated porcine anti-rabbit IgG polyclonal antibody (table 2.13) and detected by chemiluminescence (see 2.12.3 for method).
Lane 1 =unstimulated extracts (150mM NaCl), lane 2 =30min IL-1β-stimulated extracts (150mM NaCl), lane 3 =30min IL-1β-stimulated extracts (300mM NaCl), L=ladder of protein molecular weight markers (Benchmark, Gibco). ⟶ = protein band for NF1 according to molecular weight. Lower bands probably represent degradation products.

Two unlabelled competitor sequences of NF1 consensus binding sites were used to investigate the possible binding of NF1 to produce band C on EMSA with the 51bp probes 2G and 2C (see 5.2.2). NF1 consensus 1 (NF1-1) competitor contained the canonical consensus sequence for NF1 (see table 2.11), present with two base differences in the C allele probe (2C) and three in the G allele probe (2G). NF1 consensus 2 (NF1-2) competitor contained the short consensus sequence TGCCA (see table 2.11), present with the C allele but not with the G allele. Figure 5.14 shows that both NF1-1 and NF1-2 competitor probes could compete band C for radiolabelled probes 2G and 2C.

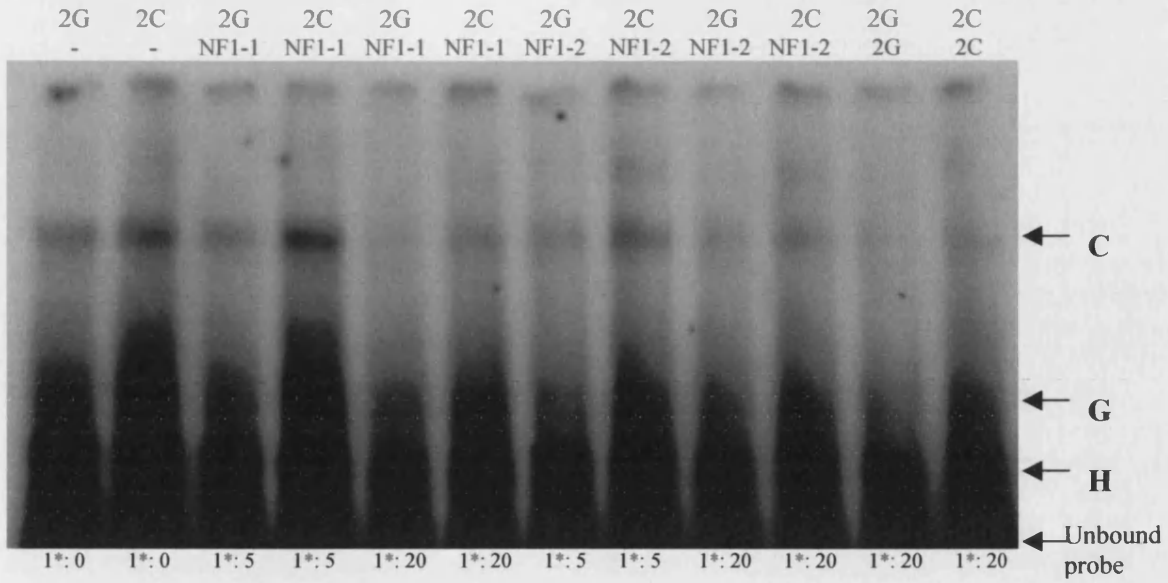

Figure 5.14. Cold competition with NF1 consensus sequences for IL-6 probes 2G and 2C incubated with 30min IL-1β-stimulated HeLa cell nuclear extracts.
Radiolabelled probe* (5pmol) was mixed with the indicated ratio of unlabelled NF1 consensus 1 (NF1-1) or NF1 consensus 2 (NF1-2) competitor (see table 2.11 for sequences), incubated with 10μg of 150mM NaCl HeLa extracts pre-incubated with poly dI.dC (10μg), and run on a 4% non-denaturing polyacrylamide gel at 4°C for 4 hours (see 2.11 for method). Red lettering= radiolabelled probe, blue lettering= unlabelled competitor, the ratio of radiolabelled to unlabelled is indicated underneath each lane.
Band C was competed out by both the NF1-1 and NF1-2 competitor sequences.

This suggested that NF1 may be involved in binding to the 2G and 2C probes to produce band C. However, supershift studies with a monoclonal antibody to the NF1 family of proteins did not result in a shift (figure 5.15). Antibody incubations of 15-60min, at 4°C as well as at room temperature (21°C) were carried out with antibody concentrations of 100-300ng per μl of reaction, added before or after incubation of extracts with the radiolabelled probe. Under similar conditions as a positive control, it was shown that the same anti-NF1 antibody resulted in a shift with radiolabelled NF1-1 consensus probe (figure 5.16). This confirmed that NF1 bound to the NF1-1 consensus probe and that supershift conditions were suitable. The band 'f' and 'h' did not compete out with cold probe suggesting that they were probably produced by non-specific protein binding. The lower band 'g' did compete out with cold NF1-1 probe, but not with random probe, suggesting that this was a specific band. This band was not shifted however by anti-NF1 antibody and may therefore have been due to an additional transcription factor binding to the sequence of the NF1-1 probe.

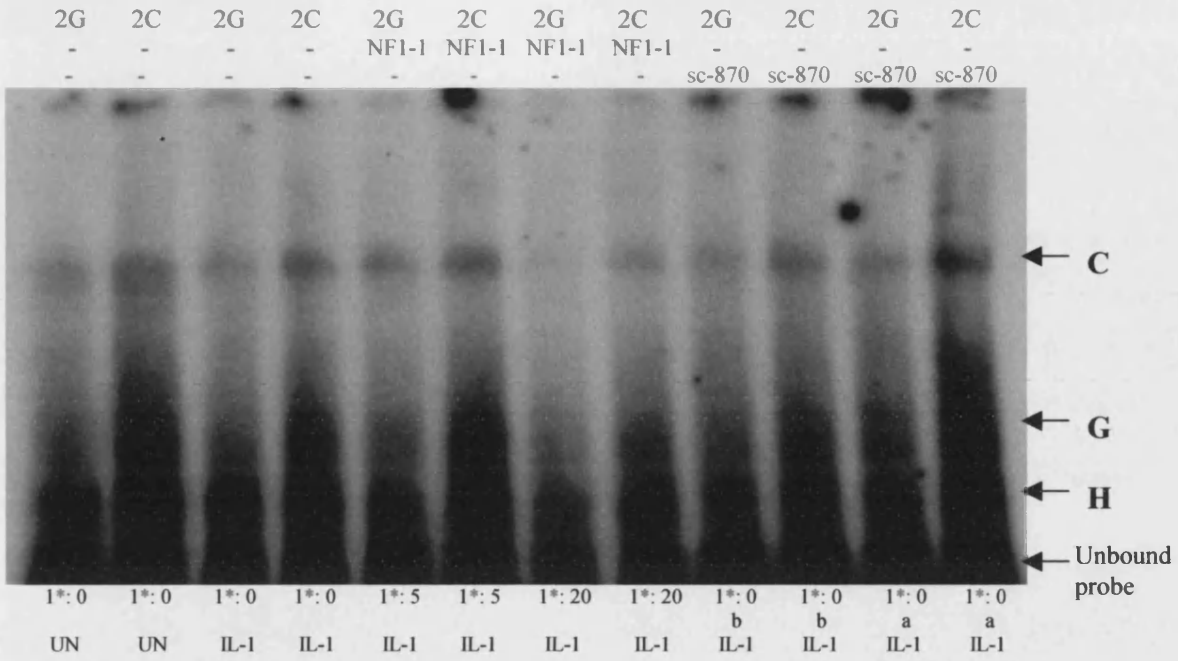

Figure 5.15. Supershift EMSA of IL-6 probes 2G and 2C with monoclonal antibody to NF1.

Radiolabelled probe* (5pmol) was mixed with the indicated ratio of unlabelled competitor NF1-1 (table 2.11) and incubated with 10μg of HeLa nuclear extracts (150mM NaCl), pre-incubated with poly dI.dC (10μg), (see 2.11 for method). For supershift reactions, 3μl of anti-NF1 antibody sc-870 (300ng/μl, table 2.12) was added either *before* or *after* radiolabelled probe and incubated at 21°C for 20min (see method 2.11.4). Reactions were run on a 4% non-denaturing polyacrylamide gel at 4°C for 4hrs. Red lettering= radiolabelled probe, blue lettering= unlabelled competitor, green lettering= specific antibody added. The ratio of radiolabelled probe to unlabelled competitor is indicated underneath each lane. 'b' and 'a' refer to whether antibody was added *before* or *after* radiolabelled probe. UN= unstimulated HeLa nuclear extracts, IL-1= 30min IL-1β-stimulated HeLa nuclear extracts.

Band C was competed by NF1-1 competitor probe, but no shift was seen with antibody to NF1 whether added *before* or *after* the binding reaction with radiolabelled probe.

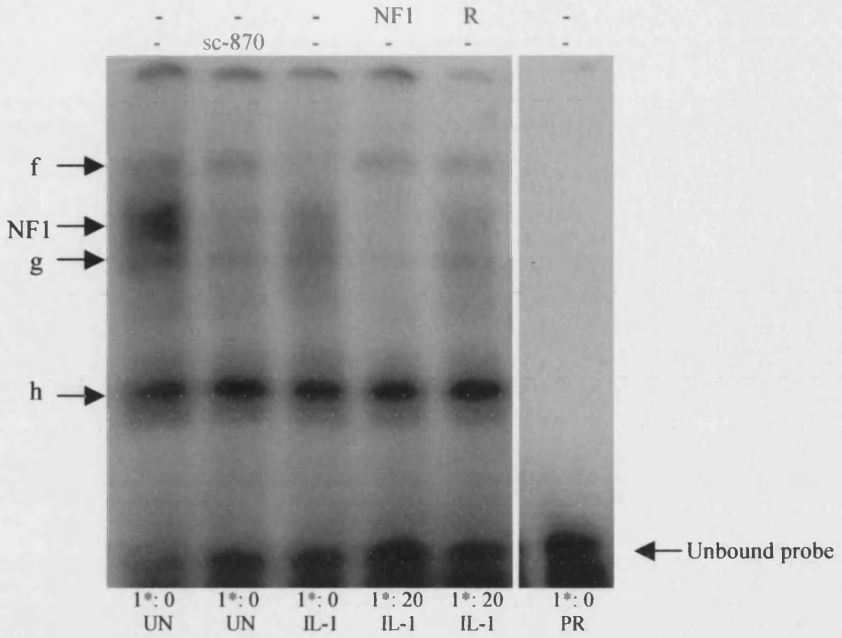

Figure 5.16. Supershift EMSA of NF1-1 consensus probe with monoclonal antibody to NF1.

Radiolabelled probe* (5pmol) was mixed with the indicated ratio of NF1-1 unlabelled competitor or random competitor R (see table 2.11 for sequences) and incubated with 10μg of HeLa nuclear extracts (150mM NaCl), pre-incubated with poly dI.dC (10μg), (see 2.11 for method). For supershift reactions, 3μl of anti-NF1 antibody sc-870 (300ng/μl, table 2.12) was added *before* radiolabelled probe and incubated at 21°C for 20min (see 2.11.4). Reactions were run on a 4% non-denaturing polyacrylamide gel at 4°C for 4hrs. Blue lettering= unlabelled competitor, the ratio to radiolabelled probe is indicated underneath each lane, green lettering= specific antibody added. UN =unstimulated HeLa extracts, IL-1= 30min IL-1β-stimulated HeLa extracts, PR= probe only.

The NF1 band was competed by NF1-1 competitor probe but not random competitor. It was shifted (lost) with antibody to NF1. Band g was competed out by NF1-1 competitor but not shifted by anti-NF1 antibody. Bands f and h were probably due to non-specific protein binding.

No alternative antibody to NF1 was available to investigate further the possibility of NF1 binding to probe 2G or 2C. It is possible that steric interactions between antibody and protein were hindered by the presence of other proteins in a complex. Despite competition from the NF1 consensus sequences, no definite conclusion can be drawn as to whether NF1 is involved in binding to probe 2G or 2C to produce band C (section 5.2.2).

5.2.4. CREB interacts equally with probes 2G and 2C

Adjacent to the –174 polymorphism in the IL-6 gene, there is a cyclic AMP response element (CRE) from –158 to –163 (ACTGCA, figure 5.5). This site confers an enhancer effect on IL-6 transcription as demonstrated by site-directed mutagenesis studies (Dendorfer et al., 1994). A family of CRE binding proteins (CREB) can bind CRE sites and include CREB-1 and ATF-1 with transactivating function, and CREM and ICERs with inhibitory functions (see section 1.3.2.3). The possibility of CREB being present as part of a complex forming EMSA band C with probes 2G and 2C (see 5.2.2) was investigated using competition studies with a CREB consensus sequence competitor (table 2.11) and in supershift studies with two specific anti-CREB antibodies (table 2.12). CREB did not appear to be involved in band C as consensus probe did not compete the band, nor antibodies to CREB-1/ATF-1 family members produce a shift of the band. However, CREB binding to the IL-6 sequence in probes 2G and 2C was confirmed. Anti-CREB antibodies resulted in an upward shift of a lower band to form two supershifted bands (bands i and j, figure 5.17). This may represent binding of two distinct members or forms of CREB (such as phosphorylated and unphosphorylated forms). This could also represent alteration of another bound-factor, or complex of factors, following removal of CREB. The co-factor CREB binding protein (CBP) only binds to the phosphorylated form of CREB and would be expected to be lost from a protein complex on removal of phosphorylated CREB. CREB was presumed to be binding at the known CREB site between –158 and –163. The –174 G and C alleles did not appear to affect CREB binding. Western blot analysis confirmed the presence of CREB-1/ATF-1 (43kD) in the IL-1β-stimulated HeLa cell nuclear extracts, with lower levels present in unstimulated cells (figure 5.18).

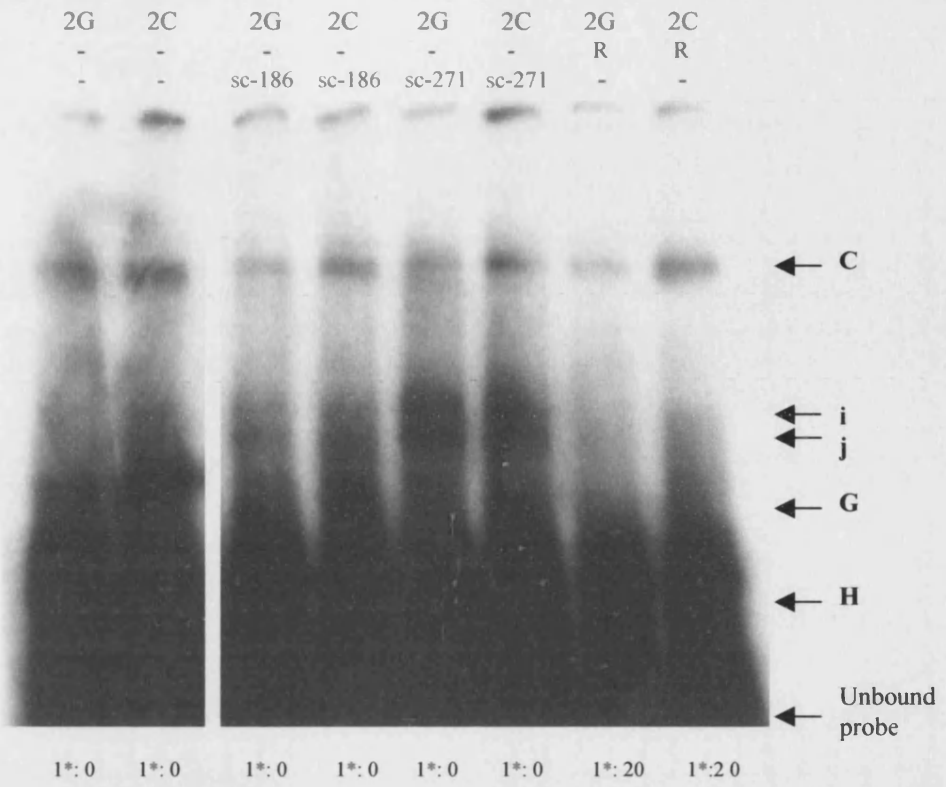

Figure 5.17. Supershift EMSA of IL-6 probes 2G and 2C with antibody to CREB.
Radiolabelled probe* (5pmol) was incubated with 10μg of 30min IL-1β-stimulated HeLa cell nuclear extracts (150mM NaCl), pre-incubated with poly dI.dC (10μg). 3μl of anti-CREB antibody sc-186 or sc271 (300ng/μl, table 2.12) was added before radiolabelled probe and incubated at 21°C for 20min (see methods 2.11.4). The indicated ratio of unlabelled random competitor (R, see underneath lane) was mixed with radiolabelled probe. Reactions were run on a 4% non-denaturing polyacrylamide gel at 4°C for 4.5hrs. Red lettering = radiolabelled probe, blue lettering = unlabelled random competitor, green lettering = specific antibody added.
Band C is not shifted by antibody to CREB, but a shift of lower bands is seen to produce bands i and j.

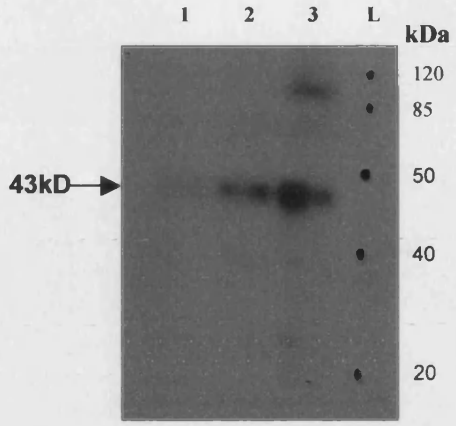

Figure 5.18. Western blot for CREB in unstimulated and IL-1β-stimulated HeLa cell nuclear extracts.

5μg of HeLa cell nuclear extract was applied per lane. CREB was detected using primary antibody Sc-271 mouse anti-CREB monoclonal antibody (table 2.12), secondary antibody HRP-conjugated rabbit anti-mouse polyclonal antibody (see table 2.13), followed by chemiluminescent detection (see 2.12.3 for method).

Lane 1= unstimulated extracts (150mM NaCl), lane 2 =30min IL-1β-stimulated extracts (150mM NaCl), lane 3=30min IL-1β-stimulated extracts (300mM NaCl), L=ladder of protein molecular weight markers (Benchmark, Gibco). ⟶= protein band for CREB according to molecular weight.

5.2.5. C/EBPβ is involved in differential binding of a transcription factor complex to probes 2G and 2C

A known binding site for C/EBPβ (TCTAACACGTTACA) occurs between bases –146 to –156 of the 2G and 2C probes (see figure 5.5). To investigate whether C/EBPβ could be involved in a transcription factor complex producing EMSA band C with probes 2G and 2C (see 5.2.2) cold competition studies were carried out with C/EBP consensus sequence (table 2.11) and supershift studies with two anti-C/EBP antibodies, one specific for C/EBPβ (table 2.12). Figure 5.19 shows that the C/EBP consensus probe competed band C, more apparent with probe 2G than 2C. Addition of anti-C/EBP and anti-C/EBPβ antibodies *before* the binding reaction resulted in a reduction in band C with both probes (figure 5.19). This indicates the involvement of C/EBPβ in EMSA band C. As band C was diminished but not lost by addition of antibody, some complex formation/binding was still able to occur. This could have been due to antibody concentration (though 300ng/μl is generally considered to be in excess of most nuclear protein concentrations) or due to antibody affinity for C/EBP. Alternatively, it could suggest that C/EBPβ has a synergistic role in the complex

formation or contributes to the stability of complex binding, when it is bound to its binding site, and may not be essential to complex formation. Antibody added *after* the binding reaction did not alter band C.

C/EBPβ was present in the nuclear extracts and as expected was up regulated in IL-1β-stimulated extracts as demonstrated by Western blot analysis (figure 5.20).

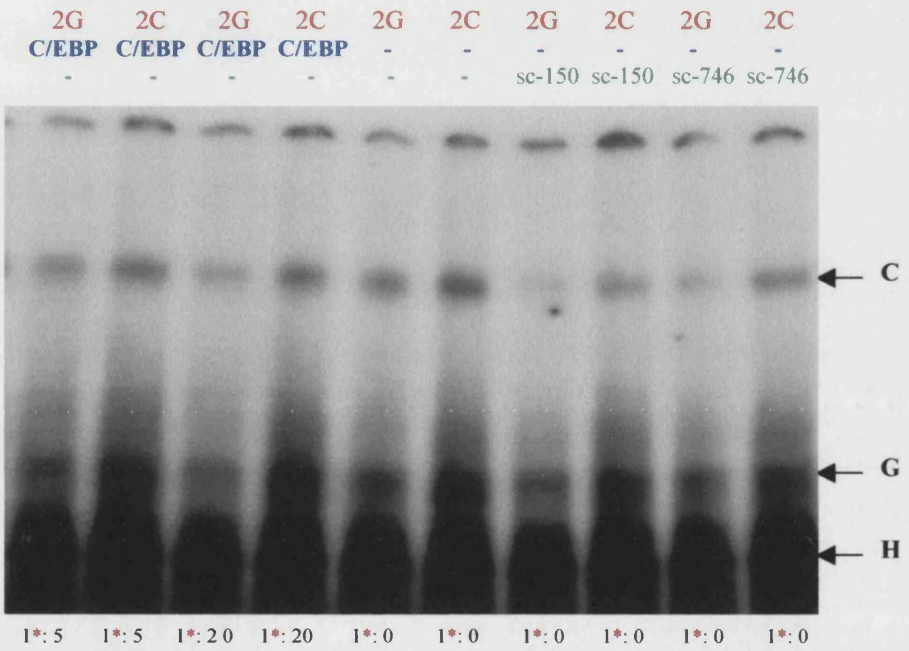

Figure 5.19. Supershift EMSA of IL-6 probes 2G and 2C with antibody to C/EBP and C/EBPβ.

Radiolabelled probe* (5pmol) was incubated with 10μg of 30min IL-1β-stimulated HeLa cell nuclear extracts (150mM NaCl), pre-incubated with poly dI.dC (10μg). 3μl of anti-C/EBPβ antibody sc-150 or anti-C/EBP antibody sc746 (300ng/μl, table 2.12) was added before radiolabelled probe and incubated at 21°C for 20min (see methods 2.11.4). For cold competition, unlabelled C/EBP consensus probe (table 2.11) was mixed with radiolabelled probe in the ratio indicated underneath each lane. Reactions were run on a 4% non-denaturing polyacrylamide gel at 4°C for 4.5hrs. Red lettering= radiolabelled probe, blue lettering= unlabelled competitor, green lettering= specific antibody added.

Band C was competed by unlabelled C/EBP consensus sequence, more noticeable for probe 2G than 2C. Band C was reduced by the addition of antibody to C/EBP and C/EBPβ.

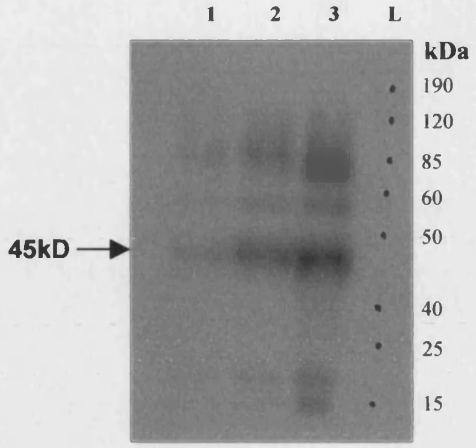

Figure 5.20. Western blot for C/EBPβ in unstimulated and IL-1β-stimulated HeLa cell nuclear extracts.

5μg of HeLa cell nuclear extract was applied per lane. C/EBPβ was detected using primary antibody sc-150 rabbit polyclonal anti-C/EBPβ antibody (table 2.12), secondary antibody HRP-conjugated porcine anti-rabbit IgG polyclonal antibody (table 2.13) and chemiluminescent detection (see method 2.12.3). Lane 1=unstimulated extracts (150mM NaCl), lane 2=30min IL-1β-stimulated extracts (150mM NaCl), lane 3=30min IL-1β-stimulated extracts (300mM NaCl), L=ladder of protein molecular weight markers (Benchmark, Gibco). →= protein band for C/EBPβ according to molecular weight.

5.2.6. Other candidate factors for differential binding to probes 2G and 2C

An alternative inhibitory factor with a known binding site within probes 2G and 2C was glucocorticoid receptor. The known binding site, demonstrated by *in vitro* foot-printing (Ray et al., 1990), occurs between bases –152 to –170. There is also a putative binding site from consensus sequence comparison between –179 and -184 (figure 5.5). However, transfection studies showed that glucocorticoids resulted in greater inhibition of transcription with the –174G rather than the C allele in HeLa cells, with resultant loss in the differential effects of the two alleles (see section 4.1.8). This would be against GR involvement in band C as the band was stronger for the C allele probe than the G allele probe. Functionally GR may have an important role in protein-protein interactions with NF-κB and C/EBP, or via competition for co-factors such as CBP, rather than direct DNA binding (see section 1.3.2.5). GR was therefore considered unlikely to be involved in production of band C with probes 2G and 2C.

The ubiquitously expressed transcription factor Sp1 has a putative binding site within the sequence of probes 2G and 2C between bases –150 and –154 (figure 5.5). In THP1 cells (human monocyte cell line) Sp1 has been shown to be involved in a complex of

factors binding to a region between –73 and –181 of the human IL-6 sequence (Sanceau et al., 1995, and see section 1.3.2.8). Sp1 is associated with constitutive activation of genes that bind this factor, although an additional regulatory role in induced levels of expression of such genes may occur via the binding of other Sp family members to an Sp1 site (Lania et al., 1997). Cold competition with an Sp1 consensus binding site sequence (see table 2.11) did not alter nuclear factors binding to the 2G or 2C probes.

Co-factors, such as CBP, may be involved via protein-protein interactions in the complex forming band C with probes 2G and 2C (see 5.2.2). These would be expected to bind in association with a DNA bound transcription factor with which they interact.

5.2.7. The –174 polymorphism does not alter transcription factor binding to the negative regulatory domain of IL-6

To investigate whether the –174 polymorphism altered any transcription factor binding to the up stream negative regulatory domain (NRD) of the IL-6 gene (from -164 to –225, see section 1.3.2.3), probes 3G and 3C were used (see figure 5.2). Probes 3G and 3C consisted of a 75bp sequence of IL-6 from –161 to –235, with a G or C allele at position –174, respectively (see table 2.10 for sequences). This sequence included a region between –201 and –210 known to bind GR (Ray et al., 1990). Probes were labelled by Klenow synthesis of a second-strand containing α^{-32}P-dCTP, from a single-strand template and primer sequence (see section 2.11.2.2 for method). EMSA studies were carried out with unstimulated and IL-1β-stimulated HeLa cell nuclear extracts of 10 and 300mM NaCl salt concentration.

With 10mM NaCl extracts, an IL-1 inducible band was seen with 30min to 2hrs IL-1β-stimulated extracts, but diminished by 3hrs (band J, figure 5.21). With 300mM NaCl extracts, two additional IL-1β-induced bands were seen (bands K and L, figure 5.22). Band L runs slightly higher than an equivalent band produced by the unstimulated extracts and could represent an additional transcription factor binding after IL-1β-stimulation to a complex present in the unstimulated conditions.

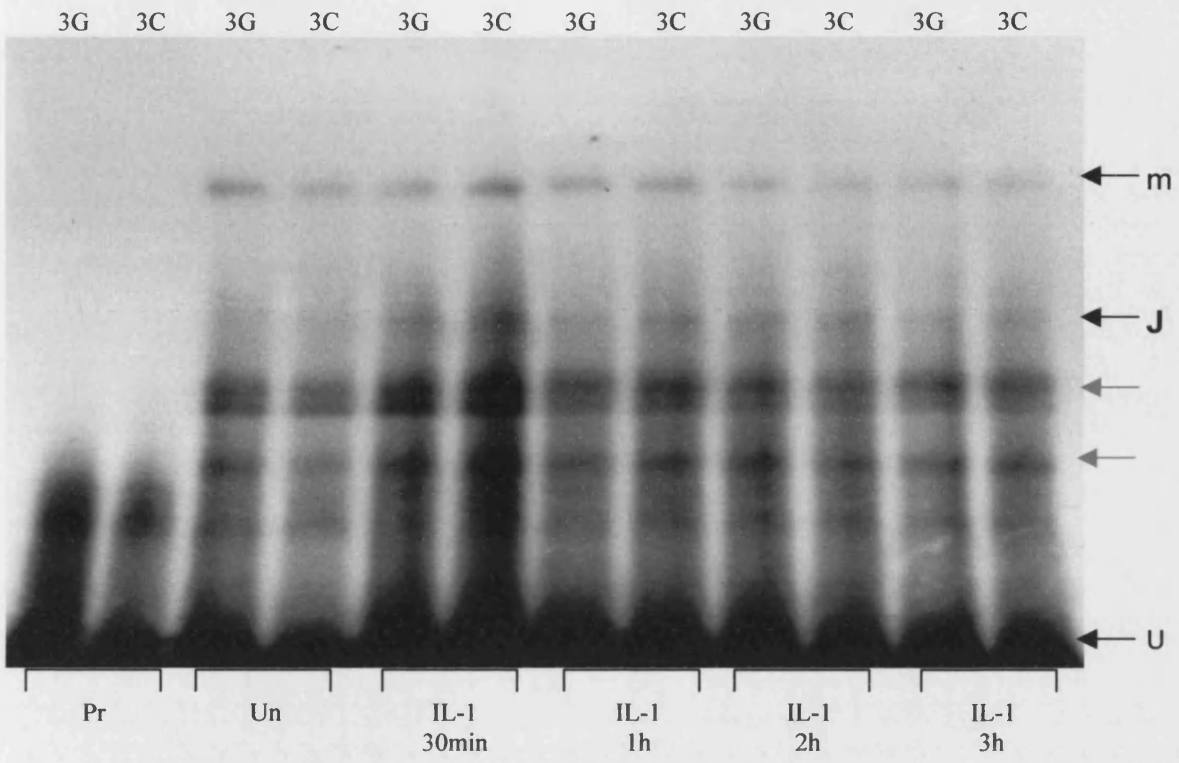

Figure 5.21. EMSA of IL-6 probes 3G and 3C incubated with unstimulated and increasing times of IL-1β-stimulated HeLa cell nuclear extracts (10mM NaCl).

5pmol radiolabelled 3G or 3C probe was incubated with 12μg of 10mM NaCl extracts pre-incubated with 10μg poly dI.dC and run on a 4% non-denaturing polyacrylamide gel at 4°C for 4.5hrs (see 2.11 for method).

Un= unstimulated extracts, IL-1= IL-1β-stimulated extracts for given length of time, Pr= probe only. m= non-specific band (could be competed out by 20μg polydI.dC). Unlabelled (grey) arrows indicate specific bands present in unstimulated and IL-1-stimulated extracts (could not be competed out by increasing concentrations of polydI.dC but could be competed out by increasing concentrations of unlabelled probe 3G or 3C). U= unbound probe.

A specific band J was produced with IL-1β-stimulated extracts 30min-2hrs and diminished by 3hrs, not present with unstimulated extracts. There was no difference between the G and C allele probes.

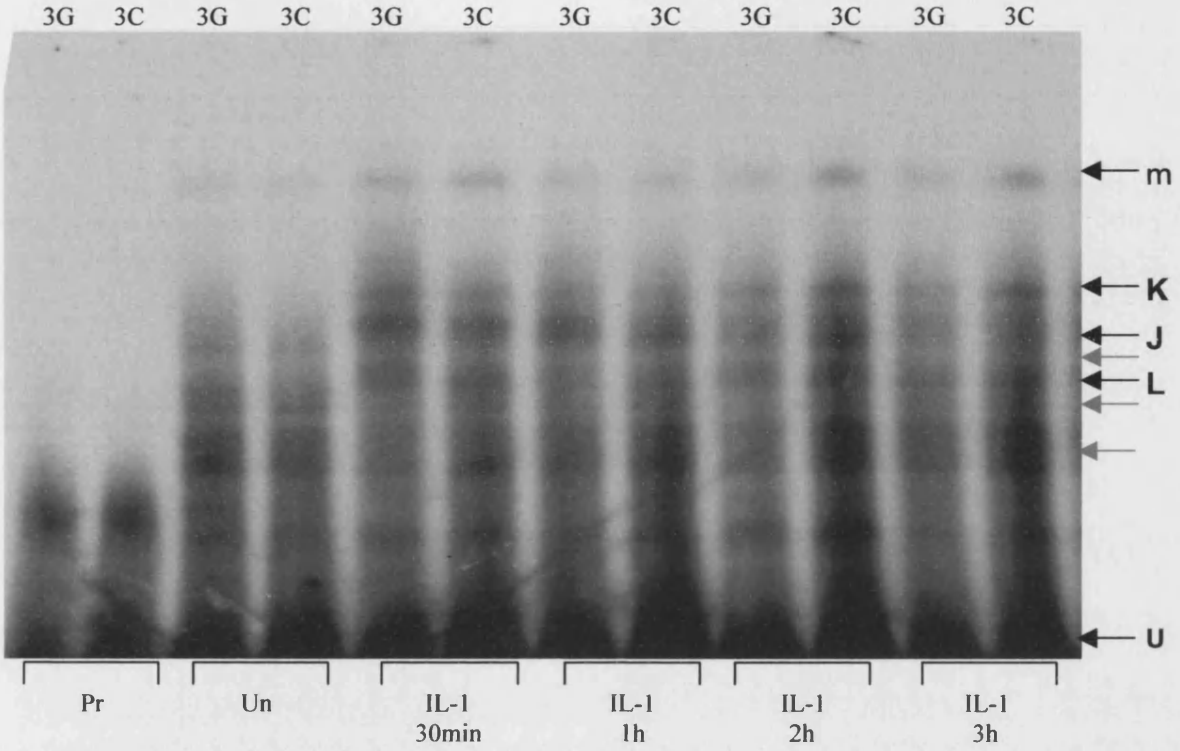

Figure 5.22. EMSA of IL-6 probes 3G and 3C incubated with unstimulated and increasing times of IL-1β-stimulated HeLa cell nuclear extracts (300mM NaCl).

5pmol radiolabelled 3G or 3C probe was incubated with 12μg of 300mM NaCl extracts pre-incubated with 10μg polydI.dC and run on a 4% non-denaturing polyacrylamide gel at 4°C for 4.5hrs (see 2.11 for method).

Un= unstimulated extracts, IL-1= IL-1β-stimulated extracts for given length of time, Pr= probe only. m= non-specific band (could be competed out by random probe). Unlabelled (grey) arrows indicate specific bands present in unstimulated extracts (could not be competed out by random probe but could be competed out by increasing concentrations of unlabelled probe). U= unbound probe.

Three specific bands J (same position as for 10mM extracts, figure 5.21), K and L (not seen with 10mM extracts) were produced with IL-1β-stimulated extracts (300mM NaCl). These bands were not seen in unstimulated extracts. Other specific bands present in the unstimulated extracts were not seen in the IL-1β-stimulated extracts. There was no difference between the G and C allele probes.

The upper most band 'm', seen with 10mM and 300mM NaCl extracts, was a non-specific band competed out by random probe (table 2.11). Specificity of the other bands was confirmed by non-competition with random probe and competition with increasing concentrations of unlabelled 3G or 3C probe. IL-1β-inducible bands J, K and L were seen from 30min to 3hrs of stimulation. There was no difference between the -174G and C allele probes.

Consensus binding sites for three known transcription factors occur within the sequence of probes 3G and 3C (figure 5.5). A GR binding site from –201 to –210 described by Ray et al., (1990), a GR consensus site GACACA from –179 to –184, an Sp1 consensus site CACGT from –198 to –202 and an NF1 consensus site TGGCA from –173 to –177 (with the –174C allele). Binding of these transcription factors was investigated by cold competition with specific transcription factor consensus sequences (table 2.11). There was no evidence that these factors bound to probe 3G or 3C as no competition was obtained with the consensus sequence probes for these factors (shown for the GR consensus probe, figure 5.23). Supershift studies with two anti-GR antibodies (table 2.12) did not produce any shift indicating that GR binding was unlikely to be present under these conditions with HeLa extracts. Glucocorticoid was present in the HeLa extracts and was reduced in IL-1β-stimulated extracts compared to unstimulated extracts as seen on Western blot analysis (figure 5.24).

The finding that IL-1β-inducible factors bind to a region of IL-6 that has previously been shown to be a negative regulatory domain, is of significant interest. As IL-1β induces IL-6 transcription, one might expect IL-1β stimulation to reduce rather than induce transcription factor binding in a negative regulatory region. The identity of these EMSA bands were not investigated further within the scope of this thesis as there was no observed differences between the -174G and C alleles to account for the functional allelic effects of this polymorphism seen in transfection studies (see chapter 4).

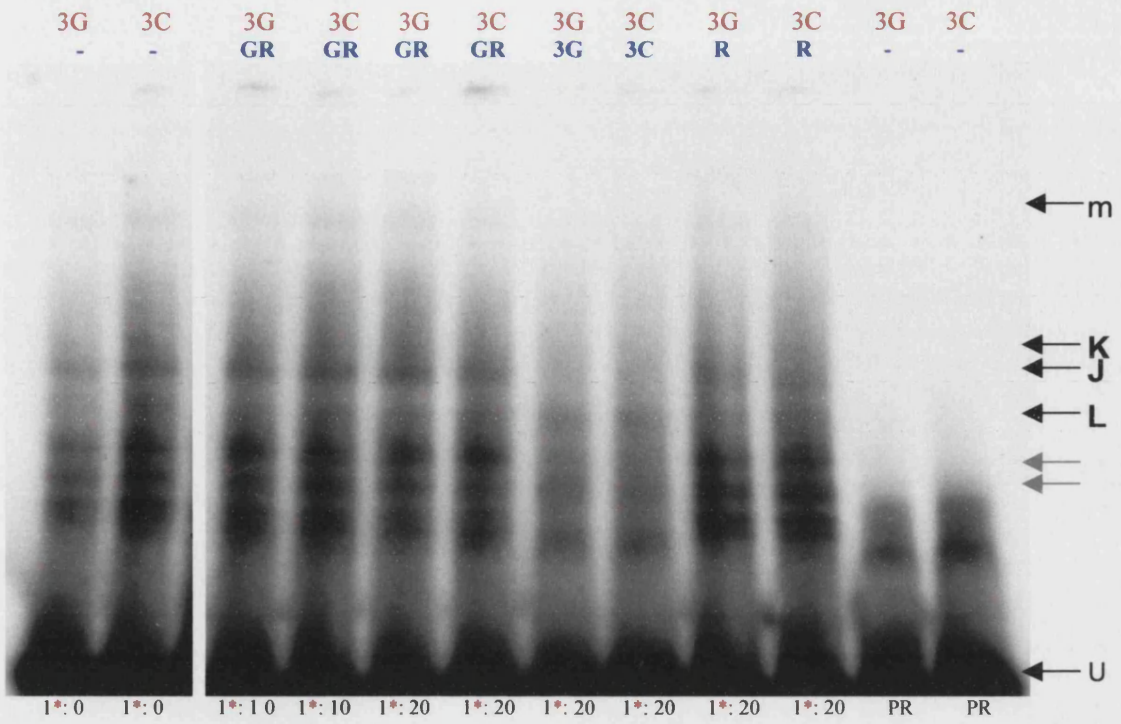

Figure 5.23. Cold competition with GR consensus sequence for IL-6 probes 3G and 3C incubated with 1hour IL-1β-stimulated HeLa cell nuclear extracts (300mM NaCl).

Radiolabelled probe* (5pmol) was mixed with the indicated ratio of unlabelled GR consensus sequence competitor (see table 2.11 for sequences), incubated with 10μg of 300mM NaCl HeLa extracts pre-incubated with polydI.dC (10μg), and run on a 4% non-denaturing polyacrylamide gel at 4°C for 4.5hrs (see 2.11 for method). Red lettering= radiolabelled probe, blue lettering= unlabelled competitor, the ratio of radiolabelled to unlabelled probe is indicated underneath each lane. GR=glucocorticoid receptor consensus sequence, R= random probe, U= unbound probe, Pr= probe only, m= non-specific upper band, unlabelled (grey) arrows indicate other specific lower bands present with unstimulated and IL-1-stimulated extracts.

None of the bands were competed out by GR consensus sequence or random probe.

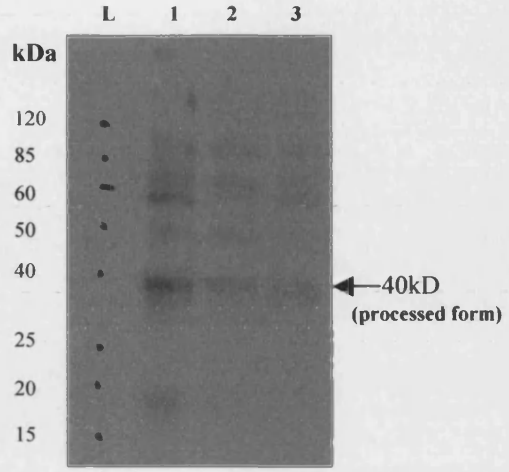

Figure 5.24. Western blot for GR in unstimulated and IL-1β-stimulated HeLa cell nuclear extracts.

5μg of HeLa cell nuclear extract was applied per lane. GR was detected using primary antibody Sc-1003 rabbit anti-GR polyclonal antibody (table 2.12), secondary antibody HRP-conjugated porcine anti-rabbit IgG polyclonal antibody (table 2.13) and chemiluminescent detection (see 2.12.3 for method).
Lane 1=unstimulated extracts (150mM NaCl), lane 2=30min IL-1β-stimulated extracts (150mM NaCl), lane 3=30min IL-1β-stimulated extracts (300mM NaCl), L=ladder of protein molecular weight markers (Benchmark, Gibco).◄ = protein band for GR (processed form) according to molecular weight. Upper bands probably represent unprocessed protein. Full size unprocessed GR=92kDa.

5.3. The effect of the –597 polymorphism on transcription factor binding

Although an independent functional effect was not attributed to the –597 polymorphism from transfection studies in HeLa or Huh7 cells, it was of interest to confirm this by investigating whether there were any differences in transcription factors binding around this polymorphic site with either allele. Double stranded probes of 75bp in length, from –539 to –613 of the IL-6 5'-flanking region sequence with either the G or the A allele at position –597, were generated by Klenow synthesis of a second-strand containing ^{32}P-dCTP from a single-strand template and primer sequence (see section 2.11.2.2). These were designated probes 4G and 4A respectively (see figure 5.25 for sequence). The allele at position –572 was kept constant at G for both probes. The probes were used in EMSA studies with unstimulated and IL-1β-stimulated HeLa nuclear extracts to compare transcription factor binding between the alleles. Conditions were as previously for probes 2 and 3 (see methods section 2.11).

```
                    A
5′-GCACGAAATTTGAGGGTGGCCAGGCAGTTCTACAACAGCCGCTCACAGGGA...
3′-CGTGCTTTAAACTCCCACCGGTCCGTCAAGATGTTGTCGGCGAGTGTCCCT...
                    G
                                                ...GAGCCAGAACACAGAAGAAC-3′
                                                ...CTCGGTCTTGTGTCTTCTTG-5′
```

Figure 5.25. Sequence and putative GR binding site for IL-6 probes 4G and 4A.
The site of the –597 polymorphism is indicated in red. The site of the –572 polymorphism is shown in blue, this was kept constant at –572G. The putative glucocorticoid receptor binding site is indicated in green.

5.3.1. GR binds to a site on probes 4G and 4A

With 10, 150 and 300mM NaCl HeLa nuclear extracts there were no differences in EMSA banding pattern between the –597G and A allele probes, for unstimulated and IL-1β-stimulated extracts (shown for 150mM NaCl extracts in figure 5.26). Several specific bands were seen to occur (bands N, O, P and Q). Probes 4G and 4A contain a putative GR-binding site from –552 to –557 (figure 5.25). Although none of the bands were seen to compete out with 20 times cold GR-consensus sequence (see table 2.11 for sequence), a supershift was obtained with two anti-GR antibodies to form band S (figure 5.27). The supershift indicates that GR binds to this region of the IL-6 sequence, probably at the putative GR site.

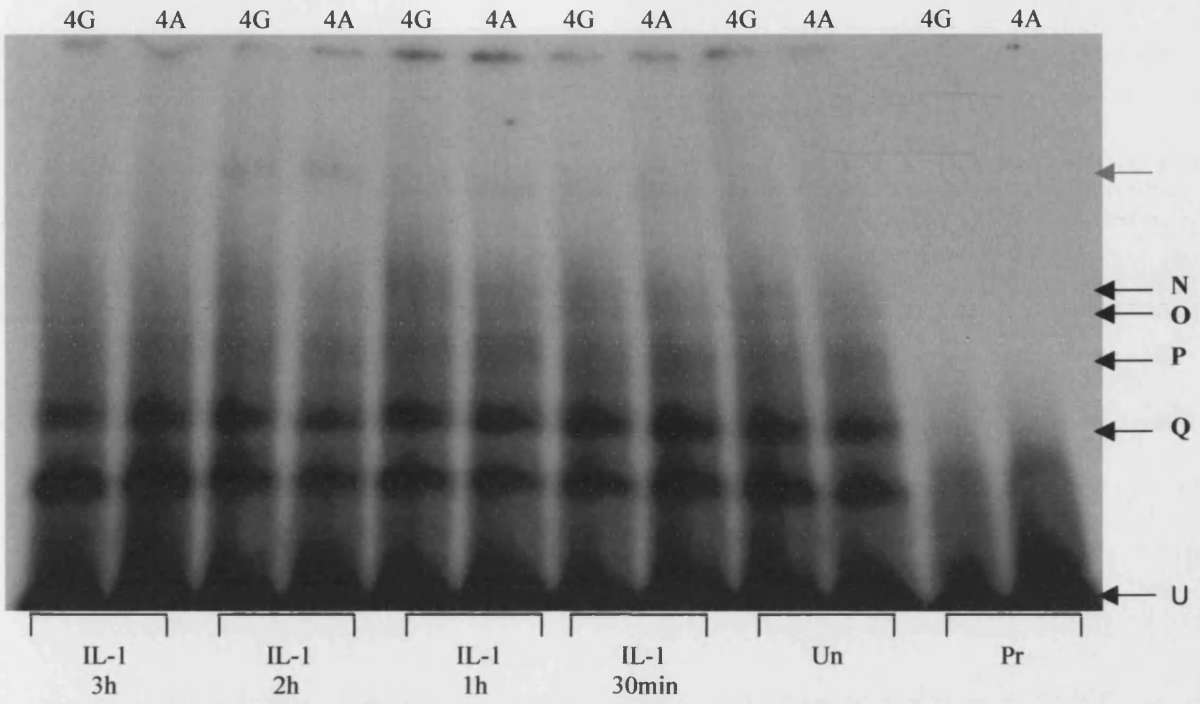

Figure 5.26. EMSA of IL-6 probes 4G and 4A incubated with unstimulated and increasing times of IL-1β-stimulated HeLa cell nuclear extracts.

5pmol radiolabelled 4G or 4A probe was incubated with 10μg of 150mM NaCl extracts pre-incubated with 10μg polydI.dC and run on a 4% non-denaturing polyacrylamide gel at 4°C for 4hrs (see 2.11 for method).

Un= unstimulated extracts, IL-1= IL-1β-stimulated extracts for given length of time, Pr= probe only. Black arrows (bands N, O, P, Q) = specific bands present in unstimulated and IL-1β-stimulated extracts (could not be competed out by random probe but could be competed by unlabelled probe 4G or 4A), the grey arrow indicates a non-specific upper band (could be competed out by random probe). U= unbound probe.

There was no difference in the EMSA banding pattern obtained for unstimulated or IL-1β-stimulated extracts with the –597G or A allele.

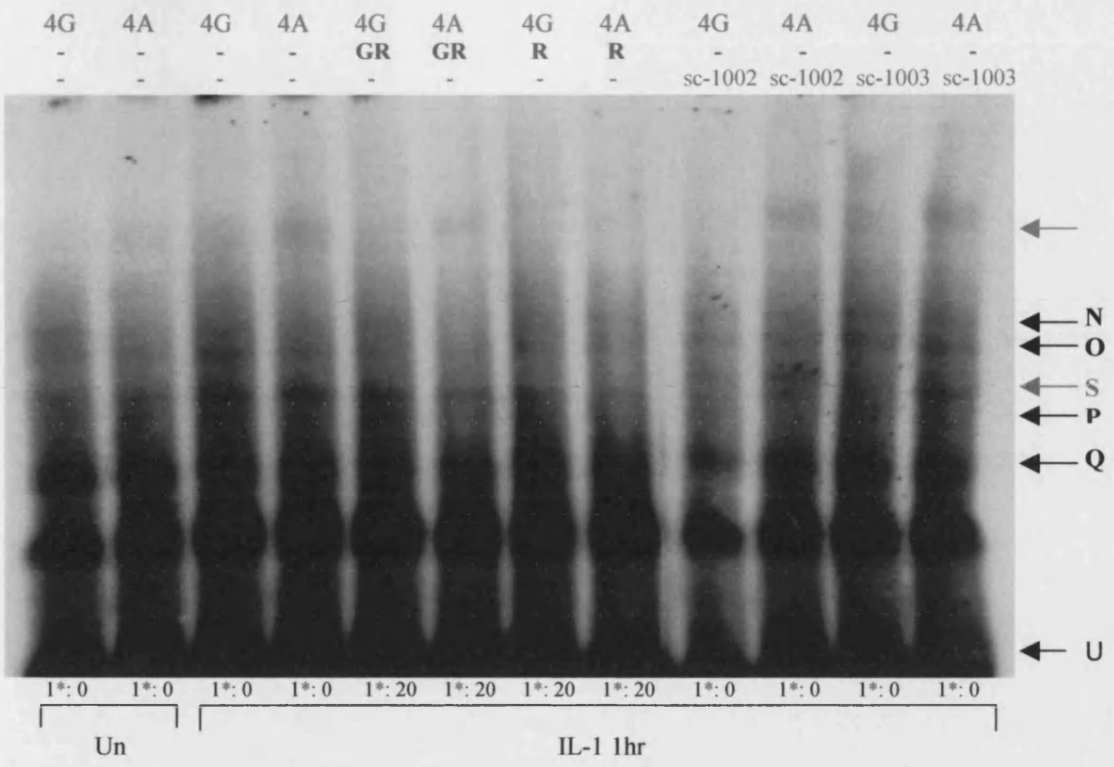

Figure 5.27. Supershift EMSA of IL-6 probes 4G and 4A with antibody to GR.

Radiolabelled probe* (5pmol) was incubated with 10μg of 1hr IL-1β-stimulated HeLa cell nuclear extracts (300mM NaCl), pre-incubated with polydI.dC (10μg). 3μl of anti-GR antibody sc-1002 or sc1003 (300ng/μl, see table 2.12) was added *before* radiolabelled probe and incubated at 21°C for 20min (see methods 2.11). For cold competition, unlabelled competitor probe was mixed with radiolabelled probe in the ratio indicated underneath each lane. Reactions were run on a 4% non-denaturing polyacrylamide gel at 4°C for 4hrs.

Red lettering= radiolabelled probe, blue lettering= unlabelled competitor, green lettering= specific antibody added. GR= glucocorticoid consensus probe, R= random probe (see table 2.11), U= unbound probe, Un= unstimulated extracts, IL-1 1hr= 1 hour IL-1-stimulated extracts. Black arrows (bands N, O, P Q) = specific bands, the green arrow (band S) = the supershifted band with anti-GR antibody, the grey arrow= a non-specific band.

A band shift occurs with anti-GR antibody although no competition is seen with 20-fold GR consensus sequence.

The possible effect of the –572 polymorphism on transcription factor binding was not investigated within this thesis. Despite the functional effects of this polymorphism in HeLa cell transfection studies. The rarity of the –572C allele in the Caucasian healthy and systemic arthritis population means this polymorphism is less significant than the –174 polymorphism.

5.4. Summary of EMSA findings

The EMSA studies in this section show that a transcription factor or complex of factors bind more strongly to the –174C than –174G allele. This is probably a transcription factor complex containing an inhibitory factor reduced by IL-1β-stimulation. C/EBPβ seems to be involved in this complex, but not GR or CREB. No conclusion could be drawn as to whether NF1 was involved in the complex. CREB binding to the probe was demonstrated but did not appear to be influenced by the –174 polymorphism. An IL-1β-induced factor(s) binds to the region of the IL-6 gene between –161 and –235, previously considered a negatively regulatory domain. GR, Sp1 and NF1 binding to this region could not be demonstrated. GR binding was however demonstrated to the IL-6 gene in the region of the –597 polymorphism, probably at the putative binding site –552 to –557.

CHAPTER 6

GENERAL DISCUSSION

6.1. Genetic susceptibility to JIA

The calculated sibling relative risk of disease (λs) for juvenile idiopathic arthritis (JIA) based on 300 JIA sib-pairs from North America was high at 15 (Glass and Giannini, 1999 and see section 1.2.10). Although this indicates that there is likely to be a relatively strong genetic component to JIA, the value is affected by the frequency of the disease in the general population. In a relatively rare disease such as JIA, the prevalence in the general population will be low and so λs will be higher. The reverse is seen for common conditions that tend to have a small λs. Rheumatoid arthritis has been calculated to have a λs of 4.9 in a population from the UK (John et al., 1997), which may reflect the higher prevalence of rheumatoid arthritis than JIA in the general population, rather than a weaker genetic component. A study of 71 sib-pairs with JIA from North America has also supported a genetic component to JIA (Moroldo et al., 1997). A higher than expected degree of concordance was found between the onset sub-type of JIA in the sib-pairs, though age at onset differed by an average of 4.4 years. The genetic component of JIA, in this complex trait with distinct sub-types and different clinical phenotypes, is likely to be polygenic (Glass and Giannini, 1999). No one major gene effect is likely to account for the calculated degree of genetic component. Rather, several genes of low penetrance with allelic heterogeneity are likely to be involved. The association of the systemic arthritis form of JIA (SA) with the –174 polymorphism of the IL-6 gene is unique in that it is the only reported genetic association specific to the SA sub-type of JIA.

6.2. IL-6 genotyping methods

The genotyping methods used for this thesis were compared and validated within this study (see 3.2.1) and are discussed in section 3.2. Compared to the gold standard of automated sequencing, heteroduplex was the most accurate of the three techniques used at 100%, followed by restriction fragment length polymorphism (RFLP) and sequence specific oligonucleotide probing (SSOP) at 96-98%. However, heteroduplex was less efficient at generating results for samples than the other two methods because of problems obtaining PCR product that would anneal to the universal heteroduplex generators. A combination of techniques was therefore used for most samples to ensure the reliability of the genotype results obtained for each population. The techniques were chosen to be cost effective and allow relatively high sample throughput. An

alternative method of RFLP using restriction endonuclease *SfaN*1 was initially considered for determining the –174 genotype. This was tried with longer PCR products to include a down-stream *SfaN*1 site in the IL-6 5'-flanking region that would have acted as an internal control for efficiency of enzyme digestion. However, PCR products including this site were less reliably produced than shorter products, and the *SfaN*1 enzyme was more sensitive to salt combinations carried over from the PCR mix. *Nla*III was therefore used in preference. Resource limitations during this thesis prevented newer techniques such as automated sequencing and Taqman allelic discrimination assay from being used on a large scale. Technology has significantly advanced recently and these techniques are now more widely available. The cost of equipment and reagents has also come down in price.

6.3. Use of association studies for IL-6 polymorphisms in SA

IL-6 is a glycoprotein involved in adaptive immune responses to inflammatory stimuli. High serum and synovial fluid levels of IL-6 and its soluble receptor agonist IL-6R in children with SA, together with the fact that levels rise and fall in parallel with disease activity, implicates IL-6 in the pathogenesis of SA. In this thesis, the IL-6 gene was investigated as a candidate gene in SA using a case-control study design. One of three single nucleotide polymorphisms (SNPs), a G to C at position –174 in the 5'-flanking region of IL-6 was shown to be associated with SA but not with other sub-types of JIA (section 3.3.1). That is to say, the null hypothesis that there was no difference in the proportion of patients carrying the putative disease allele and controls carrying the allele was not met by the results obtained for the distribution of the –174 genotype, but was for the –572 and –597 polymorphisms. A case-control study such as this is useful in the identification of genes showing association with rare diseases when only a small number of patient samples are available for study. However, of key importance is that the disease and control sample populations have the same genetic background to avoid problems of stratification where population diversity rather than disease association may result in a detected difference in genotype or allelic distribution. To avoid the effects of population stratification, the patient and control groups were ethnically and geographically matched, as much as possible (discussed in section 3.1), though complete matching was not possible. Geographical matching was to the recruitment centre location, however, the main recruitment centres (London, Birmingham and Manchester) are tertiary referral centres and it is recognised that some patients were

referred from a wider geographical location. Where samples from blood donors were used as controls, only first time donors were used to avoid potential biases of recall of individuals with a specific blood group and to ensure no individuals were sampled twice.

An alternative method to detect disease association is the transmission disequilibrium test (TDT), a family-based study that over-comes the problem of potential population stratification inherent in case-control association studies. The TDT tests for association and linkage disequilibrium (Spielman and Ewens, 1996). This requires genotype information for the candidate gene in the affected individual and at least one parent. Differences between the observed number of allele transmissions from a heterozygous parent to an affected child is compared to the null hypothesis that there would be only a 50% chance of transmission of the allele to the child under Mendelian inheritance if there was no linkage or disease association. A larger sample size is required for TDT than for case-control association study to obtain the same degree of power (Lewis, 2002). For this reason, a TDT study was not initially conducted as not enough SA samples could have been recruited from the UK. Recent on going collaborative work of the laboratory of P. Woo has confirmed the association of the –174G allele of IL-6 with SA in a multi-centre, multinational TDT study of simplex and multiplex families (Ogilvie et al., in press). Using genotype data from UK, US and French family cohorts it was shown that there was a significant excess transmission of the –174G allele to children affected with SA ($p=0.041$), whereas there was no significant difference in the frequency of allele transmission for JIA as a whole. This is a feasible approach in a disease of early onset such as SA when most parents are still alive. The disadvantage of TDT is that information cannot be used when both parents are homozygous. This is minimised when the allele frequency approximates 50% as with the –174 polymorphism. An alternative family-base study in diseases where parental information is unlikely to be available, for example one that presents later in life, is using affected sib-pairs. This method compares allelic sharing between the pair, which would be expected to be 50% if there was no gene linkage or disease association. However, with a relatively rare condition such as SA, the number of affected sib-pairs is too small to allow for such a study. Other factors (genetic or environmental) may also contribute to the low incidence of SA in sib-pairs. In the North American

collection of sib-pairs, although there are 300 JIA sib-pairs, very few have the SA sub-type (Glass and Giannini, 1999).

A difference in allele transmission was not seen in the association study in this thesis but rather a difference in genotype distribution. In the TDT study the larger number of patients allowed detection of the over transmission of the G allele in affected children, whereas the case-control study detected under representation of non-G allele carriers (that is CC genotype individuals). This is explained by the C allele occurring in a lower frequency than the G allele, so smaller numbers are needed to detect a difference in the homozygote genotype frequency. Both studies confirm an association between carriage of the G allele and susceptibility to SA.

The significant difference between the –174 genotype distribution for SA cases and controls in the association study was interpreted as a lack of the CC genotype, assuming a dominant allelic effect. This was supported by the significant difference in G-allele versus non-G allele carriage between cases and controls ($p<0.05$) and by the later TDT study results. An alternative possible interpretation is that there is a heterozygote effect with a contribution from both alleles, given that the heterozygote frequency was increased, and both the CC and GG homozygote frequencies were reduced in the association study cases compared to controls (figure 3.4). These results could also have arisen out of methodological error although every precaution had been taken to try to minimise this. A genotyping error resulting in over-calling of the heterozygotes (for example, under-cutting by RFLP) could have occurred, although all cases were genotyped by at least two methods to ensure high levels of confidence in the genotyping results. A sampling problem resulting in population stratification of the cases recruited from across the UK could have occurred with ethnic and geographic diversity, though care was taken to minimise this in the matching of control groups. Misclassification of the cases or missed cases (mainly recruited from rheumatology centres where cases under general paediatricians may have been missed) could also have contributed to the differences seen.

It is surprising given the close allelic association of the –597 and –174 polymorphisms that no association was found between the –597 polymorphism and SA. In addition to the interpretation that the main disease allele was located at –174, it could have been

due to smaller numbers in the case group analysed for the –597 polymorphism. This could be explored further using family studies. The weaker allelic association of the –572 and –174 polymorphisms, despite the strong –174/–597 allelic association may indicate that –572 is an older polymorphism.

6.4. Other genetic associations with SA

A G to C polymorphism at position –173 in the 5'-flanking region of the macrophage migration inhibitory factor (MIF) was reported to be associated with the SA sub-type of JIA in a UK study of 117 patients with SA (Donn et al., 2001a). Subsequently, an extended study in 526 UK JIA patients found that the MIF polymorphism conferred increased susceptibility to JIA irrespective of the sub-type of disease (Donn et al., 2002). The MIF polymorphism appears to have functional association (De Benedetti et al., 2003). In SA, the –173C allele of MIF was associated with higher serum and synovial fluid levels of MIF, poorer response to glucocorticosteroid treatment, higher levels of joint inflammation and poorer functional scores.

A group from Japan has reported the association of the –1031C–863A haplotype of the TNFα gene and the –857T allele (alleles associated with higher TNFα production) with an increased susceptibility to the SA sub-type of JIA in a study of 111 Japanese patients with JIA compared to ethnically matched controls (Date et al., 1999). This association was stronger in the presence of the DRB1*0405 HLA gene, suggesting that the association may be due to linkage disequilibrium between the TNFα and HLA genes. Other SNPs of the TNFα and TNF receptor genes have not been found to be associated with JIA in Caucasian populations (Ozen et al., 2002, Zeggini et al., 2002a). However, TNFα haplotype studies of nine polymorphisms within the gene, has established linkage of the TNF locus to the oligoarticular form of JIA in Caucasians (Zeggini et al., 2002b). The same group has also reported on linkage of the HLA loci with oligoarticular JIA in Caucasians (Zeggini et al., 2002c). One explanation for the reported ethnic differences may be an association with HLA, and linkage disequilibrium between HLA and TNFα or other genes. An investigation of possible HLA associations with IL-6 was beyond the scope of this thesis because of the limited number of SA samples. However, this is currently being examined.

The major histocompatibility complex (MHC) loci have been one of the main areas of study of genetic associations with JIA and other autoimmune diseases. This is because of the importance of the context in which antigen is presented on these molecules to T lymphocytes. It has been hypothesised that autoimmune reactions may develop due to altered identification of antigens (self or foreign) depending on the context of presentation. Altered levels of cytokine production may then influence cellular responses triggered by activation of specific T cells. TDT studies have shown HLA allelic associations with oligoarticular JIA (Moroldo et al., 1998, Zeggini et al., 2002c), but few clear associations with SA have been identified (discussed in section 3.3.4). Results from studies have been confusing because of the different classifications of juvenile arthritis used, the different ethnic backgrounds analysed and the relatively small size of many studies. One UK study that tried to address these issues compared the frequency of distribution of HLA class II alleles and haplotypes in over 500 Caucasian JIA patients compared to Caucasian controls. They found HLA-DRB1*08 and 11 to be associated with an increased risk of JIA (Thomson et al., 2002). The increased association with DRB1*11 was seen in the SA, persistent and extended oligoarticular sub-types of JIA (see table 1.1 for classifications). Whereas, HLA-DRB1*08 was mainly associated with the persistent and extended oligoarticular, and rheumatoid factor negative polyarticular sub-types of JIA. HLA-DQA1*05 was associated with SA and persistent oligoarthritis, and haplotype association studies showed DRB1*11-DQA1*05-DQB1*03 to occur in higher frequency in SA, persistent and extended oligoarticular arthritis. HLA-DRB1*04 was associated with a reduced risk of JIA in all sub-types except SA, enthesitis-related arthritis and rheumatoid factor positive polyarthritis. This is of interest as the DRB1*04 allele is associated with susceptibility to adult rheumatoid arthritis (Balsa et al., 2001, Jawaheer et al., 2003). Possible associations are further complicated by reported findings that HLA allelic associations may have age-specific effects (Murray et al., 1999). For example, Murray and co-workers (1999) found associations of HLA A2, DR5, DR8 and DPB1*0201 with susceptibility to the oligoarticular form of JIA occurring in the early years of life (under three years of age), whereas the association tailed off after this age, with no increased susceptibility seen after the age of 10 years. HLA B27 and DR4 were associated with protection early in life, but with an increased risk of oligoarticular and polyarticular disease later in childhood. The study reporting an HLA DR4 association with susceptibility to the SA form of JIA in North American patients, though not

reproduced in studies of European patients (see section 3.3.4), found no association of DR4 with adult Still's disease, a disease of adulthood with clinically similar manifestations to the SA form of JIA (Miller et al., 1985).

A 3'-SNP in the transcription factor interferon regulatory factor-1 (IRF-1) has been associated with susceptibility to JIA, though not specific to any one sub-type (Donn et al., 2001b). Interestingly, this study of 417 Caucasian JIA patients (63 with the SA sub-type) showed no association of the –174 polymorphism of IL-6 with JIA, nor with the SA form of the disease. This apparently contradictory result could be explained by the lower power of the study for detecting a significant difference. This thesis has more SA patients, and a larger control population resulting in higher power to detect a potential difference in genotype frequency between the groups. The fact that the association found in this thesis has subsequently been confirmed by the multi-centre TDT study supports the findings that this is a true genetic association with SA. A number of other cytokine associations have been reported with other sub-types of JIA. McDowell et al. (1995) reported the first cytokine gene association with JIA. They found the –889T allele of the IL-1 gene to be associated with early-onset oligoarticular JIA with ocular complications. However, this was not supported by the study of Donn et al. (2002b). Vencovsky et al. (2001), have subsequently reported the association of a variable number tandem repeat (VNTR) polymorphism of the IL-1 gene with JIA and a prognostic association with development of the extended oligoarticular form. Crawley et al. (1999), showed that the –1082A–819T–592A haplotype of IL-10, which was demonstrated to be associated with lower IL-10 production, was associated with the extended oligoarthritis sub-type of JIA. All these case-control studies need replication in different populations by TDT analysis. However, cytokine genes clearly play an important role in the genetic susceptibility to JIA and in some cases to the disease course. The finding that an IL-6 polymorphism is associated with SA is an important contribution to building our understanding of factors influencing the development of SA. It is likely that the IL-6 genetic effect is modulated by other, yet unidentified genetic and environmental factors. Interaction between genes can be looked for by logistic regression analysis, modelling possible types of interlocus effects. This approach has been used in diabetes mellitus (Cordell et al., 2001) and in Crohn's disease (Mizra et al., 2003) to identify genetic interactions.

6.5. Environmental susceptibility to SA

A seasonal onset of SA in children has been reported in the Prairie region of Canada with peak incidence in the autumn and early spring (Feldman et al., 1996). No correlation with viral incidence was found, and across Canada overall there was no seasonal variation in onset of SA. It is possible that 'windows of susceptibility' associated with different HLA alleles are due to differing patterns of exposure to environmental factors at different ages. This could also explain the age effect that was found for the SA association with the IL-6 polymorphism. In this study, the hypothesis would be that an environmental trigger in a genetically susceptible individual could result in the expression of disease (Brown and Wordsworth, 1998). For example an IL-6 –174G allele carrier with a certain susceptible HLA allele, exposed at a certain age to an environmental pathogen such as a virus, could predispose the child to development of SA. The reaction to some viruses is known to be different at an early age. Epstein-Barr virus in early childhood is usually asymptomatic, though in later life it is associated with infectious mononucleosis (Chan et al., 2001). Similarly, primary varicella zoster virus infection in childhood is generally less severe than in adulthood (Hardy and Gershon, 1990). Virus infection of specific cells can influence levels of IL-6 and IL-6R expression (Janaswami et al., 1992, Tomeczkowski et al., 1997). Genes that affect the metabolism or eradication of an exogenous agent may contribute to the triggering of disease expression (Dooley and Hogan, 2003). IL-6 may influence host response to a pathogen or efficacy of clearance via induction of B-cell maturation, stimulation of antibody production (see section 1.2.1), influences on T-cell differentiation (see 1.2.2), macrophage differentiation and altered antigen presentation by dendritic cells (see 1.2.3). IL-6 may result in altered levels of inflammatory response via induction of the acute phase response (see section 1.2.6) and may result in perpetuation of inflammation by acting as a 'switch' between acute and chronic inflammation (discussed in section 1.2.8&9). IL-6 is one part of a network of pro- and anti-inflammatory cytokines that act in concert when triggered by an inflammatory stimulus. Functional allelic differences within these cytokine genes may alter the balance of cytokines and influence the extent of acute or chronic inflammatory response generated to a specific environmental trigger (as for example seen with the –376 polymorphism of TNFα and severity of malaria infection, see 1.3.3.2). Different genetic factors may be important later in life and in different parts of the World, dependent upon exposure to environmental triggers. It is certainly the case that some

complications of SA are distinct between Europe and North America. Secondary amyloidosis, a complication of deposition of the inflammatory protein serum amyloid A (SAA) in multiple organs resulting in impaired organ function, is rarely seen in patients with SA in the US compared to a higher incidence within European patients (at least until recent treatment developments controlled disease activity). Work from the laboratory of P. Woo has shown that development of secondary amyloidosis in UK Caucasian patients with SA was associated with a polymorphism of the SAA gene, the SAA2 α2 allele (Faulkes and Woo, 1997).

6.6. Severity versus susceptibility

In multifactorial diseases such as JIA, genetic effects may influence disease severity rather than susceptibility. Weyand and co-workers (1992) suggested HLA DRB1 genes influence disease severity in rheumatoid arthritis when they reported the association of distinct clinical features of disease in DRB1 positive individuals. More recently, a family-based study of IL-10 polymorphisms in Finnish patients with the inflammatory arthritis ankylosing spondylitis, found association of the IL-10 G4 microsatellite marker within the IL-10 promoter with poorer functional scores (corrected for duration of disease) but not with disease occurrence (Goedecke et al., 2003). This suggests that IL-10 promoter polymorphisms may influence disease severity in ankylosing spondylitis rather than susceptibility. This may also be a feature of certain HLA genotypes in the inflammatory bowel disease ulcerative colitis (Yamamoto-Furusho et al., 2003). In a study of Mexican patients, HLA DR15 was associated with extensive colitis rather than limited distal colitis. HLA DRB1*0103 was associated with requirement for surgical intervention to manage the colitis. In family-based studies of the psychiatric condition attention deficit hyperactive disorder in children, a dose dependent association has been described between the dopamine transporter gene DAT1 and severity of a subset of symptoms of the disorder, namely hyperactive-impulsive behaviour (Waldman et al., 1998).

We found that the association of the –174 polymorphism of the IL-6 gene with SA could be accounted for by patients with early onset disease (≤ 5 years of age), (section 3.3.2). In SA, early onset disease has been shown to be associated with poorer prognosis in terms of functional outcome and requirement for surgery (Modesto et al., 2001). Although this could be explained by longer duration of disease and

complications of inflammation during earlier stages of growth and development, it is also considered to represent disease that is more aggressive and harder to control with immunosuppressive therapy. This would suggest that IL-6 genetic effects might influence the severity of SA as well as the susceptibility. A gene dose effect was not seen with age of onset, only that lack of the –174G allele protected against development of SA in the early age group. It was beyond the scope of this thesis to investigate disease course, outcome and severity markers in association with the –174 polymorphism because of the heterogeneous nature of SA, small numbers of patients and differing lengths of disease duration. However, such a prospective study would help establish any role of IL-6 in severity and not just on susceptibility within the younger age group (as discussed above). It is of interest that in the TDT study, an age association with the younger onset patients was not found and that the association was strongest for older onset patients, > 5 years of age (Ogilvie et al., in press). This may be due to a numbers effect between the two studies as the case-control study had significantly more patients in the early age at onset group, where as the TDT study had more in the older age at onset group. Overall, it would suggest that the IL-6 polymorphism might not have true effect on age of onset of SA.

6.7. IL-6 haplotype associations

IL-6 haplotype frequencies were determined in this thesis for the UK Caucasian population, estimated from the determined genotype frequencies for each polymorphism using the EH linkage-utility programme (see section 3.6). These correlated closely with haplotype frequencies published since the undertaking of this work, by another group, based on a smaller Caucasian population study (Jordanides et al., 2000). Jordanides and co-workers confirmed linkage disequilibrium of –597G with –174G, and –597A with –174C, in 73 healthy, unrelated individuals from the West of Scotland. Four haplotypes of the 5'-flanking region polymorphisms –597, –572, –174 emerged in this population. GGG (frequency 0.514), AGC (frequency 0.432), GCG (frequency 0.041) and GGC (frequency 0.014), compared to frequency 0.524, 0.374, 0.070 and 0.018, respectively, found in our study. It should be noted that the numbering of the polymorphisms by Jordanides et al., (2000) is slightly different from that used in this thesis. They used another sequence of IL-6 (Ray et al., 1988) that though it has the same initiation site, differs by several bases from the sequence of Yasukawa et al., (1987) used in this thesis (and more generally adopted), (see section

1.3). Consequently what they describe as the –172 polymorphism is the same as the –174 polymorphism described in this thesis, their –570 is the same as our –572 and their –594 the same as the –597 polymorphism described here. The paper by Jordanides and co-workers (2000) also reported linkage disequilibrium of these 5'-haplotypes with three 3'-VNTRs of the IL-6 gene. The –597A–174C haplotype was found to be in allelic association with the 3'VNTR.3 allele, and the –597G–174G haplotype with the 3'VNTR.4 & 7 alleles. Interestingly, in a study of 63 African-American healthy individuals, the distribution of haplotype frequencies was significantly different from the findings in Caucasian populations (Osiri et al., 1999). Five probable haplotypes of the 5'-flanking region polymorphisms –597, -572 and –174 were reported GGG (frequency 0.841), GCG (frequency 0.095), AGC & AGG (frequency 0.024) and GGC (frequency 0.016). The GGG haplotype was present at much higher frequency, with AGC occurring in only 2.5% compared to over 40% in the Caucasian population. It would appear that the ancestral genotype is homozygous GGG, as a genotyping study in several primate species has revealed them all as GGG (Kelberman et al., submitted, personal communications). Although these studies are in small numbers and larger studies are required to confirm the different frequency of distribution of these haplotypes compared to the Caucasian population, it would suggest that there has been some evolutionary advantage in the African population to retaining the GGG haplotype, or advantage in the Caucasian population to acquiring the AGC haplotype. This suggests a functional influence of these haplotypes on IL-6 expression, which may alter for example the way certain infections are dealt with (discussed in 6.5). Indeed, the –174GG genotype has been associated with significantly improved survival in 50 German Caucasian intensive care patients who developed sepsis post-surgery (Schluter et al., 2002).

Despite the strong allelic association between the –174 and –597 polymorphisms in the normal population this association was significantly weaker in patients with SA (section 3.6.2). This suggests that the –174 polymorphism is the functionally significant polymorphism. The weak allelic association between –174 and –572 we found in this study has not been reported in the literature, probably because in smaller studies the power would be too low to detect the association. In our larger study, we also found that all haplotype combinations were seen in the Caucasian population

though the haplotypes ACC, AGG, ACG and GCC were extremely rare, occurring in <1% of individuals (section 3.6.3).

6.8. The AT-tract polymorphism of IL-6

The frequency of distribution of AT-tract polymorphisms between –373 and –392 of IL-6 was not determined within the scope of this project. Initial attempts to sequence this region using an Applied Biosystems (ABI) PRISM® polyacrylamide gel separation sequencer and Amersham Life Science dye termination detection kit (see 2.4.8.2), resulted in base detection slippage and consequently the number of sequential A-nucleotides and T-nucleotides could not be accurately determined. Subsequent advances in the technology of the dye terminator kits available (ABI PRISM® BigDyeT Terminators version 3.0 sequencing kit) and the software available to detect base spacing on an ABI PRISM® 3100 capillary sequencing machine, has allowed the AT-tract polymorphism to be accurately determined (Twine et al., 2003). A TDT study in 100 simplex families with SA as part of the on going work from this project has identified six AnTn alleles A8T12 (frequency 0.368), A9T11 (frequency 0.268), A10T11 (frequency 0.210), A10T10 (frequency 0.150), A9T12 & A11T9 (frequency <0.010). Strong allelic association was found between the –174 and AnTn tract loci ($p<10^{-10}$), with the –174C allele almost completely carried with the A8T12 allele (haplotype frequency 0.368), whereas the –174G allele was distributed between the AnTn alleles A9T11 (haplotype frequency 0.231), A10T11 (haplotype frequency 0.225) and A10T10 (haplotype frequency 0.119), (Twine et al., 2003). Other haplotype frequencies occurred at less than 3%. No association was found between either AnTn genotype or –174/AnTn haplotype and SA, indicating that the AT-tract does not play a significant role in SA disease association. We had previously reported the AnTn tract frequency in a combined sample of 57 controls and SA patients (Fishman et al., 1998). In that cohort, in all but one case the –174C allele was associated with the A8T12 tract, while the –174G allele was found in association with a variety of other AnTn alleles, the most common being A9T11, followed by A10T10 (see table 1.3). Two other studies, a study of 78 healthy Caucasian patients (Terry et al., 2000) and a study of 132 Caucasian patients undergoing coronary artery bypass grafting (Kelberman et al., submitted, personal communication), have confirmed A8T12 as the most frequently occurring AT-tract allele with a strong allelic association with the –174C allele.

6.9. Other disease associations with the –174 polymorphism of IL-6

The results of the genetic studies presented in this thesis indicate that the –174 polymorphism of IL-6 is important in the pathogenesis of SA. We were the first to report a disease association with the –174 polymorphism (Fishman et al., 1998). Subsequently, there have been many reports of associations of this same polymorphism with other diseases in which IL-6 is implicated in the disease pathogenesis (summarised in tables 6.1&2). In primary Sjögren's syndrome, an autoimmune condition primarily affecting exocrine glands and joints, differing –174 genotypes of IL-6 were associated with specific manifestations of the disease and altered plasma levels of IL-6 in 61 Finnish patients, although no association with susceptibility was found (Hulkkonen et al., 2001). In a similar way, the –174 polymorphism was found to be associated with specific disease manifestations in the multi-system autoimmune disease systemic lupus erythematosus in 211 German patients, the –174G allele being associated with discoid skin lesions and anti-histone antibodies (Schotte et al., 2001). In 163 Spanish patients with rheumatoid arthritis, the –174 genotype was associated with a significant difference in the mean age at disease onset, indicating a possible influence on severity, but was not associated with susceptibility (Pascual et al., 2000). In relation to the effects of IL-6 on bone metabolism, Lorentzon and co-workers (2000) showed that in 90 healthy Swedish Caucasian males in late puberty, individuals with the –174CC genotype had significantly higher bone mineral density (BMD) than –174GG individuals and the genotype predicted peak bone mass. In 434 healthy North American women, the –174CC genotype was associated with lower bone resorption and a lesser decrease in BMD in the older postmenopausal women (Ferrari et al., 2001). We also found the –174CC genotype to be associated with a higher BMD in healthy post-menopausal French women, however this difference was no longer significant after correction for body height (Garnero et al., 2002).

In 53 patients with type 1 diabetes mellitus the –174GG genotype was found to occur in significantly higher frequency than in normal controls (Jahromi et al., 2000). A study in patients with type 2 diabetes mellitus suggested that the –174CC genotype was associated with an increased insulin sensitivity (Fernandez-Real et al., 2000a).

Condition	Feature	Reference
Systemic arthritis sub-type of JIA	Susceptibility	Fishman et al., 1998, Ogilvie et al., in press
Sjögren's syndrome	Specific disease manifestations	Hulkkonen et al., 2001
Systemic lupus erythematosus	Specific disease manifestations	Schotte et al., 2001
Septicaemia (post-surgery)	Improved survival	Schulter et al., 2001
Rheumatoid arthritis	Severity	Pascual et al., 2000
Type 1 diabetes mellitus	Susceptibility	Jahromi et al., 2000
Healthy subjects	Atherosclerosis-associated lipid profile	Fernandez-Real et al, 2000b
Healthy men	Asymptomatic carotid artery atherosclerosis	Rauramaa et al., 2000
Healthy subjects	Higher IL-6 serum levels	Fishman et al., 1998
Peripheral artery occlusive disease	Susceptibility	Flex et al., 2002
Coronary artery disease	Longer hospital & ITU stay, higher serum IL-6 levels post bypass graft surgery	Burzotta et al., 2001
Bone marrow transplantation	Chronic graft versus host disease (recipient genotype)	Cavet et al., 2001

Table 6.1. IL-6 genotype studies that report association with –174G.
The pathogenesis of these conditions suggests that the –174G allele is associated with higher levels of IL-6 expression than –174C.

In healthy subjects, carriers of the –174G allele were found to have significantly higher levels of plasma triglycerides, very-low-density-lipoprotein and post-glucose load free fatty acids, a lipid profile associated with an increased risk of atherosclerosis (Fernandez-Real et al., 2000b). IL-6 mediated inflammation is implicated in the pathogenesis of atherosclerosis. The –174G allele of IL-6, in association with a functional stromelysin-1 promoter polymorphism, was found to be associated with asymptomatic carotid artery atherosclerosis, measured as intima-media thickening in 109 middle-aged, Finnish men (Rauramaa et al., 2000). The –174GG genotype showed a strong association with peripheral artery occlusive vascular disease in an Italian study of 84 patients (Flex et al., 2002). Antibodies to the 60kDa heat shock protein, associated with coronary heart disease and carotid atherosclerosis, were significantly lower in –174C allele carriers than in –174G carriers, in a Hungarian study of 176 healthy male blood donors (Veres et al., 2002). In 111 Italian patients undergoing elective coronary artery bypass graft surgery, the –174GG genotype was associated with significantly higher levels of IL-6, with longer hospitalisation and the need for

longer stays in the intensive care unit post-operatively than C-allele carriers (Burzotta et al., 2001). This contrasts with the findings of Brull and co-workers (2001) who reported increased IL-6 levels post coronary artery bypass graft surgery in association with the –174CC genotype compared to –174G allele carriers, in 127 UK Caucasian patients. It is difficult to explain these contradictory results, both groups showed no baseline differences pre-operatively and were not significantly different in terms of other factors potentially affecting IL-6 levels such as age, sex and smoking status (other possible associations are discussed more fully below). The same group reports higher plasma IL-6 concentrations in patients with small abdominal aortic aneurysms who were carriers of the –174C allele compared to –174 GG homozygotes, though this was not related to rate of aneurysm growth (Jones et al., 2001). They have also reported an association of the –174C allele with increased systolic blood pressure in healthy men and increased risk of coronary artery disease, not explained simply by blood pressure effects alone (Humphries et al., 2001). In an older patient age group with both men and women, they found no association of cardiovascular incident events (angina, myocardial infarction and cerebrovascular accident) with –174C, however this allele was associated with sub-clinical cardiovascular disease as detected on magnetic resonance imaging, with a higher acute phase response and plasma IL-6 levels (Jenny et al., 2002). Two further studies in cardiovascular disease have added to these conflicting results. A large study of 640 male patients from Northern Ireland and France showed a higher carriage frequency of the –174C allele with myocardial infarction compared to age-matched controls, indicating a susceptibility association (Georges et al., 2001). However, in the French population within this study, the –174C allele was associated with fewer stenosed coronary vessels, suggesting that the –174G allele may have an influence on extent of atherosclerosis. The authors suggest that these results are compatible with a lower IL-6 secretion in association with the –174C allele. A study of 498 patients from the West of Scotland found no association of cardiovascular risk with the –174 polymorphism in patients who were not on a lipid-lowering agent (Basso et al., 2002). However, patients treated with the lipid-lowering agent, pravastatin, had a significantly lower risk of coronary artery disease in association with the –174CC genotype compared to –174G allele carriers. They found no association between the –572 polymorphism and coronary heart disease. Higher baseline C-reactive protein levels, a heritable cardiovascular risk factor, were associated with the –174C allele in 588 members of 98 nuclear Caucasian UK families

(Vickers et al., 2002). The –174C allele of the donor IL-6 gene in 145 cadaveric renal allograft transplants was associated with an increased incidence and severity of acute rejection in the recipient (Marshall et al., 2001). In 80 sibling bone marrow transplants, chronic graft-versus-host disease was associated with recipient –174GG genotype (Cavet et al., 2001).

Condition	Feature	Reference
Healthy male	Higher bone mineral density*	Lorentzon et al., 2000
Postmenopausal women (osteoporosis)	Lower bone resorption, higher BMD* (protective factor)	Ferrari et al., 2001 Garnero et al., 2002
Type 2 diabetes mellitus	Increased insulin sensitivity* (protective factor)	Fernandez-Real et al., 2000a
Coronary artery disease	Higher serum IL-6 levels post bypass graft surgery	Brull et al., 2001
Small abdominal aortic aneurysms	Higher serum IL-6 levels	Jones et al., 2001
Healthy men	Increased systolic blood pressure, increase risk of coronary artery disease	Humphries et al., 2001
Older asymptomatic subjects	Sub-clinical cardiovascular disease, higher serum IL-6 levels	Jenny et al., 2002
Myocardial infarction	Susceptibility	Georges et al., 2001
Myocardial infarction	Fewer stenosed coronary arteries	Georges et al., 2001
Cardiovascular disease	Lower risk of coronary artery disease in those taking pravastatin	Basso et al., 2002
Renal transplantation	Increased rejection of transplant (donor genotype)	Marshall et al., 2001

Table 6.2. IL-6 genotype studies that report association with –174C.
The pathogenesis of conditions marked with * suggest that the –174G allele is associated with higher levels of IL-6 expression than –174C. The other studies suggest that the –174C allele is associated with higher levels of IL-6 expression than –174G.

This plethora of IL-6 disease association studies, many of which are yet to be corroborated in an independent population or family study, nevertheless indicates a likely functional effect of the –174 polymorphism. The nature of this effect is difficult to hypothesise from the association studies alone, as some diseases associated with the –174G allele or GG genotype such as SA, would suggest that this allele would be associated with higher IL-6 expression, whereas other studies, particularly in cardiovascular disease, would suggest that the –174C allele could be associated with higher IL-6 expression. IL-6 of course, does not operate in isolation but functions as part of the cytokine network. Interactions of other cytokines and influences on the balance of cytokines operating in different disease states are likely to influence

outcome. This needs to be taken into consideration, together with the effects of possible confounders such as disease treatments (for example, steroids) or environmental risk factors for disease. Such an effect is suggested by the results of the West of Scotland study where IL-6 genetic influences were only seen to be significant in patients receiving a lipid-lowering agent (Basso et al., 2002). In addition, the possible modulation of one genetic effect by other genetic influences, and linkage between genes must be considered. Some of these possible influences are discussed below.

6.10. Transfection techniques

Transfection studies were used as an *in vitro* system to investigate the functional significance of the IL-6 5'-flanking region polymorphisms, focusing particularly on the –174 alleles. Transient transfections were initially used, and have the advantage that the transfected plasmid remains circularised within the cell nucleus with minimal disruption to the regulatory sequence under investigation. Additionally, the plasmids are independent of potential influences of host genomic DNA regulatory regions. However, transfection efficiency will vary between experiments. This was controlled for by co-transfecting with β-galactosidase (β-gal) as an internal control. An alternative option that became available during this thesis would have been to use sea pansy renilla as a control reporter. This would have allowed assay of the luciferase reporter from the constructs and the renilla control on the same sample aliquots. The choice of promoter driving renilla expression would be important. The cytomegalovirus promoter and simian virus 40 promoter (driving renilla expression in control plasmids available from Promega) are known to be induced by IL-1β and TNFα (Ritter et al., 2000, Plaetinck et al., 1989). The β-gal reporter was available on a respiratory syncitial virus promoter that was tested in our study and found not to be sensitive to IL-1, IL-6 or TNFα stimulation. Stable transfections were subsequently used to confirm transient transfection findings with the plasmid construct integrated into the genomic DNA of the host cell. While this is considered to more closely represent the *in vivo* DNA packaging, the plasmid is linearised and the regulatory region under investigation could be disrupted, or host regulatory regions influence reporter gene expression. Any influences of this nature were minimised by using pooled stable clones for each construct, representing many randomly inserted reporter

constructs. Flanking sequences to target the reporter construct to a specific region of the genome can be used. However, although this will control for comparisons between constructs inserted in the same location, it will not prevent unpredictable host genomic influences on the regulatory region under investigation. The stable transfectants allowed a wider range of inducer and repressor effects on the IL-6 polymorphisms to be investigated. Only allelic and haplotype effects were investigated using the transfection studies, not genotypic effects.

6.11. Functional effects of IL-6 haplotypes

The influence of the –597, -572, -174 haplotype on levels of IL-6 transcription was compared using 1.17kb constructs transfected into the transformed epithelial cell line HeLa cells. The constructs had a constant A9T11 AT-tract allele that proved technically difficult to mutate to allow comparison of other AT-tract alleles (see discussion in section 4.1.1). The –597G–572G–174G haplotype construct produced significantly higher levels of IL-1-induced reporter expression than –597G–572C –174G or –597A–572G–174C, but not higher than –597A–572G–174G (section 4.1.6). This indicates that in the context of the most common naturally occurring haplotypes GGG and AGC, the –174G allele produced higher levels of IL-6 transcription than the –174C allele and that this was independent of the –597 or –572 allele. It also indicates that the –572G allele produced higher levels of transcription than the –572C allele as an independent effect. With TNFα induced expression, similar results were obtained with the –174G allele producing higher levels of IL-6 expression than –174C, in the context of the naturally occurring haplotypes (see section 4.2.2). These functional effects were however cell-specific. When compared in the transformed hepatoma cell line Huh7 cells, there was a trend towards a reverse in the order of transcriptional activity of the haplotype constructs in these cells compared to HeLa cells but it did not reach statistical significance ($p=0.06$, see section 4.1.7). See discussion in section 6.17.

6.12. Functional associations *in vivo*

The –174 allelic effect identified in the transfection studies in HeLa cells corresponds to *in vivo* genotype effects on plasma IL-6 levels measured in 102 healthy individuals (Fishman et al., 1998). IL-6 levels were measured first thing in the morning to avoid effects of diurnal variation (Seiler et al., 1995). Carriers of the –174G allele had approximately two fold higher levels of plasma IL-6 than non-carriers of the G allele

(Fishman et al., 1998). There was no allelic dose effect, that is, GG homozygotes had similar levels of plasma IL-6 to GC heterozygotes. These results would support a dominant role for the –174G allelic effect. What is different in the transfection studies however, is that the –174 allelic effect was only seen with acute phase stimulation (IL-1β and TNFα), but not constitutively. This contrasts with the *in vivo* study results, where care was taken in collecting the patient samples to obtain constitutive levels of plasma IL-6, and a genetic difference in this basal level of IL-6 expression was seen. This would imply that different or additional mechanisms influence levels of IL-6 expression constitutively *in vivo* than in the HeLa cell model. This may reflect a different cell type as the main producer of constitutive levels of IL-6 *in vivo* in health, which could include adipocytes. β-adrenergic stimulation of adipocytes is associated with increased plasma IL-6 concentrations (Mohamed-Ali et al., 2001). The *in vivo* samples were taken after an over-night fast and individuals may have had increased adrenergic stimulation secondary to sympathetic activation from fasting and then attending for a blood test, which may have meant that the IL-6 levels were induced, though not by the acute phase response. Preliminary results from transfecting the same IL-6 haplotype constructs as used in the HeLa cell studies into 3T3F442A cells, a human differentiated adipocyte cell line, has yielded results with IL-1 stimulation similar to those obtained in HeLa cells, that is, –174G was associated with higher levels of IL-6 expression than –174C (L Luong, personal communications).

Reports of the influence of the –174 genotype on serum IL-6 levels in disease states have differed. A study of IL-6 protein levels produced by *ex vivo* culture of peripheral blood mononuclear cells (PBMCs) from SA patients compared to controls, showed SA patients to have significantly higher unstimulated levels of IL-6 production (Pignatti et al., 2001). There was no difference in the levels of IL-10 produced. However there was significantly reduced inhibition of IL-6 production by IL-10. These effects were not associated with the –174 polymorphism of IL-6, though small numbers limited the power of the study to detect a possible association. The most confusing results have been from Burzotta and co-workers (2001) who found higher levels of IL-6 post coronary artery bypass grafting in –174GG individuals, and Brull and co-workers (2001) who found higher levels of IL-6 post coronary artery bypass grafting in –174CC individuals. The Brull et al. study found peak IL-6 levels at 6-hours post-operative with maximum genotyping effect at 12 hours. The Burzotta et al. study did

not measure levels before 24 hours post-operative and reported the peak at 24 hours, with maximum difference in genotypic effect at 48 hours. Though the stimulant to raised IL-6 expression was considered as surgical trauma, other factors will have been involved and may have differed between the two surgical centres. For example, surgical effects such as hypoxia associated with length of operation may have differed, need for peri-operative blood transfusion and use of cooling techniques. The plastic tubing of the bypass circulation creates an inflammatory response. Different anaesthetics, or exposure to different bacterial organisms, may all have influenced the mechanism of IL-6 induction and the predominant cell type producing it. Burzotta and co-workers included only those individuals undergoing operation between 8 and 10am to avoid effects of circadian variations of IL-6 levels. Brull and co-workers reported higher peak IL-6 levels post-operatively in –572C allele carriers than in –572GG individuals. The –572 genotype distribution was similar to previously reported frequencies in Caucasian population, but no information was available for the –572 genotype in the Burzotta et al. study as to whether this could have influenced IL-6 levels post-operatively, and no information was available from either study on the AT-tract or –597 genotype (see discussion below). The fact that the time of maximum genotypic differential effect on IL-6 levels was after the time of maximum IL-6 induction, could suggest that *in vivo* factors (possibly other cytokines) contributing to perpetuation of IL-6 induction are influenced by the allelic differences. It is clear that the *in vivo* situation is much more complicated than the *in vitro* transfection model. However, the HeLa cell results seem representative of the –174 polymorphic effect in health and in some pathophysiological conditions. To date the Brull et al. (2001) study is the only report of *in vivo* –572 genotypic associations with IL-6 levels.

6.13. Other *in vitro* evidence of functional effect

Transfection studies by another group published during the preparation of this thesis, compared IL-6 5'-flanking region haplotype effects on levels of transcription in HeLa cells and ECV304 cells, thought to be an endothelial cell line* (Terry et al., 2000). Although Terry et al. reported no significant differences in levels of transcription between haplotypes in HeLa cells, this apparent discrepancy with our results could be explained by methodological differences.

*It should be noted that ECV304 cells have been recalled by the European cell line repository for further analysis as extended phenotype analyses have suggested that they may be an epithelial cell line rather than an endothelial cell line as originally thought.

In our study, construct expression was compared at the time point of maximum IL-1-induced expression using luciferase-reporter constructs; this was 6 hours post-stimulation (see section 4.1.3 and figure 4.6). At 24hrs post-stimulation, we found only a small difference in the level of transcription between haplotypes. The later time-point of 24hrs was used by Terry et al. in their study based on a time-course carried out with the chloramphenicol acetyl transferase (CAT) reporter that has a longer half-life (~50hrs) than luciferase (~3hrs). However, it was the luciferase reporter constructs that they used in the comparative studies at time point 24hrs, not the CAT reporter constructs, and so they may have over-looked an earlier haplotype effect.

In ECV304 cells, Terry and co-workers (2000) found that the up-stream context of the –174 allele was important in determining allelic effect of IL-6 expression. In the context of the –597G–572G[A9T11] haplotype, the –174G allele was associated with significantly higher levels of reporter expression than the –174C allele when induced by IL-1. However, in the context of –597A–572G[A8T12] haplotype, the –174C allele was associated with higher levels of reporter expression than the –174G allele when unstimulated or induced by IL-1. The results of Terry et al. suggest a functional role for the –597 allele of IL-6 in combination with the –174 polymorphism, in ECV304 cells. We did not see this in HeLa cells, nor did the genotype studies in SA suggest a functional role for the –597 polymorphism. In HeLa and ECV304 cells, Terry et al., found no significant difference between levels of reporter expression with the –572G and C alleles in the context of the –597G[A10T10]–174G haplotype (assayed at the 24hr time-point).

6.14. The functional influence of the AT-tract

Short constructs of the 5'-flanking region of IL-6 (611bp) containing only the –174 polymorphism (either G or C allele) and the A8T12 polymorphism (the most common AT-tract allele) produced significantly higher levels of reporter expression with –174G than –174C when induced by IL-1β, but no difference in constitutive (non-induced) levels of expression (section 4.1.3). The AT-tract was kept constant between constructs to allow comparison of –174 allelic effect alone. However, while the –174C allele is in strong allelic association with A8T12, –174G rarely occur with this AT-tract allele (see discussion section 6.8). The –174G allele occurs most commonly with A9T11. A 611bp –174G-allele construct with the A9T11 AT-tract allele was compared to the

–174G/A8T12 construct (see section 4.1.5). The AT-tract polymorphism showed functional effects independent of the –174 polymorphism with –174G/A8T12 producing higher levels of expression than –174G/A9T11, both constitutively and with IL-1 induction. Levels of reporter expression were still significantly higher for the –174G/A9T11 construct when compared to the –174C/A8T12 construct with IL-1 induced, but not constitutive expression (data not shown).

Comparison of haplotype constructs differing by the AT-tract allele transfected into ECV304 cells showed that the more A-nucleotides in the AT-tract the lower the levels of associated IL-1-induced reporter expression (Terry et al., 2000). AT-tract allele A9T11 was associated with significantly higher levels of IL-1-induced expression than either A10T10 or A10T11 alleles in the context of the –597G–572G–174G haplotype. This is in agreement with the findings in our study of the AT-tract allelic effects on IL-6 transcription in HeLa cells, though we found these effects in unstimulated as well as IL-1-induced expression. Alterations in the tertiary DNA structure by the AT-tract may alter ease of strand opening and access for transcription (see section 1.3.3.3). Alternatively, variations in the helical structure resulting in bending of the DNA may produce steric hindrance or facilitation of transcription factor binding to adjacent regions of the DNA. Electrophoretic mobility shift assays would yield information as to whether any transcription factors bind at the AT-tract itself. The functional effects of the AT-tract alleles in transfection studies suggest significance, though in the context of SA, the genotype studies did not identify an association between AnTn or the –174/AnTn haplotype and disease. *In vivo* effects of the AT-tract polymorphisms on levels of IL-6 transcription have been investigated following coronary artery by-pass graft as a stimulus to IL-6 production (Kelberman et al., submitted, personal communications). They found significantly higher post-operative IL-6 levels in A9T11 homozygotes compared to A10T11 homozygotes, in the context of the –597GG–572GG–174GG genotype. This supports the *in vitro* reporter assay results for functional effects of the AT-tract polymorphism.

6.15. Information from deletion mutant studies

The use of deletion mutants of the 611bp 5'-flanking region constructs of IL-6, showed a functional effect on transcriptional activation for a region within –310 to –550 (section 4.1.4). This region included the AT-tract. The finding that even in the absence

of the AT-tract, the –174G allele produced higher levels of IL-1 induced reporter expression than the –174C allele confirmed an independent effect of the –174 polymorphism. The lower levels of expression with deletion of the region –310 to –550 may have been due to removal of the AT-tract with reduced strand accessibility to transcription. The only other known site within the deleted region is a putative GRE at –461 to –466 that if functional would be expected to repress IL-6 transcriptional activation rather than activate it. With deletion of the region –220 to –310 a further functional element of IL-6 transcription was removed (section 4.1.4). A region within this appeared to interact with the –174 polymorphism resulting in a differential reduction in the levels of reporter expression with the –174G allele compared to the C allele. Two binding sites have been identified within the deleted region both enhancing IL-6 transcription, an AP1 site at –277 to –283 mediating cAMP responsiveness (Dendorfer et al., 1994) and an IRF-1 site at position –254 to –267 shown in HeLa cells to up-regulated IL-6 expression in the co-presence of down-stream NF-κB (Faggioli et al., 1997). Either of these sites could be involved. A 3'UTR polymorphism in IRF-1 has been associated with susceptibility to JIA (Donn et al., 2001b). Although to date, no functional effect has been ascribed to this polymorphism, functional effects on levels of expression in transfection studies have been found with promoter region polymorphisms of the IRF-1 gene that may be in allelic association with the 3'UTR polymorphism (Saito et al., 2001). This could link a susceptibility factor for JIA with risk of developing the SA form of disease in IL-6 –174G carrying individuals, via the IRF-1 binding site in the IL-6 5'-flanking region. Alternatively, the co-activator CBP required for transcriptional activation by Fos-Jun complexes via the AP1 site may be available when the AP1 site is absent to bind co-operatively with GRE and allow increased repression of IL-6 transcription (see sections 1.3.2.4 & 5). Site-directed mutagenesis studies would allow these possibilities to be investigated further.

6.16. The influence of glucocorticoids on polymorphic effects

Dexamethasone has a differential inhibitory effect on the –174G and C alleles (see section 4.1.8). With the 611bp constructs, dexamethasone resulted in more inhibition of IL-1-induced transcription with the –174G allele than the –174C allele, though levels of transcription were not returned to unstimulated levels. With the 1.17kb haplotype constructs, a similar effect was seen. The –174G allele showed significant inhibition of IL-1-induced reporter expression in the presence of dexamethasone, in the

context of its common natural haplotype –597G–572G–174G, and in the context of –597A–572G–174G. In contrast, the –174C allele showed no significant inhibition of IL-1-induced transcription with dexamethasone in the context of its naturally occurring haplotype –597A–572G–174C. In fact, the differential allelic effect of the –174 G/C polymorphism with IL-1 stimulation was lost in the presence of dexamethasone inhibition. The mechanism underlying this effect could be due to influences on GRE binding to DNA, GRE co-factor competition, prevention of activating transcription factor binding or altered levels of NF-κB availability for binding. For example, the –174G allele may facilitate GRE binding compared to –174C. GRE may compete the transcriptional co-factor CBP that could be involved in differential up-regulation of the –174G allele with IL-1 stimulation compared to the –174C allele, via AP1, CREB or other enhancer sites. GRE may directly block transcription factor binding to DNA (for example, by steric hindrance of CREB binding at the overlapping GRE and CREB sites, -145 to –173) or indirectly by protein-to-protein interactions (for example, with Fos and Jun, or NF-κB), involved in up-regulation of the –174G allele compared to –174C. Alternatively, GRE could result in reduced availability of a transcriptional enhancer such as NF-κB, via indirect influences on release of the active form of protein (see section 1.3.2.1&5). Electrophoretic mobility shift assays and site-directed mutagenesis would help to differentiate these possibilities. It should be noted that ethanol was present in the medium for the dexamethasone studies, as it was required to dissolve the crystalline form of dexamethasone (Sigma). This form of the drug was used in preference to water-soluble dexamethasone (Sigma) that contained a high molar ratio of cyclodextrins to dexamethasone (>20-fold), with unpredictable cellular effects. Although ethanol has been reported to inhibit NF-κB activation, the concentrations reported to produce such inhibitory effects were of the order of 100-fold higher than the concentrations present in our studies (Mandrekar et al., 1999). The ethanol concentration was standardised in the medium of all comparative wells within the dexamethasone study and no inhibitory effect of ethanol alone at these levels was detected.

Interestingly, the effects of dexamethasone inhibition differed with the –174 allele in unstimulated compared to IL-1-stimulated transcription (see section 4.1.8). With unstimulated transcription, dexamethasone resulted in more inhibition of the –174C

allele compared to the –174G allele, and resulted in significantly higher levels of reporter expression with –174G than –174C. This can only be explained by a different inhibitory mechanism of dexamethasone acting under unstimulated compared to IL-1 stimulated conditions. It may be that effects are modulated via a different GRE site. Any of the mechanisms discussed above could be effective, however in the unstimulated situation, the –174C allele would favour GRE binding/inhibition. This suggests that a constitutively bound factor, binding more strongly to the –174C than G allele is likely to be involved, to convert the inhibitory mechanisms for GRE in favour of the –174C allele instead of G allele. Alternatively, an IL-1-induced factor could bind more strongly to the –174G allele to favour GRE binding with IL-1 exposure, however EMSA study results do not support this hypothesis (see discussion 6.23).

Dexamethasone inhibition of IL-1-induced expression of the –597G–572G–174G haplotype construct compared to –597G–572C–174G showed that only the –572G allele was significantly inhibited (see section 4.1.9). This is most likely due to facilitated GRE binding by the –572G allele at one of the adjacent GRE sites (position –461 to –466 & –552 to –557). EMSA studies within this thesis have confirmed GRE binding to the region –539 to –613 with the –572G allele, though comparison with the –572C allele have not been made (see section 5.3.1). Site-directed mutagenesis would allow identification of the binding site for GRE in this region. No effect of the –597 polymorphism was seen on dexamethasone inhibition nor on GRE binding in this region.

6.17. Cell-specific transcriptional effects

The results for the transient transfections in HeLa cells were confirmed in the stable transfections of these cells (see 4.2.1). In contrast, no significant differential effect of the –174 polymorphism was seen in Huh7 cells, for IL-1 stimulation or dexamethasone inhibition (section 4.1.7&8). IL-1-induced transcription of IL-6 was not inhibited by dexamethasone in Huh7 cells. This cell-specific difference is unlikely to be due to insensitivity of Huh7 cells to dexamethasone as mRNA levels of the acute phase protein serum amyloid A have been shown to be up regulated by dexamethasone in Huh7 cells (Steel et al., 1996). It may therefore reflect differences in the mechanism of IL-1-induction of IL-6 transcription between the cell types, or differences in the mechanisms of glucocorticoid inhibition in Huh7 cells. In ECV304 cells, Terry et al.

(2000) found no difference in the effect of dexamethasone inhibition on the –174 or –572 alleles with IL-1-induced expression of IL-6, though IL-1-induction alone resulted in allelic differences in expression. They reported a small difference with the AT-tract polymorphism, in the context of the –597G–572G–174G haplotype. Dexamethasone inhibition of IL-1-induced expression of IL-6 was less for A9T11 than A10T11, though there was no difference between the two most common haplotypes –597A–572G[A8T12] –174C and –597G–572G[A9T11]–174G. These results support the case that cell-specific differences occur in regulation of IL-6 transcription. Such differences may explain the array of gene association results in different disease states (see 6.9), where the effects of IL-6 polymorphisms may vary dependent on the predominant cell-type involved in IL-6 production.

Cell-type differences in the expression and regulation of certain transcription factors, and isoforms of a transcription factor, influence levels of IL-6 transcription (discussed in section 1.3.2) and may therefore alter the –174 allelic effect. One such candidate transcription factor is C/EBPβ. NF-κB and CREB can up regulate the expression of C/EBPβ in hepatoma cells (Niehof et al., 2001a). Inflammatory stimuli, including cytokines, alter the nuclear localisation of C/EBP isoforms within hepatocytes, up regulating nuclear concentrations of C/EBPβ and δ and down regulating C/EBPα (Yin et al., 1996). Dexamethasone can induce C/EBPβ expression at the level of transcription in hepatocytes and increase C/EBPβ DNA-binding activity (Matsuno et al., 1996). In addition, the ratio of the activating to the repressor isoforms of C/EBPβ (LAP to LIP, see section 1.3.2.2) may vary with inflammatory stimuli and between cell types. In HepG2 (hepatoma) cells, the albumin promoter can be activated by C/EBPβ. However, in HeLa or L (fibroblastic) cells, C/EBPβ activation of the promoter was inhibited, dependent on the presence of the repressor region of C/EBPβ (Williams et al., 1995). All of these mechanisms could influence cell-specific activation of IL-6 transcription via C/EBPβ. If C/EBPβ acts differentially with the –174 G and C allele, as suggested by the involvement of C/EBPβ in the differential binding of a protein complex to these alleles in EMSA studies (see section 5.2.5 & 6.27), then this could influence the level of induced transcription for each allele and determine cell-specific effects.

6.18. The effect of stripped FCS

Stripped FCS was used in comparing the dexamethasone effect to try to reduce any hormonal or glucocorticoid influences the cells were exposed to from the serum. Of interest, the use of activated charcoal and dextran to strip the FCS resulted in loss of the inhibiting effect of dexamethasone on IL-6 transcription, reduction of the IL-1 stimulatory effect, and loss of the –572 allelic effect on IL-1 induced reporter expression (see section 4.1.10). The loss of inhibition with dexamethasone may have been due to dextran remaining in the stripped medium, binding the dexamethasone and preventing its interaction with the cells. Similarly, if the –572 allelic differences were due to differential inhibition by glucocorticoids then this could have been lost if glucocorticoids were removed from the serum by the stripping of FCS. EMSA studies showed that GR does bind at a site adjacent to the –572 polymorphism (see sections 5.3.1 and 6.29), though possible influences of the –572 polymorphism on this binding were not investigated. The reduction in IL-1β-induced transcription of IL-6 with stripped FCS medium may also have been due to effects of residual dextran in the medium, possibly binding IL-1 and reducing bioavailability for cell stimulation. A fluorescence-activated cell sorter (FACS) was used to determine the percentage of cells carrying detectable levels of IL-1RI (the signalling molecule of the tri-molecular IL-1R complex) on HeLa cells and Huh7 cells after exposure to medium containing 2% FCS or stripped FCS (see section 2.10.7.2 for method). Both 2% FCS and stripped FCS significantly increased the proportion of HeLa and Huh7 cells expressing detectable levels of cell surface IL-1RI (data not shown). For HeLa cells this was maximal from 1-6 hours ($p<0.03$) and for Huh7 cells at 4-6 hours ($p\leq0.03$) post change of medium. This would explain the increased level of IL-6 expression following medium change alone and the later time to peak IL-6 expression with Huh7 cells. Overall levels of detectable IL-1RI expression on HeLa and Huh7 cells were low (6-8%) compared to B-cells or monocytes (75-80%). Neither IL-1 nor dexamethasone had any significant effect on the number of HeLa cells expressing IL-1R, however, consistent with reported findings in murine hepatocytes (Ito et al., 1999), the number of Huh7 cells expressing detectable levels of IL-1RI significantly increased with dexamethasone exposure ($p=0.046$). This provides a possible explanation as to why inhibition of IL-6 expression was not seen with dexamethasone in Huh7 cells. Increased IL-1 induction of IL-6 may have counteracted any inhibitory actions of dexamethasone on IL-6 expression. Overall the use of 2% FCS (unstripped) was

considered a better model for studying IL-6 transcription in HeLa and Huh7 cells. *In vivo* serum factors would be present.

6.19. What drives IL-6 expression in SA?

Since in several cell types no difference was seen between constitutive levels of IL-6 production with the –174 allele, it raises the question as to what may be inducing IL-6 in the pathogenesis of SA to result in the –174G allele association. We have already said that IL-1β and TNFα, the acute-phase inducers of IL-6 used in the transfection model, are not elevated pre-IL-6 levels rising in SA, in comparison to other inflammatory states (see section 1.2.10). Traditionally other cytokines have been considered. However, recent evidence suggests that regulators of cell cycle activity may be important. The cyclin-dependent kinase inhibitor p21 in synovial fibroblasts has been found to arrest cell growth in the G(0)/G(1) phase of the cell cycle (Perlman et al., 2003). Lack of p21 has been associated with significantly increased IL-6 expression (up to 100-fold higher) and enhanced activation of the transcription factor AP1. Perlman and co-workers found significantly lower levels of expression of p21 in synovial fibroblasts from the inflammatory synovium of rheumatoid arthritis compared to the synovium of the degenerate arthropathy osteoarthritis. This has not been investigated in the context of SA, nor in other cell types, however, it suggests a possible mechanism for differential expression of IL-6 that could be modified by the –174 allelic effects. It is also possible that more than one inducing factor is important and may vary between cell-type and stage of cell differentiation. In mouse mononuclear phagocytes, the stage of cellular differentiation has been shown to be important in determining the response to monocyte-macrophage colony-stimulating factor and hence the cell sensitivity to a secondary stimulus such as lipopolysaccharide to induce IL-6 expression (Kamdar et al., 1996).

6.20. Other factors that modulate genotypic effects

The genotypic effects of IL-6 are also subject to modulation by other factors. At the extremes of age, the effects of the –174 polymorphism appear to differ, and may be associated with a different spectrum of benefits versus disadvantage. In healthy, full term neonates born by normal vaginal delivery or elective caesarian section, the –174CC genotype was associated with higher IL-6 plasma levels taken at delivery and higher levels of in vitro production of IL-6 from cultured mononuclear cells (Kilpinen

et al., 2001). In a control group of healthy adults, no effect of the –174 polymorphism was found on *in vitro* or *in vivo* IL-6 levels. In contrast, another group found in a more elderly population that PBMCs from healthy adults of mean age 60 years produced lower levels of IL-6 in vitro with –174C-allele carriers compared to non-C-allele carriers (Olivieri et al., 2002). They found lower plasma IL-6 levels in association with –174C-allele carriage in males but not females, and found a significant under-representation of the –174GG genotype in centenarian males, but not females (Bonafe et al., 2001). This lead to the proposition that in men the –174GG genotype results in a disadvantage for longevity. Differential influences on IL-6 levels of varying levels of oestrogens and androgens with age could contribute to these effects (see section 1.3.2.6). Together, the results suggest that while the production of IL-6 is genetically controlled, the control may also be age and gender dependent. Although we found age-at-onset associated differences with IL-6 genotype in the SA patients, no associated differences were found with gender (section 3.3.3).

6.21. Electrophoretic mobility shift assay technique

EMSAs are a useful technique to compare transcription factor binding between sequences and investigate specific transcription factors that may bind to certain DNA sequences. However, there are limitations that must be taken into account. Only a limited length of DNA can be used as a probe. As a result, interactions may be missed of transcription factor sites over long distances of DNA, even 1000s of bases as for the immunoglobulin heavy chain gene (Lieberson et al., 1995). Once transcription factor binding has been established *in vitro*, this needs to be confirmed *in vivo*. For example the glucocorticoid receptor can bind *in vitro* without the presence of glucocorticoids, however *in vivo* it requires glucocorticoids to induce a conformational change and facilitate binding (Wilmann & Beato, 1986). The context and configuration of the DNA sequence, influenced by flanking DNA sequences, may be different *in vivo*. In a similar way, factors that could bind *in vivo* may not be found to bind *in vitro*. *In vitro*, the optimal conditions for each transcription factor to bind a DNA sequence may vary with different salt conditions and varying protein to DNA concentrations of the binding reaction. This will also influence the formation of non-specific bands. Similar factors apply when it comes to cold competition studies and antibody binding for supershift studies. Antibody binding is also dependent on the epitope to which they are raised and on whether this is exposed on the DNA-bound protein. The use of Trizma®

(Sigma) in the polyacrylamide gel and running buffers, as in this study, instead of Tris-base that has a lower salt concentration, may affect the running and clarity of the bands on electrophoresis and the degree of dissociation of protein from DNA. Some degradation of nuclear protein was seen on Western blot analysis. This probably reflects over-heating or mechanical sheer during the dounce homogenisation process (see method section 2.11.1), although this was carried out on ice. Up to 100 strokes were required to lyse the HeLa cell membranes, even with the additional use of Triton. This was more than normally utilised for other cell-types such as HepG2 cells. Use of chemical lysis with a short freeze-thaw step would be an alternative method of cell extract preparation that may have reduced this (Schreiber et al., 1989). Co-factors required for transcription factor binding and/or function may also be altered or lost by the preparation process or binding conditions. The identity of a bound factor can only be determined by cold competition and supershift assay if the nuclear factor can be hypothesised or is known to bind, and if antibodies are available to it. A factor may not be hypothesised to bind if it is part of a protein complex involved in protein-to-protein interactions rather than direct DNA binding. Once a transcription factor has been identified as binding to a sequence of DNA on EMSA, site-directed mutagenesis and/or foot-printing studies are required to determine the exact site of binding. Isolation and purification of the protein factor may be necessary to identify an unknown factor. Functional studies are then required with transfected protein and site-directed mutated constructs to confirm functional effects of the factor on the gene (discussed further in section 6.30).

EMSAs were used in this study to identify any differences in the pattern of transcription factor binding between the IL-6 single nucleotide variance –174G or C, and when a difference was detected to begin to identify factors involved, within the limitations of the technique.

6.22. Choice of EMSA probes

Probes were chosen to encompass the –174 allele with surrounding down-stream or up-stream, known and putative transcription factor binding sites. Probes of less than 100bp were chosen to avoid too many binding sites that would have given complex, multiple bands on EMSA and made interpretation more difficult. The shortest probe was 26bp (probes 1G and 1C, figure 5.2). This included the putative NF1 binding

sequence around the –174 allele and 10 bases on either side to allow one helical turn of the DNA to try to ensure correct orientation of the site. This principle was followed for the other probes; there were no less than 10 bases at the end of each probe from the sites of interest. Probes 2G & 2C were designed to include the CRE and C/EBPβ site downstream of –174 and probes 3G & 3C were designed to include the up-stream negative regulatory domain (figure 5.2). Probes 4G & 4A were used to investigate transcription factor binding around the –597 polymorphism and included 1 of the putative GRE sites.

The specific-activity of the labelled probes was compared by serial dilutions counted with a Geiger counter at a fixed distance, and run on an agarose gel. As far as could be determined, the probes used were of equal activity though this was a rather crude method of comparison. Had the facility been available, comparing the level of activity between the two allelic probes using a scintillation counter would have been more accurate.

6.23. Implications of EMSA findings

Probes 2G & 2C were identical apart from the allele at position –174. A nuclear protein (or protein complex) was found to bind more strongly to the –174C than G allele (see section 5.2.2). Not only was the band stronger with the C-allele, but also the C-allele could compete out the band at lower concentrations than the G-allele, whether added before or after the binding reaction. To account for the transfection results obtained in HeLa cells, this factor was hypothesised to have an inhibitory influence on IL-6 transcription, with a stronger residual influence on the –174C allele than G after partial removal of the effect following IL-1 stimulation.

It is also possible that despite HPLC purification and OD_{260} quantification of the oligonucleotide probes obtained from the manufacturer (see table 2.10) that the C-allele probe was at slightly higher concentration than the G-allele probe. The lyophilised oligonucleotides were dissolved in water and the concentration re-checked by OD_{260} and by serial dilutions on an agarose gel. This would not however have been sensitive enough to detect a difference in concentration of as little as 1-2% which may have been enough to account for a stronger band with the C-allele probe when radio-labelled and stronger cold competition. One way to check this would have been to

obtain re-synthesized probes and repeat the experiment. Alternatively, cold competition of the probes 2G and 2C with probes 1, 3 or longer probes covering the –174 region, could have been used to compare the effect on the bound complex.

6.24. NF1 consensus binding site

Members of the transcription factor family nuclear factor 1 (NF1) are expressed in HeLa cells, in fact NF1-C was initially purified from HeLa nuclear extracts (Santoro et al., 1988). Four NF1 proteins have been identified, NF1-A, -B, -C and -X. All four have been shown to bind to a common DNA sequence GCCAAT (Osada et al., 1999), however only NF1-A from rat origin has been shown to bind to the sequence TGGCA (Paonessa et al., 1988). The TGGCA sequence is present with the –174C allele of IL-6, though it is not established whether NF1-A from human cells or other members of the NF1 family will bind to this sequence. Members of the NF1 family have also been shown to bind a canonical DNA sequence NNTGGNNNNNNGCCAAN (Chodosh et al., 1988, Jones et al., 1987). This canonical binding sequence differs from the sequence of IL-6 between –171 and –186 by three bases for the –174G allele and by only two bases for the –174C allele (figure 5.6). It was hypothesised that NF1 may bind both alleles of IL-6 (by either of the NF1 consensus sequences) but with differing affinity, resulting in altered levels of transcription between the alleles. NF1 has been shown to act as a transcriptional repressor of some genes, human metallothionein IIA (Osada et al., 1997b) and rat hepatic aldehyde dehydrogenase 3 (Lindahl et al., 1999). However, it can act as a transcriptional activator of other genes, adenoviral RNA polymerase II (Jones et al., 1987) and rat α_{1b} adrenergic receptor (Gao et al., 1996). If NF1 bound preferentially to the –174C allele form of IL-6, in HeLa cells this could result in repression of IL-6 transcription and hence explain the lower levels of C allele expression in transfected HeLa cells. From the cold competition studies with either NF1 consensus sequence, the protein band was competed out from probes 2G & 2C, suggesting that NF1 may be involved in this complex (section 5.2.3). However, this was not confirmed by supershift studies with an antibody to NF1 and no definite conclusion could be drawn as to whether NF1 was involved. Availability of purified NF1 protein could have helped clarify whether this factor bound to probes 2G and 2C.

An alternative strategy was tried whereby two mutated sequences were generated of the NF1 consensus binding-site (NF1mut1 and NF1mut2, see table 2.11) so that NF1

would no longer bind (confirmed by EMSA, see figure 2.12). The probes were otherwise similar to the NF1 consensus 1 sequence probe. The mutated probes were used in cold competition studies with probes 2G & 2C. The theory was that if the factor competing for probe 2G & 2C binding was NF1, mutating this site should reduce competition. This was the case for NF1mut2, but not for NF1mut1 (data not shown). It was therefore not possible to clarify whether NF1 was involved in the complex binding to probes 2G and 2C. The mutation sequence of NF1mut1 may have introduced an artefact. To investigate the components of the protein binding complex on probes 2G and 2C, further studies with foot-printing and protein isolation would be necessary (see section 6.30).

6.25. Possible transcriptional co-factors in an IL-6 bound complex

The possible role of co-factors needs to be considered. Many transcription factors can associate with co-regulatory molecules that will influence their regulatory actions on transcription (Lemon and Tjian, 2000). Five classes of co-factors have been described in eukaryotes, with functions as diverse as the general co-regulatory factors involved in the RNA polymerase II transcriptional activity, factors that associate with sequence-specific transcription factors to alter DNA specificity or interaction with other transcription factors, and factors that alter chromatin structure. A transcriptional co-factor, common to transcription factors bound to the NF1 consensus, NF1mut1 and IL-6 2G & 2C probes would be an alternative explanation for the competition results obtained. There were no known transcription factor sites other than NF1 that were common to these probes (Sigscan analysis), so the transcription factors binding a co-factor may have differed. CBP is an example of a possible co-factor. This transcriptional co-factor is involved in protein-protein interactions with multiple transcription factors including CREB, c-Jun, Fos, GR, oestrogen receptor, TATA binding protein, transcription factor IIB and YY1 (Chan and La Thangue, 2001). CBP can act as a co-activator with these transcription factors by acting as a bridge between DNA-bound transcription factors and the basal transcription machinery, providing a 'scaffold' for complex formation or by modifying transcription factors and chromatin through acetylation. It is possible that CBP is involved in the transcription factor complex differentially bound to the IL-6 –174G & C probe, and that it is CBP that is competed out by its involvement in a transcription factor complex bound to the NF1 consensus and NF1mut1 probes. (The NF1 consensus and NF1mut1 probes have a

common YY1 site on Sigscan analysis, which the NF1mut2 probe does not). The possibility of CBP involvement in the IL-6 probe-protein complex was not explored in the context of this thesis, but remains to be investigated.

6.26. CREB binding to IL-6

CREB binding to the IL-6 gene between –134 to –184 was confirmed with supershift studies (section 5.2.4), although this binding was not altered by the identity of the –174 allele. Two supershift bands were produced which probably represents two forms of CREB bound to this region of the gene. Only the phosphorylated form of CREB will bind CBP, though dephosphorylated CREB will bind to the CRE. The two bands may represent the presence of phosphorylated and dephosphorylated CREB on the IL-6 sequence with the phosphorylated form associated with CBP, running more slowly through the gel. Alternatively, CREB may be associated with another factor such as c-Jun in one of the bands. The transcription factor c-Jun can form heterodimers with a variety of other transcription factors including ATF/CREB family members (Hai and Curran, 1991). The binding of c-Jun to CREB, results in altered DNA binding specificity. Western blot analysis did not test for the phosphorylation state of CREB, and the protein was denatured so associations would have been lost.

6.27. C/EBP binding to the –174G and C allele

Competition and supershift studies confirmed that C/EBPβ bound to the IL-6 gene between –134 and –184 and was involved in the differential binding of a protein complex to the –174G and C allele (section 5.2.5). Even with antibody concentrations that were expected to be in excess of the C/EBP protein concentration (up to 300ng/μl), the protein complex was not completely competed out. This, together with the transfection study results showing that the –174G was associated with higher levels of IL-6 expression than the –174C allele, though the EMSA band was bound more strongly with the –174C allele, makes it unlikely that C/EBPβ alone accounted for the EMSA band. It is more likely that C/EBPβ is involved either directly or in-directly in a complex of proteins binding to this region of the IL-6 gene. EMSA studies with site-directed mutagenesis of the C/EBP site in the IL-6 probes would help establish the role of C/EBP. DNA-bound C/EBPβ may stabilise the formation of the differentially bound protein complex rather than forming a direct component of the complex. Different

isoforms of C/EBP may bind the IL-6 probe in this region as heterodimers with C/EBPβ (see section 1.3.2.2 & 6.17). Supershift studies with anti-bodies to other isoforms of C/EBP may provide evidence to support this possibility. Alternatively, disruption of synergistic co-operation between C/EBPβ and NF-κB (see 1.3.2.2) by an inhibitory protein(s) bound differentially to the –174G and C alleles could explain the differential levels of expression seen in the HeLa cell transfection studies (section 4.1.3).

6.28. Factor binding to the negative regulatory domain

EMSA studies showed transcription factor binding to the negative regulatory domain (NRD) of IL-6 though these were not influenced by the –174 alleles (section 5.2.7). This region contains a known GR binding site, however GR binding was not demonstrated by cold competition or supershift studies. This may have been due to the EMSA conditions. *In vitro* foot-printing had previously demonstrated GR binding from –201 to –210 (Ray et al., 1990).

The EMSA studies showed that an IL-1-inducible factor bound within the NRD. The NRD contains an Sp1-consensus binding site between –198 and –202 (figure 5.5). The transcription factor Sp1 was initially identified in HeLa cells as an activator of *in vitro* transcription of the SV40 viral promoter binding to a repetitive GGGGCGGGGC sequence called the GC box (Dynan and Tjian, 1983). Two distinct regions of the Sp1 protein are responsible for DNA-binding specificity and affinity. It belongs to a subgroup of factors that are phosphorylated upon promoter sequence binding by a DNA-dependent protein kinase, Sp1 kinase (Jackson et al., 1990), therefore binding does not necessarily determine activity. In THP1 cells, Sp1 was found to be present in a protein-complex binding to a negative regulatory region between –73 to –181 of the IL-6 gene (see section 1.3.2.8). Cold competition studies were conducted for the Sp1 consensus sequence (see table 2.11) with the NRD IL-6 probes (3G and 3C) and HeLa cell nuclear extracts to investigate the possibility that Sp1 bound to this region of the IL-6 gene. No competition was observed (data not shown) and so it was considered unlikely that Sp1 was involved in the IL-1 inducible complexes bound to the NRD. It remains to be established what IL-1 inducible factor binds to this region.

6.29. The –597 G/A polymorphism

Consistent with the transfection studies in HeLa cells that showed no independent effect of the –597 allele on levels of IL-6 transcription, no differences were seen between transcription factor binding around this site with either allele (section 5.3).

GR binding to the IL-6 gene at a site between –539 and –613 was identified by supershift studies (section 5.3.1). This binding was not influenced by the allele at –597. GR binding was identified in the context of the –572G allele, the effect of the –572C allele was not investigated but it would be interesting to compare as this polymorphism showed independent functional effects on IL-6 transcription in transfection studies (see section 4.1.6). The –572C allele was associated with lower levels of IL-6 expression than the G allele. For differences in GR binding to explain the –572 allelic effect, the –572C allele would have to bind GR more strongly, or facilitate GR binding to a second site. The site of GR binding was not established in this study but could be determined by site-directed mutagenesis or foot-printing studies. It was presumed that this was most likely to be at one of the two putative GR binding sites (see figure 5.2). No other transcription factor sites are known for this region of the IL-6 gene, nor were consensus sequences identified using the Sigscan programme.

6.30. Alternatives to EMSA

Although EMSA studies can be useful in identifying transcription factor(s) that bind to DNA sequence motifs, the technique is limited when the possible identity of the factor(s) is wide, or novel. *In vitro* foot-printing studies could narrow-down the identity of the specific sequence and site where the factor(s) are bound. Purified protein of hypothesised factors could be used instead of cellular nuclear extracts. However, this has the disadvantage that co-operative binding, factor complexes and non-direct DNA binding will be missed. *In vitro* foot-printing is currently underway as on-going work in the laboratory of P. Woo. It should yield more information on the site of factors bound to the –174G and C sequences, which may provide information on the identity of the factor(s) and allow a shorter probe sequence to be used for isolation and purification of the factor(s). With a shorter DNA probe, this could be biotinylated and incubated with HeLa cell nuclear extracts under the same conditions as for the EMSA studies. Protein bound probe passed over strepdavidin-coated magnetic micro-beads would adhere. The probe bound transcription factors could be

cautiously eluted and if pure protein bands were identified in elution fractions (for example on a silver-stained gel), identification could be attempted by matrix-assisted laser desorption ionisation time-of-flight (MALDI TOF) mass spectrometry, which identifies proteins by peptide mass fingerprinting. This would be an adaptation of a method successfully used to isolate and identify BiP, an auto-antigen identified from rheumatoid arthritis patients (Corrigall et. al., 2001).

The results of *in vitro* studies must be interpreted in the context of functional studies. Transfection studies using constructs that have been manipulated by site-directed mutagenesis to abolish a transcription factor binding site thought to be important, would help support an '*in vivo*' role for that factor in a specific cell type. Alternatively, transfection into a cell line deficient in a certain transcription factor may yield information. However, alternative transcription mechanisms may over-come a deficiency if the factor is not essential, with many biological systems displaying redundancy. Re-introduction of the deficient factor by transfection of an expression plasmid may enable the role of the transcription factor to be identified. True *in vivo* studies using knockout animals deficient for a transcription factor are often difficult because many such mutations will be lethal due to the multiple functions of transcription factors on multiple genes, some of which may be essential. Developments in mouse 'knock-out' technology has meant that methods are available to flank a gene with a 'knock-out' sequence that can be induced to 'switch off' the gene expression after the birth or development of the animal, for example on exposure to an antibiotic. This could provide specific information *in vivo*.

6.31. Implications of the findings from this study

A number of novel findings arose from this thesis: The association of the –174 polymorphism but not the –572 or –597 polymorphism with SA; the independent functional effects of the –174 polymorphism in HeLa cells with IL-1β & TNFα induction and glucocorticoid inhibition; the functional effects of the –572 and AT-tract polymorphisms in HeLa cells; the differential binding of a transcription factor(s) to the –174 C & G alleles in HeLa cells; the binding of an IL-1β-induced transcription factor(s) to the NRD of the IL-6 gene; the binding of GR to a region adjacent to the –597 & –572 polymorphisms. These results indicate the importance of genetic influences on the regulation of IL-6 gene expression and that cell-specific differences

may result in different genetic effects in different cell types, possibly accounting for the different associations reported *in vivo*. In SA, carriage of the –174G allele may identify a poorer prognosis group who would warrant early aggressive immunosuppressive therapy. It is possible that this group would respond better to treatments aimed to reduce or inhibit IL-6 production or IL-6 effects. Glucocorticoid therapy may be more effective as the –174G allele was associated with increased sensitivity to glucocorticoid repression than the –174C allele. In addition, the –174G allele carriers, with associated higher levels of IL-6 production, may respond better to anti-IL-6 therapy with antibodies blocking IL-6 receptor binding and signalling. In –174CC genotype individuals, factors other than the regulation of IL-6 levels may play a more significant role. It is certainly evident that IL-6 is one of several multi-factorial genetic and environmental influences determining the susceptibility and out-comes of SA.

6.32. Future work

Now that it has been established that there is disease association with the –174 polymorphism of IL-6 and SA, and that this polymorphism has functionality, the down-stream effects need to be investigated. Paired plasma samples and peripheral blood mononuclear cells from patients before and after first-time treatment with glucocorticosteroids, or on stable immunosuppressive therapy during quiescent disease and at the time of disease activity flare, can be used to investigate *in vivo* genotypic effects on IL-6 mRNA and protein levels in association with disease. Similar paired samples from children during and after an acute phase response, secondary to for example an infection, or before and after glucocorticosteroid therapy for another indication (for example an acute asthma exacerbation) would allow comparison of genotype effects in a different population. A prospective study of clinical disease course, disease activity and responsiveness to therapy in association with genotype analysis could also yield information on the role of IL-6 in SA, although diverse ethnic and geographical back-grounds would be difficult to control for. In addition, prior standardised protocols for the classification of disease activity, ratings of improvement and remission, and therapeutic strategies used, would have to be established and verified.

In parallel, further investigations of *in vitro* functional effects of the IL-6 polymorphisms will yield more information on the mechanisms involved. Transfection studies in a wider range of cell types and in primary cell lines rather than transformed cell lines are planned. Synovial biopsies from children with SA would allow fibroblast-like synoviocytes to be isolated and used for transfection studies. Bone biopsies at the time of joint replacements would allow primary osteoblasts and osteoclasts to be isolated for use in transfection studies and may provide more insight into the role of IL-6 in osteoporosis. *In vitro* foot-printing studies, mutation studies and transcription factor isolation are underway to identify differentially bound transcription factor(s) around the –174G/C polymorphism (as discussed in section 6.30).

The ultimate test of whether IL-6 is involved in the pathogenesis of SA will be the use of anti-IL-6 treatments to control disease. In adults with rheumatoid arthritis where IL-6 is implicated down-stream of other inflammatory mediators in the production of synovial inflammation, recombinant human anti-IL-6 receptor monoclonal antibody (MRA), that inhibits the biological activity of IL-6, has produced significant improvement in disease activity scores and acute phase response (Choy et al., 2002, Nishimoto et al., 2002). In the first trial, 45 patients were randomised to a single dose of MRA or placebo and 5mg/kg of MRA produced significant improvement by 2-weeks post-treatment compared with placebo or lower treatment doses. In the second trial, 164 rheumatoid arthritis patients were randomised to placebo or MRA therapy every 4 weeks for 3 months. A dose of 8mg/kg of MRA produced a significant reduction in disease activity at 12-weeks compared to a dose of 4mg/kg or placebo. The drug was well tolerated. MRA has had encouraging results in two children with SA treated for 1 year in Japan (Yokota et al., 2002). Both boys, aged 6-7 years who had failed to respond to, and had complications from, other forms of treatment, improved with fortnightly MRA infusions (half-life of the antibody ~10days). Within 1 week of the initiation of treatment, the acute phase response and disease activity fell and remained suppressed for the 18 months of follow-up. In addition, over the year their functional ability improved, they grew 10cm in height, gained in bone mineral density and were able to reduce glucocorticosteroid therapy. Neither experienced any adverse reactions to treatment. A 23-year old patient with adult onset Still's disease (a condition very similar to the SA form of JIA and also thought to involve IL-6 in the pathogenesis) improved significantly in systemic and articular symptoms with MRA

treatment (Iwamoto et al., 2002). Controlled phase II trials are underway for MRA in Europe for children with SA.

6.33 Conclusion

IL-6 is involved in the pathogenesis of the systemic arthritis form of juvenile idiopathic arthritis. The 5'-flanking region polymorphism –174G of IL-6 is associated with disease. This polymorphism alters levels of IL-6 expression in a cell-specific manner and forms functional allelic associations with other IL-6 5'-flanking region polymorphisms. Transcription factor binding is altered by the –174 polymorphism and involves C/EBPβ. These advances in our understanding of the role of IL-6 in SA and the mechanisms of control of IL-6 transcription could lead to development of more effective and specific treatment for SA.

REFERENCES

Akashi M, Loussararian AH, Adelman DC, Saito M and Koeffler HP (1990). Role of lymphotoxin in expression of interleukin 6 in human fibroblasts. Stimulation and regulation. *J Clin Invest*, **85**, 121-9.

Akerblom IE, Slater EP, Beato M, Baxter JD and Mellon PL (1988). Negative regulation by glucocorticoids through interference with a cAMP responsive enhancer. *Science*, **241**, 350-3.

Akira S and Kishimoto T (1997). NF-IL6 and NF-kappa B in cytokine gene regulation. *Adv Immunol*, **65**, 1-46.

Akira S, Isshiki H, Sugita T, Tanabe O, Kinoshita S, Nishio Y, Nakajima T, Hirano T and Kishimoto T (1990). A nuclear factor for IL-6 expression (NF-IL6) is a member of a C/EBP family. *EMBO J*, **9**, 1897-1906.

Alam T, An MR and Papaconstantinou J (1992). Differential expression of three C/EBP isoforms in multiple tissues during the acute phase response. *J Biol Chem*, **267**, 5021-4.

Alonzi T, Fattori E, Lazzaro D, Costa P, Probert L, Kollias G, De Benedetti F, Poli V and Ciliberto G (1998). Interlekin-6 is required for the development of collagen-induced arthritis. *J Exp Med*, **187**, 461-8.

Anguita J, Rincón M, Samanta S, Barthold SW, Flavell RA and Fikrig E (1997). Borrelia burgdorferi-infected interleukin-6-deficient mice have decreased Th2 responses and increased lyme arthritis. *J Infect Dis*, **178**, 1512-5.

Anhuf D, Weissenbach M, Schmitz J, Sobota R, Hermanns HM, Radtke S, Linnemann S, Behrmann I, Heinrich PC and Schaper F (2000). Signal transduction of IL-6, leukemia-inhibitory factor, and oncostatin M: structural receptor requirements for signal attenuation. *J Immunol*, **165**, 2535-43.

Balsa A, Barrera P, Westhovens R, Alves H, Maenaut K, Pascual-Salcedo D, Cornelis F, Bardin T, Riente L, Radstake TR, de Almeida G, Lepage V, Stravopoulos C, Spaepen M, Lopes-Vaz A, Charron D, Martinez M, Prudhomme JF, Migliorini P, Fritz P and European Consortium on Rheumatoid Arthritis Families (ECRAF) (2001). Clinical and immunogenetic characteristics of European multicase rheumatoid arthritis families. *Ann Rheum Dis*, **60**, 573-6.

Balto K, Sasaki H and Stashenko P (2001). Interleukin-6 deficiency increases inflammatory bone destruction. *Infection and Immunity*, **69**, 744-50.

Bank U, Kupper B, Reinhold D, Hoffmann T and Ansorge S (1999). Evidence for a crucial role of neutrophil-derived serine proteases in the inactivation of interleukin-6 at sites of inflammation. *FEBS Lett*, **461**, 235-40.

Banks RE, Wicher JT, Thompson D and Bird HA (1998). Acute phase response. In *Oxford Textbook of Rheumatology*, Maddison PJ, Isenberg DA, Woo P and Glass DN, editors. Oxford Medical Publications, **2nd ed**, 623-31.

Basso F, Lowe GD, Rumley A, McMahon AD and Humphries SE (2002). Interleukin-6 – 174G>C polymorphism and risk of coronary heart disease in West of Scotland coronary prevention study (WOSCOPS). *Arterioscler Thromb Vasc Biol*, **22**, 599-604.

Baumann H and Gauldie J (1994). "The acute phase response". *Immunol Today*, **15**, 74-80.

Bazan JF (1990). Structural design and molecular evolution of a cytokine receptor superfamily. *Proc Natl Acad Sci (USA)*, **87**, 6934-8.

Bedford PA, Ansell BM, Hall PJ and Woo P (1992). Increased frequency of DR4 in systemic onset juvenile chronic arthritis. *Clin Exp Rheumatol*, **10**, 189-93.

Bell S, Matthews JR, Jaffray E and Hay RT (1996). I(kappa)B(gamma) inhibits DNA binding of NF-kappa B p50 homodimers by interacting with residues that contact DNA. *Mol Cell Biol*, **16**, 6477-85.

Berghe WV, Plaisance S, Boone E, De Bosscher K, Schmitz ML, Fiers W and Haegeman G (1998). P38 and extracellular signal-regulated kinase mitogen-activated protein kinase pathways are required for nuclear factor-κB p65 transactivation mediated by tumor necrosis factor. *J Biol Chem*, **273**, 3285-90.

Berkowitz B, Huang DB, Chen-Park FE, Sigler PB and Ghosh G (2002). The x-ray crystal structure of the NF-kappa B p50.p65 heterodimer bound to the interferon beta-kappa B site. *J Biol Chem*, **277**, 24694-700.

Betts JC, Cheshire JK, Akira S, Kishimoto T and Woo P (1993). The role of NF-kappa B and NF-IL6 transactivating factors in the synergistic activation of human serum amyloid A gene expression by interleukin-1 and interleukin-6. *J. Biol. Chem*, **268**, 25624-31.

Betts JC and Nabel GJ (1996). Differential regulation of NF-κB2 (p100) processing and control by amino-terminal sequences. *Mol Cell Biol*, **16**, 6363-71.

Birnboim HC and Doly J (1979). A rapid alkaline extraction procedure for screening recombinant plasmid DNA. *Nuc Acid Res*, **7**, 1513-23.

Bismar H, Diel I, Ziegler R and Pfeilschfter J (1995). Increased cytokine secretion by human bone marrow cells after menopause or discontinuation of estrogen replacement. *J Clin Endocrinol Metab*, **80**, 3351-5.

Bjorck P, Larsson S, Andang M, Ahrlund-Richter L and Paulie S (1998). IL-6 antisense oligonucleotides inhibit IgE production in IL-4 and anti-CD40-stimulated human B-lymphocytes. *Immunol Lett*, **61**, 1-5.

Blank V, Kourilsky P and Israel A (1991). Cytoplasmic retention, DNA binding and processing of the NFκB p50 precursor are controlled by a small region in its C terminus. *EMBO J*, **10**, 4159-67.

Bode JG, Nimmesgern A, Schmitz J, Schaper F, Schmitt M, Frisch W, Haussinger D, Heinrich PC and Graeve L (1999). LPS and TNFalpha induce SOCS3 mRNA and inhibit IL-6-induced activation of STAT3 in macrophages. *FEBS Lett*, **463**, 365-70.

Bonafe M, Olivieri F, Cavallone L, Giovagnetti S, Mayegiani F, Cardelli M, Pieri C, Marra M, Antonicelli R, Lisa R, Rizzo MR, Paolisso G, Monti D and Franceschi C (2001). A gender-dependent genetic predisposition to produce high levels of IL-6 is detrimental for longevity. *Eur J Immunol*, **31**, 2357-61.

Boulton TG, Zhong Z, Wen Z, Darnell JE, Stahl N and Yancopoulos GD (1995). STAT3 activation by cytokines utilizing gp130 and related transducers involves a secondary modification requiring an H7-sensitive kinase. *Proc Natl Acad Sci (USA)*, **92**, 6915-9.

Bowater RP, Aboulela F and Lilley DM (1994). Large-scale opening of A+T rich regions within super coiled DNA molecules is suppressed by salt. *Nuc Acid Res*, **22**, 2042-50.

Bowcock AM, Kidd JR, Lathrop M, Danshvar L, May LT, Ray A, Sehgal PB, Kidd KK and Cavallisforza LL (1988). The human "interferon-beta 2/hepatocyte stimulating factor/interleukin-6" gene: DNA polymorphism studies and localization to chromosome 7p21. *Genomics*, **3**, 8-16.

Bowcock AM, Ray A, Erlich H, Sehgal PB (1989). Rapid detection and sequencing of alleles in the 3'-flanking region of the interleukin 6 gene. *Nuc Acid Res*, **17**, 6855-64.

Brach MA, Cicco NA, Riedel D, Hirano T, Kishimoto T, Mertelsmann RH and Herrmann F (1990). Mechanisms of differential regulation of interleukin-6 mRNA accumulation by tumor necrosis factor alpha and lymphotoxin during monocytic differentiation. *FEBS Lett*, **263**, 349-54.

Brakenhoff JP, de Hon FD, Fontaine V, ten Boekel E, Schooltink H, Rose-John S, Heinrich PC, Content J and Aarden LA (1994). Development of a human interleukin-6 receptor antagonist. *J Biol Chem*, **269**, 86-93.

Bravo J, Staunton D, Heath JK and Jones Y (1998). Crystal structure of a cytokine-binding region of gp130. *EMBO J*, **17**, 1665-74.

Bronstein I, Fortin J, Stanley PE, Stewart GS and Kricka LJ (1994). Chemiluminescent and bioluminescent reporter gene assays. *Anal Biochem*, **219**, 169-81.

Brown MA and Wordsworth BP (1998). Genetic studies of common rheumatological diseases. *Br J Rheumatol*, **37**, 818-23.

Brown K, Park S, Kanno T, Franzoso G and Sibenlist U (1993). Mutual regulation of the transcriptional activator NFκB and its inhibitor, IκB-α. *Proc Natl Acad Sci (USA)*, **90**, 2532-6.

Brown AM, Linhoff MW, Stein B, Wright KL, Baldwin AS Jr, Basta PV and Ting JP (1994). Function of NF-kappa B/Rel binding sites in the major histocompatibility complex class II invariant chain promoter dependent on cell-specific binding of different NF-kappa B/Rel subunits. *Mol Cell Biol*, **14**, 2926-35.

Brown K, Gerstberger S, Carlson L, Franzoso G and Siebenlist U (1995). Control of I kappaB-alpha proteolysis by site-specific, signal induced phosphorylation. *Science*, **267**, 1485-8.

Brull DJ, Montgomery HE, Sanders J, Dhamrait S, Luong L, Rumley A, Lowe GD and Humphries SE (2001). Interleukin-6 gene –174g>c and –572g>c promoter polymorphisms are strong predictors of plasma interleukin-6 levels after coronary artery bypass surgery. *Arterioscler Thromb Vasc Biol*, **21**, 1458-63.

Buck M, Zhang L, Halasz NA, Hunter T and Chojkier M (2001). Nuclear export of phosphorylated C/EBPβ mediates the inhibition of albumin expression by TNFα. *EMBO J*, **20**, 6712-23.

Burzotta F, Iacoviello L, Di Castelnuovo A, Glieca G, Luciani N, Zamparelli R, Schiavello R, Donati MB, Maseri A, Possati G and Andreotti F (2001). Relation of the –174 G/C polymorphism of interleukin-6 to interleukin-6 plasma levels and to length of hospitalisation after surgical coronary revasculatization. *Am J Cardiol*, **88**, 1125-8.

Cao X, Cai R, Ju DW, Tao Q, Yu Y and Wang J (1998). Augmentation of hematopoiesis by fibroblast-mediated interleukin-6 gene therapy in mice with chemotherapy. *J Interferon Cytokine Res*, **18**, 227-33.

Cassidy JT, Levinson JE, Bass JC, Baum J, Brewer EJ Jr, Fink CW, Hanson V, Jacobs JC, Masi AT and Scaller JG (1986). A study of classification criteria for a diagnosis of juvenile rheumatoid arthritis. *Arthritis Rheum*, **29**, 274-81.

Cavet J, Dickinson AM, Norden J, Taylor PR, Jackson GH and Middleton PG (2001). Interferon-gamma and interleukin-6 gene polymorphisms associate with graft-versus-host disease in HLA-matched sibling bone marrow transplantation. *Blood*, **98**, 1594-600.

Chan HM and La Thangue NB (2001). p300/CBP proteins: HATs for transcriptional bridges and scaffolds. *J Cell Sci*, **114**, 2363-73.

Chan GC, Hess P, Meenakshi T, Carlstedt-Duke J, Gustafsson J-A and Payvar F (1991). Delayed secondary glucocorticoid response elements. *J Biol Chem*, **266**, 22634-44.

Chan KH, Tam JS, Peiris JS, Seto WH and Ng MH (2001). Epstein-Barr virus (EBV) infection in infancy. *J Clin Virol*, **21**, 57-62.

Chen X, Vinkemeier U, Zhao Y, Jeruzalmi D, Darnell JE and Kuriyan J (1998a). Crystal structure of a tyrosine phosphorylated STAT-1 dimer bound to DNA. *Cell*, **93**, 827-39.

Chen FE, Huang DB, Chen YQ and Ghosh G (1998b). Crystal structure of p50/p65 heterodimer of transcription factor NF-kappaB bound to DNA. *Nature*, **391**, 410-3.

Chen Y-Q, Ghosh S and Ghosh G (1998c). A novel DNA recognition mode by NFκB p65 homodimer. *Nat Struct Biol*, **5**, 67-73.

Chevalier S, Fourcin M, Robledo O, Wijdenes J, Pouplard-Barthelaix A and Gascan H (1996). Interleukin-6 family of cytokines induced activation of different functional sites expressed by gp130 transducing protein. *J Biol Chem*, **271**, 14764-72.

Chiao PJ, Miyamoto S and Verma IM (1994). Autoregulation of IκB-α activity. *Proc Natl Acad Sci (USA)*, **91**, 28-32.

Chodosh LA, Baldwin AS, Carthew RW and Sharp PA (1988). Human CCAAT-binding proteins have heterologous subunits. *Cell*, **53**, 11-24.

Chomarat P, Banchereau J, Davoust J and Palucka AK (2000). IL-6 switches the differentiation of monocytes from dendritic cells to macrophages. *Nature Immunology*, **1**, 510-4.

Chow D-C, He X-L, Snow AL, Rose-John S and Carcia KC (2001). Structure of an extracellular gp130 cytokine receptor signalling complex. *Science*, **291**, 2150-5.

Choy EH, Isenberg DA, Garrood T, Farrow S, Ioannou Y, Bird H, Cheung N, Williams B, Hazleman B, Price R, Yoshizaki K, Nishimoto N, Kishimoto T and Panayi GS (2002). Therapeutic benefit of blocking interleukin-6 activity with an anti-interleukin-6 receptor monoclonal antibody in rheumatoid arthritis: a randomised, double-blind, placebo-controlled, dose-escalation trial. *Arthritis Rheum*, **46**, 3143-50.

Chrivia JC, Kwok RP, Lamb N, Hagiwara M, Montminy MR and Goodman RH (1993). Phosphorylated CREB binds specifically to the nuclear protein CBP. *Nature*, **365**, 855-9.

Chung CT, Niemela SL and Miller RH (1989). One-step preparation of competent Escherichia coli: transformation and storage of bacterial cells in the same solution. *Proc Natl Acad Sci (USA)*, **86**, 2172-5.

Chung CD, Liao J, Liu B, Rao X, Jay P, Berta P and Shaui K (1997). Specific inhibition of Stat3 signal transduction by PIAS3. *Science*, **278**, 1803-5.

Cooper C, Johnson D, Roman C, Avitahl N, Tucker P and Calame K (1992). The C/EBP family of transcriptional activators is functionally important for Ig VH promoter activity in vivo and in vitro. *J Immunol*, **149**, 3225-31.

Cooper C, Henderson A, Artandi S, Avihahl N and Calame K (1995). Ig/EBP (C/EBPγ) is a transdominant negative inhibitor of C/EBP family of transcriptional activators. *Nucleic Acids Res*, **23**, 4371-7.

Cordell HJ, Todd JA, Hill NJ, Lord CJ, Lyons PA, Peterson LB, Wicker LS and Clayton DG (2001). Statistical modelling of interlocus interactions in a complex disease: rejection of the multiplicative model of epistasis in type I diabetes. *Genetics*, **158**, 357-67.

Corrigall VM, Bodman-Smith MD, Fife MS, Canas B, Myers LK, Wooley PH, Soh C, Staines NA, Pappin DJ, Berlo SE, van Eden W, van der Zee R, Lanchbury JS and Panayi GS (2001). The human endoplasmic reticulum molecular chaperone BiP is an autoantigen for rheumatoid arthritis and prevents the induction of experimental arthritis. *J Immunol*, **166**, 1492-8.

Crawley E, Kay R, Sillibourne J, Patel Pritash, Hutchinson I and Woo P (1999). Polymorphic haplotypes of the interleukin-10 5'-flanking region determine variable interleukin-10 transcription and are associated with particular phenotypes of juvenile rheumatoid arthritis. *Arthritis Rheum*, **42**, 1101-8.

Crilly A, Bartlett JM, White A, Stirling D, Capell H and Madhok R (2001). Investigation of novel polymorphisms within the 3' region of the IL-6 gene in patients with rheumatoid arthritis using genescan analysis. *Cytokine*, **13**, 109-12.

Date Y, Seki N, Kamizono S, Higuchi T, Hirata T, Miyata K, Ohkuni M, Tatsuzawa O, Yokota S, Joo K, Ueda K, Sasazuki T, Kimura A, Itoh K and Kato H (1999). Identification of a genetic risk factor for systemic juvenile rheumatoid arthritis in the 5'-flanking region of the TNFα gene and HLA genes. *Arthritis Rheum*, **42**, 2577-82.

Davies UM, Jones J, Reeve J, Camacho-Hubner C, Charlett A, Ansell BM, Preece MA and Woo PM (1997). Juvenile rheumatoid arthritis. Effects of disease activity and recombinant human growth hormone on insulin-like growth factor 1, insulin-like growth factor binding proteins 1 and 3, and osteocalcin. *Arthritis Rheum*, **40**, 332-40.

Day IN, Humphries SE, Richards S, Norton D and Reid M (1995). High-throughput genotyping using horizontal polyacrylamide gels with wells arranged for microplate array diagonal gel electrophoresis (MADGE). *Biotechniques*, **19**, 830-5.

De Benedetti F, Massa M, Robbioni P, Ravelli A, Burgio GR and Martini A (1991). Correlation of serum interleukin-6 levels with joint involvement and thrombocytosis in systemic juvenile rheumatoid arthritis. *Arthritis Rheum*, **34**, 1158-63.

De Benedetti F, Robbioni P, Massa M, Viola S, Albabi S and Martini A (1992). Serum interluekin-6 levels and joint involvement in polyarticular and pauciarticular juvenile chronic arthritis. *Clin Exp Rheumatol*, **10**, 493-8.

De Benedetti F, Massa M, Pignatti P, Albani S, Novick D and Martini A (1994). Serum soluble IL-6 receptor and IL-6/soluble receptor complex in systemic juvenile rheumatoid arthritis. *J Clin Invest*, **93**, 2114-9.

De Benedetti F, Pignatti P, Massa M, Sartirana P, Ravelli A and Martini A (1995). Circulating levels of interleukin 1 beta and of interleukin 1 receptor antagonist in systemic juvenile chronic arthritis. *Clin Exp Rheumatol*, **13**, 779-84.

De Benedetti F, Alonzi T, Moretta A, Lazzaro D, Costa P, Poli V, Martini A, Ciliberto G and Fattori E (1997a). Interleukin 6 causes growth impairment in transgenic mice through a decrease in insulin-like growth factor-I. A model for stunted growth in children with chronic inflammation. *J Clin Invest*, **99**, 643-50.

De Benedetti F, Pignatti P, Gerlloni V, Massa M, Sartirana P, Caporali R, Montecucco CM, Corti A, Fantini F and Martini A (1997b). Differences in synovial fluid cytokine levels between juvenile and adult rheumatoid arthritis. *J Rheumatol*, **24**, 1403-9.

De Benedetti F, Meassa C, Vivarelli M, Rossi F, Pistorio A, Lamb R, Lunt M, Thomson W, Ravelli A, Donn R, Martini A and British Paediatric Rheumatology Study Group (2003). Functional and prognostic relevance of the –173 polymorphism of the macrophage migration inhibitory factor gene in systemic-onset juvenile idiopathic arthritis. *Arthritis Rheum*, **48**, 1171-6.

de Hon FD, ten Boekel E, Herrman J, Clement C, Ehlers M, Taga T, Yasukawa K, Ohsugi Y, Kishimoto T, Rose-John S, Wijdenes J, Kastelein R, Aarden LA and Brakenhoff JP (1995). Functional distinction of two regions of human interleukin 6 important for signal transduction via gp130. *Cytokine*, **7**, 398-407.

de Hooge AS, van de Loo FA, Arntz OJ and van den Berg WB (2000). Involvement of IL-6, apart form its role in immunity, in mediating a chronic response during experimental arthritis. *Am J Pathol.*, **157**, 2081-91.

de Hooge AS, van de Loo FA, Kolbe T, Mueller M, Levy DE, Bennink M, Arntz OJ and van den Berg WB (2002). STAT1 and STAT3 activation during the course of experimental arthritis. *Arthritis Rheum*, **46** Suppl 9, S596.

Dendorfer U, Oettgen P and Libermann TA (1994). Multiple regulatory elements in the interleukin-6 gene mediate induction by prostaglandins, cyclic AMP and lipopolysaccharide. *Mol Cell Biol*, **14**, 4443-54.

Deng WP and Nickoloff JA (1992). Site-directed mutagenesis of virtually any plasmid by eliminating a unique site. *Anal Biochem*, **200**, 81-8.

Desaymard C, Kaplan C, Fournier C, Manigne P, Hayem F, Kahn MF and Prieur AM (1996). Major histocompatibility complex markers and disease heterogeneity in one hundred eight patients with systemic onset juvenile chronic arthritis. *Rev Rheum (Engl Ed)*, **63**, 9-16.

Descombes P and Schibler U (1991). A liver-enriched transcriptional activator protein, LAP, and a transcriptional inhibitory protein, LIP, are translated form the same mRNA. *Cell*, **67**, 569-79.

Devlin RD, Bone HG 3rd and Roodman GD (1996). Interleukin-6: a potential mediator of the massive osteolysis in patients with Gorham-Stout disease. *J Clin Endocrinol Metab*, **81**, 1893-7.

Devlin RD, Reddy SV, Savino R, Ciliberto G and Roodman GD (1998). IL-6 mediates the effects of IL-1 or TNF, but not PTHrP or 1,25(OH)2D3, on osteoclast-like cell formation in normal human bone marrow cultures. *J Bone Miner Res*, **13**, 393-9.

Diamant M, Rieneck K, Mechti N, Zhang XG, Svenson M, Bendtzen K and Klein B (1997). Cloning and expression of an alternatively spliced mRNA encoding a soluble form of the human interleukin-6 signal transducer gp130. *FEBS Lett*, **412**, 379-84.

Didonato J, Mercurio F, Rosette C, Wu-Li J, Suyang H and Ghosh S (1996). Mapping of the inducible I-kappaB phosphorylation sites that signal its ubiquitination and degradation. *Mol Cell Biol*, **16**, 1295-1304.

Diehl S, Anguita J, Hoffmeyer A, Zapton T, Ihle JN, Fikrig E and Rincón M (2000). Inhibition of Th1 differentiation by IL-6 is mediated by SOCS1. *Immunity*, **13**, 805-15.

Dignam JD, Lebovitz RM and Roeder RG (1983). Accurate transcription initiation by RNA polymerase II in a soluble extract from isolated mammalian nuclei. *Nucleic Acids Res*, **11**, 1475-89.

Dittrich E, Haft CR, Muys L, Heinrich PC and Graeve L (1996). A di-leucine motif and an upstream serine in the interleukin-6 (IL-6) signal transducer gp130 mediate ligand-induced endocytosis and down-regulation of the IL-6 receptor. *J Biol Chem*, **271**, 5487-94.

Donn RP, Shelley E, Ollier WE, Thomson W and British Paediatric Rheumatology Study Group (2001a). A novel 5'-flanking region polymorphism of macrophage migration inhibitory factor is associated with systemic-onset juvenile idiopathic arthritis. *Arthritis Rheum*, **44**, 1782-5.

Donn RP, Barrett JH, Farhan A, Stopford A, Pepper L, Shelley E, Davies N, Ollier WE and Thomson W (2001b). Cytokine gene polymorphisms and susceptibility to juvenile idiopathic arthritis. British Paediatric Rheumatology Study Group. *Arthritis Rheum*, **44**, 802-10.

Donn R, Alourfi Z, De Benedetti F, Meazza C, Zeggini E, Lunt M, Stevens A, Shelley E, Lamb R, Ollier WE, Thomson W, Ray D and British Paediatric Rheumatology Study Group (2002). Mutation screening of the macrophage migration inhibitory factor gene: positive association of a functional polymorphism of macrophage migration inhibitory factor with juvenile idiopathic arthritis. *Arthritis Rheum*, **46**, 2402-9.

Dooley MA and Hogan SL (2003). Environmental epidemiology and risk factors for autoimmune disease. *Curr Opin Rheumatol*, **15**, 99-103.

Doucas V, Spyrou G and Yaniv M (1991). Unregulated expression of c-Jun or c-Fos proteins but not Jun D inhibits oestrogen receptor activity in human breast cancer derived cells. *EMBO J*, **10**, 2237-45.

Drakesmith H, O'Neil D, Schneider SC, Binks M, Medd P, Sercarz E, Beverley P and Chain B (1998). *In vivo* priming of T cells against cryptic determinants by dendritic cells exposed to interleukin 6 and native antigen. *Proc Natl Acad Sci USA*, **95**, 14903-8.

Droogmans L, Cludts I, Cleuter Y, Kettmann R and Burny A (1992). Nucleotide sequence of the bovine interleukin-6 gene promoter. *DNA Seq*, **3**, 115-7.

Drouin J, Sun YL, Chamberland M, Ganthier Y, De Lean A, Nemer M and Schmidt TJ (1993). Novel glucocorticoid receptor complex with DNA element of the hormone repressed POMC gene. *EMBO J*, **12**, 145-56.

Dynan WS and Tjian R (1983). The promoter-specific transcription factor Sp1 binds to upstream sequences in the SV40 early promoter. *Cell*, **35**, 79-87.

Ehlers M, Grotzinger J, de Hon FD, Mullberg J, Brakenhoff JP, Liu J, Wollmer A and Rose-John S (1994). Identification of two novel regions of human IL-6 responsible for receptor binding and signal transduction. *J Immunol*, **153**, 1744-53.

Elias JA and Lentz V (1990). IL-1 and tumor necrosis factor synergistically stimulate fibroblast IL-6 production and stabilize IL-6 messenger RNA. *J Immunol*, **145**, 161-6.

Endo TA, Masuhara M, Yokouchi M, Suzuki R, Sakamoto H, Misui K, Matsumoto A, Tanimura S, Ohtsubo M, Misawa H, Miyazaki T, Leonor N, Taniguchi T, Fujita T, Kanakura Y, Komiya S and Yoshimura A (1997). A new protein containing an SH2 domain that inhibits JAK kinases. *Nature*, **387**, 921-4.

Eray M, Postila V, Eeva J, Ripatti A, Karjalainen-Lindsberg ML, Knuutila S, Andersson LC and Pelkonen J (2003). Follicular lymphoma cell lines, an in vitro model for antigenic selection and cytokine-mediated growth regulation of germinal centre B cells. *Scand J Immunol*, **57**, 545-55.

Ernst M, Inglese M, Waring P, Campbell IK, Bao S, Clay FJ, Alexander WS, Wicks IP, Tarlinton DM, Novak U, Heath JK and Dunn AR (2001). Defective gp130-mediated signal transducer and activator of transcription (STAT) signalling results in degenerative joint disease, gastrointestinal ulceration, and failure of uterine implantation. *J Exp Med*, **194**, 189-203.

Faggioli L, Merola M, Hiscott J, Furia A, Monese R, Tovey M and Palmieri M (1997). Molecular mechanisms regulating induction of interleuin-6 gene transcription by interferon-gamma. *Eur J Immunol*, **27**, 3022-30.

Fattori E, Cappelletti M, Costa P, Sellitto C, Cantoni L, Carelli M, Faggioni R, Fantuzzi G, Ghezzi P and Poli V (1994). Defective inflammatory response in interleukin 6-deficient mice. *J Exp Med*, **180**, 1243-50.

Faulds G, Fishman D, Woo P and Humphries S (1998). Novel Fok I polymorphism in the 5'-flanking region of the human IL-6 gene. *Genbank/EMBL*, Accession number AF048692.

Faulkes DJ and Woo P (1997). "Do alleles at the serum amyloid A locus influence susceptibility to reactive amyloidosis in systemic onset juvenile chronic arthritis". *Amyloid: Int J Exp Clin Invest*, **4**, 75-9.

Feldman BM, Birdi N, Boone JE, Dent PB, Duffy CM, Ellsworth JE, Lang BA, Laxer RM, Lewkonia RM, Malleson PN, Oen KG, Paquin JD, Rosenberg AM, Schneider R and Silverman ED (1996). Seasonal onset of systemic-onset juvenile rheumatoid arthritis. *J Pediatr*, **129**, 512-8.

Feldmann M, Brennan FM and Maini R (1998). Cytokines in autoimmune disorders. *Int Rev Immunol*, **17**, 217-28.

Fenske M (1991). Protein binding of cortisol by means of competitive adsorption: application to cortisol binding by serum of sixteen eutherian mammals. *Comp Biochem Physiol A*, **98**, 61-6.

Fernandez-Real JM, Broch M, Vendrell J, Gutierrez C, Casamitjana R, Pugeat M, Richart C and Ricart W (2000a). Interlekin-6 gene polymorphism and insulin sensitivity. *Diabetes*, **49**, 517-20.

Fernandez-Real JM, Broch M, Vendrell J, Richart C and Ricart W (2000b). Interelukin-6 gene polymorphism and lipid abnormalities in healthy subjects. *J Clin Endocrinol Metal*, **85**, 1334-9.

Fernandez-Real J-M, Vendrell J, Richart C, Gutierrez C and Ricart W (2001). Platelet count and interleukin 6 gene polymorphism in healthy subjects. *BMC Medical Genetics*, **2**, 6-9.

Ferrari SL, Garnero P, Emond S, Montgomery H, Humphries SE and Greenspan SL (2001). A functional polymorphic variant in the interleukin-6 gene promoter associated with low bone resorption in postmenopausal women. *Arthritis Rheum*, **44**, 196-201.

Firestein GS, Alvaro-Garcia JM and Maki R (1990). Quantitative analysis of cytokine gene expression in rheumatoid arthritis. *J Immunol*, **144**, 3347-53.

Fishman D, Faulds G, Jeffery R, Mohamed-Ali V, Yudkin JS, Humphries S and Woo P (1998). The effect of novel polymorphisms in the interleukin-6 (IL-6) gene on IL-6 transcription and plasma IL-6 levels, and an association with systemic-onset juvenile chronic arthritis. *J Clin Invest*, **102**, 1369-76.

Fleiss JL, Tytun A and Ury HK (1980). A simple approximation for calculating sample sizes for comparing independent proportions. *Biometrics*, **36**, 343-6.

Flex A, Gaetani E, Pola R, Santoliquido A, Aloi F, Papaleo P, Dal Lago A, Pola E, Serricchio M, Tondi P and Pola P (2002). The –174 G/G polymorphism of the interleukin-6 gene promoter is associated with peripheral artery occlusive disease. *Eur J Vasc Endovasc Surg*, **24**, 264-8.

Fried M and Crothers DM (1981). Equilibria and kinetics of lac repressor-operator interactions by polyacrylamide gel electrophoresis. *Nucleic Acid Res*, **9**, 6505-25.

Gao B, Jiang L and Kunos G (1996). Transcriptional regulation of α_{1b} adrenergic receptors (α_{1b}AR) by nuclear factor 1 (NF1): a decline in the concentration of NF1 correlates with the down regulation of α_{1b}AR gene expression in regenerating liver. *Mol Cell Biol*, **16**, 5997-6008.

Garner MM and Revzin A (1981). A gel electrophoresis method for quantifying the binding of proteins to specific DNA regions: application to components of the *Escherichia coli* lactose operon regulatory system. *Nucleic Acid Res*, **9**, 3047-60.

Garnero P, Borel O, Sornay-Rendu E, Duboeuf F, Jeffery R, Woo P and Delmas PD (2002). Association between a functional interleukin-6 gene polymorphism and peak bone mineral density and postmenopausal bone loss in women: the OFELY study. *Bone*, **31**, 43-50.

Gastl G, Plante M, Finstad CL, Wong GY, Federici MG, Bander NH and Rubin SC (1993). High IL-6 level in ascitic fluid correlate with reactive thrombocytosis in patients with epithelial ovarian cancer. *Br J Haematol*, **83**, 433-41.

Gauldie J, Richards C, Harnish D, Lansdrop P and Baumann H (1987). Interferon 2/B-cell stimulatory factor type 2 shares identity with monocyte-derived hepatocyte-stimulating factor and regulates the major acute phase protein response in liver cells. *Proc Natl Acad Sci USA*, **84**, 7251-5.

Georges JL, Loukaci V, Poirier O, Evans A, Luc G, Arveiler D, Ruidavets JB, Cambien F and Tiret L (2001). Interleukin-6 gene polymorphisms and susceptibility to myocardial infarction: the ECTIM study. Etude Cas-Temmoin de l'Infarctus du Myocarde. *J Mol Med*, **79**, 300-5.

Gerhartz C, Heesel B, Sasse J, Hemmann U, Landgraf C, Schneider-Mergener J, Horn F, Heinrich PC and Graeve L (1996). Differential activation of acute phase response factor/STAT3 and STAT1 via the cytoplasmic domain of the interleukin-6 signal transducer gp130. 1. Definition of a novel phosphotyrosine motif mediating STAT1 activation. *J Biol Chem*, **271**, 12991-8.

Ghosh S, Gifford AM, Rivere LR, Tempest P, Nolan GP and Baltimore D (1990). Cloning of p50 DNA binding subunit of NFκB: homology to rel and dorsal. *Cell*, **62**, 1019-29.

Ghosh G, van Duyne G, Ghosh S and Sigler PB (1995). Structure of NFκB p50 homodimer bound to a κB site. *Nature*, **373**, 303-10.

Gibson RM, Schiemann WP, Prichard LB, Reno JM, Ericsson LH and Nathanson NM (2000). Phosphorylation of human gp130 at Ser-782 adjacent to the di-leucine internalization motif. Effects on expression and signaling. *J Biol Chem*, **275**, 22574-82.

Girasole G, Jilka RL, Passeri G, Boswell S, Boder G, Williams D and Manolagas SC (1992). 17β-estradiol inhibits interleukin-6 production by bone marrow-derived stromal cells and osteoblasts in vitro: a potential mechanism for the antiosteoporotic effect of estrogens. *J Clin Invest*, **89**, 883-91.

Glass DN and Giannini EH (1999). Juvenile rheumatoid arthritis as a complex genetic trait. *Arthritis Rheum*, **42**, 2261-8.

Glass CK, Rose DW and Rosenfeld MG (1997). Nuclear receptor co-activators. *Curr Opin Cell Biol*, **9**, 222-32.

Goedecke V, Crane AM, Jaakkola E, Kaluza W, Laiho K, Weeks DE, Wilson J, Kauppi M, Kaarela K, Tuomilehto J, Wordsworth BP and Brown MA (2003). Interleukin 10 polymorphisms in ankylosing spondylitis. *Genes Immun*, **4**, 74-6.

Gojobori T and Nei M (1984). Concerted evolution of the immunoglobulin VH gene family. *Mol Biol Evol*, **1**, 195-212.

Gonzalez-Crespo S and Levine M (1994). Related target enhancers for dorsal and NFκB signalling pathways. *Science*, **264**, 255-8.

Gorgoni B, Maritano D, Marthyn P, Righi M and Poli V (2002). C/EBPβ gene inactivation causes both impaired and enhanced gene expression and inverse regulation of IL-12 p40 and p35 mRNAs in macrophages. *J Immunol*, **168**, 4055-62.

Graham F L and van der Eb A J (1973). A new technique for the assay of infectivity of human adenovirus 5 DNA. *Virology*, **52**, 456.

Graziano M, St-Pierre Y, Beauchemin C, Desrosiers M and Potworowski EF (1998). The fate of thymocytes labelled in vivo with CFSE. *Exp Cell Res*, **240**, 75-85.

Greenfield EM, Gornik SA, Horowitz MC, Donahue HJ and Shaw SM (1993). Regulation of cytokine expression in osteoblasts by parathyroid hormone: rapid stimulation of interleukin-6 and leukemia inhibitory factor mRNA. *J Bone Miner Res*, **8**, 1163-71.

Greenfield EM, Shaw SM, Gornik SA and Bank MA (1995). Adenyl cyclase and interleukin 6 are downstream effectors of parathyroid hormone resulting in stimulation of bone resorption. *J Clin Invest*, **96**, 1238-44.

Greiser JS, Stross C, Heinrich PC, Behrmann I and Hermanns HM (2002). Orientational constraints of the gp130 intracellular juxtamembrane domain for signaling. *J Biol Chem*, **277**, 26959-65.

Grötzinger J, Kurapkat G, Wollmer A, Kalai M and Rose-John S (1997). The family of the IL-6 cytokines: specificity and promiscuity of the receptor complexes. *Proteins*, **27**, 96-109.

Guerne PA, Zuraw BL, Vaughan JH, Carson DA and Lotz M (1989). Synovium as a source of interleukin 6 in vitro. Contribution to local and systemic manifestations of arthritis. *J Clin Invest*, **83**, 585-92.

Haan C, Hermanns HM, Heinrich PC and Behrmann I (2000). A single amino acid substitution (Trp666Ala) in the interbox1/2 region of the interleukin-6 signal transducer gp130 abrogates binding of JAK1, and dominantly impairs signal transduction. *Biochem J*, **349**, 261-6.

Haan C, Heinrich PC and Behrmann I (2002). Structural requirements of the interleukin-6 signal transducer gp130 for its interaction with Janus kinase 1: the receptor is crucial for kinase activation. *Biochem J*, **361**, 105-11.

Haegeman G, Content J, Volckaert G, Derynck R, Tavernier J and Fiers W (1986). Structural analysis of the sequence coding for an inducible 26-kDa protein in human fibroblasts. *Eur J Biochem*, **159**, 625–32.

Hai T and Curran T (1991). Cross-family dimerization of transcription factors Fos/Jun and ATF/CREB alters DNA binding specificity. *Proc Natl Acad Sci USA*, **88**, 3720-4.

Hardy IR and Gershon AA (1990). Prospects for use of a varicella vaccine in adults. *Infect Dis Clin North Am*, **4**, 159-73.

Haspel RL and Darnell JE (1999). A nuclear protein tyrosine phosphatase is required for the inactivation of Stat1. *Proc Natl Acad Sci USA*, **96**, 10188-93.

Haspel RL, Salditt-Georgieff M and Darnell JE (1996). The rapid inactivation of nuclear tyrosine phosphorylated Stat1 depends upon a protein tyrosine phosphatase. *EMBO J*, **15**, 6262-8.

Heinrich PC, Behrmann I, Müller-Newen G, Schaper F and Graeve L (1998). Interleukin-6 type cytokine signalling through the gp130/Jak/STAT pathway. *Biochem J*, **334**, 297-314.

Heinrich PC, Behrmann I, Haan S, Hermanns HM, Müller-Newen G and Schaper F (2003). Principles of IL-6-type cytokine signalling and its regulation. *Biochem J*, Epub ahead of print.

Heinzel T, Lavinsky RM, Mullen TM, Soderstrom M, Laherty CD, Torchia J, Yang WM, Brard G, Ngo SD, Davie JR, Seto E, Eisenman RN, Rose DW, Glass CK and Rosenfeld MG (1997). A complex containing N-CoR, mSin3 and histone deacetylase mediates transcriptional repression. *Nature*, **387**, 16-7.

Heits F, Stahl M, Ludwig D, Stange EF and Jelkmann W (1999). Elevated serum thrombopoietin and interleukin-6 concentrations in thrombocytosis associated with inflammatory bowel disease. *J Interferon Cytokine Res*, **19**, 757-60.

Hel Z, Di Marco S and Radzioch D (1998). Characterization of the RNA binding proteins forming complexes with a novel putative regulatory region in the 3'-UTR of TNF-α mRNA. *Nucleic Acid Res*, **26**, 2803-12.

Hemman U, Gerhartz C, Heesel B, Sasse J, Kurapkat G, Grötzinger J, Wollmer A, Zhong Z, Darnell JE, Graeve L, Heinrich P and Horn F (1996). Differential activation of acute phase response factor/stat3 and stat1 via the cytoplasmic domain of the interleukin 6 signal transducer gp130. *J Biol Chem*, **271**, 12999-13007.

Henkel T, Zabel U, van Zee K, Muller JM, Fanning E and Baeuerle PA (1992). Intramolecular masking of the nuclear location signal and dimerization domain in the precursor for the p50 NFκB subunit. *Cell*, **68**, 1121-33.

Heron E, Deloukas P and van Loon AP (1995). The complete exon-intron structure of the 156-kb human gene NFKB1, which encodes the p105 and p50 proteins of transcription factors NF-kappa B and I kappa B-gamma: implications for NF-kappa B-mediated signal transduction. *Genomics*, **30**, 493-505.

Higuchi T, Seki N, Kamizono S, Yamada A, Kimura A, Kato H and Itoh K (1998). Polymorphism of the 5'-flanking region of human tumor necrosis factor (TNF)-a gene in Japanese. *Tissue Antigens*, **51**, 605-12.

Hill RJ, Warren MK, Stenberg P, Levin J, Corash L, Drummond R, Baker G, Levin F and Mok Y (1991). Stimulation of megakaryocytopoiesis in mice by human recombinant interleukin-6. *Blood*, 77, 42-8.

Hirano T, Taga T, Nakano N, Yasukawa K, Kashiwamura S, Shimizu K, Nakajima K, Pyun KH and Kishimoto T (1985). Purification to homogeneity and characterization of human B-cell differentiation factor (BCDF or BSFp-2). *Proc Natl Acad Sci USA*, **82**, 5490-4.

Hirano T, Yasukawa K, Harada H, Taga T, Watanabe Y, Matsuda T, Kashiwamura S, Nakajima K, Koyama K, Iwamatsu A, Tsunasawa S, Sakiyama F, Matsui H, Takahara Y, Taniguchi T and Kishimoto T (1986). Complementary DNA for a novel human interleukin (BSF-2) that induces B lymphocytes to produce immunoglobulin. *Nature*, **324**, 73-6.

Hirano T, Suematsu S, Matsusaka T, Matsuda T and Kishimoto T (1992). The role of interleukin 6 in plasmacytomagenesis. *Ciba Found Symp*, **167**, 188-200.

Hofer MF, Mouy R and Prieur AM (2001). Juvenile idiopathic arthritides evaluated prospectively in a single center according to the Durban Criteria. *J Rheumatol*, **28**, 1083-90.

Holloway JW, Beghe B, Turner S, Hinks LJ, Day IN and Howell WM (1999). Comparison of three methods for single nucleotide polymorphism typing for DNA bank studies: sequence-specific oligonucleotide probe hybridisation, TaqMan liquid phase hybridisation, and microplate array diagonal gel electrophoresis (MADGE). *Human Mutation*, **14**, 340-7.

Holt I, Davie MW and Marshall MJ (1996). Osteoclasts are not the major source of interleukin-6 in mouse parietal bones. *Bone*, **18**, 221-6.

Horlein AJ, Naar AM, Heinzel T, Torchia J, Gloss B, Kurokawa R, Ryan A, Kamei Y, Soderstrom M and Glass CK (1995). Ligand-independent repression by the thyroid hormone receptor mediated by a nuclear receptor co-repressor. *Nature*, **377**, 387-8.

Horowitz MC, Xi Y, Wilson K and Kacena MA (2001). Control of osteoclastogenesis and bone resorption by members of the TNF family of receptors and ligands. *Cytokine and growth factor reviews*, **12**, 9-18.

Horsten U, Müller-Newen G, Gerhartz C, Wollmer A, Wijdenes J, Heinrich PC and Grötzinger J (1997). Molecular modeling-guided mutagenesis of the extracellular part of gp130 leads to the identification of contact sites in the interleukin-6 (IL-6)-IL-6 receptor-gp130 complex. *J Biol Chem*, **272**, 23748-57.

Hoyland JA, Freemont AJ and Sharpe PT (1994). Interleukin-6, IL-6 receptor, and IL-6 nuclear factor gene expression in Paget's disease. *J Bone Miner Res*, **9**, 75-80.

Hsu W, Kerppola TK, Chen PL, Curran T and Chen-Kiang S (1994). Fos and Jun repress transcriptional activation by NF-IL6 through association at the basic leucine zipper region. *Mol Cell Biol*, **14**, 268-76.

Hsu H, Shu HB, Pan MG and Goeddel DV (1996). TRADD-TRAF2 and TRADD-FADD interactions define two distinct TNF receptor 1 signal transduction pathways. *Cell*, **84**, 299-308.

Hu HM, Baer M, Williams SC, Johnson PF and Schwartz RC (1998). Redundancy of C/EBPα, -β, and –δ in supporting the lipopolysaccharide-induced transcription of IL-6 and monocyte chemoattractant protein-1. *J Immunol*, **160**, 2334-42.

Hulkkonen J, Pertovaara M, Antonen J, Pasternack A and Hurme M (2001). Elevated interleukin-6 plasma levels are regulated by the promoter region polymorphism of the IL-6 gene in primary Sjogren's syndrome and correlate with the clinical manifestations of the disease. *Rheumatology*, **40**, 656-61.

Humphries SE, Luong LA, Ogg MS, Hawe E and Miller GJ (2001). The interleukin-6 –174 G/C promoter polymorphism is associated with risk of coronary heart disease and systolic blood pressure in healthy men. *Eur Heart J*, **22**, 2243-52.

Ishimi Y, Miyaura C, Jin CH, Akatsu T, Abe E, Nakamura Y, Yamaguchi A, Yoshiki S, Matsuda T, Hirano T, Kishimoto T and Suda T (1990). IL-6 is produced by osteoblasts and induces bone resorption. *J Immunol*, **145**, 3297-303.

Isshiki H, Akira S, Tanabe O, Nakajima T, shimamoto T, Hirano T and Kishimoto T (1990). Constitutive and interleukin-1 (IL-1)-inducible factors interact with the IL-1-responsive element in the IL-6 gene. *Mol Cell Biol*, **10**, 2757-64.

Ito A, Takii T, Matsumura T and Onozaki K (1999). Augmentation of type I IL-1 receptor expression and IL-1 signalling by IL-6 and glucocorticoid in murine hepatocytes. *J Immunol*, **162**, 4260-5.

Iwamoto M, Nara H, Hirata D, Minota S, Nishimoto N, Yoshizaki K (2002). Humanized monoclonal anti-interleukin-6 receptor antibody for treatment of intractable adult-onset Still's disease. *Arthritis Rheum*, **46**, 3388-9.

Jackson ME (1991). Negative regulation of eukaryotic transcription. *J Cell Sci*, **100**, 1-7.

Jackson SP, MacDonald JJ, Lees-Miller S and Tjian R (1990). GC box binding induces phosphorylation of Sp1 by a DNA-dependent protein kinase. *Cell*, **63**(1), 155-65.

Jahromi MM, Millward BA and Demaine AG (2000). A polymorphism in the promoter region of the gene for interleukin-6 is associated with susceptibility to type I diabetes mellitus. *J Interferon Cytokine Res*, **20**, 885-8.

Janaswami PM, Kalvakolanu DV, Zhang Y and Sen GC (1992). Transcriptional repression of interleukin-6 gene by adenoviral E1A proteins. *J Biol Chem*, **267**, 24886-91.

Janknecht R and Hunter T (1996). A growing co-activator network. *Nature*, **383**, 22-3.

Jawaheer D, Seldin MF, Amos CI, Chen WV, Shigeta R, Etzel C, Damle A, Xiao X, Chen D, Lum RF, Monteiro J, Kern M, Criswell L, Albani S, Nelson JL, Clegg DO, Pope R, Schroeder HW Jr, Bridges S Jr, Pisetsky DS, Ward R, Kastner DL, Wilder RL, Pincus T, Callaha LF, Flemming D, Wener MH, Gregersen PK and North American Rheumatoid Arthritis Consortium (2003). Screening the genome for rheumatoid arthritis susceptibility genes: a replication study and combined analysis of 512 multicase families. *Arthritis Rheum*, **48**, 906-16.

Jego G, Bataille R and Pellat-Deceunynck C (2001). Interleukin-6 is a growth factor for non-malignant human plasmablasts. *Blood*, **97**, 1817-22.

Jenny NS, Tracy RP, Ogg MS, Luong LA, Kuller LH, Arnold AM, Sharrett AR and Humphries SE (2002). In the elderly, interleukin-6 plasma levels and the –174G>C polymorphism are associated with the development of cardiovascular disease. *Arterioscler Thromb Vasc Biol*, **22**, 2066-71.

John S, Hajeer A, Marlow A, Myerscough A, Silman AJ, Ollier WE and Worthington J (1997). Investigation of candidate disease susceptibility genes in rheumatoid arthritis: principles and strategies. *J Rheumatol*, **24**, 199-201.

Johnson PF (1993). Identification of C/EBP basic residues involved in DNA sequence recognition and half-site spacing preference. *Mol Cell Biol*, **13**, 6919-30.

Jones KA, Kadonaga JT, Rosenfeld PJ, Kelly TJ and Tjian R (1987). A cellular DNA-binding protein that activates eukaryotic transcription and DNA replication. *Cell*, **48**, 79-89.

Jones KG, Brull DJ, Brown LC, Sian M, Greenhalgh RM, Humphries SE and Powell JT (2001). Interleukin-6 (IL-6) and the prognosis of abdominal aortic aneurysms. *Circulation*, **103**, 2222-4.

Jordan M, Otterness IG, Ng R, Gessner A, Rollinghoff M and Beuscher HU (1995). Neutralization of endogenous IL-6 suppresses induction of IL-1 receptor antagonist. *J. Immunol.*, **154**, 4081-90.

Jordanides N, Eskdale J, Stuart R and Gallacher G (2000). Allele associations reveal four prominent haplotypes at the human interleukin-6 (IL-6) locus. *Genes and Immunity*, **1**, 451-5.

Jorgensen C, Apparailly F, Couret I, Canovas F, Jacquet C and Sany J (1998). Interleukin-4 and interleukin-10 are chondroprotective and decrease mononuclear cell recruitment in human rheumatoid synovium in vivo. *Immunology*, **93**, 518-23.

Joseph SB, Miner KT and Croft M (1998). Augmentation of naïve, Th1 and Th2 effector CD4 responses by IL-6, IL-1 and TNF. *Eur J Immuno*, **28**, 277-89.

Kalai M, Montero-Julian FA, Grötzinger J, Fontaine V, Vandenbussche P, Deschuyteneer R, Wollmer A, Brailly H and Content J (1997). Analysis of the human interleukin-6/human interleukin-6 receptor binding interface at the amino acid level: proposed mechanism of interaction. *Blood*, **89**, 1319-33.

Kamdar SJ, Chapoval AI, Phelps J, Fuller JA and Evans R (1996). Differential sensitivity of mouse mononuclear phagocytes to CSF-1 and LPS: the potential in vivo relevance of enhanced IL-6 gene expression. *Cell Immunol*, **174**, 165-72.

Kamei Y, Xu L, Heinzel T, Torchia J, Kurokawa R, Gloss S, Lin SC, Heyman RA, Rose DW, Glass CK and Rosenfeld MG (1996). A CBP integrator complex mediates transcriptional activation and AP-1 inhibition by nuclear receptors. *Cell*, **85**, 403-14.

Kamimura D, Fu D, Matsuda Y, Atsumi T, Ohtani T, Park SJ, Ishihara K and Hirano T (2002). Tyrosine 759 of the cytokine receptor gp130 is involved in Listeria monocytogenes susceptibility. *Genes Immun*, **3**, 119-22.

Kang SH, Brown DA, Kitajima I, Xu X, Heidenreich O, Gryaznov S and Nerenberg M (1996). Binding and functional effects of transcription factor Sp1 on the murine interleukin-6 promoter. *J Biol Chem*, **271**, 7330-5.

Kannabiran C, Zeng X and Vales LD (1997). The mammalian transcriptional repressor RBP (CBF1) regulates interleukin-6 gene expression. *Mol Cell Biol*, **17**, 1-9.

Kao HY, Ordentlich P, Koyano-Nakagawa N, Tang Z, Downes M, Kintner CR, Evans RM and Kadesch T (1998). A histone deacetylase corepressor complex regulates the Notch signal transduction pathway. *Genes Dev*, **12**, 2269-77.

Kaptein A, Paillard V and Saunders M (1996). Dominant negative Stat3 mutant inhibits interleukin-6-induced Jak-STAT signal transduction. *J Biol Chem*, **271**, 5961-4.

Karin M, Liu ZG and Zandi E (1997). AP-1 function and regulation. *Curr Opin Cell Biol*, **9**, 240-6.

Kaser A, Brandacher G, Steurer W, Kaser S, Offner FA, Zoller H, Theurl I, Widder W, Molnar C, Ludwiczek O, Atkins MB, Mier JW and Tilg H (2001). Interleukin-6 stimulates thrombopoiesis through thrombopoietin: role in inflammatory thrombocytosis. *Blood*, **98**, 2720-5.

Kelberman D, Rockman MV, Brull DJ, Fife M, Sanders J, Woo P and Humphries SE (in press). Analysis of common IL-6 promoter SNP variants and the AnTn tract in humans and primates and effects on plasma IL-6 levels following coronary artery bypass graft surgery. *BBA-Molecular Mechanisms of Disease*.

Keller ET, Chang C and Ershler WB (1996). Inhibition of NFkappaB activity through maintenance of IkappaBalpha levels contribute to dihydrotestosterone-mediated repression of the interleukin-6 promoter. *J Biol Chem*, **271**, 26267-75.

Keul R, Heinrich PC, Muller-Newen G, Muller K and Woo P (1998). A possible role for soluble IL-6 receptor in the pathogenesis of systemic onset juvenile chronic arthritis. *Cytokine*, **10**, 729-34.

Kilpinen S, Hulkkonen J, Wang XY and Hurme M, 2001. The promoter polymorphism of the interleukin-6 gene regulates interleukin-6 production in neonates but not in adults. *Eur Cytokine Netw*, **12**, 62-8.

Kim H, Hawley TS, Hawley RG and Baumann H (1998). Protein tyrosine phosphatase 2 (SHP-2) moderates signalling by gp130 but is not required for the induction of acute-phase plasma protein genes in hepatic cells. *Mol Cell Biol*, **18**, 1525-33.

Kinoshita S, Akira S and Kishimoto T (1992). A member of the C/EBP family, NF-IL6β, forms a heterodimers and transcriptionally synergizes with NF-IL6. *Proc Natl Acad Sci USA*, **89**, 1473-6.

Kitamura H, Kawata H, Takahashi F, Higuchi Y, Furuichi T and Ohkawa H (1995). Bone marrow neutrophilia and suppressed bone turnover in human interleukin-6 transgenic mice: A cellular relationship among hematopoietic cells, osteoblasts, and osteoclasts mediated by stromal cells in bone marrow. *Am J Pathol,* **147,** 1682-92.

Knight JC, Udalova I, Hill AVS, Greenwood BM, Peshu N, Marsh K and Kwiatkowski D (1999). A polymorphism that affects OCT-1 binding to the TNF promoter region is associated with severe malaria. *Nature Genetics,* **22,** 145-50.

Kobayashi H, Ohshima S, Nishioka K, Yamaguchi N, Umeshita-Sasa M, Ishii T, Mima T, Kishimoto T, Kawase I and Saeki Y (2002). Antigen induced arthritis (AIA) can be transferred by bone marrow transplantation: evidence that interleukin 6 is essential for induction of AIA. *J Rheumatol*, **29**, 1176-82.

Kopf M, Baumann H, Freer G, Freudenberg M, Lamers M, Kishimoto T, Zinkernagel R, Bluethmann H and Kohler G (1994). Impaired immune and acute-phase responses in interleukin-6-deficient mice. *Nature,* **368**, 339-42.

Kopf M, Herren S, Wiles MV, Pepys MB and Kosco-Vilbois MH (1998). Interleukin 6 influences germinal center development and antibody production via a contribution of C3 complement component. *J Exp Med*, **188**, 1895-906.

Kunkel LM, Smith KD, Boyer SH, Borgaonkar DS, Wachtel SS, Miller OJ, Breg WR, Jones HW Jr and Rary JM (1977). Analysis of human Y-chromosome-specific reiterated DNA in chromosome variants. *Proc. Natl. Acad. Sci. USA,* **74**, 1245-9.

Kunsch C, Ruben S and Rosen C (1992). Selection of optimal κB-Rel DNA binding motifs; interaction of both subunits of NFκB with DNA is required for transcriptional activation. *Mol Cell Biol,* **12,** 4412-21.

Kurebayashi S, Miyashita Y, Hirose T, Kasayama S, Akira S and Kishimoto T (1997). Characterization of mechanisms of interleukin-6 gene repression by estrogen receptor. *J Steroid Biochem Mol Biol,* **60,** 11-7.

Kurihara N, Bertolini D, Suda T, Akiyama Y and Roodman GD (1990). IL-6 stimulates osteoclast-like multinucleated cell formation in long term human marrow cultures by inducing IL-1 release. *J Immunol,* **144,** 4226-30.

Kuwana M, Medsger TA and Wright TM (2000). Analysis of soluble and cell surface factors regulating anti-DNA topoisomerase I autoantibody production demonstrates synergy between Th1 and Th2 autoreactive cells. *J Immunol,* **164,** 6138-46.

La Flamme AC and Pearce EJ (1999). The absence of IL-6 does not affect Th2 cell development in vivo, but does lead to impaired proliferation, IL-2 receptor expression and B cell responses. *J Immunol,* **162,** 5829-37.

Laemmli UK (1970). Cleavage of structural proteins during the assembly of the head of bacteriophage T4. *Nature,* **227,** 680-5.

Lamb P, Seidel HM, Haslam J, Milocco L, Kessler LV, Stein RB and Rosen J (1995). STAT protein complexes activated by interferon-gamma and gp130 signaling molecules differ in their sequence preference and transcriptional induction properties. *Nucleic Acids Res,* **23,** 3283-9.

Lamph WW, Wamsley P, Sassone-Corsi P and Verma IM (1988). Induction of proto-oncogene Jun/AP1 by serum and TPA. *Nature,* **334,** 629-31.

Land H, Parada LF and Weinberg R (1983). Cellular oncogenes and multistep carcinogenesis. *Science,* **222,** 771-8.

Landschultz WH, Johnson PF and McKnight SL (1989). The DNA binding domain of the rat liver nuclear protein C/EBP is bipartitie. *Science,* **243,** 1681-8.

Lania L, Majello B and De Luca P (1997). Transcriptional regulation by the Sp family proteins. *Int J Biochem Cell Biol,* **29,** 1313-23.

Latchman D (1998). *Eukaryotic transcription factors.* 3rd ed. London, Academic Press.

Laxer RM and Schneider R (1998). Systemic-onset juvenile chronic arthritis. In *Oxford Textbook of Rheumatology*, Maddison PJ, Isenberg DA, Woo P and Glass DN, editors, Oxford Medical Publications, **2nd ed**, 1114-31.

Leger-Ravet MB, Peuchmaur M, Devergne O, Audouin J, Raphael M, Van-Damme J, Galanaud P, Diebold J and Emilie D (1991). Interleukin-6 gene expression in Castleman's disease. *Blood,* **78**, 2923-30.

Lekstrom-Himes J and Xanthopoulos KG (1998). Biological role of the CCAAT/Enhancer-binding protein family of transcription factors. *J Biol Chem*, **273**, 28545-8.

Lemon B and Tjian R (2000). Orchestrated response: a symphony of transcription factors for gene control. *Genes Dev*, **14**, 2551-2569.

Lepore L, Pennesi M, Saletta S, Perticarari S, Presani G and Prodan M (1994). Study of IL2, IL6, TNF alpha, IFN gamma and beta in serum and synovial fluid of patients with juvenile chronic arthritis. *Clin Exp Rheumatol,* **12**, 561-5.

Lewis CM (2002). Genetic association studies: design, analysis and interpretation. *Brief Bioinform,* **3**, 146-53.

Libermann TA and Baltimore D (1990). Activation of interleukin-6 gene expression through the NF-kappa B transcription factor. *Mol CellBiol,* **10**, 2327-34.

Lieberson R, Ong J, Shi X and Eckhardt LA (1995). Immunoglobulin gene transcription ceases upon deletion of a distant enhancer. *EMBO J*, **14**, 6229-38.

Lim CS, Zheng S, Kim YS, Ahn C, Han JS, Kim S, Lee JS and Chae DW (2002). The –174 G to C polymorphism of interleukin-6 gene is very rare in Koreans. *Cytokine,* **19**, 52-4.

Lin L and Ghosh S (1996). A glycine-rich region in NFκB p105 functions as a processing signal for the generation of the p50 subunit. *Mol Cell Biol,* **16**, 2248-54.

Lindahl R, Xiao GH, Falkner KC and Prough RA (1999). Negative regulation of rat hepatic aldehyde dehydrogenase 3 by glucocorticoids. *Adv Exp Med Biol,* **463,** 159-64.

Linker-Israeli M, Deans RJ, Wallace DJ, Prehan J, Ozeri-Chen T and Klinenberg JR (1991). Elevated levels of endogenous IL-6 in systemic lupus erythematosus. A putative role in pathogenesis. *J Immunol,* **147,** 117-23.

Liu J, Fan Q, Sodeoka M, Lane W and Verdine G (1994). DNA binding by an amino acid residue in the C-terminal half of the Rel homology region. *Chem Biol,* **1,** 47-55.

Liu B, Liao J, Rao X, Kushner SA, Chung CD, Chang DD and Shuai K (1998). Inhibition of Stat1-mediated gene activation by PIAS1. *Proc Natl Acad Sci USA,* **95,** 10626-31.

Liu B, Gross M, ten Hoeve J and Shuai K (2001). A transcriptional co repressor of Stat1 with an essential LXXLL signature motif. *Proc Natl Acad Sci USA,* **98,** 3203-7.

Lorentzon M, Lorentzon R and Nordstrom P (2000). Interleukin-6 gene polymorphism is related to bone mineral density during and after puberty in healthy white males: a cross-sectional and longitudinal study. *J Bone Miner Res,* **15,** 1944-9.

Lu-Kuo JM, Austen KF and Katz HR (1996). Post-transcriptional stabilization by interleukin-1β of interleukin-6 mRNA induced by c-*kit* ligand and interleukin-10 in mouse bone marrow-derived mast cells. *J Biol Chem,* **271,** 22169-74.

Lyons AB and Parish CR (1994). Determination of lymphocyte division by flow cytometry. *J Imm Methods,* **171,** 131-7.

Malinin NL, Boldin MP, Kovalenko AV and Wallach D (1997). MAP3K-related kinase involved in NF-kappa B induction by TNF, CD95 and IL-1. *Nature,* **385,** 540-4.

Mandrekar P, Catalano D and Szabo G (1999). Inhibition of lipopolysaccharide-mediated NFκB activation by ethanol in human monocytes. *Int Immunology,* **11,** 1781-90.

Mangelsdorf DJ and Evans RM (1995). The RXR heterodimers and orphan receptors. Cell, 83, 841-50.

Mangelsdorf DJ, Thummel C, Beato M, Herrlich F, Schutz G, Umesono K, Blumberg B, Kustner P, Mark M, Chambon P and Evans RM (1995). The nuclear receptor superfamily: the second decade. *Cell,* **83**, 835-9.

Marin V, Montero-Julian FA, Grès S, Boulay V, Bongrand P, Farnarier C and Kaplanski G (2001). The IL-6-soluble IL-6Ralpha autocrine loop of endothelial activation as an intermediate between acute and chronic inflammation: an experimental model involving thrombin. *J. Immunol.* **167**, 3435-42.

Marshall SE, McLaren AJ, McKinney EF, Bird TG, Haldar NA, Bunce M, Morris PJ and Welsh KI (2001). Donor cytokine genotype influences the development of acute rejection after renal transplantation. *Transplantation,* **71**, 469-76.

Martens AS, Bode JG, Heinrich PC and Graeve L (2000). The cytoplasmic domain of the interleukin-6 receptor gp80 mediates its basolateral sorting in polarized madin-darby canine kidney cells. *J Cell Sci,* **113**, 3593-602.

Martincic K, Campbell R, Edwalds-Gilbert G, Souan L, Lotze MT and Milcarek C (1998). Increase in the 64-kDa subunit of the polyadenylation/cleavage stimulatory factor during the G_0 to S phase transition. *Proc Natl Acad Sci USA,* **95**, 11095-100.

Matsuno F, Chowdhury S, Gotoh T, Iwase K, Matsuzaki H, Takatsuki K, Mori M and Takiguchi M (1996). Induction of the C/EBPβ gene by dexamethasone and glucagon in primary-cultured rat hepatocytes. *J Biochem (Tokyo),* **119**, 524-32.

Matsusaka T, Fujikawa K, Nishio Y, Mukaida N, Matsushima K, Kishimoto T and Akira S (1993). Transcription factors NF-IL6 and NF-kB synergistically activate transcription of the inflammatory cytokines, interleukin 6 and interleukin 8. *Proc Natl Acad Sci USA,* **90**, 10193-7.

May MJ and Ghosh S (1998). Signal transduction through NF-kappa B. *Immunol Today,* **19**, 80-8.

May LT, Ghrayeb H, Santhanam U, Tatter SB, Sthoeger Z, Helfgott DC, Chiorazzi N, Grieninger G and Sehgal PB (1988). Synthesis and secretion of multiple forms of beta 2-interferon/B-cell differentiation factor 2/hepatocyte-stimulating factor by human fibroblasts and monocytes. *J Biol Chem,* **263**, 7760-6.

McDonald NQ, Panayotatos and Hendrickson WA (1995a). Crystal structure of dimeric human ciliary neurotrophic factor determined by MAD phasing. *EMBO J,* **14**, 2689-99.

McDonald PP, Castella MA, Bald A, Maggi E, Romaghani S, Gruss HJ and Pizzolo G (1995b). CD30 ligation induces nuclear factor NF-kappaB activation in human T cell lines. *Eur J Immunol,* **25**, 2870-6.

McDowell TL, Symons JA, Ploski R, Forre O and Duff GW (1995). A genetic association between juvenile rheumatoid arthritis and a novel interleukin-1 alpha polymorphsim. *Arthritis Rheum,* **38**, 221-8.

McKnight GS, Clegg CH, Uhler M, Chrivia JC, Cudd GG, Correll LA and Otten AD (1988). Analysis of the cAMP-dependent protein kinase system using molecular genetic approaches. *Recent Progress in Hormone Research,* **44**, 307-31.

Medzhitov R, Preston-Hurlburt P and Janeway CA Jr. (1997). A human homologue of the Drosophila toll protein signals activation of adaptive immunity. *Nature*, **388**, 394-7.

Mellits KH, Hay RT and Goodbourn S (1993). Proteolytic degradation of MAD3 (I kappa B alpha) and enhanced processing of the NF-kappa B precursor p105 are obligatory steps in the activation of NF-kappa B. *Nucleic Acids Res,* **21**, 5059-66.

Mihara M, Kotoh M, Nishimoto N, Oda Y, Kumagai E, Takagi N, Tsunemi K, Ohsugi Y, Kishimoto T, Yoshizaki K and Takeda Y (2001). Humanized anitibody to human interleukin-6 receptor inhibits the development of collagen arthritis in Cynomolgus monkeys. *Clinical Immunology,* **98**, 319-26.

Miller ML, Aaron S, Jackson J, Fraser P, Cairns L, Hoch S, Borel Y, Larson M and Glass DN (1985). HLA gene frequencies in children and adults with systemic onset juvenile rheumatoid arthritis. *Arthritis Rheum.* **28**, 146-50.

Miller GJ, Bauer KA, Barzegar S, Cooper JA and Rosenberg RD (1996). Increased activation of the haemostatic system in men at high risk of fatal coronary heart disease. *Thromb Haemost,* **75**, 767-71.

Mitchell PJ and Tjian R (1989). Transcriptional regulation in mammalian cells by sequence-specific DNA binding proteins. *Science,* **245,** 371-8.

Miyazawa K, Mori A, Yamamoto K, and Okudaira H (1998a). Transcriptional roles of CCAAT/enhancer binding protein-beta, nuclear factor-kappaB, and C-promoter binding factor 1 in interleukin (IL)-1beta-induced IL-6 synthesis by human rheumatoid fibroblast-like synoviocytes. *J Biol Chem,* **273,** 7620-7.

Miyazawa K, Mori A, Miyata H, Akahane M, Ajisawa Y and Okudaira H (1998b). Regulation of interleukin-1β-induced interleukin-6 gene expression in human fibroblast-like synoviocytes by p38 mitogen-activated protein kinase. *J Biol Chem,* **273,** 24832-8.

Miyazawa K, Mori A and Okudaira H (1998c). Regulation of interleukin-1beta-induced interleukin-6 gene expression in human fibroblast-like synoviocytes by glucocorticoids. *J Biochem (Japan),* **124,** 1130-7.

Mizra MM, Fisher SA, King K, Cuthbert AP, Hampe J, Sanderson J, Mansfield J, Donaldson P, Macpherson AJS, Forbes A, Schreiber S, Lewis CM and Mathew CG (2003). Genetic evidence for interaction of the 5q31 cytokine locus and the CARD15 gene in Crohn Disease. *Am J Hum Genet,* **72,** 1018-22.

Modesto C, Woo P, Garcia-Consuegra J, Merino R, Garcia-Granero M, Arnal C and Prieur A-M (2001). Systemic onset juvenile chronic arthritis, polyarticular pattern and hip involvement as markers for bad prognosis. *Clinical and Experimetal Rheumatology,* **19,** 211-7.

Mohamed-Ali V, Flower L, Sethi J, Hotamisligil G, Gray R, Humphries SE, York DA and Pinkney J (2001). Beta-adrenergic regulation of IL-6 release from adipose tissue: in vivo and in vitro studies. *J Clin Endocrinol Metab,* **86,** 5864-9.

Montminy M (1997). Transcriptional regulation by cyclic AMP. *Ann Rev Biochem,* **66,** 870-822.

Mori N, Shirakawa F, Shimizu H, Murakami S, Oda S, Yamamoto K and Eto S (1994). Transcriptional regulation of the human interleukin-6 gene promoter in human T-cell leukemia virus type I-infected T-cell lines: evidence for the involvement of NF-kappa B. *Blood,* **84,** 2904-11.

Moritz RL, Ward LD, Tu GF, Fabri LJ, Ji H, Yasukawa K and Simpson RJ (1999). The N-terminus of gp130 is critical for the formation of the high-affinity interleukin-6 receptor complex. *Growth Factors,* **16,** 265-78.

Moroldo MB, Tague BL, Shear ES, Glass DN and Giannini EH (1997). Juvenile rheumatoid arthritis in affected sib pairs. *Arthritis Rheum,* **40,** 1962-6.

Moroldo MB, Donnelly P, Saunders J, Glass DN and Giannini EH (1998). Transmission disequilibrium as a test of linkage and association between HLA alleles and pauciarticular-onset juvenile rheumatoid arthritis. *Arthritis Rheum,* **41,** 1620-4.

Morse HR, Olomolaiye OO, Wood NA, Keen LJ and Bidwell JL (1999). Induced heteroduplex genotyping of TNF-alpha, IL-1beta, IL-6 and IL-10 polymorphisms associated with transcriptional regulation. *Cytokine* **11,** 789-95.

Mowen KA, Tang J, Zhu W, Schurter BT, Shuai K, Herschman HR and David M (2001). Arginine methylation of STAT1 modulates IFNalpha/beta-induced transcription. *Cell,* **104,** 731-41.

Müller-Newen G, Köhne C, Keul R, Hemman U, Müller-Esterl W, Wlijdenes J, Brakenhoff JP, Hart MH and Heinrich PC (1996). Purification and characterisation of the soluble interleukin-6 receptor from human plasma and identification of an isoform generated through alternative spicing. *Eur J Biochem,* **236,** 837-42.

Müller-Newen G, Kuster A, Hemman U, Keul R, Horsten U, Martens A, Graeve L, Wijdenes J and Heinrich PC (1998). Soluble IL-6 receptor potentiates the antagonistic activity of soluble gp130 on IL-6 responses. *J Immunol,* **161,** 6347-55.

Müller-Newen G, Kuster A, Wijdenes J, Schaper F and Heinrich PC (2000). Studies on the interleukin-6-type cytokine signal transducer gp130 reveal a novel mechanism of receptor activation by monoclonal antibodies. *J Biol Chem,* **275,** 4579-86.

Munck PC, Davidsen O, Moestrup SK, Sonne O, Nykjaer A and Moller BK (1990). Cellular targets and receptors for interleukin-6. II. Characterization of IL-6 binding and receptors in peripheral blood cells and macrophages. *Eur J Clin Invest,* **20**, 377-84.

Muraguchi A, Hirano T, Tang B, Matsuda T, Horii Y, Nakajima K and Kishimoto T (1988). The essential role of B cell stimulatory factor 2 (BSF-2/IL-6) for the terminal differentiation of B cells. *J Exp Med,* **167**, 332-44.

Murakami M, Narazaki M, Hibi M, Yawata H, Yasukawa K, Hamaguchi M, Taga T and Kishimoto T (1991). Critical cytoplasmic region of the interleukin 6 signal transducer gp130 is conserved in the cytokine receptor family. *Proc Natl Acad Sci USA,* **88**, 11349-53.

Murakami M, Hibi M, Nakagawa N, Nakagawa T, Yasukawa K, Yamanishi K, Taga T and Kishimoto T (1993). IL-6 induced homodimerization of gp130 and associated activation of a tyrosine kinase. *Science,* **260**, 1808-10.

Murphy KM (1998). T lymphocyte differentiation in the periphery. *Curr Opin Immunol,* **10**, 226-32.

Murray RE, McGuigan F, Grant SF, Reid DM and Ralston SH (1997). Polymorphisms of the interleukin-6 gene are associated with bone mineral density. *Bone,* **21**, 89-92.

Murray KJ, Moroldo MB, Donnelly P, Prahalad S, Passo MH, Giannini EH and Glass DN (1999). Age-specific effects of juvenile rheumatoid arthritis-associated HLA alleles. *Arthritis Rheum,* **42**, 1843-53.

Naka T, Narazaki M, Hirata M, Matsumoto T, Minamoto S, Aono A, Nishimoto N, Kajita T, Taga T, Yoshizaki K, Akira S and Kishimoto T (1997). Structure and function of a new STAT-induced STAT inhibitor. *Nature,* **387**, 924-9.

Nakajima T, Kinoshita S, Sasagawa T, Sasaki K, Naruto M, Kishimoto T and Akira S (1993). Phosphorylation at threonine-235 by a ras-dependent mitogen-activated protein kinase cascade is essential for transcription factor NF-IL6. *Proc Natl Acad Sci USA,* **90**, 2207-11.

Nakajima T, Uchida C, Anderson SF, Parvin JD and Montminy M (1997). Analysis of a cAMP-responsive activator reveals a two component system for transcriptional activation via signal dependent factors. *Genes Dev,* **11**, 738-47.

Nakajima T, Ota N, Yoshida H, Watanabe S, Suzuki T and Emi M (1999). Allelic variants in the interleukin-6 gene and essential hypertension in Japanese women. *Gene Immun,* **1**, 115-9.

Nakama A, Kuroda K and Yamada A (1995). Induction of cytochrome P450-dependent monooxygenase in serum-free cultured Hep G2 cells. *Biochem. Pharmacol.,* **50**, 1407-12.

Nakano H, Oshima H, Chung W, Willians-Abbott L, Ware CF, Yagita H and Okumura K (1996). Traf 5, an activator of NF-kappaB and putative signal transducer for the lymphotoxin-beta receptor. *J Biol Chem,* **271**, 14661-4.

Narazaki M, Witthuhn BA, Yoshida K, Sivennoinen O, Yasukawa K, Ihle JN, Kishimoto T and Taga T (1994). Activation of JAK2 kinase mediated by interleukin signal transducer gp130. *Proc Natl Acad Sci USA,* **91**, 2285-9.

Natkunam Y, Zhang X, Liu Z and Chen-Kiang S (1994). Simultaneous activation of Ig and Oct-2 synthesis and reduction of surface MHC class II expression by IL-6. *J Immuno,* **153**, 3476-84.

Nawata Y, Eugui EM, Lee SW and Allison AC (1989). IL-6 is the principal factor produced by synovia of patients with rheumatoid arthritis that induces B-lymphocytes to secrete immunoglobulins. *Ann N Y Acad Sci,* **557**, 230-8.

Neininger A, Kontoyiannis D, Kotlyarov A, Winzen R, Eckert R, Volk HD, Holtmann H, Kollias G and Gaestel M (2002). MK2 targets AU-rich elements and regulates biosynthesis of tumor necrosis factor and interleukin-6 independently at different post-transcriptional levels. *J Biol Chem,* **277**, 3065-8.

Nicholson SE, Willson TA, Farley A, Starr R, Zhang JG, Baca M, Alexander WS, Metcalfe D, Hilton DJ and Nicola NA (1999). Mutational analyses of the SOCS proteins suggest a dual domain requirement but distinct mechanisms for inhibition of LIF and IL-6 signal transduction. *EMBO J,* **18**, 375-85.

Niehof M, Manns MP and Trautwein C (1997). CREB controls LAP/C/EBP β transcription. *Mol Cell Biol*, **17**, 3600-13.

Niehof M, Kubicka S, Zender L, Manns MP and Trautwein C (2001a). Autoregulation enables different pathways to control CCAAT/enhancer binding protein β (C/EBPβ) transcription. *J Mol Biol*, **309**, 855-68.

Niehof M, Streetz K, Rakemann T, Bischoff SC, Manns MP, Horn F and Trautwein C (2001b). Interleukin-6-induced tethering of STAT3 to the LAP/C/EBP β promoter suggests a new mechanism of transcriptional regulation by STAT3. *J Biol Chem*, **276**, 9016-27.

Nishimoto N, Sasai M, Shima Y, Nakagawa M, Masumoto T, Shirai T, Kishimoto T and Yoshizake K (2000). Improvement in Castleman's disease by humanized anti-interleukin-6 receptor antibody therapy. *Blood*, **95**, 56-61.

Nishimoto N, Yoshizaki K, Miyasaka N, Yamamoto K, Kawai S, Takeuchi T, Hashimoto J, Azuma J and Kishimoto T (2002). A multi-center, randomised, double-blind, placebo-controlled trial of humanized anti-interleukin-6 (IL-6) receptor monoclonal antibody (MRA) in rheumatoid arthritis (RA). *Arthritis Rheum*, **46** Suppl 9, S1499.

Nolan GP, Fujita T, Bhatia K, Huppi C, Liou HC, Scott ML and Baltimore D (1993). The Bcl-3 proto-oncogene encodes a nuclear IκB-like molecule that preferentially interacts with NFκB p50 and p52 in a phosphorylation-dependent manner. *Mol Cell Biol*, **13**, 3557-66.

Northemann W, Braciak TA, Hattori M, Lee F and Fey GH (1989). Structure of the rat interleukin 6 gene and its expression in macrophage-derived cells. *J Biol Chem*, **264**, 16072-82.

Ogilvie EM, Fife MS, Thompson SD, Twine N, Tsoras M, Fisher SA, Lewis CM, Prieur AM, Glass DN and Woo P (2003). A multi-centre study using simplex and multi-case families demonstrates that the –174G allele of the interleukin-6 promoter confers susceptibility to systemic arthritis in children. *Arthritis Rheum*, **48**, 3302-6.

Ogryzko VV, Schiltz L, Russanova V, Howard BH and Nakatani Y (1996). The transcriptional coactivators p300 and CBP are histone acetyltransferases. *Cell*, **87**, 953-9.

Ohshima S, Saeki Y, Mima T, Sasai M, Nishioka K, Nomura S, Kopf M, Katuda Y, Tanaka T, Suemura M and Kishimoto T (1998). Interleukin-6 plays a key role in the development of antigen-induced arthritis. *Proc Natl Acad Sci* USA, **95**, 8222-6.

Olave I, Reinberg D and Vales LD (1998). The mammalian transcriptional repressor RBP (CBF1) targets TFIID and TFIIA to prevent activated transcription. *Genes Dev*, **12**, 1621-37.

Olencki T, Finke J, Tubbs R, Elson P, Mclain D, Herzog P, Budd GT, Gunn H and Bukowski RM (2000). Phase 1 trial of subcutaneous IL-6 in patients with refractory cancer: clinical and biological effects. *J Immunother*, **23**, 549-56.

Olivieri F, Bonafe M, Cavallone L, Giovagnetti S, Marchegiani F, Cardelli M, Mugianesi E, Giampieri C, Moresi R, Stecconi R, Lisa R and Franceschi C (2002). The –174C/G locus affects in vitro/in vivo IL-6 production during aging. *Exp Gerentol*, **37**, 309-14.

Olomolaiye O, Wood NA and Bidwell JL (1998). A novel NlaIII polymorphism in the human IL-6 promoter. *Eur J Immunogenet*, **25**, 267.

Osada S, Yamamoto H, Nishihara T and Imagawa M (1997a). DNA binding specificity of the CCAAT/enhancer-binding protein transcription factor family. *J Biol Chem*, **271**, 3891-6.

Osada S, Ikeda T, Xu M, Nishihara T and Imagawa M (1997b). Identification of the transcriptional repression domain of nuclear factor 1-A. *Biochem Biophys Res Commun*, **238**, 744-7.

Osada S, Matsubara T, Daimon S, Terazu Y, Xu M, Nishihara T and Imagawa M, (1999). Expression, DNA-binding specificity and transcriptional regulation of nuclear factor 1 family proteins from rat. *Biochem J*, **342**, 189-98.

Osiri M, McNicholl J, Moreland LW and Bridges SL Jr (1999). A novel single nucleotide polymorphism and five probable haplotypes in the 5'-flanking region of the IL-6 gene in African-Americans. *Genes Immun*, **1**, 166-7.

Ozen S, Alikasifoglu M, Bakkaloglu A, Duzova A, Jarosova K, Nemcova D, Besbas N, Vencovsky J and Tuncbilek E (2002). Tumour necrosis factor alpha G to A –238 and G to A –308 polymorphisms in juvenile idiopathic arthritis. *Rheumatology*, **41**, 223-7.

Pabo CO and Sauer RT (1992). Transcription factors: structural families and principle of DNA recognition. *Annu Rev Biochem,* **61**, 1053-95.

Palmieri M, Sasso MP, Monese R, Merola M, Faggioli L, Tovey M and Furia A (1999). Interaction of the nuclear protein CBF1 with the kappaB site of the IL-6 gene promoter. *Nuc Acids Res*, **27**, 2785-91.

Paonessa G, Gounari F, Frank R and Cortese R (1988). Purification of a NF1-like DNA-binding protein from rat liver and cloning of the corresponding cDNA. *EMBO J,* **7**, 3115-23.

Paonessa G, Graziani R, De Serio A, Savino R, Ciapponi L, Lahm A, Salvati AL, Toniatti C and Ciliberto G (1995). Two distinct and independent sites on IL-6 trigger gp130 dimer formation and signalling. *EMBO J*, **14**, 1942-51.

Parganas E, Wang D, Stravopodis D, Topham DJ, Marine JC, Teglund S, Vanin EF, Bodner S, Colamonicic OR, van Deursen JM, Grosveld G and Ihle JN (1998). Jak2 is essential for signalling through a variety of cytokine receptors. *Cell,* **93**, 385-95.

Parissis JT, Mentzikof D, Georgopoulou M, Gikopoulos M, Kanapitsas A, Merkouris K and Kefalas C (1996). Correlation of interleukin-6 gene expression to immunologic features in patients with cardiac myxomas. *J Interferon Cytokine Res*, **16**, 589-93.

Pascual M, Nieto A, Mataran L, Balsa A, Pascual-Salcedo D and Martin J (2000). IL-6 promoter polymorphisms in rheumatoid arthritis. *Genes Immun,* **1**, 338-40.

Paul R, Koedel U, Winkler F, Kiesseier BC, Fontana A, Kopf M, Hartung HP and Pfister HW (2003). Lack of IL-6 augments inflammatory response but decreases vascular permeability in bacterial meningitis. *Brain*, **126**, 1873-82.

Peng SS, Chen CA, and Shyu A (1996). Functional characterization of a non-AUUUA AU-rich element from the c-*jun* proto-oncogene mRNA: evidence for a novel class of AU-rich elements. *Mol Cell Biol,* **16**, 1490-9.

Perlman H, Bradley K, Liu H, Cole S, Shamiyeh E, Smith RC, Walsh K, Fiore S, Koch AE, Firestein GS, Haines GK and Pope RM (2003). IL-6 and matrix metalloproteinase-1 are regulated by the cyclin-dependent kinase inhibitor p21 in synovial fibroblasts. *J Immunol,* **170,** 838-45.

Petty RE, Southwood T, Baum J, Bhettay E, Glass D, Manners P, Maldonado-Cocco J, Suarez-Almazor M, Orozco-Alcala J, Prieur AM (1998). Revision of the proposed classification criteria for juvenile idiopathic arthritis: Durban, 1997. *J Rheum,* **25,** 1991-4.

Pignatti P, Vivarelli M, Meazza C, Rizzolo MG, Martini A and De Benedetti F (2001). Abnormal regulation of interleukin 6 in systemic juvenile idiopathic arthritis. *J Rheumatol,* **28,** 1670-6.

Plaetinck G, Combe MC, Corthesy P, Seckinger P and Nabholz M (1989). Interleukin 1 and tumor necrosis factor enhance transcription from the SV40 early promoter in a T cell line. *Eur J Immunol,* **19,** 897-904.

Plaisance S, Vanden Berghe W, Boone E, Fiers W and Haegeman G (1997). Recombination signal sequence binding protein Jk is constitutively bound to the NF-kB site of the interleukin-6 promoter and acts as a negative regulatory factor. *Mol Cell Biol,* **17,** 3733-43.

Plaskin D, Baeuerle PA and Eisenbach L (1993). κBF1 (p50 NFκB homodimer) acts as a repressor of H-2k (b) gene expression in metastatic tumour cells. *J Exp Med,* **177,** 1651-62

Poli V, Mancini FP and Cortese R (1990). IL-6DBP, a nuclear protein involved in interleukin-6 signal transduction, defines a new family of leucine zipper proteins related to C/EBP. *Cell,* **63,** 643-53

Poli V, Balena R, Fattori E, Markatos A, Yamamoto M, Tanaka H, Ciliberto G, Rodan GA and Costantini F (1994). Interleukin-6 deficient mice are protected from bone loss caused by oestrogen depletion. *EMBO J,* **13,** 1189-96

Poli V (1998). The role of C/EBP isoforms in the control of inflammatory and native immunity functions. *J. Biol. Chem,* **273,** 29279-82.

Poll T, Keogh CV, Guirao X, Buurman WA, Kopf M and Lowry SF (1997). Interleukin-6 gene-deficient mice show impaired defense against Pneumococcal pneumoniae. *J Infect Dis,* **176**, 439-44.

Pottratz ST, Bellido T, Mocharla H, Crabb D and Manolagas SC (1994). 17β-estradiol inhibits expression of human interleukin-6 promoter-reporter constructs by a receptor-dependent mechanism. *J Clin Invest,* **93**, 944-50.

Poupart P, Vandenabeele P, Cayphas S, Van-Snick J, Haegeman G, Kruys V, Fiers W and Content J (1987). B cell growth modulating and differentiating activity of recombinant human 26-kd protein (BSF-2, HuIFN-beta 2, HPGF). *EMBO J,* **6**, 1219-24.

Pratt WB (1997). The role of the hsp90 based chaperone system in signal transduction by nuclear receptors and receptor signalling via MAP kinase. *Ann Rev Pharm Tox,* **37**, 297-326.

Prestridge DS (1991). SIGNAL SCAN: a computer program that scans DNA sequences for eukaryotic transcriptional elements. *CABIOS,* **7**, 203-6.

Prieur AM, Roux Lombard P and Dayer JM (1996). Dynamics of fever and the cytokine network in systemic juvenile arthritis. *Rev Rhuem Engl Ed,* **63**, 163-70.

Ptashne M (1986). Gene regulation by proteins acting nearby and at a distance. *Nature,* **322**, 697-701.

Ptashne M (1988). How eukaryotic transcriptional activators work. *Nature,* **335**, 683-9.

Radhakrishnan I, Perez-Alvardo GC, Parker D, Dyson HJ, Montminy MR and Wright P (1997). Solution structure of the KIX domain of CBP bound to the transctivation domain of CREB a model for activator: co-activator interactions. *Cell,* **91**, 74-52.

Ralston SH (1994). Analysis of gene expression in human bone biopsies by polymerase chain reaction: Evidence for enhanced cytokine expression in postmenopausal osteoporosis. *J Bone Miner Res,* **9**, 883-90.

Ramji DP and Foka P (2002). CCAAT/enhancer-binding proteins: structure, function and regulation. *Biochem J,* **365**, 561-75.

Rauramaa R, Vaisanen SB, Luong LA, Schmidt-Trucksass A, Penttila IM, Bouchard C, Toyry J and Humphries SE (2000). Stromelysin-1 and interleukin-6 gene promoter polymorphisms are determinants of asymptomatic carotid artery atherosclerosis. *Arterioscler Thromb Vasc Biol,* **20**, 2657-62.

Rauscher FJ, Cohen DR, Curran T, Bos RJ, Bogt PK, Bohmann D, Tjian R and Franza BR (1988). Fos-associated protein p39 is the product of c-jun oncogene. *Science,* **240**, 1010-6.

Ray A and Prefontaine KE (1994). Physical association and functional antagonism between the p65 subunit of transcription factor NF-kappa B and the glucocorticoid receptor. *Proc Natl Acad Sci USA,* **91**, 752-6.

Ray A and Ray BK (1994). Serum amyloid A gene expression under acute-phase conditions involves participation of inducible C/EBPβ and C/EBPδ and their activation by phosphorylation. *Mol Cell Biol,* **14**, 4324-32.

Ray A, Tatter SB, May LT and Sehgal PB (1988). Activation of the human 'beta 2-interferon/hepatocyte-stimulating factor/interleukin 6' promoter by cytokines, viruses, and second messenger agonists. *Proc Natl Acad Sci USA,* **85**, 6701-5.

Ray A, Sassone-Corsi P and Sehgal PB (1989). A multiple cytokine- and second messenger-responsive element in the enhancer of the human interleukin-6 gene: similarities with c-fos gene regulation. *Mol Cell Biol,* **9**, 5537-47.

Ray A, LaForge KS and Sehgal PB (1990). On the mechanism for efficient repression of the interleukin-6 promoter by glucocorticoids: enhancer, TATA box, and RNA start site (Inr motif) occlusion. *Mol Cell Biol,* **10**, 5736-46.

Ray A, Prefontaine KE and Ray P (1994). Down-modulation of interleukin-6 gene expression by 17β-estradiol in the absence of high affinity DNA binding by the estrogen receptor. *J Biol Chem,* **269**, 12940-6.

Ray P, Ghosh SK, Zhang DH and Ray A (1997). Repression of interleukin-6 gene expression by 17 beta-estradiol: inhibition of the DNA-binding activity of the transcription factors NF-IL6 and NF-kappa B by the estrogen receptor. *FEBS Lett,* **409**, 79-85.

Raynal MC, Liu ZY, Hirano T, Mayer L, Kishimoto T and Chen-Kiang S (1989). Interleukin 6 induces secretion of IgG1 by coordinated transcriptional activation and differentiatial mRNA accumulation. *Proc atl Acad Sci USA,* **86,** 8024-8.

Rice NR, MacKichan ML and Israel A (1992). The precursor of NF-kappaB p50 has I kappa B-like functions. *Cell,* **71,** 243-53.

Richards HB, Satoh M, Shaw M, Libert C, Poli V and Reeves WH (1998). Interleukin 6 dependence of anti-DNA antibody production: evidence for two pathways of autoantibody formation in pristane-induced lupus. *J Exp Med,* **188,** 985-90.

Rincón M, Anguita J, Nakamura T, Fikrig E and Flavell RA (1997). Interleukin (IL)-6 directs the differentiation of IL-4-producing CD4+ T cells. *J Exp Med,* **185,** 461-9.

Ritter T, Brandt C, Prosch S, Vergopoulos A, Vogt K, Kolls J and Volk HD (2000). Stimulatory and inhibitory action of cytokines on the regulation of hCMV-IE promoter activity in human endothelial cells. *Cytokine,* **12,** 1163-70.

Robinson RC, Grey LM, Staunton D, Vankelecom H, VErnallis AB, Moreau JF, STuart DI, Heath JK and Jones EY (1994). The crystal structure and biological function of leukemia inhibitory factor: implications for receptor binding. *Cell,* **77,** 1101-16.

Rodig SJ, Meraz MA, White JM, Arthur CD, King KL, Sheehan KCF, Yin L, Pennica D, Johnson EM and Schreiber RD (1998). Disruption of the Jak1 gene demonstrates obligatory and nonredundant roles of the Haks in cytokine-induced biologic responses. *Cell,* **93,** 373-83.

Rola-Pleszczynski M and Stankova J (1992). Leukotriene B4 enhances interleukin-6 (IL-6) production and IL-6 messenger RNA accumulation in human monocytes in vitro: transcriptional and post-transcriptional mechanisms. *Blood,* **80,** 1004-11.

Rollwagen FM, Yu ZY, Li YY and Pacheco ND (1998). IL-6 rescues enterocytes from haemorrhage induced apoptosis in vivo and in vitro by a bcl-2 mediated mechanism. *Clin. Immunol. Immunopathol,* **89,** 205-13.

Romani L, Mencacci A, Cenci E, Spaccapelo R, Toniatti C, Puccetti P, Bistoni F and Poli V (1996). Impaired neutrophil response and CD4+ T helper cell 1 development in interleukin 6-deficient mice infected with Candida albicans. *J Exp Med*, **183**, 1345-55.

Roodman GD, Kurihara N, Ohsaki Y, Kukita A, Hosking D, Demulder A, Smith JF and Singer FR (1992). Interleukin 6: a potential autocrine/paracrine factor in Paget's disease of bone. *J Clin Invest*, **89**, 46-52.

Rooney M, David J, Symons J, Di Giovine F, Varsani H and Woo P (1995). Inflammatory cytokine responses in juvenile chronic arthritis. *Br J Rheumatol*, **34**, 454-60.

Ruocco MR, Chen X, Ambrosino C, Dragonetti E, Liu W, Mallardo M, Falco GD, Palmieri C, Franzoso G, Quinto I, Venuta S and Scala G (1996). Regulation of HIV-1 long terminal repeats by interaction of C/EBP(NF-IL6) and NF-kappaB/Rel transcription factors. *J Biol Chem*, **271**, 22479-86.

Saito H, Tada S, Ebinuma H, Wakabayashi K, Takagi T, Saito Y, Nakamoto N, Kurita S and Ishii H (2001). Interferon regulatory factor 1 promoter polymorphism and response to type 1 interferon. *J Cell Biochem*, **Suppl 36**, 191-200.

Saklatvala J, Dean J and Finch A, 1999. Protein kinase cascades in intracellular signalling by interleukin-1 and tumour necrosis factor. *Biochem Soc Symp.* **64**, 63-77.

Sanceau J, Kaisho T, Hirano T and Wietzerbin J (1995). Triggering of the human interleukin-6 gene by interferon-γ and tumor necrosis factor-α in monocytic cells involves cooperation between interferon regulatory factor-1, NFκB, and Sp1 transcription factors. *J Bio Chem*, **270**, 27920-31.

Santhanam U, Ghrayeb J, Sehgal PB and May LT (1989). Post-translational modifications of human interleukin-6. *Arch Biochem Biophys*, **274**, 161-70.

Santoro C, Mermod N, Andrews PC and Tjian R (1988). A family of human CCAAT-box binding proteins active in transcription and DNA replication: cloning and expression of multiple cDNAs. *Nature*, **334**, 218-224.

Sassone-Corsi P (1998). Coupling gene expression to cAMP signalling: role of CREB and CREM. *Int J Biochem Cell Biol,* **30,** 27-38.

Savino R, Lahm A, Giorgio M, Cabibbo A, Tramontano A and Ciliberto G (1993). Saturation mutagenesis of the human interleukin 6 receptor-binding site: implications for its three-dimensional structure. *Proc Natl Acad Sci USA,* **90,** 4067-71.

Schaper F, Gendo C, Eck M, Schmitz J, Grimm C, Anhuf D, Kerr IM and Heinrich PC (1998). Activation of the protein tyrosine phosphatase SHP2 via the interleukin-6 signal transducing receptor gp130 requires tyrosine kinase Jak1 and limits acute-phase protein expression. *Biochem J,* **335,** 557-65.

Scheidt-Nave C, Bismar H, Leidig-Bruckner G, Woitge H, Seibel MJ, Ziegler R and Pfeilschifter J (2001). Serum interleukin 6 is a major predictor of bone loss in women specific to the first decade past menopause. *J Clin Endocrinol Metab.* **86,** 2032-42.

Scheinman RI, Cogswell PC, Lofquist AK and Baldwin AS Jr (1995). Role of transcriptional activation of I kappa B alpha in mediation of immunosuppression by glucocorticoids. *Science,* **270,** 283-6.

Schleif R (1992). DNA looping. *Annu Rev Biochem,* **61,** 199-223.

Schluter B, Raufhake C, Erren M, Schotte H, Kipp F, Rust S, Van AH, Assmann G and Berendes D (2002). Effect of the interleukin-6 promoter polymorphism (-174 G/C) on the incidence and outcome of sepsis. *Crit Care Med,* **30,** 32-7.

Schmid RM, Perkins ND, Duckett CS, Andrews PC and Nabel GC (1991). Cloning of an NF-kappaB subunit which stimulates HIV transcription in synergy with p65. *Nature,* **352,** 733-6.

Schmitz J, Weissenbach M, Haan S, Heinrich PC and Schaper F (2000). SOCS3 exerts its inhibitory function on interleukin-6 signal transduction through the SHP2 recruitment site of gp130. *J Biol Chem,* **275,** 12848-56.

Schotte H, Schluter B, Rust S, Assmann G, Domschke W and Gaubitz M (2001). Interleukin-6 promoter polymorphism (-174 G/C) in Caucasian German patients with systemic lupus erythematosus. *Rheumatology,* **40,** 393-400.

Schreiber E, Matthias P, Muller MM and Schafner W (1989). Rapid detection of octamer binding proteins with 'mini-extracts', prepared from a small number of cells. *Nucleic Acids Res*, **17**, 6419.

Screpanti I, Musiani P, Bellavia d, Cappelletti M, Aiello FB, Maroder M, Frati L, Modesti A, Gulino A and Poli V (1996). Inactivation of the IL-6 gene prevents development of multicentric Castleman's disease in C/EBP β-deficient mice. *J Exp Med*, **184**, 1561-6.

Sehgal PB, Grienger G and Tosata G (1989). Multiple forms of human interleukin-6. *Ann NY Acad Sci*, **557**, 1-583.

Seidel HM, Milocco LH, Lamb P, Darnell JE, Stein RB and Rosen J (1995). Spacing of palindromic half sites as a determinant of selective STAT (signal transducers and activators of transcription) DNA binding and transcriptional activity. *Proc Natl Acad Sci USA*, **92**, 3041-5.

Seiler W, Muller H and Hiemke C (1995). Diurnal variations of plasma interleukin-6 in man: methodological implications of continuous use of indwelling cannulae. *Ann NY Acad Sci*, **762**, 468-70.

Sen R and Baltimore D (1986). Multiple nuclear factors interact with the immunoglobulin enhancer sequences. *Cell* **46**, 705-16.

Sengchanthalangsy LL, Datta S, Huang DB, Anderson E, Braswell E and Ghosh G (1999). Characterization of the dimer interface of transcription factor NFκB p50 homodimer. *J Mol Biol*, **289**, 1029-40.

Sheppard KA, Phelps KM, Williams AJ, Thanos D, Glass CK, Rosenfeld MG, Gerritsen ME and Collins T (1998). Nuclear integration of glucocorticoid receptor and nuclear factor-kappaB signalling by CREB-binding protein and steroid receptor coactivator-1. *J Biol Chem*, **273**, 29291-4.

Shikama N, Lyon J and La Thangue NB (1997). The p300/CBP family: integrating signals with transcription factors and chromatin. *Trend Cell Biol*, **7**, 230-6.

Shimizu H, Mitomo K, Watanabe T, Okamoto S and Yamamoto K-I (1990). Involvement of a NF-kB like transcription factor in the activation of the interleukin-6 gene by inflammatory lymphokines. *Mol Cell Biol,* **10**, 561-8.

Shuai K, Horvath CM, Huang LH, Qureshi SA, Cowburn D and Darnell JE (1994). Interferon activation of the transcription factor Stat91 involves dimerization through SH2-phosphotyrosyl peptide interactions. *Cell,* **76**, 821-8.

Shuai K, Stark GR, Kerr IM and Darnell JE (1993). A single phosphotyrosine residue of Stat91 required for gene activation by interferon-gamma. *Science,* **261**, 1744-6.

Siebenlist U (1979). RNA polymerase unwinds an 11-base pair segment of a phage T7 promoter. *Nature,* **279**, 651-2.

Skoog T, van't Hooft FM, Kallin B, Jovinge S, Boquist S, Nilsson J, Eriksson P and Hamsten A (1999). A common functional polymorphism (C→A substitution at position –863) in the promoter region of the tumour necrosis factor-alpha (TNF-alpha) gene associated with reduced circulating levels of TNF-alpha. *Hum Mol Genet,* **8**, 1443-9.

Smith CL and Hager GL (1997). Transcriptional regulation of mammalian gene *in vivo. J Biol Chem,* **272**, 27493-6.

Somers W, Stahl M and Seehra JS (1997). 1.9A crystal structure of interleukin 6: implications for a novel mode of receptor dimerization and signalling. *EMBO J,* **16**, 989-97.

Sonne O, Davidsen O, Moller BK, Munck PC (1990). Cellular targets and receptors for interleukin-6. I. In vivo and in vitro uptake of IL-6 in liver and hepatocytes. *Eur J Clin Invest,* **20**, 366-76.

Spielman RS and Ewens WJ (1996). The TDT and other family-based tests for linkage disequilibrium and association. *Am J Hum Genetics,* **59**, 983-9.

Stahl N, Boulton TG, Farruggella T, Ip NY, Davis S, Witthuhn BA, Quelle FW, Silvennoinen O, Barbeiri G, Pellegrini S (1994). Association and activation of Jak-Tyk kinases by CNTF-LIF-OSM-IL6 beta receptor components. *Science,* **263**, 92-5.

Stahl N, Farruggella TJ, Boulton TG, Zhong Z, Darnell JE and Yancopouos GD (1995). Choice of STATs and other substrates specified by modular tyrosine-based motifs in cytokine receptors. *Science,* **267**, 1349-53.

Starr R, Willson TA, Viney EM, Murray LJL, Rayner JR, Jenkins BJ, Gonda TJ, Alexander WS, Metcalf D, Nicola NA and Hilton DJ (1997). A family of cytokine-inducible inhibitors of signalling. *Nature,* **387**, 917-21.

Stauber C, Altschmied J, Akerblom IE, Marron JL and Mellon PL (1992). Mutual cross-interference between glucocorticoid receptor and CREB inhibits transactivation in placental cells. *New Biol*, **4**, 527-40.

Steel DM, Donoghue FC, O'Neill RM, Uhlar CM and Whitehead AS (1996). Expression and regulation of constitutive and acute phase serum amyloid A mRNAs in hepatic and non-hepatic cell lines. *Scand J Immunol*, **44**, 493-500.

Stein B and Yang MX (1995). Repression of the interleukin-6 promoter by estrogen receptor is mediated by NF-κB and C/EBPβ. *Mol Cell Biol,* **15**, 4971-9.

Sugiyama T (2001). Involvement of interleukin-6 and prostaglandin E2 in periarticular osteoporosis of postmenopausal women with rheumatoid arthritis. *J Bone Miner Metab,* **19**, 89-96.

Sureau A, Soret J, Vellard M, Crochet J and Perbal B (1992). The PR264/c-myb connection: expression of a splicing factor modulated by a nuclear protooncogene. *Proc Natl Acad Sci USA,* **89**, 11683-7.

Symmons D, Jones M, Osborne J, Sills J, Southwood T and Woo P (1996). Paediatric rheumatology in the United Kingdom: data from the British Paediatric Rheumatology Group National Diagnostic Register *J Rheum,* **23**, 1975-80.

Taga T and Kishimoto T (1997). GP130 and the interleukin-6 family of cytokines. *Ann Rev Immunol*, **15**, 797-819.

Takagaki Y, Seipelt RL, Peterson ML and Manley J (1996). The polyadenylation factor CstF-64 regulates alternative processing of IgM heavy chain pre-mRNA during B cell differentiation. *Cell*, **87**, 941-52.

Takahashi-Tezuka M, Yoshida Y, Fukada T, Ohtani T, Yamanaka Y, Nishida K, Hibi M and Hirano T (1998). Gab1 acts as an adapter molecule linking the cytokine receptor gp130 to ERK mitogen-activated protein kinase. *Mol Cell Biol*, **18**, 4109-17.

Takai Y, Wong GG, Clark SC, Blurakoff SJ and Herrmann SH (1988). B cell stimulatory factor-2 is involved in the differentiation of cytotoxic T lymphocytes. *J Immunol*, **140**, 508-12.

Takatsu K (1997). Cytokines involved in B-cell differentiation and their sites of action. *Proc Soc Exp Biol Med*, **215**, 121-33.

Takeshita S, Gage JR, Kishimoto T, Vredevoe DL and Martinez-Maza O (1996). Differential regulation of IL-6 gene transcription and expression by IL-4 and IL-10 in human monocytic cell lines. *J Immunol*, **156**, 2591-8.

Tamura T, Udagawa N, Takahashi N, Miyaura C, Tanaka S, Yamada Y, Koishihara Y, Ohsugi Y, Kumaki K and Taga T (1993). Soluble interleukin-6 receptor triggers osteoclast formation by interleukin 6. *Proc. Natl. Acad. Sci. USA*, **90**, 11924-8.

Tanabe O, Akira S, Kamiya T, Wong GG, Hirano T and Kishimoto T (1988). Genomic structure of the murine IL-6 gene: High degree conservation of potential regulatory sequences between mouse and human. *J Immunol*, **141**, 3875-81.

Tanaka T, Akira S, Yoshida K, Umemoto M, Yonida Y, Shirafuji N, Fujiwara H, Suematsu S, Yoshida N and Kishimoto T (1995). Targeted disruption of the NF-IL6 gene discloses its essential role in bacterial killing and tumor cytotoxicity by macrophages. *Cell*, **80**, 353-61.

Tanaka T, Katada Y, Higa S, Fujiwara H, Wang W, Saeki Y, Ohshima S, Okuda Y, Suemura M and Kishimoto T (2001). Enhancement of T helper$_2$ response in the absence of interleukin (IL-)6; an inhibitor of IL-4-mediated T helper$_2$ cell differentiation by IL-6. *Cytokine*, **13**, 193-201.

Tanner JE and Tosato G (1992). Regulation of B-cell growth and immunoglobulin gene transcription by interleukin-6. *Blood*, **79**, 452-9.

Tanner JW, Chen W, Young RL, Longmore GD and Shaw AS (1995). The conserved box 1 motif of cytokine receptors is required for association with JAK kinases. *J Biol Chem*, **270**, 6523-30.

Tengku-Muhammad TS, Hughes TR, Ranki H, Cryer A and Ramji DP (2000). Differential regulation of macrophage CCAAT-enhancer binding isoforms by lipopolysaccharide and cytokines. *Cytokine*, **12**, 1430-6.

Terry CF, Loukaci V and Green FR (2000). Cooperative influence of genetic polymorphisms on interleukin 6 transcriptional regulation. *J Biol Chem*, **275**, 18138-44.

Terstegen L, Gatsios P, Bode JG, Schaper F, Heinrich PC and Graeve L (2000). The inhibition of interleukin-6-dependent STAT activation by mitogen-activated protein kinases depends on tyrosine 759 in the cytoplasmic tail of glycoprotein 130. *J Biol Chem*, **275**, 18810-7.

Terwilliger JD and Ott J (1994). *Handbook of human genetic linkage*. John Hopkins University Press, Batlimore, MD.

Theil S, Behrmann I, Dittrich E, Muys L, Tavernier J, Wijdenes J, Heinrich PC and Graeve L (1998). Internalization of the interleukin 6 signal transducer gp130 does not require activation of the Jak/STAT pathway. *Biochem J*, **330**, 47-54.

Thompson J, Phillips R, Erdjument-Bromage H, Tempest P and Ghosh S (1995). IκB-β regulates the persistent response in a biphasic activation of NFκB. *Cell*, **80**, 573-82.

Thomson W, Barrett JH, Donn R, Pepper L, Kennedy LJ, Ollier WER, Silman AJS, British Paediatric Rheumatology Study Group, Woo P and Southwood T (2002). Juvenile idiopathic arthritis classified by the ILAR criteria: HLA associations in UK patients. *Rheumatology*, **41**, 1183-9.

Tilg H, Trehu E, Atkins MB, Dinarello CA and Meir JW (1994). Interleukin-6 (IL-6) as an anti-inflammatory cytokine: induction of circulating IL-1 receptor antagonist and soluble tumor necrosis factor receptor p55. *Blood*, **83**, 113-8.

Timmermann A, Pflanz S, Grotzinger J, Kuster A, Kurth I, Pitard V, Heinrich PC and Müller-Newen G (2000). Different epitopes are required for gp130 activation by interleukin-6, oncostatin M and leukemia inhibitory factor. *FEBS Lett,* **468,** 120-4.

Toledano MB, Ghosh D, Trinh F and Leonard WJ (1993). N-terminal DNA-binding domains contribute to differential DNA-binding specificities of NFκB p50 and p65. *Mol Cell Biol,* **13,** 852-60.

Tomeczkowski J, zur Stadt U, Reiter A, Welte K and Sykora KW (1997). Absence of IL-6 receptor expression in fresh childhood Burkitt's lymphoma cells and induction of IL-6 receptors by Epstein-Barr virus in vitro. *Br J Haematol,* **97,** 400-8.

Tonouchi N, Miwa K, Karasuyama H and Matsui H (1989). Deletion of 3' untranslated region of human BSF-2 mRNA causes stabilization of the mRNA and high-level expression in mouse NIH3T3 cells. *Biochem Biophys Res Communication,* **163,** 1056-62.

Torchia J, Glass C and Rosenfeld MG (1998). Co-activators and co-repressors in the integration of transcriptional responses. *Curr Opin Cell Biol,* **10,** 373-83.

Towbin H, Strehelin T and Gordon J (1979). Electrophoretic transfer of proteins from polyacrylamide gels to nitrocellulose sheets: procedures and some applications. *Proc. Natl. Acad. Sci,* **76,** 4350-4.

Turner DM, Williams DM, Sankaran D, Lazarus M, Sinnott PJ and Hutchinson IV (1997). An investigation of polymorphism in the interleukin 10 gene promoter. *Eur J Immunogenet,* **24,** 1-8.

Twine NA, Fife MS, Ogilvie EM, Lewis CM, Jeffery R and Woo P (2003). Does the IL6 AnTn tract modify the effect of the –174 polymorphism in systemic arthritis? *Rheumatol,* **42** suppl 1, 89.

Udagawa N, Takahashi N, Katagiri T, Tamura T, Wada S, Findlay DM, Martin TJ, Hirota H, Taga T, Kishimoto T (1995). Interleukin (IL)-6 induction of osteoclast differentiation depends on IL-6 receptors expressed on osteoblastic cells but not on osteoclast progenitors. *J Exp Med,* **182,** 1461-8.

Udalova IA, Richardson A, Denys A, Smith C, Ackerman H, Foxwell B and Kwiathowski D (2000). Functional consequences of a polymorphism affecting NF-kappaB p50-p50 binding to the TNF promoter region. *Mol Cell Biol,* **20**, 9113-9.

Ulich TR, Yin S, Guo K, Yi ES, Remick D and del Castillo J, 1994. Intratracheal injection of endotoxin and cytokines. II. Interleukin-6 and transforming growth factor beta inhibit acute inflammation. *Am. J. Pathol.* **138,** 1097-101.

Ungureanu D, Saharinen P, Junttila I, Hilton DJ and Silvennoinen O (2002). Regulation of Jak2 through the ubiquitin-proteasome pathway involves phosphorylation of Jak2 on Y1007 and interaction with SOCS-1. *Mol Cell Biol,* **22**, 3316-26.

Vales LD and Friedl EM (2002). Binding of C/EBP and RBP (CBF1) to overlapping sites regulates interleukin-6 gene expression. *J Biol Chem,* **277**, 42438-46.

Van Damme J, Cayphas S, Van Snick J, Conings R, Put W, Lenaerts JP, Simpson RJ and Billiau A (1987). Purification and characterization of human fibroblast-derived hybridoma growth factor identical to T-cell-derived B-cell stimulatory factor-2 (interleukin-6). *Eur J Biochem,* **168**, 543-50.

Van Kooten C, Van Oers MH and Aarden LA (1990). Interleukin-6 enhances human Ig production, but not as a terminal differentiation factor for B-lymphocytes. *Res Immunol,* **141**, 341-56.

Vannier E and Dinarello C (1994). Histamine enhances interleukin (IL)-1-induced IL-6 gene expression and protein synthesis via H2 receptors in peripheral blood mononuclear cells. *J Biol Chem,* **269**, 9952-6.

Vencovsky J, Jarosova K, Ruzickova S, Nemcova D, Niederlova J, Ozen S, Alikasifoglu M, Bakkaloglu A, Ollier WE and Mageed RA (2001). Higher frequency of allele 2 of the interleukin-1 receptor antagonist gene in patients with juvenile idiopathic arthritis. *Arthritis Rheum,* **44**, 2387-91.

Veres A, Prohaszka Z, Kilpinen S, Singh M, Fust G and Hurme M (2002). The promoter polymorphism of the IL-6 gene is associated with levels of antibodies to 60-kDa heat-shock proteins. *Immunogenetics*, **53**, 851-6.

Verma IM, Stevenson JK, Schwarz EM, Van Antwerp D and Miyamoto S (1995). Rel/NF-κB/IκB family: intimate tales of association and dissociation. *Genes Dev,* **9**, 2723-35.

Vickers MA, Green FR, Terry C, Mayosi BM, Julier C, Lathrop M, Ratcliffe PJ, Watkins HC and Keavney B (2002). Genotype at a promoter polymorphism of the interleukin-6 gene is associated with baseline levels of plasma C-reactive protein. *Cardiovasc Res,* **53**, 1029-34.

Vinson CR, Hai T and Boyd SM (1993). Dimerization specificity of the leucine zipper-containing bZIP motif on DNA binding: prediction and rational design. *Genes Dev,* **7**, 1047-58.

Wade PA, Pruss D and Wolffe AP (1997). Histone acetylation: chromatin in action. *Trend Biochem Sci,* **22**, 128-32.

Waldman ID, Rowe DC, Abramowitz A, Kozel ST, Mohr JH, Sherman SL, Cleveland HH, Sanders ML, Gard JM and Stever C (1998). Association and linkage of the dopamine transporter gene and attention-deficit hyperactivity disorder in children: heterogeneity owing to diagnostic subtype and severity. *Am J Hum Genet,* **63**, 1767-76.

Wallace and Levinson (1991). Juvenile rheumatoid arthritis: outcome and treatment for the 1990s. *Rheum Dis Clin North Am,* **17**, 891-905.

Wang L, Wang J, Sauter N and Pearce D (1995). Steroid receptor homodimerisation demonstrated in vitro and in vivo. *Proc Natl Acd Sci USA,* **92**, 12480-4.

Wang LH, Yang XY, Mihalic K, Xiao W, Li D and Farrar WL (2001). Activation of estrogen receptor blocks interleukin-6-inducible cell growth of human multiple myeloma involving molecular cross-talk between estrogen receptor and STAT3 mediated by co-regulator PIAS3. *J Biol Chem,* **276**, 31839-44.

Ward LD, Howlett GJ, Discolo G, Yasukawa K, Hammacher A, Moritz RL and Simpson RJ (1994). High affinity interleukin-6 receptor is a hexameric complex consisting of two molecules each of interleukin-6, interleukin-6 receptor, and gp-130. *J Biol Chem,* **269**, 23286-9.

Ward LD, Hammacher A, Howlett GJ, Matthews JM, Fabri L, Moritz RL, Nice EC, Weinstock J and Simpson RJ (1996). Influence of interleukin-6 (IL-6) dimerization on formation of the high affinity hexameric IL-6.receptor complex. *J Biol Chem*, **271**, 20138-44.

Ward NS, Waxman AB, Homer RJ, Mantell LL, Einarsson O, Du Y and Elias JA (2000). Interleukin-6-inducd protection in hyperoxic acute lung injury. *Am J Respir Cell Mol Biol*, **22**, 535-42.

Wegenka UM, Buschmann J, Lütticken C, Heinrich PC and Horn F (1993). Acute-phase response factor, a nuclear factor binding to acute-phase response elements, is rapidly activated by interleukin-6 at the posttranslational level. *Mol Cell Biol*, **13**, 276-88.

Weir BS (1996). Disequilibrium. In *Genetic Data Analysis II*, Sinauer Associates Incorporated, 98-101.

Weissenbach J, Chernajovsky Y, Zeevi M, Shulman L, Soreq H, Nir U, Wallach D, Perricuadet M, Tiollais P and Revel M (1980). Two interferon mRNAs in human fibroblasts: in vitro translation and Escherichia coli cloning studies. *Proc Natl Acad Sci USA*, **77**, 7152-6.

Wen Z and Darnell JE (1997). Mapping of Stat3 serine phosphorylation to a single residue (727) and evidence that serine phosphorylation has no influence on DNA binding of Stat1 and Stat3. *Nucleic Acids Res*, **25**, 2062-7.

Wesche H, Henzel WJ, Shillinglaw W, Li S and Cao ZD (1997). MyD88 – an adapter that recruits IRAK to the IL-1 receptor complex. *Immunity*, **7**, 837-47.

Weyand CM, Hicok KC, Conn DL and Goronzy JJ (1992). The influence of HLA-DRB1 genes on disease severity in rheumatoid arthritis. *Ann Intern Med*, **117**, 801-6.

Whiteside ST, Epinat JC, Rice NR and Israel A (1997). IκB epsilon, a novel member of the IκB family, controls rel A and c-rel NFκB activity. *EMBO J*, **16**, 1413-26.

Wigler M, Silverstein S, Lee LS, Pellicer A, Cheng Y and Axel R (1977). Transfer of purified herpes virus thymidine kinase gene to cultured mouse cells. *Cell*, **11**, 223-32.

Wijdenes J, Heinrich PC, Muller-Newen G, Roche C, Gu ZJ, Clement C and Klein B (1995). Interleukin-6 signal transducer gp130 has specific binding sites for different cytokines as determined by antagonistic and agonistic anti-gp130 monoclonal antibodies. *Eur J Immunol,* **25**, 3473-81.

Williams SC, Baer M, Dillner AJ and Johnson PF (1995). CRP2 (C/EBP beta) contains a bipartite regulatory domain that controls transcriptional activation, DNA binding and cell specificity. *EMBO J,* **14**, 3170-83.

Wilmann T and Beato M (1986). Steroid-free glucocorticoid receptor binds specifically to mouse mammary tumour DNA. *Nature*, **324**, 688-91.

Wolber EM and Jelkmann W (2000). Interleukin-6 increases thrombopoietin production in human hepatoma cells HepG2 and Hep3B. *J Interferon Cytokine Res*, **20**, 499-506.

Wood PH (1978). Nomenclature and classification of arthritis in children. In *The care of Rheumatic children*, Munthe E, editor, EULAR, **Basel** ed, 47-50.

Xia C, Cheshire J, Patel H and Woo P (1997). Cross talk between transcription factors NF-kappa B and C/EBP in the transcriptional regulation of genes. *Int J Biochem Cell Biol,* **29**, 1525-39.

Xing Z, Gauldie J, Cox G, Baumann H, Jordana M, Lei XF and Achong MK (1998). IL-6 is an anti-inflammatory cytokine required for controlling local or systemic acute inflammatory responses. *J Clin Invest*, **101**, 311-20.

Yamamoto-Furusho JK, Uscanga LF, Vargas-Alarcon G, Ruiz-Morales JA, Higuera L, Cutino T, Rodriguez-Perez JM, Villarreal-Garza C and Granados J (2003). Clinical and genetic heterogeneity in Mexican patients with ulcerative colitis. *Hum Immunol*, **64**, 119-23.

Yan H, Piazza F, Krishan K, Pine R and Krolewski JJ (1998). Definition of the interferon-alpha receptor-binding domain on the TYK2 kinase. *J Biol Chem,* **273**, 4046-51.

Yang-Yen HF, Chambard JC, Sun YL, Smeal T, Schmidt TJ, Drouin J and Karin M (1990). Transcriptional interference between c-Jun and the glucocorticoid receptor: mutual inhibition of DNA binding due to direct protein-protein interaction. *Cell*, **62**, 1205-15.

Yasukawa K, Hirano T, Watanabe Y, Muratani K, Matsuda T, Nakai S and Kishimoto T (1987). Structure and expression of human B cell stimulatory factor-2 (BSF-2/IL-6) gene. *EMBO J,* **6,** 2939–45.

Yawata H, Yasukawa K, Natsuka S, Murakami M, Yamasaki K, Hibi M, Taga T and Kishimoto T (1993). Structure-function analysis of human IL-6 receptor: dissociation of amino acid residues required for IL-6 binding and for IL-6 signal transduction through gp130. *EMBO J,* **12,** 1705-12.

Yin M, Yang SQ, Lin HG, Lane MD, Chatterjee S and Diehl AM (1996). Tumor necrosis factor alpha promotes nuclear localization of cytokine-inducible CCAAT/enhancer binding protein isoforms in hepatocytes. *J Biol Chem,* **271,** 17974-8.

Yin T, Shen R, Feng GS and Yang YC (1997). Molecular characterization of specific interactions between SHP-2 phosphatase and JAK tyrosine kinases. *J Biol Chem,* **272,** 1032-7.

Yokota S, Miyamae T, Imagawa T, Nishimoto N, Yoshizaki K, Mori M and Hirsch R (2002). Long-term therapeutic efficacy of humanized anti-IL 6-receptor antibody for systemic juvenile idiopathic arthritis. *Arthritis Rheum,* **46** Suppl 9, S1270.

Yoshizaki K, Nakagawa T, Fukunaga K, Tseng LT, Yamamura Y and KishimotoT (1984). Isolation and characterization of B cell differentiation factor (BCDF) secreted from a human B lymphoblastoid cell line. *J Immunol,* **132,** 2948-54.

Zak M and Pedersen FK (2000). Juvenile chronic arthritis into adulthood: a long-term follow-up study. *Rheumatology,* **39,** 198-204.

Zeggini E, Thomson W, Alansari A, Ollier W, Donn R and British Paediatric Rheumatology Study Group (2002a). Tumour necrosis factor receptor II polymorphism and juvenile idiopathic arthritis. *Rheumatology,* **41,** 462-5.

Zeggini E, Thomson W, Kwiatkowski D, Richardson A, Ollier W, Donn R and British Paediatric Rheumatology Study Group (2002b). Linkage and association studies of single-nucleotide polymorphism-tagged tumor necrosis factor haplotypes in juvenile oligoarthritis. *Arthritis Rheum,* **46,** 3304-11.

Zeggini E, Donn RP, Ollier WE, Thomson W and British Paediatric Rheumatology Study Group (2002c). Evidence for linkage of HLA loci in juvenile idiopathic oligoarthritis: independent effects of HLA-A and HLA-DRB1. *Arthritis Rheum*, **46**, 2716-20.

Zeidler C, Kanz L, Hurkuck F, Rittmann KL, Wildfang I, Kadoya T, Mikayama T, Souza L and Welte K (1993). In vivo effects of interleukin-6 on thrombopoiesis in healthy and irradiated primates. *Blood*, **81**, 2819-20.

Zhai R, Liu G, Yang C, Huang C, Wu C and Christiani DC (2001). The G to C polymorphism at –174 of the interleukin-6 gene is rare in a Southern Chinese population. *Pharmacogenetics*, **11**, 699-701.

Zhang X and Darnell JE (2001). Functional importance of Stat3 tetramerization in activation of the alpha2-macroglobulin gene. *J Biol Chem*, **276**, 33576-81.

Zhang YH, Lin JX and Vicek J (1990). Interleukin-6 induction by tumour necrosis factor and interleukin-1 in human fibroblasts involves activation of a nuclear factor binding to a kappa B-like sequence. *Mol Cell Biol*, **10**, 3818-23.

Zhang Y, Broser M and Rom W (1994). Activation of the interleukin 6 gene by *Mycobacterium tuberculosis* or lipopolysaccharide is mediated by nuclear factors NF-IL6 and NF-κB. *Proc Natl Acad Sci USA*, **91**, 2225-9.

Zhang X, Blenis J, Li HC, Schindler C and Chen-Kiang S (1995). Requirement of serine phosphorylation for formation of STAT-promoter complexes. *Science*, **267**, 1990-4.

Zhang JG, Farley A, Nicholson SE, Willson TA, Zugaro LM, Simpson RJ, Moritz RL, Cary D, Richardson R, Hausmann G, Kile BJ, Kent SB, Alexander WS, Metcalf D, Hilton DJ, Nicola NA and Baca M (1999). The conserved SOCS box motif in suppressors of cytokine signalling binds to elongins B and C and may couple bound proteins to proteasomal degradation. *Proc Natl Acad Sci USA*, **96**, 2071-6.

Zilberstein A, Ruggieri R, Korn JH and Revel M (1986). Structure and expression of cDNA and genes for human interferon-beta-2, a distinct species inducible by growth-stimulatory cytokines. *EMBO J*, **5**, 2529-37.

Zohlnhofer D, Graeve L, Rose-John S, Schooltink H, Dittrich E and Heinrich PC (1992). The hepatic interleukin-6 receptor. Down-regulation of the interleukin-6 binding subunit (gp80) by its ligand. *FEBS Lett*, **306**, 219-22.